

Technische Universität München

Max-Planck-Institut für Physik
(Werner-Heisenberg-Institut)

Differential Equations and the Magnus Exponential for multi-loop multi-scale Feynman Integrals

Ulrich Schubert-Mielnik

Vollständiger Abdruck der von der Fakultät für Physik
der Technischen Universität München zur Erlangung des akademischen Grades eines
Doktors der Naturwissenschaften (Dr. rer. nat.)
genehmigten Dissertation.

Vorsitzender: Prof. Dr. St. Schönert
Prüfer der Dissertation: 1. Hon.-Prof. Dr. W. F. L. Hollik
2. Priv.-Doz. Dr. A. Vairo

Die Dissertation wurde am 05.07.2016
bei der Technischen Universität München eingereicht und
durch die Fakultät für Physik am 14.07.2016 angenommen.

This thesis is based on the author's work conducted at the Max Planck Institute for Physics (Werner-Heisenberg-Institute) in Munich. Parts of this work have already been published in Refs. [1–8]

Articles

- [1] M. Argeri, S. Di Vita, P. Mastrolia, E. Mirabella, J. Schlenk, U. Schubert, and L. Tancredi, *Magnus and Dyson Series for Master Integrals*, *JHEP* **1403** (2014) 082, arXiv:1401.2979
- [2] S. Di Vita, P. Mastrolia, U. Schubert, and V. Yundin, *Three-loop master integrals for ladder-box diagrams with one massive leg*, *JHEP* **09** (2014) 148, [arXiv:1408.3107]
- [3] P. Mastrolia, A. Primo, U. Schubert, and W. J. Torres Bobadilla, *Off-shell currents and color-kinematics duality*, *Phys. Lett.* **B753** (2016) 242–262, [arXiv:1507.0753]
- [4] S. Borowka, N. Greiner, G. Heinrich, S. P. Jones, M. Kerner, J. Schlenk, U. Schubert, and T. Zirke, *Higgs boson pair production in gluon fusion at NLO with full top-quark mass dependence*, arXiv:1604.0644
- [5] R. Bonciani, S. Di Vita, P. Mastrolia, and U. Schubert, *Two-Loop Master Integrals for the mixed EW-QCD virtual corrections to Drell-Yan scattering*, arXiv:1604.0858

Proceedings

- [6] H. van Deurzen, G. Luisoni, P. Mastrolia, E. Mirabella, G. Ossola, T. Peraro, and U. Schubert, *Multi-loop Integrand Reduction via Multivariate Polynomial Division*, *PoS RADCOR2013* (2013) 012, [arXiv:1312.1627]
- [7] T. Peraro, H. van Deurzen, G. Luisoni, P. Mastrolia, E. Mirabella, G. Ossola, and U. Schubert, *Integrand reduction at NLO and beyond*, *PoS EPS-HEP2013* (2013) 449
- [8] P. Mastrolia, M. Argeri, S. Di Vita, E. Mirabella, J. Schlenk, U. Schubert, and L. Tancredi, *Magnus and Dyson Series for Master Integrals*, *PoS LL2014* (2014) 007

Abstract

The upcoming Run II of the Large Hadron Collider will measure scattering events at uncharted luminosities and energy scales. In order to exploit the measurements to their full potential it is essential to describe scattering processes at very high accuracy. The intended accuracies require the computation of higher loop amplitudes including the mass effects stemming from electroweak bosons and the top quark. The inclusion of mass effects does not only pose a challenge due to the increased number of kinematic scales, but also because of the absence of symmetries, which facilitated the computations in massless theories.

In this thesis we discuss the underlying algebraic structure of scattering amplitudes aiming at the development of novel techniques for their efficient computation. The techniques we will discuss can be applied to generic amplitudes including the aforementioned mass effects. In particular we will examine the algebra of the relations obeyed by dimensional regulated integrals allowing us to find a basis of integrals, called master integrals. By definition the latter span the whole space of Feynman integrals for a given process, allowing us to derive differential equations for the master integrals. The choice of master integrals is by no means unique and some choices can simplify the form of the differential equation and therefore their solution. A particular convenient choice is indicated by a so-called canonical differential equation, where the dependence on the dimensional regularization parameter is factorized from the kinematics. The solution of such a canonical form can be obtained algebraically and its analytic structure is evidently inherited from the associated matrix.

In this work we will focus on systems having a linear dependence on the dimensional regularization parameter and exploit the Magnus theory for differential equations in order to readily write down their solution as a kinematic evolution operator, describing the evolution from a boundary point to any point in the kinematic space. The evolution operator is given as a product of two Magnus exponentials, where the first exponential can be understood as a rotation in the space of master integrals, transforming the linear differential equation into its canonical form and where the second Magnus exponential solves the corresponding canonical form. We embodied this strategy for the computation of the master integrals for the ladder-box diagram with one massive leg, which enter the next-to-next-to-next-to-leading order virtual corrections to processes like the three-jet production mediated by vector boson decay, $V^* \rightarrow jjj$, as well as the Higgs plus one-jet productions in gluon fusion, $pp \rightarrow Hj$. Furthermore we computed the master integrals for the mixed QCD-EW corrections to Drell-Yan scattering.

Finally we presented the calculation of the cross section and invariant mass distribution for Higgs boson pair production in gluon fusion at next-to-leading order (NLO) in QCD, with the full top-mass dependence. The occurring integrals have been calculated numerically using the program SECDEC. Since our results include the full top-quark mass, we are able to assess the validity of various approximations proposed in the literature, which we also recalculate. We find substantial derivations between the NLO result and the different approximations, which emphasizes the importance of including the full top-quark mass dependence.

Zusammenfassung

Im bevorstehenden Run II am Large Hadron Collider(LHC) werden Streuprozesse von unerreichter Luminosität und Energie gemessen. Um das volle Potential dieser Messungen auszuschöpfen, müssen Streuprozesse mit großer Genauigkeit beschrieben werden. Die angestrebten Genauigkeiten erfordern die Berechnung von höheren Ordnungen in der Störungstheorie inklusive der Masseneffekte von elektroschwachen Vektorbosonen und des Top-Quarks. Die Berücksichtigung dieser Masseneffekte ist nicht nur wegen der erhöhten Anzahl der Massenskalen kompliziert, sondern auch weil Symmetrien gebrochen werden, welche die Berechnungen in masselosen Theorien vereinfacht haben.

In dieser Dissertation werden wir die zugrundeliegenden algebraischen Strukturen von Streuamplituden erkunden mit dem Ziel neue Methoden zu ihrer Berechnung zu entwickeln. Die hier beschriebenen Methoden sind für alle Streuamplituden inklusive der vorher beschriebenen Masseneffekte gültig. Insbesondere werden wir die Algebra der Relationen zwischen dimensional regulierten Integralen diskutieren. Diese Relationen erlauben es uns eine Integralbasis, die sogenannten Hauptintegrale, zu finden. Die Hauptintegrale spannen per Definition den gesamten Raum der Feynman Integrale für einen bestimmten Streuprozess und erlauben uns Differential Gleichungen für deren Bestimmung herzuleiten. Die Auswahl der Hauptintegrale ist in keiner Hinsicht eindeutig und manche Auswahlmöglichkeiten können die dazugehörigen Differentialgleichungen und deren Lösungen vereinfachen. Eine besonders gute Basis zeigt sich durch eine sogenannte kanonische Differentialgleichung, bei der der dimensionale Regularisationsparameter von der Kinematik faktorisiert. Die Lösung einer kanonischen Form kann algebraisch bestimmt werden und deren analytische Struktur folgt offensichtlich aus der zugehörigen Matrix.

In dieser Arbeit werden wir uns auf Systeme fokussieren, die linear vom dimensionalem Regularisationsparameter abhängen und werden mit Hilfe der Magnus Theorie deren Lösung direkt als einen kinematischen Entwicklungsoperator darstellen. Dieser Operator beschreibt die Entwicklung von einem Randpunkt zu einem beliebigen Punkt im kinematischen Raum und besteht aus dem Produkt zweier Magnus Exponentialfunktionen. Die erste Exponentialfunktion kann als Rotation im Raum der Hauptintegrale, welche die Differentialgleichung in ihre kanonische Form bringt, interpretiert werden. Die zweite Exponentialfunktion beschreibt die Lösung dieser kanonischen Form. Wir haben diese Strategie zur Berechnung der Hauptintegrale des Leiterboxdiagramms mit einer massiven äußeren Linie angewendet. Diese Integrale tragen zu den virtuellen Korrekturen in der dritten Ordnung der Störungstheorie für Streuprozesse bei. Beispiele für solche Streuprozesse sind die drei Teilchenjetproduktion vermittelt durch den Zerfall eines Vektorbosons $V^* \rightarrow jjj$ oder der Produktion von einem Higgsteilchen mit einem Teilchenjet durch Gluonfusion, $pp \rightarrow Hj$. Zusätzlich haben wir noch die Hauptintegrale für die gemischten ES-QCD Korrekturen zur Drell-Yan Streuung berechnet.

Zum Abschluss präsentieren wir die Berechnung des Wirkungsquerschnitts und der invarianten Massenverteilung für die Produktion eines Higgspaars durch die Fusion zweier Gluonen in der ersten Ordnung der Störungstheorie unter voller Berücksichtigung der Topmasseneffekte. Die auftretenden Hauptintegrale wurden numerisch mit der Hilfe des Programms

SECDEC berechnet. Da unser Ergebnis die vollen Topmasseneffekte berücksichtigt, können wir mehrere vorgeschlagene Approximationen untersuchen. Wir finden bedeutende Unterschiede zwischen unserem Ergebnis und den verschiedenen Approximationen, was die Bedeutung der Topmasseneffekte unterstreicht.

Contents

1. Introduction	12
2. From Feynman Diagrams to Master Integrals	18
2.1. Tensor Decomposition	18
2.2. Feynman Integral Classification	19
2.3. Reduction to Master Integrals	20
2.3.1. Symmetry Relations	20
2.3.2. Lorentz Invariance Identities	20
2.3.3. Integration-by-parts Identities	21
2.3.4. Finding Master Integrals	22
3. Differential Equations for Feynman Integrals	24
3.1. Deriving Differential Equations	24
3.2. Solution	28
3.3. Canonical Form	30
3.4. Boundary Conditions	32
4. The Magnus Method for Differential Equations	36
4.1. The Magnus Theorem	37
4.2. Proof of the Magnus Theorem	38
4.3. Graphical Representation of the Magnus Expansion	40
4.4. Magnus and Dyson Series Expansion	44
5. Differential Equations in Canonical Form	46
5.1. Pure Functions of Uniform Weight	47
5.1.1. Unit Leading Singularity and Unitarity Cuts	48
5.1.2. Feynman Parameter Representation	50

5.2.	Canonical Systems and Magnus Exponential Matrix	51
5.2.1.	Preface: On time-dependent Perturbation Theory	51
5.2.2.	Changing the Basis of Master Integrals	52
5.2.3.	An Algorithm based on the Magnus Expansion	53
5.2.4.	Extension to Polynomial ϵ Dependence	55
5.3.	Canonical Systems and Deflation	56
5.3.1.	Eigenvalue Deflation	56
5.3.2.	An Algorithm based on Eigenvalue Deflation	60
5.4.	The QED Sunrise	64
5.4.1.	Canonical Form with the Magnus Exponential	65
5.4.2.	Canonical Form with Eigenvalue Deflation	66
5.5.	Irrational Terms within Differential Equations	68
5.5.1.	Landau Variables	69
6.	Iterated Integrals	71
6.1.	Chen's Iterated Integrals	71
6.1.1.	Properties of Chen's iterated integrals	73
6.1.2.	Path Invariance	75
6.2.	Goncharov Polylogarithms	78
6.3.	Mixed Chen-Goncharov Representation	82
7.	Magnus Series for Master Integrals	83
7.1.	One-Loop Bhabha Scattering	83
7.2.	Two-Loop QED Vertices	86
7.3.	Massless $2 \rightarrow 2$ Scattering at Two-Loop	89
8.	Associated Higgs plus One Jet Production	93
8.1.	Introduction	93
8.2.	Differential Equations and Magnus Exponential	94
8.3.	Canonical System	97
8.4.	Two-Loop Master Integrals	98
8.4.1.	Planar Topology	98
8.4.2.	Easy non-planar Topology	100
8.4.3.	Hard non-planar Topology	102
8.5.	Three-Loop Master Integrals	103
8.6.	Boundary Conditions	108
8.7.	Conclusions	112
9.	Mixed EW and QCD Corrections to Drell-Yan Scattering	113
9.1.	Introduction	113
9.2.	Notations and Conventions	116
9.3.	System of Differential Equations for Master Integrals	120
9.3.1.	Constant <i>GPLs</i>	121

9.4. One-Mass Master Integrals	121
9.4.1. One-Loop	122
9.4.2. Two-Loop	124
9.5. Two-Mass Master Integrals	125
9.5.1. Variables for the two-mass Integrals	125
9.5.2. One-Loop	128
9.5.3. Two-Loop	130
9.6. Conclusions	134
10. Higgs Boson Pair Production in Gluon Fusion at NLO	136
10.1. Introduction	136
10.2. Analytic Computation of Master Integrals	138
10.2.1. Notations and Conventions	138
10.2.2. Canonical System and Boundary Conditions	140
10.2.3. Outlook for the Double Higgs Master Integrals	141
10.3. Numerical Integration via Sector Decomposition	142
10.4. NLO Calculation	144
10.4.1. Amplitude Structure	145
10.4.2. The virtual two-loop Amplitude	147
10.4.3. Real Radiation	147
10.5. Numerical Results	148
10.6. Conclusions	150
11. Conclusion	151
Acknowledgements	153
Appendices	154
A. Computing Leading Singularities	155
A.1. One-Loop massless Box	155
A.2. One-Loop massless Bubble in two Dimensions	157
A.3. Two-Loop non-planar massless Box	158
B. Master Integrals for the two-loop QED vertices	160
C. Matrices for Associated Higgs plus One Jet Production	169
C.1. Canonical Matrices at Two-Loop	169
C.2. Canonical Matrices at Three-Loop	171
D. Two-Loop dlog-forms	186
D.1. One-mass	186
D.2. Two-mass	190

It is a great achievement of particle physics that the rich world of subatomic particles can be described by a simple model, the so-called Standard Model(SM). Within the SM particles are described as quantum excitations of physical fields and the forces between them are generated by symmetries of the SM. In particular the SM is invariant under gauge transformations generated by the group $SU(3)_C \times SU(2)_L \times U(1)_Y$, where $SU(3)_C$ corresponds to the strong force and $SU(2)_L \times U(1)_Y$ generates the electroweak force. The interactions under the strong force define the theory of Quantum Chromodynamics(QCD), which is an exact symmetry of nature. This is in contrast to the electroweak theory, where the symmetry is spontaneously broken by the Brout-Englert-Higgs mechanism at low energies. The excitations of the corresponding Higgs field describe the famous Higgs boson, which is the only spin zero particle within the SM and responsible for the masses of all other SM particles.

The SM was tested by an extensive series of experiments and it is therefore one of the best confirmed models in physics. Some of the discoveries, which underlined the validity of the SM were the W and Z bosons by the UA1 and UA2 experiment at the Super Proton Synchrotron [9–11], the top quark by the CDF and DØ experiment at the Tevatron [12,13], the τ neutrino by the DONUT experiment at the Tevatron [14] and the Higgs boson by ATLAS and CMS experiment at the Large Hadron Collider(LHC) [15,16].

Despite this huge success we also know that the SM can not be a complete model of the subatomic world. From the observed neutrino flavor oscillations [17,18], it can be concluded that the neutrino must have a mass, which is not explained within the SM. In addition the cosmic microwave background allows us to make estimations about the energy distribution in the universe [19]. From this distribution we can conclude that the SM only describes around five percent of the universe leaving the two most significant contributions dark energy and dark matter unexplained. Furthermore the SM only allows for a slight derivation from the otherwise symmetric production of matter and anti-matter, which is not able to account for the current excess of matter in our universe. Additionally the SM does not describe the

gravitational force and it remains an open question if gravity can be consistently described by any quantum field theory at all.

Physics beyond the Standard Model(BSM) might provide answers to these open questions of particle physics and the search for BSM physics is one of the main goals of the LHC. BSM physics might manifest itself at the LHC either by the direct production of new heavy particles or by slight derivations from the precisely measured SM parameters. These derivations might then be explained within an extension of the SM or even a complete new theory. Currently the LHC is exploring the SM at previously unknown energy scales and measures many of our SM parameters at an incredible precision. In order to fully exploit this advancement and hopefully answer some of the remaining open questions, it is essential that we vastly improve our theory predictions.

The nature of the LHC as an hadron collider provides several challenges for the theoretical description of a scattering event, due to the strongly interacting hadrons. In fact our ability to make any theoretical prediction for a hadron collision relies on the QCD factorization theorem [20–22], which allows us to factor the short distance effects from the long distance effects. This is essential, since only at short distances (high energies) the strong coupling constant is small enough to justify the use of perturbation theory, whereas the long distance effects get non-perturbative contributions. The long distance effects encode the inner structure of the hadron, which consists of valence and sea quarks. While the valence quarks determine the quantum properties of the hadron, the sea quarks are virtual quark-antiquark pairs, which are constantly created and destroyed within the hadron. All this structure can be conveniently combined in the parton distribution functions(PDFs), which provide us with the probability to find a certain parton, carrying a fraction of the hadron momentum, at a specific energy. Due to their non-perturbative nature, they are determined by a global fit of deep inelastic scattering data at lower energies and then evolved to higher energies through the Dokshitzer-Gribov-Lipatov-Altarelli-Parisi (DGLAP) equations [23–25].

The hadron scattering at the LHC happens at such high energies, that the asymptotic freedom of QCD allows us to regard the partons of the hadrons as free particles. For this reason we essentially have a hard scattering event between only two partons each carrying a momentum fraction of the corresponding hadrons. The momentum fraction and the type of parton is described by the PDFs, while the hard scattering event can be calculated within the framework of perturbation theory. The resulting particles, provided they interact with the strong force, radiate of virtual gluons which may radiate of gluons and quark-antiquark pairs. This process is known as a parton shower and will continue until we reach the hadronisation scale at around $\Lambda_{\text{QCD}} \sim 1\text{GeV}$. At this scale the partons will start to form hadrons, which may decay into more stable particles before they are measured in the detector.

Within this framework it is important to describe the underlying hard scattering as precise as possible, since a deeper understanding of the hard scattering event may provide us

with insight into BSM physics. The core ingredient for the description of the hard scattering process are scattering amplitudes, which give us the probability that our initial partons scatter to a certain set of final state particles. A scattering amplitude can be computed by Feynman diagrams, which encode every possibility for the particles to interact. Perturbation theory allows us to expand the hard scattering event in the number of interactions, where at each order we may either add an additional final state particle or a closed loop. With the increasing number of loops and final state particles scattering amplitudes become harder and harder to compute and therefore limit our precision with which we can describe the hard scattering event.

Up to recent years most relevant processes for the LHC were only known up to leading order(LO) precision. By now it is clear that these LO calculations are insufficient and may get unexpected large corrections from the higher orders in the perturbation theory, which in some cases exceeded the estimate error for the truncation of the series (see e.g. Higgs production through gluon fusion [26]). For this reason we can only obtain reliable predictions for our hard scattering event by including higher order corrections, which require the computation of loop-level scattering amplitudes.

For most loop-level scattering amplitudes a direct integration of the appearing Feynman integrals is prohibitive, due to their sheer number and complexity. It is fruitful to think about this problem in the context of linear algebra. The loop-level scattering amplitude can be thought of as a point in a space, which is spanned by the appearing Feynman integrals. But it turns out that most of the Feynman integrals are not linearly independent and therefore only a small subset of integrals, called master integrals (MI's) is needed to span the space. After projecting our amplitude on this new basis, the computation of the MI's is still an open problem, but it usually reduces the number of integrals by several orders of magnitude.

At one-loop level the basis of MI's was first identified through the Passarino-Veltmann reduction [27] as a set of scalar integrals with up to four loop propagators. This knowledge allowed for the development of efficient projection techniques onto this basis, where especially methods based on unitarity were extremely successful. The unitarity of the S-matrix follows from the conservation of probability and directly implies the optical theorem, by which the imaginary part of the forward scattering amplitude is proportional to the total cross section. The former can only develop an imaginary part, if some of its propagators vanish (are cut), such that their $i\epsilon$ description becomes relevant. This idea was worked out by Cutkosky [28], who showed that the imaginary part of the forward scattering amplitude can be computed as the sum of all possible two propagator cuts. By definition a cut propagator is on-shell and therefore our amplitude factorizes into a product of lower-loop amplitudes. By considering complex kinematics it becomes possible to cut even more than two propagators at once, as long as all cut conditions can be satisfied simultaneously by the loop momenta [29–32]. This framework is known as generalized unitarity and allows us to group the Feynman diagrams according to their multi-particle factorization channels. A scattering amplitude can

be reconstructed by systematically considering all possible factorization channels. Furthermore we can completely circumvent the use of Feynman diagrams, by using the fact that amplitudes factorize on each cut into a product of lower-loop amplitudes.

Although these techniques were originally developed to be used after integration, they can also be applied at the integrand level at the cost of introducing spurious terms, which vanish after integration [33, 34]. This decomposition of the integrand in its multi-particle factorization channels, known as the OPP decomposition, is completely independent of the kinematics of the process and therefore can be applied to any one-loop scattering amplitude. The automation of this integrand decomposition [35–37] and the implementation within one-loop generators [38–46] greatly boosted our ability to perform one-loop calculations.

Trying to generalize these techniques to the two-loop level and beyond provides us with several challenges. Already at the level of Feynman diagrams we encounter a new type of diagrams, so-called non-planar diagrams. The latter can only be drawn with crossing internal edges or having external edges end within the diagram. Even though this might seem like a pettiness these diagrams and their corresponding integrals have a much richer singularity structure than their planar counter parts, which can impede the calculation. In contrast to one-loop a general integral basis is not known at the two-loop level and beyond, instead the integral basis has to be determined process by process. Similarly the appearing MI's are only known for specific processes and their analytic expressions involve a variety of complicated functions, making the corresponding amplitude much harder to handle analytically and slow to evaluate numerically.

Even though these challenges have been overcome for a number of processes, keeping up with the ever increasing experimental accuracy requires us to calculate numerous processes at two-loop accuracy with an increasing number of external legs, which we can only be achieved through automation. A first step in this direction was done by the extension of integrand reduction techniques to higher loops, which was first achieved in [47]. Later the OPP decomposition was understood as the result of a polynomial division between the numerator and the propagators, a concept which was then generalized to higher loops [48–50]. Through a better understanding of the physical degrees of freedom for each multi particle factorization channel and by a priori integrating them out the efficiency of this algorithm was greatly improved [51]. In addition generalized unitarity has been extended to the two-loop level in the form of the maximal unitarity approach [52–55], which aims to directly obtain the coefficients of the master integrals by choosing suitable integration contours in the complex plane.

After the coefficients of the MI's are determined the question of their calculation arises. We can achieve this either by direct or indirect integration. For the former we find a convenient parametrization of the integrand, which allows us to directly integrate our Feynman integral, e.g. Feynman parametrization and sector decomposition [56–64] or Mellin-Barnes representation [65–68], whereas for the latter we derive a system of equations, whose solution will be the Feynman integrals; examples for this approach are the difference [69–71]

and differential equations [72–74].

This thesis is dedicated to the calculation of master integrals, especially via the method of differential equations. The idea to use differential equation was first introduced by Kotikov for internal masses [72] and then extended to all external invariants by Remiddi [73] and Gehrmann and Remiddi [74]. The solution of the differential equation provides us with an evolution operator, which describes the kinematic evolution from the boundary point to any point in the kinematic plane. The singularity structure of the evolution operator is in general much richer than the singularity structure of the corresponding MI's, therefore providing the boundary point amounts to choosing the physical set of singularities, which corresponds to our MI's. In fact we can turn this argument around and fix the boundary constants by demanding the absence of unphysical thresholds from our solution.

Recently an additional way to derive a differential equation was suggested in [75]. By cleverly rescaling some of the external momenta, we can derive a differential equation in respect to this rescaling parameter, which after a solution has been obtained is taken back to one. This method has been recently used in the computation of the planar five-point two-loop massless MI's with one off-shell leg [76].

For any given process the set of master integrals is not unique and their choice is rather arbitrary. Initially the master integrals are identified by the Laporta algorithm [69], but then we may choose any convenient set. A proper set of MI's can significantly simplify the differential equation and therefore simplify the calculation of the MI's. In fact a particular good choice of master integrals is characterized by the factorization of the dimensional regularization parameter from the kinematics [77]. The canonical form does not only make the singularity structure especially transparent, but it also simplifies the integration to a completely algebraic procedure.

It remains an open question if a canonical form can be found for any process and the answer to this question is tightly connected to the existence of a general algorithm that transforms any set of MI's to the corresponding canonical set of MI's. Nevertheless the qualitative properties of canonical MI's can be turned into quantitative tools like unit leading singularity criterion and the *dlog* representation in terms of Feynman parameters [78–80]. Furthermore we can attempt to find a rotation matrix in the space of master integrals, yielding a canonical form, through an appropriate ansatz, which is based on the polynomial structure of the dimensional regularization parameter in the initial differential equation [81]. In cases, where we have several master integrals in one topology, we can identify canonical master integrals by exploiting the structure of the higher order differential equation, which are independent from the choice of the other master integrals [82]. In addition there exists an algorithm for processes depending only on two kinematic invariants based on the deflation of eigenvalues [83]. This algorithm suggests that not all systems can be transformed into a canonical form, since this is related to the 21st Hilbert problem, which has a negative

answer [84]. Furthermore if we are able to choose an initial set of MI's such that our differential equation is linear in ϵ , we can use the Magnus exponential to obtain a canonical set of master integrals [1]. The latter two algorithms will be discussed in detail within this thesis.

We will first show how the algorithm based on the Magnus series can be used to recompute known MI's and then later used to compute the 85 MI's of the three-loop ladder-box topology with one massive leg [2]. These master integrals are part of the next-to-next-to-next-to leading order(NNNLO) virtual correction to scattering processes like Higgs plus one-jet production through gluon fusion in the heavy top limit. In addition we show how this algorithm can be used to compute the MI's for the mixed EW-QCD virtual corrections to Drell-Yan scattering [5], which are approximately at the same order of accuracy as the NNNLO QCD corrections.

Finally we will apply the algorithm based on the Magnus series to the computation of the MI's for Higgs production through gluon fusion, which previously have been computed without the canonical basis [85]. The computed MI's belong to a subset of integrals needed for the computation of the NLO correction to Higgs boson pair production through gluon fusion including the top mass effects, presented in [4]. Due to the expected appearance of elliptic integrals we embodied a numerical approach for the computation of the remaining MI's. Nevertheless we computed the cross section and the invariant mass distribution for this process, which will be important for the determination of the Higgs boson self coupling in the upcoming Run II of the LHC. In addition the full result allows us to check various approximations, which have been proposed in the literature [86–97].

This thesis is organized as follows: First we will describe how a scattering amplitude, given by its Feynman diagram expansion, can be expressed as a linear combination of master integrals. In the next chapter we will introduce the method of differential equations for the computation of Feynman integrals and discuss two strategies for their solution one where we solve the differential equation line by line and one based on the canonical form. After this chapter we will discuss the Magnus theory for differential equations and then move to the question how we can find a canonical differential equation. Here we will first discuss some properties, which indicate a canonical master integral and then present an algorithm based on the Magnus series and an algorithm based on eigenvalue deflation, which both under certain assumptions allow us to find a canonical basis of MI's. Afterwards we will discuss the solution of differential equations in terms of iterated integrals. In particular we will discuss Chen's iterated integrals and its special case the Goncharov polylogarithm. In the following chapter we will show some easy examples, where the algorithm based on the Magnus expansion has been applied and later we discuss the calculation of the MI's belonging to the three-loop ladder-box with one off-shell leg as well as the calculation of the master integrals for the mixed EW-QCD virtual corrections to Drell-Yan scattering. Finally we will elaborate on the NLO correction to Higgs boson pair production through gluon fusion including the full top-mass effects.

From Feynman Diagrams to Master Integrals

During the calculation of quantum corrections to a given process via loop-level Feynman diagrams, we encounter an abundance of difficult Feynman integrals, describing the generalization of averaging over non-observable degrees of freedom. The calculation of each individual Feynman integral can be difficult and time consuming, therefore each identity, relating different Feynman integrals, can greatly simplify the problem of their determination and consequently the calculation of the quantum correction as a whole. In order to reduce the number of Feynman integrals to a minimal set, we usually follow a three step procedure, which will be described in the following sections.

2.1. Tensor Decomposition

In the first step we separate the Lorentz and Dirac structures in the Feynman diagrams from the integrals. One efficient way in doing so is given by the method of tensor decomposition, where we first expose all external polarization vectors

$$\mathcal{M} = \epsilon_1^{\mu_1} \dots \epsilon_k^{\mu_k} \mathcal{M}_{\mu_1 \dots \mu_k} , \quad (2.1)$$

and then write an ansatz for the tensor $\mathcal{M}_{\mu_1 \dots \mu_k}$ in terms of the independent Lorentz vectors and tensors¹ and the possible Dirac structures

$$\mathcal{M}_{\mu_1 \dots \mu_k} = \sum_i T_{\mu_1 \dots \mu_k; i} f_i . \quad (2.2)$$

The size of the ansatz can be further reduced by imposing physical constraints like the transversality condition and the Ward identity. After an adequate ansatz is obtained we can compute the form factors f_i directly from our Feynman diagrams by defining projectors,

¹E.g. for four external gluons there are two Lorentz tensors: the metric $g^{\mu\nu}$ and the epsilon tensor $\epsilon^{\alpha\beta\mu\nu}$ and three independent Lorentz vectors namely three of the four external momenta

which single out specific tensor structures in (2.2)

$$P_i \mathcal{M} = f_i . \quad (2.3)$$

Through the tensor decomposition the numerators of the Feynman integrals appearing in the form factors f_i may only include scalar products build from the external momenta and the loop momenta.

2.2. Feynman Integral Classification

A typical L -loop Feynman integral within the form factor is given by²

$$\int \prod_{i=1}^L d^d k_i \frac{\mathcal{N}(k, p)}{D_1^{\alpha_1} \dots D_{N'}^{\alpha_{N'}}} . \quad (2.4)$$

The number of different scalar products appearing in the numerator can be calculated as

$$N_{sp} = L(n - 1) + \frac{L(L + 1)}{2} = L \left(n + \frac{L}{2} - \frac{1}{2} \right) , \quad (2.5)$$

where n is the number of external legs. Beyond one-loop the number of scalar products is always bigger than the number of propagators, preventing us from writing every scalar product as a combination of propagators and therefore from expressing the numerator in terms of propagators. A way of dealing with these irreducible scalar products is to artificially enlarge the set of propagators with so called auxiliary propagators, such that we are able to write every scalar product in terms of propagators. Consequently we are able to express each scalar product in the numerator completely in terms of the enlarged set of propagators

$$\int \prod_{i=1}^L d^d k_i \frac{1}{D_1^{\alpha_1} \dots D_N^{\alpha_N}} . \quad (2.6)$$

We should note that some of the α_i might be negative, especially the ones related to the auxiliary propagators are always non-positive. At this step we can define:

Definition 2.2.1 *An integral family is given by a full set of propagators, which spans the complete space of scalar products.*

Definition 2.2.2 *A topology is a subset of the integral family, where all powers of the propagators are positive and which corresponds to a graph with momentum conservation at each vertex.*

Definition 2.2.3 *A subtopology is a subset of a topology, which also can be drawn as a graph with momentum conservation at each vertex.*

²We promoted the integral to $d = 4 - 2\epsilon$ dimensions, in order to conveniently encode its UV and IR divergences as poles in ϵ within the framework of dimensional regularization.

Going back to our form factors we can now classify each set of propagators stemming from a Feynman integral as either a topology or a subtopology. In general each topology may generate an integral family, but it is convenient to choose the auxiliary propagators in a way that we can group all topologies in as few integral families as possible. It is important to note that some of the subtopologies may belong to several integral families which may lead to over counting of master integrals and unnoticed cancellations. Partly we already resolved these overlaps by grouping the maximal number of topologies into each integral family, but nevertheless the remaining overlapping subtopologies still have to be identified and mapped to each other.

2.3. Reduction to Master Integrals

It turns out that most of the Feynman integrals in a topology are actually related to each other by symmetry relations, Lorentz invariance identities and integration-by-parts (IBP) identities [98,99], which are based on general properties of Feynman integrals, namely graph symmetries, the Lorentz invariance and shift invariance of the loop momenta of the integral respectively. By exploiting these relations we are able to express all integrals within our topology in terms of a much smaller set of master integrals.

2.3.1. Symmetry Relations

The first set of relations between different integrals can be derived from discrete shifts of the loop momenta, which leave the value of the integral unchanged or in other words, which have a trivial Jacobian. From the whole set of shifts two are especially useful to us, ones which map different topologies into each other and ones which map the topology onto itself. The former allows us to decrease the number of independent topologies, whereas the latter allows us to derive identities between integrals in our topologies. E.g. whenever we have a bubble insertion we can shift the loop momenta, which runs in the bubble such that we exchange the two bubble propagators. This will not only lead to the identity that we can exchange the powers of the corresponding propagators, but also to more involved identities especially if we consider non-trivial numerators.

2.3.2. Lorentz Invariance Identities

The Feynman integrals contained in the form factors in (2.2) are by construction only Lorentz scalars, therefore they are invariant under all Lorentz transformations. Under an infinitesimal shift of the external momenta $p_i^\mu \rightarrow p_i^\mu + w^{\mu\nu} p_{i,\nu}$, where $w^{\mu\nu}$ is some totally antisymmetric tensor, our Feynman integral transforms in the following way

$$\int \prod_{i=1}^L d^d k_i \frac{1}{D_1^{\alpha_1} \dots D_N^{\alpha_N}} \rightarrow \left(1 + w^{\mu\nu} \sum_i^n p_{i,\nu} \frac{\partial}{\partial p_i^\mu} \right) \int \prod_{i=1}^L d^d k_i \frac{1}{D_1^{\alpha_1} \dots D_N^{\alpha_N}}. \quad (2.7)$$

The Lorentz invariance of the latter expression allows us to obtain relations of the form

$$\sum_i^n \left(p_{i,\nu} \frac{\partial}{\partial p_i^\mu} - p_{i,\mu} \frac{\partial}{\partial p_i^\nu} \right) \int \prod_{i=1}^L d^d k_i \frac{1}{D_1^{\alpha_1} \dots D_N^{\alpha_N}} = 0 , \quad (2.8)$$

which can be contracted with all possible antisymmetric tensors built from the external momenta.

2.3.3. Integration-by-parts Identities

As it has been described in [100,101] a Feynman integral is invariant under shifts in the loop momenta k_1, \dots, k_L by any combination of loop and external momenta p_1, \dots, p_n

$$k_i \rightarrow A_{ij} k_j + B_{ij} p_j , \quad (2.9)$$

with A_{ij} being an invertible $L \times L$ matrix and B_{ij} an rectangular $L \times n$ matrix. This shift symmetry actually forms a general linear group $GL(n, \mathcal{R})$ of dimension L .

Considering the action of an infinitesimal shift of our loop momenta ³

$$k_i^\mu \rightarrow k_i^\mu + \beta_{ij} q_j^\mu , \quad \text{with} \quad q_j^\mu = \{k_1^\mu, \dots, k_L^\mu, p_1^\mu, \dots, p_n^\mu\} , \quad (2.10)$$

on to our Feynman integral

$$\int \prod_{i=1}^L d^d k_i \frac{1}{D_1^{\alpha_1} \dots D_N^{\alpha_N}} \rightarrow \int \prod_{i=1}^L d^d k_i \left(1 + \beta_{ij} \left(d\delta_{ij} + q_j^\mu \frac{\partial}{\partial q_{\mu,i}} \right) \right) \frac{1}{D_1^{\alpha_1} \dots D_N^{\alpha_N}} \quad (2.11)$$

$$= \int \prod_{i=1}^L d^d k_i \beta_{ij} \left(1 + \frac{\partial}{\partial q_{\mu,i}} q_j^\mu \right) \frac{1}{D_1^{\alpha_1} \dots D_N^{\alpha_N}} , \quad (2.12)$$

allows us to identify the generator of the Lie group

$$O_{ij} = \frac{\partial}{\partial q_{\mu,i}} q_j^\mu , \quad (2.13)$$

and its structure constants

$$[O_{ij}, O_{kl}] = \delta_{il} O_{kj} - \delta_{kj} O_{il} . \quad (2.14)$$

The shift invariance of our Feynman integral can be formulated in a simple equation, which generates all IBP identities for a given Feynman integral

$$\int \prod_{i=1}^L d^d k_i \frac{\partial}{\partial k_{\mu,i}} \left(\frac{q_j^\mu}{D_1^{\alpha_1} \dots D_N^{\alpha_N}} \right) = 0 . \quad (2.15)$$

³In order to have a well defined shift we require that $\mathbb{1} + \beta_{i,j}$ is invertible, where $\beta_{i,j}$ is the minor with $i = 1, \dots, L$ and $j = 1, \dots, L$.

The form of this equation also exposes another origin of the integration-by-parts identities namely Stokes theorem, which states that integrating over a manifold of a total derivative equals the integral over the boundary of the manifold, which given that our integrand vanishes sufficiently fast is zero.

We should also note that after differentiation we will get a sum of integrals with rational integrands, where the numerators consists of scalar products involving the loop and the external momenta and denominator is build from the propagators. After expressing all scalar products involving the loop momenta back in terms of our propagators, we obtain relations between the different integrals. The rational coefficients of the integrals will be build from the kinematic invariants and the space time dimensions d . Furthermore neither the derivative nor replacing the scalar products in the numerator will introduce propagators in the denominator with positive powers α_i , which were not already present in the corresponding generating function. Therefore an IBP identity will only involve integrals from the same topology or its subtopologies.

2.3.4. Finding Master Integrals

Since the exponents of the propagators are left arbitrary in the generating equation for the IBP identities (2.15), we can generate an infinite number of equations for an infinite number of integrals within a given topology. Fortunately the number of equations is growing faster than the number of involved integrals indicating that most equations are redundant [102]. Indeed it has been shown that we can always solve these systems in terms of a finite number of master integrals [103]. In addition the infinite set of equations also contains all information from the Lorentz invariance identities relating them to the IBP identities.

In practice we will only generate equations up to a total power of propagators $r = \sum_i \alpha_i$, where we only consider positive exponents α_i and up to a total power of propagators in the numerator $s = -\sum_i \alpha_i$, where we only consider negative exponents α_i . It is important to find a balance between a high enough s and t to find the correct number of master integrals, but also a low enough s and t , such that we are able to solve the system with the available computer resources. The resulting system can then be solved by the Laporta algorithm [69], which introduces an ordering for each integral and then solves the system by Gauss substitution.

In theory any increasing function based on the powers of the propagators α_i can be used for this ordering, but in practice some orderings may facilitate the solution of the system. After an adequate ordering is chosen we can solve equation by equation with the Gauss substitution rule, where we replace the integral with the highest weight, in terms of integrals with lower weight. This step is repeated until only a very small subset of integrals with the lowest possible weight are left, which are the master integral of our topology. We may also encounter so-called reducible topologies which have no master integrals and can be completely expressed in terms of their subtopologies.

We should note that restricting ourselves to some r and s , where we stop the generation of the IBP system may also comes with some drawbacks. Firstly we can't rule out that an IBP identity with higher r and/or s may relate some master integrals, we thought were

independent, therefore further reducing the number of master integrals. Secondly whereas the Lorentz invariance identities were related to the IBP identities for the full system, this might not be the case if we restrict ourselves to a system with a specific r and s , therefore in many applications we still consider the Lorentz invariance identities, in order to reduce the necessary algebra, which needs to be performed.

All in all the symmetry relations, IBP and Lorentz invariance identities are essential tools for any multi-loop computation, since they reduce the number of Feynman integrals by several orders of magnitude. For a typical two-loop problem they reduce the total number of independent Feynman integrals from $\mathcal{O}(10000)$ down to $\mathcal{O}(100)$. With such huge simplifications it is no surprise, that there are several implementations of them in public computer codes [104–107].

Differential Equations for Feynman Integrals

Even after the reduction of the Feynman integrals to a small set of master integrals is completed, the evaluation of the latter remains an open question. There are two different approaches for their analytical computation. Either we attempt to integrate them directly or we use a method, which performs the integration only indirectly. In the former method we manipulate the integrand in a way that allows for a direct integration. Examples of such methods are the Feynman parametrization of an integral and the Mellin-Barnes representation [65–68], which have been very successful at one-loop and even for lower scale problems at the multi loop level. Two examples for indirect integration methods are given by difference [69–71] and differential equations [72–74], where the former are functional relations between integrals, which are shifted by discrete values of e.g. the space time dimensions and where the latter describe how Feynman integrals behave under continuous changes in the kinematical invariants. The idea to use differential equations in order to calculate Feynman integrals was first proposed for internal masses by Kotikov [72] and then latter extended to all external invariants by Remiddi [73] and Gehrmann and Remiddi [74]. Since then differential equations have proven to be an essential tool for the analytic calculation of multi-loop and multi-scale Feynman integrals.

3.1. Deriving Differential Equations

The first step to derive a differential equation is to find an integral basis for the process under consideration, which can be done with the help of the symmetry relations, Lorentz invariance identities and IBP identities. Solving these identities results in a set of master integrals, which span the whole space of Feynman integrals for the given process. This will be essential when we start taking derivatives of the kinematic invariants of our process. We will first consider only derivatives with respect to internal masses, which will already include all main features of the method and only later we will extend the discussion to general external invariants.

When we act with a derivative with respect to an internal mass on a master integral we

essentially raise the power of the corresponding propagator by one

$$\partial_{m_i^2} \int \prod_{i=1}^L d^d k_i \frac{1}{D_1^{\alpha_1} \dots D_i^{\alpha_i} \dots D_N^{\alpha_N}} = -\alpha_i \int \prod_{i=1}^L d^d k_i \frac{1}{D_1^{\alpha_1} \dots D_i^{\alpha_i+1} \dots D_N^{\alpha_N}}, \quad (3.1)$$

where the propagators are defined as $D_i = K_i^2 - m_i^2$ with K_i being a sum of loop and external momenta. Since the latter integral still involves the same set of propagators, we have not left the space of Feynman integrals, which was spanned by our master integrals. Consequently there exists an IBP identity, which brings us back to a linear combination of the original integral and other master integrals, which for simplicity we will omit for now

$$\partial_{m_i^2} \int \prod_{i=1}^L d^d k_i \frac{1}{D_1^{\alpha_1} \dots D_i^{\alpha_i} \dots D_N^{\alpha_N}} = A_{m_i^2} \int \prod_{i=1}^L d^d k_i \frac{1}{D_1^{\alpha_1} \dots D_i^{\alpha_i} \dots D_N^{\alpha_N}}. \quad (3.2)$$

This is a first example of a differential equation, which we will later solve in order to obtain analytic expression for the master integrals. We should note that the prefactor $A_{m_i^2}$ is a rational function of the space time dimensions and the kinematic invariants of our process, since it inherits these properties directly from the IBP identities.

The previous steps show how a differential equation for each master integral can be derived. It is convenient to group all differential equations together in one coupled system

$$\partial_{m_i^2} \mathbf{F} = A_{m_i^2} \mathbf{F}, \quad (3.3)$$

where \mathbf{F} is a vector of master integrals and $A_{m_i^2}$ has been promoted to a matrix. If we order our master integrals by the size of the topology, we also realize that the matrix $A_{m_i^2}$ is block triangular, since both the derivative and the IBP identities will only involve integrals from the same topology or its subtopology. In fact the only reason, why $A_{m_i^2}$ is only block diagonal instead of diagonal is because there are topologies with several master integrals. This concludes our discussion of differential equations for internal masses and we are now ready to extend our discussion to general kinematic invariants.

First we should note that we can build $\frac{n(n-1)}{2}$ different scalar products from our n external legs, which we will conveniently group together in one vector

$$\vec{\hat{x}} = \{\hat{x}_1, \dots, \hat{x}_{\frac{n(n-1)}{2}}\} = \{s_{11}, s_{12}, \dots, s_{\frac{n(n-1)}{2} \frac{n(n-1)}{2}}\} \quad \text{with } s_{ij} = p_i \cdot p_j. \quad (3.4)$$

Since the integrand of a Feynman integral depends on the external momenta instead of the invariants we have to use the chain rule to obtain a differential operator involving the external momenta

$$p_k^\mu \frac{\partial}{\partial p_{\mu,i}} = \sum_j p_k^\mu \frac{\partial \hat{x}_j}{\partial p_{\mu,i}} \frac{\partial}{\partial \hat{x}_j}, \quad (3.5)$$

where we already multiplied our equation with another external momenta p_k in order to obtain a scalar differential operator which does not introduce uncontracted Lorentz indices.

If we have more than two external legs the system of equations in (3.5) is overdetermined. In detail we have $(n - 1)^2$ equations in the over constraint system, which give us

$$(n - 1)^2 - \frac{n(n - 1)}{2} = \frac{(n - 1)(n - 2)}{2} , \quad (3.6)$$

additional equations. These additional equations prevent us from solving our system in a unique way. The different differential operators we get by solving different subsets of the equations in (3.5), may at first look inconsistent, however there are exactly $\frac{(n-1)(n-2)}{2}$ Lorentz invariance identities, which guarantee us that all differential operators are equivalent.

Including the internal masses into our vector of kinematic invariants \vec{x} we arrive at the most general form for our differential equation

$$\partial_{\vec{x}} F = A_{\vec{x}} F , \quad (3.7)$$

At this point we should make a couple of remarks.

As denoted by \vec{x} we usually have a whole set of differential equations, namely one for each kinematical invariant of our process. It is convenient to perform a change of variable in order to have only one invariant with mass dimensions and a set of dimensionless invariants. The differential equation of the dimensionful invariant can be trivially solved and just give us the mass dimension of each integral, which we could have immediately accessed through power counting. The remaining set of differential equations can then be solved sequentially, where the integration constant at each step will only depend on a subset of kinematic invariants, which correspond to the still unsolved differential equations. After all differential equations have been solved the integration constant will be a constant in respect to all kinematic invariants, which can be fixed by the boundary conditions. This algorithm must succeed, since the integrability condition

$$\partial_{x_i} A_{x_j} - \partial_{x_j} A_{x_i} + [A_{x_j}, A_{x_i}] = 0 , \quad (3.8)$$

which can be derived from the Schwarz integrability condition for F , ensures that non-factorisable terms which depend on several kinematic invariants are common to all corresponding differential equations. With this procedure in my mind we will mostly consider only one of the differential equations, which is derived from a dimensionless variable, knowing that we can solve the differential equations of the other dimensionless invariants sequentially. In the case, where we only have one kinematic invariant, the differential equation gives us only the mass dimensions for each integral. For that reason all the desired information is in the boundary constants, which need to be provided independently. Nevertheless it has been shown that by introducing an additional kinematical invariant, solving the now meaningful differential equation and then carefully taking that kinematical invariant to zero one can still solve integrals depending on one kinematical invariant with the method of differential equations [108].

We should also note that the derivation of the differential operator was only based on the structure of the external and internal kinematics and is therefore completely independent

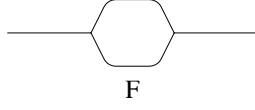


Figure 3.1.: The massless bubble F is shown.

of the loop order. The most limiting factor in the derivation of differential equations is in fact the derivation of the IBP identities, which are needed to reduce the derivative of our master integral back to the basis of master integrals. In fact deriving the IBP identities for a difficult two-loop process can be already beyond the current technologies. But with growing computing power and a better understanding of the underlying structure [109–111] we might be able to push this threshold to even more scales/loops in the near future.

The massless one-loop Bubble

Let us show the steps we described in the previous section with an easy one-loop example: the one-loop massless bubble, with an off-shell external leg $\hat{x} = p^2 \neq 0$ ¹

$$F(\epsilon, p^2) = \int d^d k \frac{1}{k^2(k-p)^2}, \quad (3.9)$$

which is depicted in figure 3.1. In the first step we construct the differential operator

$$p^\mu \frac{\partial}{\partial p_\mu} = p^\mu \frac{\partial p^2}{\partial p_\mu} \frac{\partial}{\partial p^2} = 2p^2 \frac{\partial}{\partial p^2} \quad (3.10)$$

$$\Rightarrow \frac{\partial}{\partial p^2} = \frac{1}{2} \frac{p^\mu}{p^2} \frac{\partial}{\partial p_\mu}, \quad (3.11)$$

which in this case is solely done by the chain rule, since the system (3.5) is not overdetermined. Applying the differential operator to our integral we find

$$\frac{\partial}{\partial p^2} \int d^d k \frac{1}{k^2(k-p)^2} = \frac{p^\mu}{2p^2} \frac{\partial}{\partial p_\mu} \int d^d k \frac{1}{k^2(k-p)^2} \quad (3.12)$$

$$= \frac{1}{p^2} \int d^d k \frac{k \cdot p - p^2}{k^2(k-p)^4} \quad (3.13)$$

$$= -\frac{1}{2p^2} \int d^d k \left(\frac{1}{k^2(k-p)^2} - \frac{1}{(k-p)^4} + \frac{p^2}{k^2(k-p)^4} \right), \quad (3.14)$$

where in the last step we replaced the scalar product in terms of our propagators $k \cdot p = -\frac{1}{2}((k-p)^2 - k^2 - p^2)$. We can perform a shift in the loop momenta $k \rightarrow k+p$ in the

¹The massless bubble with an on-shell external leg is vanishing in dimensional regularization, since it does not depend on any kinematic invariant

second integral to realize that it does not depend on any kinematic invariant and therefore vanishes in dimensional regularization

$$\frac{\partial}{\partial p^2} \int d^d k \frac{1}{k^2(k-p)^2} = -\frac{1}{2p^2} \int d^d k \left(\frac{1}{k^2(k-p)^2} + \frac{p^2}{k^2(k-p)^4} \right). \quad (3.15)$$

As it was advertised earlier the derivative of our integral is now expressed in terms of integrals in the same topology or its subtopologies. In the next step we use an IBP identity in order to express all integrals back in terms of our master integral. For this example we can actually directly derive the IBP directly from its generating equation (2.15)

$$0 = \int d^d k \frac{\partial}{\partial k_\mu} \frac{k^\mu}{k^2(k-p)^2}, \quad (3.16)$$

where we put the loop momenta k^μ in the numerator. Taking the derivative we find a relation between the bubble with a squared propagator and the scalar bubble

$$0 = \int d^d k \frac{D}{k^2(k-p)^2} - 2 \frac{k^2}{k^4(k-p)^2} - \frac{2k^2 - 2k \cdot p}{k^2(k-p)^4} \quad (3.17)$$

$$= \int d^d k \frac{D-3}{k^2(k-p)^2} + \frac{p^2}{k^2(k-p)^4} \quad (3.18)$$

$$\Rightarrow \int d^d k \frac{1}{k^2(k-p)^4} = -\frac{d-3}{p^2} \int d^d k \frac{1}{k^2(k-p)^2}. \quad (3.19)$$

Going back to equation (3.15) and applying the IBP identity we just derived we are able to find a differential equation for our master integral

$$\frac{\partial}{\partial p^2} \int d^d k \frac{1}{k^2(k-p)^2} = -\frac{1}{2p^2} \int d^d k \left(\frac{1}{k^2(k-p)^2} - \frac{d-3}{k^2(k-p)^4} \right) \quad (3.20)$$

$$= \frac{d-4}{2p^2} \int d^d k \frac{1}{k^2(k-p)^2}. \quad (3.21)$$

In fact for this differential equation we can immediately write down the solution

$$F(\epsilon, p^2) = (p^2)^{-2\epsilon} F(\epsilon, x_0), \quad (3.22)$$

with the dimensional regularization parameter $\epsilon = \frac{4-d}{2}$ and boundary constant $F(\epsilon, x_0)$. We should note that we could have obtained this result directly from power counting the mass dimensions of our integral, since we have only one scale with mass dimension in our problem. Therefore the most difficult part of calculation is actually to determine the boundary constant, which at least in this case has to be provided as an independent input.

3.2. Solution

There are two main strategies to solve the system of coupled first ordered differential equation (3.7). In the first way we make use of the block triangular form of the differential equation

and solve each block individually. As we progress through the blocks we will notice that the integrals, we solved in previous blocks, enter as the inhomogeneous part of the later blocks, which step-by-step increases their complexity. In the second way we first bring our differential equation into a special form, where the dependence on the dimensional regulator ϵ factorizes [77], called the canonical form and then integrate it. In fact here the integration can be performed simply by matrix multiplication, but this comes at the cost that finding such a canonical form can be a formidable task. Let us first discuss how we can solve a differential equation block by block and then later we will elaborate more on the canonical form.

Each topology in our vector of master integrals defines a block in the otherwise already triangular differential equation, therefore our differential equation is already factorized up to blocks of the form,

$$\begin{aligned} \partial_x F_i &= \sum_{j=1}^{i+k} A_{x;i,j} F_j \\ &\vdots \\ \partial_x F_{i+k} &= \sum_{j=1}^{i+k} A_{x;i+k,j} F_j , \end{aligned} \tag{3.23}$$

where k is the size of the block and equivalently the number of master integrals in this topology. Furthermore it is convenient to split the differential equation into the homogeneous part C and the inhomogeneous part D

$$\begin{aligned} \partial_x F_i &= \sum_{j=1}^{i-1} D_{x;i,j} F_j + \sum_{j=i}^{i+k} C_{x;i,j} F_j \\ &\vdots \\ \partial_x F_{i+k} &= \sum_{j=1}^{i-1} D_{x;i+k,j} F_j + \sum_{j=i}^{i+k} C_{x;i+k,j} F_j . \end{aligned} \tag{3.24}$$

Solving such coupled systems is a difficult task, especially since all entries in the homogeneous part C might be non-zero, therefore we will first consider a system with trivial block size $k = 1$ and later discuss strategies for solving systems with non trivial block sizes $k > 1$.

For a trivial block size

$$\partial_x F_i = \sum_{j=1}^{i-1} D_{x;i,j} F_j + C_{x;i,i} F_i , \tag{3.25}$$

we can formally write down the solution to the differential equation as

$$F_i(\epsilon, x) = H(\epsilon, x) \left[1 + \int_{x_0}^x \left(dx \sum_{j=1}^{i-1} \frac{D_{x;i,j} F_j(\epsilon, x)}{H(\epsilon, x)} \right) \right] F_i(\epsilon, x_0) , \tag{3.26}$$

with the integrating factor

$$H(\epsilon, x) = \exp\left(\int_{x_0}^x dx C_{x;i,i}\right), \quad (3.27)$$

which can be obtained by solving the homogeneous part of the differential equation. We should note the formal solution in (3.26) can be interpreted as an kinematical evolution operator, which takes our solution from a boundary point x_0 to some other point x . Especially in the case where our end point $x = x_0$ we see that all integrals vanish and we are only left with our boundary constant $F_i(\epsilon, x_0)$ as we would expect. Let us mention one more time that in the case where we have several dimensionless variables this boundary constant would depend on the remaining variables and could be fixed up to a true constant by sequentially solving the other differential equations.

In the case where we have a non trivial block size $k > 1$ we can not write down a meaningful solution of the form (3.26), because the integrating factor of the solution would involve other integrals from the same block which we consider still unknown to us. Furthermore there is no general algorithm how such a system can be solved at all. However in some cases we can obtain a solution to such coupled system by first transforming the system of k coupled first order differential equations into an equivalent k th order differential equation

$$\begin{aligned} \partial_x F_i &= \sum_{j=1}^{i+k} A_{x;i,j} F_j \\ &\vdots \\ \partial_x F_{i+k} &= \sum_{j=1}^{i+k} A_{x;i+k,j} F_j \end{aligned} \quad \Rightarrow \quad \sum_{j=0}^k \hat{A}_{x;j} \partial_x^j F_i + \sum_{j=1}^{i-1} \hat{A}_{x;j} F_j = 0, \quad (3.28)$$

and then recognizing the higher order differential equation as a differential equation of some well studied function like hyper-geometric functions, which allows us to immediately write down the solution of our integrals in terms of these functions.

Another way of solving such a coupled system is to find a special form, where the system triangularizes in the limit $d \rightarrow 4$ or equivalently $\epsilon \rightarrow 0$. For most systems this can be achieved by finding a suitable rotation of our master integrals build from IBP identities, Lorentz invariance identities and sector symmetries, which is equivalent to considering different sets of master integrals from the same topology. Once such a set is found the non-trivial block decouples into trivial blocks at each order in ϵ . For that reason we can solve each ϵ -order of the integrals just as if they would belong to a trivial block.

3.3. Canonical Form

In this section we take the idea that a system triangularizes in the limit $\epsilon \rightarrow 0$ to the next level. We are going back to our full differential equation and search for a system, where the

dimensional regularization parameter ϵ has completely factorized from our kinematics

$$\partial_x \mathbf{I} = \epsilon A_x \mathbf{I} , \quad (3.29)$$

where the matrix A_x is now independent of ϵ . Let us delay the discussion on how such a canonical form can be found to chapter 5 and first investigate the advantage of having a system in this form.

For most applications we are actually interested in the Laurent series around $\epsilon = 0$ of our master integrals

$$\mathbf{F} = \sum_k \mathbf{F}^{(k)} \epsilon^k . \quad (3.30)$$

Expanding a general differential equation in ϵ , we obtain separate differential equations for each coefficient of the Laurent series e.g. at order k we have

$$\partial_x \mathbf{F}^{(k)} = \sum_j A_{x,k-j} \mathbf{F}^{(j)} , \quad (3.31)$$

where $A_{x,k-j}$ is the $(k-j)$ th coefficient of the Laurent series in ϵ of the matrix A_x . Even though the expanded differential equations are simpler, since we traded the dependence on ϵ for a larger set of easier differential equations, their solution is still highly non trivial. Especially we might still encounter non-trivial unfactorized blocks. If we consider the Laurent expansion around $\epsilon = 0$ for our canonical form instead

$$\partial_x \mathbf{I}^{(k)} = A_x \mathbf{I}^{(k-1)} , \quad (3.32)$$

we immediately notice that the solution of the k th order only depends on integrals of order $k-1$. For convenience in the following discussion let us multiply all integrals by an appropriate factor of ϵ in order to turn their Laurent expansion into a Taylor expansion. Then the zeroth order differential equation is particular simple since all integrals are now finite in ϵ

$$\partial_x \mathbf{I}^{(0)} = 0 , \quad (3.33)$$

which implies that the zeroth order of all our integrals is a constant.

In addition for a canonical differential equation it is convenient to employ a different strategy for solution of multi scale problems. Instead of considering the differential equations sequentially we will combine them in a total differential

$$d\mathbf{I} = \epsilon dA \mathbf{I} , \quad (3.34)$$

which would have been also possible for a non-canonical differential equation, but only in this form we avoid the resummation of logarithms into rational factors. Empirically the matrix dA is composed of constant rational matrices multiplied by a $d\log(\eta)$, where the latter encode all the kinematic information. Therefore the arguments η allow us to identify

all physical and unphysical thresholds and their set defines the so-called alphabet of our process. Formally the solution to such a $d\log$ form is given by Chen's iterated integrals

$$I(\epsilon, \vec{x}) = \left(\mathbb{1} + \epsilon \int_{\gamma} dA + \epsilon^2 \int_{\gamma} dA dA + \dots \right) I(\epsilon, \vec{x}_0) , \quad (3.35)$$

which we will further discuss in chapter 6. For now let us just notice that the solution is expressed as iterated path integrals over different $d\log$ s and their coefficients can be simply obtained by matrix multiplication. Also at each order in ϵ we have the same number of integrations over a $d\log$ or in other words all terms at each order in ϵ have the same weight, which is the defining criteria for a function of uniform weight. Furthermore all integrals in the canonical form trivially satisfy a conjecture made about all Feynman integrals.

Conjecture 3.3.1 *In $d = 4 - 2\epsilon$ dimensions, the Laurent coefficient of ϵ^k of an L -loop amplitude contains at most terms of weight $2L + k$*

In fact the integrals in this form will have only terms of weight $2L + k$ in the ϵ^k coefficient. We should also note that our solution is free of rational factors in the kinematical invariants, since all kinematical information is encoded in the arguments of the $d\log$ s. This will be helpful when we compute the boundary conditions of our integrals, since it separates possible logarithmic divergences from power divergences.

3.4. Boundary Conditions

The solution of a differential equation describes the kinematical evolution from a boundary point x_0 to the point of interest x . In this section we will present two strategies how we can determine this boundary point. Firstly we can try to compute the integral in a specific kinematical limit by either direct integration or by using an asymptotic expansion [112–114]. Secondly the differential equation itself can at least minimize the number of boundary constants that have to be provided. For that we need to investigate the divergent behavior of our differential equation. Already the non-canonical form allows us to identify the physical and unphysical thresholds of our solution as poles in the differential equation. We can remove the unphysical poles from our differential equation and therefore the corresponding thresholds from our solution by an appropriate choice of boundary constants. In particular we can derive a relation between different integrals by demanding that the coefficients of the corresponding poles in the differential equation vanish, whenever the pole diverges. After solving the differential equations we can demand that our solutions satisfy these all order relations, which will imply relations between the boundary constants of the involved integrals. These relations may greatly reduce the number of boundary constants that have to otherwise be provided independently. We will illustrate this procedure on a small toy example.

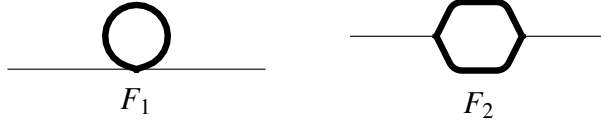


Figure 3.2.: The masters F_1 and F_2 are shown, where the thick line represent massive propagators.

The massive one-loop Bubble

Let us consider the differential equation of the massive one-loop bubble with an off-shell leg $p^2 \neq 0$

$$\partial_{p^2} F_2 = -\frac{d-2}{p^2(p^2+4m^2)} F_1 + \frac{1}{2} \left(\frac{d-3}{p^2+4m^2} - \frac{1}{p^2} \right) F_2, \quad (3.36)$$

where the massive tadpole F_1 and the massive bubble F_2 , which are shown in figure 3.2, are given by

$$F_1 = \int d^d k \frac{1}{k^2 - m^2} F_2 = \int d^d k \frac{1}{(k^2 - m^2)((k-p)^2 - m^2)}. \quad (3.37)$$

For both the tadpole and the bubble the divergence at $p^2 \rightarrow 0$ is unphysical, due to the massive propagators. Therefore we can multiply both sides of the differential equation by p^2

$$p^2 \partial_{p^2} F_2 = -\frac{d-2}{(p^2+4m^2)} F_1 + \frac{1}{2} \left(\frac{(d-3)p^2}{p^2+4m^2} - 1 \right) F_2, \quad (3.38)$$

and then take the limit $p^2 \rightarrow 0$

$$\lim_{p^2 \rightarrow 0} p^2 \partial_{p^2} F_2 = \lim_{p^2 \rightarrow 0} \left[-\frac{d-2}{(p^2+4m^2)} F_1 + \frac{1}{2} \left(\frac{(d-3)p^2}{p^2+4m^2} - 1 \right) F_2 \right] \quad (3.39)$$

$$\Rightarrow 0 = -\frac{d-2}{4m^2} \lim_{p^2 \rightarrow 0} F_1 - \frac{1}{2} \lim_{p^2 \rightarrow 0} F_2 \quad (3.40)$$

$$\Rightarrow \lim_{p^2 \rightarrow 0} F_2 = -\frac{d-2}{2m^2} \lim_{p^2 \rightarrow 0} F_1, \quad (3.41)$$

where in the second line we used that the integrals F_1 and F_2 and their derivatives are finite in the limit $p^2 \rightarrow 0$. Together with the solution of our differential equation, (3.41) connects the boundary constant of the massive bubble to the one of the tadpole, which can be easily obtained by direct integration.

Boundary Conditions for a Canonical Form

The procedure we described for a non canonical system becomes even easier if we were able to obtain a canonical differential equation

$$dI = \epsilon dA I , \quad (3.42)$$

where dA is a $d\log$ -form with

$$dA = \sum_{i=1}^n \mathbb{M}_i d\log \eta_i . \quad (3.43)$$

Here we can obtain the all order relation for the finiteness of our solution at the unphysical threshold η_i by demanding that the product of the corresponding coefficient matrix times the vector of master integrals vanishes in the limit where the unphysical threshold diverges

$$\lim_{\eta_i \rightarrow 0} \mathbb{M}_i I = 0 . \quad (3.44)$$

We can prove that this equation implies the finiteness of our solution at the unphysical threshold η_i by induction.

Before we start the prove let us rewrite the formal solution to our canonical differential equation (3.35) in a form that will be more suitable for the prove. If we are just interested in the k th coefficient of the Taylor expansion we can easily write down its solution as

$$I^{(k)}(x) = \int_{\gamma} dA \dots dA = \int_{\gamma} dA I^{(k-1)} , \quad (3.45)$$

where we recognized the first $k - 1$ integration as the $k - 1$ Taylor coefficient $I^{(k-1)}$. With this relation we are now ready to prove that equation (3.44) implies the finiteness of the solution at the unphysical threshold.

At order zero our solution is simply given by a constant and therefore finite under any limit. The first non-trivial step is at the first order in ϵ , where our solution is given by

$$I^{(1)}(x) = \int_{\gamma} dA I^{(0)} . \quad (3.46)$$

Taking the limit $\eta_i \rightarrow 0$ introduces a possible end point singularity of our path integral

$$\lim_{\eta_i \rightarrow 0} I^{(1)}(x) = \lim_{\eta_i \rightarrow 0} \int_{\gamma} d\log(\eta_i) \mathbb{M}_i I^{(0)} + \text{finite} , \quad (3.47)$$

where all other terms were finite because both the arguments of the $d\log$ s and the zeroth order of our integrals $I^{(0)}$ are finite. The only way for this divergence to be absent and therefore for our integrals to be finite is if its coefficient vanishes in the limit $\lim_{\eta_i \rightarrow 0} \mathbb{M}_i I^{(0)} = 0$, which is exactly the ϵ^0 term of equation (3.44).

Assuming that $I^{(k-1)}$ is finite we can prove our inductive step by considering the solution at k th order in ϵ

$$I^{(k)}(x) = \int_{\gamma} dA I^{(k-1)} , \quad (3.48)$$

and taking the limit where the unphysical threshold diverges $\eta_i \rightarrow 0$

$$\lim_{\eta_i \rightarrow 0} I^{(k)}(x) = \lim_{\eta_i \rightarrow 0} \int_{\gamma} d\log(\eta_i) \mathbb{M}_i I^{(k-1)} + \text{finite} . \quad (3.49)$$

We see that our solution is only finite if the coefficient of the divergence vanishes in the limit $\lim_{\eta_i \rightarrow 0} \mathbb{M}_i I^{(k-1)} = 0$.

By this inductive prove we see that each order in ϵ our condition has to be satisfied and therefore we can conclude that the condition has to be correct also for the whole Taylor series.

In addition to this simpler derivation of the all order relations also solving them becomes easier, since first of all at each order in ϵ we only deal with functions of uniform weight and second of all we only encounter log divergences, whereas in general a Feynman integral can also have power divergences. In fact we can obtain another set of all order relations if we investigate the canonical master integral further. A canonical master integral is typically given as a linear combination of different integrals each with a kinematical prefactor. If there is a limit, where all the kinematical prefactors vanish, while the integrals remain finite, also our canonical master integral will vanish in this limit. This provides us with an easy all order relation, which can be use to fix the boundary of our canonical master integral.

The Magnus Method for Differential Equations

The Magnus theorem was first described in a paper by Willhelm Magnus [115] in 1954 and generalizes the exponential solution of a homogeneous differential equation to systems of coupled homogeneous differential equations. The work by Magnus was stimulated by developments in theoretical physics at the time, especially by the theory of linear operators in quantum mechanics [116] and by work of Feynmann in quantum electrodynamics [117]. This shows that from the very beginning the work by Magnus was closely related to physics and it has still impact today.

Let us consider the initial value problem related to a linear differential equation

$$\partial_x Y(x) = A(x)Y(x) , \quad Y(x_0) = Y_0 , \quad (4.1)$$

depending on the form of $Y(x)$ and $A(x)$ we can distinguish four different cases of increasing complexity:

- a) $Y(x) : \mathbb{R} \rightarrow \mathbb{C}$ and $A(x) : \mathbb{R} \rightarrow \mathbb{C}$

In this case both $Y(x)$ and $A(x)$ are complex scalar functions, therefore we have an uncoupled first order differential equation, which can be solved by quadrature

$$Y(x) = \exp\left(\int_{x_0}^x d\tau A(\tau)\right) Y_0 . \quad (4.2)$$

- b) $Y(x) : \mathbb{R} \rightarrow \mathbb{C}^n$ and $A(x) : \mathbb{R} \rightarrow \mathbb{M}_n(\mathbb{C})$

Now $Y(x)$ is a complex vector valued function and $A(x)$ is a $n \times n$ matrix of complex functions resulting in a coupled system of differential equations. Only in very special cases, where the commutator $[A(\tau_1), A(\tau_2)]$ vanishes, are we still able to solve the system by quadrature and obtain a solution of the form (4.2). In the more general cases we will get corrections to the exponential, which are described by the Magnus expansion.

- c) $Y(x) : \mathbb{R} \rightarrow \mathbb{M}_n(\mathbb{C})$ and $A(x) : \mathbb{R} \rightarrow \mathbb{M}_n(\mathbb{C})$

Here both $Y(x)$ and $A(x)$ are complex matrix valued functions, but the discussion of the previous case applies as well and in fact both cases can be solved with the Magnus exponential. One example of such a case is when $Y(x)$ is an element of a Lie group and $A(x)$ is its corresponding Lie algebra, which underlines the importance for physics applications.

- d) $Y(x)$ and $A(x)$ are operators

In the most general case both $Y(x)$ and $A(x)$ are operators which map one vector space into another without any restrictions. One example for such a differential equation is the time dependent Schrödinger equation.

For our purposes we will consider cases b) and c), which can be treated equivalently. The basic idea is to write down a exponential solution to our differential equation, which is similar to (4.2), but in general we get corrections to the exponential, because the matrices $A(\tau)$ may be non-commuting. These corrections are given by the Magnus expansion and come in the form of commutators between the matrices $A(\tau)$. Especially in the case, where we have an underlying Lie algebra, this is advantageous, since the Lie algebra structure is preserved at each order of the Magnus expansion.

4.1. The Magnus Theorem

Consider a generic linear matrix differential equation [118]

$$\partial_x Y(x) = A(x)Y(x) , \quad Y(x_0) = Y_0 . \quad (4.3)$$

If $A(x)$ commutes with its integral $\int_{x_0}^x d\tau A(\tau)$, *e.g.* in the scalar case, the solution can be written as

$$Y(x) = e^{\int_{x_0}^x d\tau A(\tau)} Y_0 . \quad (4.4)$$

In the general non-commutative case, one can use the *Magnus theorem* [115] to write the solution as,

$$Y(x) = e^{\Omega(x,x_0)} Y(x_0) \equiv e^{\Omega(x)} Y_0 , \quad (4.5)$$

where $\Omega(x)$ is written as a series expansion, called *Magnus expansion*,

$$\Omega(x) = \sum_{n=1}^{\infty} \Omega_n(x) . \quad (4.6)$$

The first three terms of the expansion (4.6) read as follows:

$$\begin{aligned}
\Omega_1(x) &= \int_{x_0}^x d\tau_1 A(\tau_1) , \\
\Omega_2(x) &= \frac{1}{2} \int_{x_0}^x d\tau_1 \int_{x_0}^{\tau_1} d\tau_2 [A(\tau_1), A(\tau_2)] , \\
\Omega_3(x) &= \frac{1}{6} \int_{x_0}^x d\tau_1 \int_{x_0}^{\tau_1} d\tau_2 \int_{x_0}^{\tau_2} d\tau_3 [A(\tau_1), [A(\tau_2), A(\tau_3)]] + [A(\tau_3), [A(\tau_2), A(\tau_1)]] . \quad (4.7)
\end{aligned}$$

We remark that if A and its integral commute, the series (4.6) is truncated at the first order, $\Omega = \Omega_1$, and we recover the solution (4.4). As a notational aside, in the following we will use the symbol $\Omega[A](x)$ to denote the Magnus expansion obtained using A as kernel.

4.2. Proof of the Magnus Theorem

We closely follow the discussion of ref. [119]. Given an operator, Ω , we define the derivative of Ω^k w.r.t. Ω by its action on a generic operator H :

$$\left(\frac{d}{d\Omega} \Omega^k \right) H \equiv H\Omega^{k-1} + \Omega H\Omega^{k-2} + \dots + \Omega^{k-1} H . \quad (4.8)$$

This definition guarantees that, when $\Omega = \Omega(x)$ and $H = \partial_x \Omega$,

$$\partial_x \Omega^k = \left(\frac{d}{d\Omega} \Omega^k \right) \partial_x \Omega . \quad (4.9)$$

The definition (4.8) reduces to $kH\Omega^{k-1}$ when $[\Omega, H] = 0$, therefore it is natural to write it as $kH\Omega^{k-1}$ plus correction terms involving (iterated) commutators. Using the adjoint operator

$$\text{ad}_\Omega(H) \equiv [\Omega, H] , \quad (4.10)$$

and its iterated application ad_Ω^i we obtain

$$\begin{aligned}
\left(\frac{d}{d\Omega} \Omega^2 \right) H &= H\Omega + \Omega H = 2H\Omega + \text{ad}_\Omega(H) \\
\left(\frac{d}{d\Omega} \Omega^3 \right) H &= H\Omega^2 + \Omega H\Omega + \Omega^2 H = 3H\Omega^2 + 3[\Omega, H]\Omega + \text{ad}_\Omega^2(H) \\
&\vdots \\
\left(\frac{d}{d\Omega} \Omega^k \right) H &= \sum_{i=0}^{k-1} \binom{k}{i+1} \text{ad}_\Omega^i(H) \Omega^{k-i-1} . \quad (4.11)
\end{aligned}$$

The last equation can be obtained by induction using the relation

$$\Omega \text{ad}_\Omega^i(H) = \text{ad}_\Omega^i(H) \Omega + \text{ad}_\Omega^{i+1}(H) \quad (4.12)$$

The exponential of a matrix Ω is defined via a series expansion:

$$e^\Omega \equiv \sum_{k \geq 0} \frac{1}{k!} \Omega^k . \quad (4.13)$$

The derivative and the inverse of the exponential of a matrix can be straightforwardly obtained by using the previous results:

Lemma 4.2.1 (Derivative of the exponential) *The derivative of the matrix exponential can be derived from its action on a generic operator H and reads as follows*

$$\left(\frac{d}{d\Omega} e^\Omega \right) H = d \exp_\Omega(H) e^\Omega , \quad d \exp_\Omega(H) \equiv \sum_{k \geq 0} \frac{1}{(k+1)!} \text{ad}_\Omega^k(H) . \quad (4.14)$$

Lemma 4.2.2 (Inverse of the exponential) *If the eigenvalues of ad_Ω are different from $2\ell\pi i$ with $\ell \in \{\pm 1, \pm 2, \dots\}$, then $d \exp_\Omega$ is invertible, and*

$$d \exp_\Omega^{-1}(H) = \sum_{k \geq 0} \frac{\beta_k}{k!} \text{ad}_\Omega^k(H) , \quad (4.15)$$

where β_k are the Bernoulli numbers, whose generating function is

$$\frac{t}{e^t - 1} = \sum_{k=0}^{\infty} \frac{\beta_k}{k!} t^k . \quad (4.16)$$

We have now all the ingredients to prove the following [115]

Theorem 4.2.1 (Magnus) *The solution of a generic linear matrix differential equation*

$$\partial_x Y = A(x)Y , \quad Y(x_0) = Y_0 \quad (4.17)$$

can be written as

$$Y(x) = e^{\Omega(x, x_0)} Y(x_0) \equiv e^{\Omega(x)} Y_0 \quad (4.18)$$

where $\Omega(x)$ can be computed by solving the differential equation,

$$\partial_x \Omega = d \exp_\Omega^{-1} (A(x)) , \quad \Omega(x_0) = 0 . \quad (4.19)$$

Proof Let us consider the derivative of (4.18). Using the definition (4.13) and the property (4.9) we have

$$\partial_x Y = \left(\frac{d}{d\Omega} e^\Omega \right) \partial_x \Omega Y_0 = d \exp_\Omega(\partial_x \Omega) e^\Omega Y_0 = d \exp_\Omega(\partial_x \Omega) Y(x).$$

The *r.h.s.* is equal to $A(x)Y(x)$ when

$$d \exp_\Omega(\partial_x \Omega) = A(x). \quad (4.20)$$

The relation (4.19) is thus proven by applying the operator $d \exp_\Omega^{-1}$ to both sides of (4.20). \square

The differential equation for Ω explicitly reads,

$$\partial_x \Omega = A(x) - \frac{1}{2}[\Omega, A(x)] + \frac{1}{12}[\Omega, [\Omega, A(x)]] + \dots, \quad (4.21)$$

and the solution can be written as a series, called *Magnus expansion*,

$$\Omega = \sum_{n=1}^{\infty} \Omega_n(x), \quad \Omega_n(x) = \sum_{j=1}^{n-1} \frac{\beta_j}{j!} \int_{x_0}^x S_n^{(j)}(\tau) d\tau. \quad (4.22)$$

The coefficients β_j are the Bernoulli numbers while the integrands $S_n^{(j)}$ can be computed recursively,

$$\begin{aligned} S_n^{(1)} &= [\Omega_{n-1}, A], \\ S_n^{(j)} &= \sum_{m=j-1}^{n-j} [\Omega_m, S_{n-m}^{(j-1)}] \quad 2 \leq j \leq n-2, \\ S_n^{(n-1)} &= [\Omega_1, A]. \end{aligned} \quad (4.23)$$

4.3. Graphical Representation of the Magnus Expansion

An alternative way of representing the Magnus Expansion is given by full rooted binary trees as it was worked out in [120]. A full rooted binary tree starts out from a root vertex, which has either zero or two children. In the latter case each of the children are vertices themselves, which again may have zero or two children. A good example of such a tree is the ancestry chart of a person. In fact this is even a special so-called perfect rooted binary tree, since each person has exactly two parents.

Let us now formulate the above rules within a mathematical framework. First we define a single rooted tree with one vertex

$$\mathcal{T}_0 = \{ \bullet \} \quad (4.24)$$

and then all other trees are defined recursively with

$$\mathcal{T}_m = \left\{ \begin{array}{c} \tau_1 \\ \diagdown \quad \diagup \\ \tau_2 \end{array} : \tau_1 \in \mathcal{T}_{k_1}, \tau_2 \in \mathcal{T}_{k_2}, k_1 + k_2 = m - 1 \right\}. \quad (4.25)$$

These trees can be mapped to the corresponding terms in the Magnus expansion through a simple set of rules. The single rooted tree with one vertex can be identified with our matrix $A(\tau)$

$$\bullet \rightsquigarrow A(\tau) \quad (4.26)$$

and a vertex τ with two children τ_1 and τ_2 defines a commutator of the form

$$H_\tau(x) = \left[\int_{x_0}^x H_{\tau_1}(\xi) d\xi, H_{\tau_2}(x) \right] \quad \text{with} \quad \tau = \begin{array}{c} \tau_1 \\ \diagdown \quad \diagup \\ \tau_2 \end{array}, \quad (4.27)$$

where $H_{\tau_i}(\xi)$ corresponds to an expression stemming from another tree τ_i , e.g. in the case where $\tau_i \in \mathcal{T}_0$ we have $H_{\tau_i}(\xi) = A(\xi)$. With the help of these rules we can map each binary rooted tree τ into an expression involving iterated integrals and their commutators, which in return allows us to map the Magnus expansion to a sum of binary trees

$$\Omega(x) = \sum_{m=0}^{\infty} \sum_{\tau \in \mathcal{T}_m} \alpha(\tau) \int_{x_0}^x H_\tau(\xi) d\xi, \quad (4.28)$$

with the numerical factor $\alpha(\bullet) = 1$ and, in general

$$\alpha(\tau) = \frac{\beta_s}{s!} \prod_{l=1}^s \alpha(\tau_l). \quad (4.29)$$

Here β_s are the Bernoulli numbers and s is as well as $\alpha(\tau_l)$ with $l = 1 \dots s$ best defined graphically as

$$\tau = \begin{array}{c} \tau_s \\ \diagdown \quad \diagup \\ \tau_3 \\ \diagdown \quad \diagup \\ \tau_2 \\ \diagdown \quad \diagup \\ \tau_1 \end{array}, \quad (4.30)$$

where each τ_i might be a rooted tree itself.

From equation (4.28) we can see that the first orders of the Magnus expansion are given by sums over the sets of rooted graphs \mathcal{T}_m . In order to write down the Magnus expansion in terms of binary trees let us first examine the first three orders for these sets. The zeroth order set \mathcal{T}_0 was already defined in (4.24) and has only one element

$$\mathcal{T}_0 = \{ \bullet \}. \quad (4.31)$$

For the first order set \mathcal{T}_1 we will use the recursive definition (4.25) and the fact that both children have to be zeroth order sets $k_1 = k_2 = 0$

$$\tau_1 = \bullet, \quad \tau_2 = \bullet, \quad \Rightarrow \quad \tau = \begin{array}{c} \bullet \\ | \\ \diagup \quad \diagdown \\ \bullet \quad \bullet \end{array} \quad \alpha(\tau) = -\frac{1}{2}, \quad (4.32)$$

where we calculated the numerical factor $\alpha(\tau)$ according to formula (4.29) by using that the graph τ has $s = 1$.

For the second order either k_1 or k_2 have to be a zeroth order set, while the other one is a first order set.

$$\begin{array}{l} \tau_1 = \bullet, \quad \tau_2 = \begin{array}{c} \bullet \\ | \\ \diagup \quad \diagdown \\ \bullet \quad \bullet \end{array} \quad \Rightarrow \quad \tau = \begin{array}{c} \bullet \\ | \\ \diagup \quad \diagdown \\ \bullet \quad \bullet \\ | \quad | \\ \bullet \quad \bullet \end{array}, \quad \alpha(\tau) = \frac{1}{12}, \\ \tau_1 = \begin{array}{c} \bullet \\ | \\ \diagup \quad \diagdown \\ \bullet \quad \bullet \end{array}, \quad \tau_2 = \bullet \quad \Rightarrow \quad \tau = \begin{array}{c} \bullet \\ | \\ \diagup \quad \diagdown \\ \bullet \quad \bullet \\ | \quad | \\ \bullet \quad \bullet \end{array} \quad \alpha(\tau) = \frac{1}{4}. \end{array} \quad (4.33)$$

The factor $\alpha(\tau)$ for the first graph is calculated with

$$\alpha(\tau) = \frac{\beta_2}{2} \prod_{l=1}^2 \alpha(\tau_l) = \frac{1}{12} \alpha(\bullet) \alpha(\bullet) = \frac{1}{12} \quad (4.34)$$

and for the second graph we have

$$\alpha(\tau) = \frac{\beta_1}{1} \prod_{l=1}^1 \alpha(\tau_l) = -\frac{1}{2} \alpha \left(\begin{array}{c} \bullet \\ | \\ \diagup \quad \diagdown \\ \bullet \quad \bullet \end{array} \right) = \frac{1}{4}. \quad (4.35)$$

Collecting all the information above we can write out the first terms in the Magnus expansion in terms of our binary trees

$$\Omega(t) = \begin{array}{c} \bullet \\ | \\ \bullet \end{array} - \frac{1}{2} \begin{array}{c} \bullet \\ | \\ \diagup \quad \diagdown \\ \bullet \quad \bullet \\ | \\ \bullet \end{array} + \frac{1}{4} \begin{array}{c} \bullet \\ | \\ \diagup \quad \diagdown \\ \bullet \quad \bullet \\ | \quad | \\ \bullet \quad \bullet \end{array} + \frac{1}{12} \begin{array}{c} \bullet \\ | \\ \diagup \quad \diagdown \\ \bullet \quad \bullet \\ | \quad | \\ \bullet \quad \bullet \end{array} + \dots \quad (4.36)$$

As a last little exercise let us show that this expansion is indeed equivalent to the expressions we wrote down in (4.7). The first term is easily transformed

$$\begin{array}{c} \bullet \\ | \\ \bullet \end{array} = \int_{x_0}^x d\xi H_{\bullet}(\xi) = \int_{x_0}^x d\xi A(\xi) = \Omega_1(x). \quad (4.37)$$

For the second term we have to apply our recursion relation for the first time

$$-\frac{1}{2} \begin{array}{c} \bullet \\ | \\ \diagup \quad \diagdown \\ \bullet \quad \bullet \end{array} = -\frac{1}{2} \int_{x_0}^x d\xi_1 H_{\vee}(\xi_1) \quad (4.38)$$

$$= -\frac{1}{2} \int_{x_0}^x d\xi_1 \left[\int_{x_0}^{\xi_1} d\xi_2 H_{\bullet}(\xi_2), H_{\bullet}(\xi_1) \right] \quad (4.39)$$

$$= -\frac{1}{2} \int_{x_0}^x d\xi_1 \left[\int_{x_0}^{\xi_1} d\xi_2 A(\xi_2), A(\xi_1) \right] \quad (4.40)$$

$$= \frac{1}{2} \int_{x_0}^x d\xi_1 \int_{x_0}^{\xi_1} d\xi_2 [A(\xi_1), A(\xi_2)] \quad (4.41)$$

$$= \Omega_2(x), \quad (4.42)$$

The third term

$$\frac{1}{4} \begin{array}{c} \bullet \\ | \\ \diagup \quad \diagdown \\ \bullet \quad \bullet \\ | \\ \bullet \end{array} = \frac{1}{4} \int_{x_0}^x d\xi_1 \int_{x_0}^x d\xi_2 [H_{\vee}(\xi_2), H_{\bullet}(\xi_1)] \quad (4.43)$$

$$= \frac{1}{4} \int_{x_0}^x d\xi_1 \int_{x_0}^{\xi_1} d\xi_2 \int_{x_0}^{\xi_2} d\xi_3 [[A(\xi_3), A(\xi_2)], A(\xi_1)], \quad (4.44)$$

together with the fourth term

$$\frac{1}{12} \begin{array}{c} \bullet \\ | \\ \diagup \quad \diagdown \\ \bullet \quad \bullet \\ | \\ \bullet \end{array} = \frac{1}{12} \int_{x_0}^x d\xi_1 \int_{x_0}^{\xi_1} d\xi_2 [H_{\bullet}(\xi_2), H_{\vee}(\xi_1)] \quad (4.45)$$

$$= \frac{1}{12} \int_{x_0}^x d\xi_1 \int_{x_0}^{\xi_1} d\xi_2 \int_{x_0}^{\xi_1} d\xi_3 [A(\xi_2), [A(\xi_3), A(\xi_1)]] , \quad (4.46)$$

can be rewritten as

$$\frac{1}{4} \begin{array}{c} \bullet \\ | \\ \diagup \quad \diagdown \\ \bullet \quad \bullet \\ | \\ \bullet \end{array} + \frac{1}{12} \begin{array}{c} \bullet \\ | \\ \diagup \quad \diagdown \\ \bullet \quad \bullet \\ | \\ \bullet \end{array} = \frac{1}{4} \int_{x_0}^x d\xi_1 \int_{x_0}^{\xi_1} d\xi_2 \int_{x_0}^{\xi_2} d\xi_3 [[A(\xi_3), A(\xi_2)], A(\xi_1)] \quad (4.47)$$

$$+ \frac{1}{12} \int_{x_0}^x d\xi_1 \int_{x_0}^{\xi_1} d\xi_2 \int_{x_0}^{\xi_1} d\xi_3 [A(\xi_2), [A(\xi_3), A(\xi_1)]]$$

$$= \frac{1}{6} \int_{x_0}^t d\xi_1 \int_{x_0}^{\xi_1} d\xi_2 \int_{x_0}^{\xi_2} d\xi_3 [A(\xi_1), [A(\xi_2), A(\xi_3)]] + [A(\xi_3), [A(\xi_2), A(\xi_1)]] , \quad (4.48)$$

where in the last line we used the formula

$$\int_{x_0}^x d\xi_1 \int_{x_0}^{\xi_1} d\xi_2 f(\xi_1, \xi_2) = \int_{x_0}^x d\xi_2 \int_{x_0}^x d\xi_1 f(\xi_1, \xi_2) - \int_{x_0}^x d\xi_2 \int_{x_0}^{\xi_2} d\xi_1 f(\xi_1, \xi_2) , \quad (4.49)$$

to rewrite the commutators in a more symmetric way.

Even though, as we have just shown, the graph approach and the recursion relation in (4.23) are both valid ways to generate the Magnus expansion the latter seems to be more efficient in the generation of high order terms. This can be explained by two reasons. Firstly the number of terms, which is needed to generate a higher order term in the expansions is very large and secondly the most of these graphs are redundant, calling for a careful graph theoretical analysis.

4.4. Magnus and Dyson Series Expansion

The Magnus series is related to the Dyson series [118], and their connection can be obtained starting from the Dyson expansion of the solution of the system (4.3),

$$Y(x) = Y_0 + \sum_{n=1}^{\infty} Y_n(x) , \quad Y_n(x) \equiv \int_{x_0}^x d\tau_1 \dots \int_{x_0}^{\tau_{n-1}} d\tau_n A(\tau_1)A(\tau_2) \cdots A(\tau_n) , \quad (4.50)$$

in terms of the *time-ordered* integrals Y_n . Comparing Eq. (4.5) and (4.50) we have

$$\sum_{j=1}^{\infty} \Omega_j(x) = \log \left(Y_0 + \sum_{n=1}^{\infty} Y_n(x) \right) , \quad (4.51)$$

and the following relations

$$\begin{aligned} Y_1 &= \Omega_1 , \\ Y_2 &= \Omega_2 + \frac{1}{2!} \Omega_1^2 , \\ Y_3 &= \Omega_3 + \frac{1}{2!} (\Omega_1 \Omega_2 + \Omega_2 \Omega_1) + \frac{1}{3!} \Omega_1^3 , \\ &\vdots \\ Y_n &= \Omega_n + \sum_{j=2}^n \frac{1}{j} Q_n^{(j)} . \end{aligned} \quad (4.52)$$

The matrices $Q_n^{(j)}$ are defined as

$$Q_n^{(j)} = \sum_{m=1}^{n-j+1} Q_m^{(1)} Q_{n-m}^{(j-1)} , \quad Q_n^{(1)} \equiv \Omega_n , \quad Q_n^{(n)} \equiv \Omega_1^n . \quad (4.53)$$

Similarly we can define the terms in our Magnus expansion in terms of coefficients of the Dyson series

$$\begin{aligned}\Omega_1 &= Y_1 , \\ \Omega_2 &= Y_2 - \frac{1}{2}Y_1^2 , \\ \Omega_3 &= Y_3 - \frac{1}{2}(Y_1Y_2 + Y_2Y_1) + \frac{1}{3}Y_1^3 .\end{aligned}\tag{4.54}$$

In the following chapter, we will use both the Magnus and the Dyson series in order to formulate an efficient algorithm to bring a differential equation into the canonical form.

Differential Equations in Canonical Form

For any given scattering process the set of MI's is not unique, and, in practice, their choice is rather arbitrary. Usually MI's are identified after applying the Laporta reduction algorithm [69]. Afterward, convenient manipulations of the basis of MI's may be performed.

Proper choices of MI's can simplify the form of the systems of differential equations and, hence, of their solution, although general criteria for determining such optimal sets are not available. An important step in this direction has been taken in Ref. [77], where Henn proposes to solve the systems of DE's for MI's with algebraic methods. The key observation is that a *good* choice of MI's allows one to cast the system of DE's in a *canonical form*, where the dependence on ϵ , is factorized from the kinematic. The integration of a system in canonical form trivializes and the analytic properties of its general solution are manifestly inherited from the matrix associated to the system, which is the kernel of the representation of the solutions in terms of repeated integrations.

As pointed out in [77], finding an algorithmic procedure which, starting from a generic set of MI's, leads to a set MI's fulfilling a canonical system of DE's is a formidable task. In practice, the quest for the suitable basis of MI's is determined by qualitative properties required for the solution, such as finiteness in the $\epsilon \rightarrow 0$ limit, and homogeneous transcendentality, which turn into quantitative tools like the unit leading singularity criterion and the *dlog* representation in terms of Feynman parameters [78–80]. Furthermore we can also attempt to find a rotation matrix in the space of master integrals, yielding a canonical form. This rotation matrix can be build through appropriate ansatz, which is based on the polynomial structure of ϵ in the original DE [81]. Especially in the case where we have several master integrals in one topology finding a set of canonical master integrals can be difficult. In such a case the structure of the higher order differential equation can be exploited in order to identify a canonical master integral, independent from the choice of the other master integrals in the same topology [82].

In this chapter we will first discuss pure functions of uniform weight and how we can identify them without deriving the differential equations and then present two algorithms to

transform a differential equation into a canonical form. For the first algorithm we suggest a convenient form of the initial system of MI's, which allows us to find the transformation matrix yielding a canonical system. In particular, we choose a set of MI's obeying to a system of DE's which has a *linear* ϵ -dependence, and we find a transformation which absorbs the $\mathcal{O}(\epsilon^0)$ term and leads to a new system of DE's where the ϵ -dependence is factorized. This transformation is obtained by using Magnus and Dyson series expansions [115, 118, 121]. The procedure we propose can be generalized to the case of systems that are *polynomial* in ϵ . Nevertheless, for the cases, which have been considered so far [1, 2, 5], we have succeeded to begin from a set of MI's obeying a system that is linear in ϵ .

Second we will consider a system, which depends on one dimensionless variable and has an arbitrary polynomial ϵ -dependence. We will present an algorithm, which is based on the deflation of eigenvalues. First we will deflate the eigenvalues of the higher poles, reducing each pole in our differential equation to a simple pole and second we shift all eigenvalues of the pole matrices to be multiples of ϵ , which then allows us to find the canonical form through a simple similarity transformation.

5.1. Pure Functions of Uniform Weight

Let us recall that the solution to a differential equation in canonical form

$$dI = \epsilon dA I , \tag{5.1}$$

where dA is a $d\log$ -form with

$$dA = \sum_{i=1}^n \mathbb{M}_i d\log \eta_i , \tag{5.2}$$

is given by Chen's iterated integrals of the form

$$I(\epsilon, \vec{x}) = \left(\mathbb{1} + \epsilon \int_{\gamma} dA + \epsilon^2 \int_{\gamma} dA dA + \dots \right) I(\epsilon, \vec{x}_0) . \tag{5.3}$$

Furthermore let us recall the definition of the weight of a function as the number of integrations or equivalently the number of $d\log$ s, which appear under the integral sign. Expanding the matrices dA as $d\log$ s in our formal solution we see that our solutions has the same weight at each order in ϵ . In addition the Chen's iterated integrals are also pure functions in the sense that a derivative strictly lowers their weight by one, which can be easily seen by expanding the differential equation in ϵ

$$\partial_x I^{(k)} = A_x I^{(k-1)} , \tag{5.4}$$

and observing that at each order in ϵ the weight is increased by one. For this reason it is convenient to assign a weight $W(\epsilon) = -1$ to ϵ , such that our sum of Chen's iterated

integrals have a uniform weight of zero. The only term that can spoil this property for the whole solution is the boundary constant $I(\epsilon, \vec{x}_0)$.

The most common constants that appear are $\pi, \zeta(n), \gamma_E, \log(2), \log(3)$, which have the following weight

$$\begin{aligned} \log(-1 + i\delta) = \pi & \Rightarrow W(\pi) = 1, \\ \int_{\gamma} d\log(1-x) \underbrace{d\log(x) \dots d\log(x)}_{(k-1)\text{-times}} = (-1)^k \zeta(k) & \Rightarrow W(\zeta(k)) = k, \\ W(\gamma_E) = 1 & \end{aligned}$$

where the path γ in the last equation goes from $x_0 = 0$ to $x = 1$ and γ_E is the Euler-Mascheroni constant. We should note that the weight of a product of functions is given by the sum of the weights of the factors

$$W(A * B) = W(A) + W(B). \quad (5.5)$$

With these rules in mind we can asses from the explicit expression if a functions is of uniform weight or not. However what we really need to find are criteria, which allow us to asses a function before we even evaluate it. There have been several conjectures, which properties lead to pure functions of uniform weight, which we will discuss in the following.

5.1.1. Unit Leading Singularity and Unitarity Cuts

Conjecture 5.1.1 *Integrals with a constant leading singularity are pure functions [77, 122, 123].*

As an first example let us consider the massless box at one-loop. We can obtain the leading singularity by replacing all four propagators with delta functions, which allow us to trivially perform the integration and our result will only be the Jacobian (see Appendix A for a detailed derivation)

$$\text{Box} = \frac{1}{2} \frac{1}{s t}. \quad (5.6)$$

Therefore multiplying the box by a factor of $s t$ will result in a unit leading singularity, which is conjectured to be a pure function. Indeed when we look at the first orders of the Taylor series around $\epsilon = 0$ we find¹

$$\begin{aligned} \epsilon^2 s t \text{Box} & \\ = 4 - \epsilon \left(2 \log(-s) + 2 \log\left(\frac{t}{s}\right) \right) + \epsilon^2 \left(2 \log(-s)^2 + 2 \log(-s) \log\left(\frac{t}{s}\right) - \pi^2 \right) + \mathcal{O}(\epsilon^3), & \quad (5.7) \end{aligned}$$

¹We normalized the result such that the massless bubble is 1 to all orders in ϵ .

a one-loop integral with five propagators. It can be shown that such an integral is not a function of uniform weight, therefore we expect the non-planar box also to not be a function of uniform weight. But we can choose the numerator of the non-planar box in a way that it will cancel the propagators, which came from the Jacobian of the box cut. This gives us two potential master integral of uniform weight

$$\int d^d k_1 d^d k_2 \frac{(k_1 - p_3)^2}{k_1^2 k_2^2 (k_1 - k_2)^2 (k_1 + p_1)^2 (k_2 - p_3)^2 (k_1 + p_1 + p_2)^2 (k_1 - k_2 - p_4)^2}, \quad (5.16)$$

$$\int d^d k_1 d^d k_2 \frac{(k_1 - p_4)^2}{k_1^2 k_2^2 (k_1 - k_2)^2 (k_1 + p_1)^2 (k_2 - p_3)^2 (k_1 + p_1 + p_2)^2 (k_1 - k_2 - p_4)^2}, \quad (5.17)$$

which together with the correct kinematical prefactor give us two pure functions of uniform weight. This example also illustrates another important point. We are able to reuse the information gained at one-loop for higher loop integrals.

5.1.2. Feynman Parameter Representation

Another way of seeing a priori if an integral is a function of uniform weight is to investigate the Feynman parameter representation of that integral. As an example of how this can be achieved we will consider the one-loop massless vertex with two legs on-shell $p_1^2 = p_2^2 = 0$ and one leg off-shell $p_3^2 = s$. If we express our integral in terms of Feynman parameters and integrate over the loop momentum we find

$$\text{triangle} = \int d^d k \frac{1}{k^2 (k + p_1)^2 (k + p_1 + p_2)^2} \quad (5.18)$$

$$= -\Gamma(1 - \epsilon) \int_0^\infty dz_1 dz_2 dz_3 \delta(1 - z_1 - z_2 - z_3) \frac{(z_1 + z_2 + z_3)^{-1+2\epsilon}}{(-s z_1 z_3)^{1-\epsilon}}. \quad (5.19)$$

The idea is to transform this function into a form, from which we can see that the resulting integral has uniform weight. To do this we first perform the integration over z_3 with the delta function

$$\text{triangle} = -\Gamma(1 - \epsilon) \int_0^1 dz_1 \int_0^{1-z_1} dz_2 \frac{1}{(-s z_1 (1 - z_1 - z_2))^{1-\epsilon}}, \quad (5.20)$$

and then the integration over z_2

$$\text{triangle} = \frac{\Gamma(1 - \epsilon)}{\epsilon s} \int_0^1 dz_1 \frac{1}{z_1 (s z_1 (-1 + z_1))^\epsilon} \quad (5.21)$$

$$= \frac{\Gamma(1 - \epsilon)}{\epsilon s} \int d\log(z_1) \frac{1}{(s z_1 (-1 + z_1))^\epsilon}. \quad (5.22)$$

Expanding the integrand around $\epsilon = 0$ we see that it is a function with uniform weight 0 and therefore our integral will be a function of uniform weight one. In order to make our

integral also a pure function we have to cancel the kinematic prefactor by multiplying the integral by s . Putting everything together we conclude that the integral

$$
(5.23)$$

should be a pure function of uniform weight. In fact we can confirm this statement by using an IBP identity. The triangle graph we have just discussed is actually not a master integral, since it can be connected to the massless bubble

$$
(5.24)$$

which is a pure function of uniform weight (5.13).

Even though the above mentioned ideas are mathematical quite appealing, the described analysis can become quite cumbersome for processes with a lot of master integrals. For that reason an approach, which can be automatized is more desirable. In the following two sections we will describe two algorithms, which take steps in this directions.

5.2. Canonical Systems and Magnus Exponential Matrix

Before we present the algorithm to obtain the canonical form, let us first recall a quantum mechanical example that inspired the study of the Magnus theorem.

5.2.1. Preface: On time-dependent Perturbation Theory

Given an Hamiltonian operator H , we consider the Schrödinger equation ($\partial_t \equiv \partial/\partial t$)

$$i\hbar \partial_t |\Psi(t)\rangle = H(t) |\Psi(t)\rangle. \quad (5.25)$$

Let us assume that H can be split in two terms as

$$H(t) = H_0(t) + \epsilon H_1(t), \quad (5.26)$$

where H_0 is a solvable Hamiltonian and $\epsilon \ll 1$ is a small perturbation parameter. We may move to the *interaction picture* by performing a transformation via a unitary operator B . In this representation any operator A transforms according to

$$A(t) = B(t) A_I(t) B^\dagger(t). \quad (5.27)$$

In the interaction picture one imposes that only H_1 (H_0) enters the time evolution of the states (of the operators), thus B is obtained by imposing

$$i\hbar \partial_t U_I(t) = \epsilon H_{1,I}(t) U_I(t) + \left(H_{0,I}(t) - i\hbar B^\dagger(t) \partial_t B(t) \right) U_I(t) \stackrel{!}{=} \epsilon H_{1,I}(t) U_I(t), \quad (5.28)$$

so that B fulfills

$$i\hbar \partial_t B(t) = H_0(t)B(t) . \quad (5.29)$$

In the interaction picture the Schrödinger equation can be cast in a *canonical form*,

$$i\hbar \partial_t |\Psi_I(t)\rangle = \epsilon H_{1,I}(t) |\Psi_I(t)\rangle , \quad (5.30)$$

where the ϵ -dependence is factorized. If the Hamiltonian H_0 at different times commute, the solution of Eq. (5.29) is

$$B(t) = e^{-\frac{i}{\hbar} \int_{t_0}^t d\tau H_0(\tau)} . \quad (5.31)$$

The important remark in this derivation is that, as a consequence of the linear ϵ -dependence of the original Hamiltonian Eq. (5.26), the states fulfill an equation in a canonical form by means of a transformation matrix B that obeys the differential equation (5.29). This simple quantum mechanical example contains the two main guiding principles for building canonical systems of differential equations for Feynman integrals:

- choose a set of Master Integrals obeying a system of differential equations linear in ϵ ;
- find the transformation matrix by solving a differential equation governed by the constant term.

In this example $H_0(t)$ and $B(t)$ commute. In the case of Feynman integrals, no assumption can be made on the properties of the matrix associated to the systems of differential equations built out of IBP identities. Therefore, in the following, we need to consider the generic case of non-commutative operators.

5.2.2. Changing the Basis of Master Integrals

Let us now come back to our coupled system of first order differential equations

$$\partial_x F = A_x F , \quad (5.32)$$

where F is a vector of master integrals, while x is the set of dimensionless variables depending on kinematic invariants and masses. In general the matrix A_x admits a Laurent expansion in ϵ

$$A_x = \sum_{i=-a}^n A_{x,i} \epsilon^i . \quad (5.33)$$

A general change of basis can be described with the help of a rotation matrix B in the form

$$F = B \mathbf{H} , \quad (5.34)$$

which results in a new differential equation of the form

$$\partial_x \mathbf{H} = \hat{A}_x \mathbf{H} \quad \text{with} \quad (5.35)$$

$$\hat{A}_x = B^{-1} A_x B - B^{-1} \partial_x B . \quad (5.36)$$

Expanding the latter equation in ϵ and demanding that the new differential equation matrix \hat{A} is proportional to ϵ allows us to reformulate the problem of finding a canonical basis in terms of a differential equation for the rotation matrix B

$$\partial_x B = A_x B - \epsilon B \hat{A}_{x,1} . \quad (5.37)$$

Unfortunately solving this differential equation is in general as hard as the initial differential equation for the master integrals.

Nevertheless under the assumption of a differential equation, which linear in ϵ

$$A_x = A_{x,0} + \epsilon A_{x,1}, \quad (5.38)$$

the differential equation for the rotation matrix B simplifies significantly

$$\partial_x B = A_{x,0} B . \quad (5.39)$$

This differential equation now falls into the class of differential equations, which can be solved by the Magnus expansion.

5.2.3. An Algorithm based on the Magnus Expansion

The algorithm we describe in this section works for any number of dimensionless variables, but for convenience we will restrict ourselves to two variables $\vec{x} = \{x_1, x_2\}$, which already exhibits all features of the multi variable case.

Our starting point are the two systems of first order differential equations

$$\partial_{x_1} F = A_{x_1}^{[0]} F \quad (5.40)$$

$$\partial_{x_2} F = A_{x_2}^{[0]} F , \quad (5.41)$$

with each matrix $A_{x_i}^{[1]}$ being linear in ϵ . We will proceed by finding the change of basis for the MI's via the Magnus expansion obtained by using each $A_{x_i,0}^{[1]}$ as kernel.

1. First we decompose $A_{x_1,0}^{[0]}$ in a diagonal term $D_{x_1,0}^{[0]}$ and a off-diagonal one $N_{x_1,0}^{[0]}$,

$$A_{x_1,0}^{[0]} = D_{x_1,0}^{[0]} + N_{x_1,0}^{[0]} , \quad (5.42)$$

and use only the diagonal part for the next basis change,

$$A_{x_i}^{[0]} \rightarrow A_{x_i}^{[1]}, \quad B^{[1]} \equiv e^{\Omega[D_{x_1,0}^{[0]}]} . \quad (5.43)$$

Note that the Magnus expansion stops after the first term, since all diagonal matrices commute.

2. We repeat as before and split $A_{x_2,0}^{[1]}$ into its diagonal and off-diagonal parts,

$$A_{x_2,0}^{[1]} = D_{x_2,0}^{[1]} + N_{x_2,0}^{[1]}, \quad (5.44)$$

and we build the Magnus exponential again using the diagonal part

$$A_{x_i}^{[1]} \rightarrow A_{x_i}^{[2]}, \quad B^{[2]} \equiv e^{\Omega[D_{x_2,0}^{[1]}]}. \quad (5.45)$$

3. Now the matrix $A_{x_1,0}^{[2]}$, has no diagonal term left,

$$A_{x_1,0}^{[2]} = N_{x_1,0}^{[2]}, \quad (5.46)$$

therefore we build the Dyson series using the off-diagonal part $N_{x_1,0}^{[2]}$ as a kernel

$$A_{x_i}^{[2]} \rightarrow A_{x_i}^{[3]}, \quad B^{[3]} \equiv e^{\Omega[N_{x_1,0}^{[2]}]} = \mathbb{1} + \sum_{i=1}^n Y_n(x_1) \quad (5.47)$$

$$\text{with } Y_n(x_1) \equiv \int d\tau_1 \dots \int d\tau_n N_{\tau_1,0}^{[2]} N_{\tau_2,0}^{[2]} \dots N_{\tau_n,0}^{[2]}. \quad (5.48)$$

The sum is guaranteed to stop if the matrix $N_{x_1,0}^{[2]}$ is nilpotent.

4. The matrix $A_{x_2,0}^{[3]}$ has no diagonal term as well,

$$A_{x_2,0}^{[3]} = N_{x_2,0}^{[3]}, \quad (5.49)$$

so we can define the last basis change

$$A_{x_i}^{[3]} \rightarrow A_{x_i}^{[4]}, \quad B^{[4]} \equiv e^{\Omega[N_{x_2,0}^{[3]}]} = \mathbb{1} + \sum_{i=1}^n Y_n(x_2) \quad (5.50)$$

$$\text{with } Y_n(x_2) \equiv \int d\tau_1 \dots \int d\tau_n N_{\tau_1,0}^{[3]} N_{\tau_2,0}^{[3]} \dots N_{\tau_n,0}^{[3]}. \quad (5.51)$$

After the last transformation we observe that

$$A_{x_1,0}^{[4]} = 0 = A_{x_2,0}^{[4]}. \quad (5.52)$$

This means that the basis change which brings us to the canonical form with the matrix B is given by

$$B \equiv B^{[1]} B^{[1]} B^{[2]} B^{[3]} B^{[4]} = e^{\Omega[D_{x_1,0}^{[1]}]} e^{\Omega[D_{x_2,0}^{[1]}]} e^{\Omega[N_{x_1,0}^{[2]}]} e^{\Omega[N_{x_2,0}^{[3]}]}, \quad (5.53)$$

absorbs the constant terms of A_{x_1} and A_{x_2} in the ϵ -linear system (5.41) and transforms it into

$$\partial_{x_1} I = \epsilon \hat{A}_{x_1} I \quad (5.54)$$

$$\partial_{x_2} I = \epsilon \hat{A}_{x_2} I , \quad (5.55)$$

with $I = B^{-1} F$.

Let us remark that the previously described algorithm is equivalent to solving, first, the *homogeneous* system

$$\partial_x F_H = A_{x,0} F_H , \quad (5.56)$$

whose solution reads,

$$F_H(\epsilon, x) = B_0 I(\epsilon, x_0) , \quad (5.57)$$

and, then, to find the solution of the full system by Euler constants' variation. In fact, by promoting $I(\epsilon, x_0)$ to be function of x ,

$$F_H(\epsilon, x) \rightarrow F(\epsilon, x) = B_0 I(\epsilon, x) , \quad (5.58)$$

and by requiring F to be solution of Eq. (5.41), one finds that $I(\epsilon, x)$ obeys the canonical differential equation

$$\partial_x I = \epsilon A_x I . \quad (5.59)$$

Furthermore we should emphasize the fact that the described algorithm can easily be generalized to problems with more than two variables, by simply sequentially transforming all diagonal diagonal parts first and then sequentially transforming all off-diagonal terms.

5.2.4. Extension to Polynomial ϵ Dependence

In the previous discussion we only considered cases, where an initial choice of master integrals F obeyed a system of differential equations linear in ϵ . We cannot be sure that such a choice exists for any scattering process in dimensional regularization. Nevertheless, the use of the Magnus series enables us to generalize our algorithm to the case of systems of differential equations whose matrix is a *polynomial* in ϵ . In fact, let us consider a system of equations where A is of degree κ in ϵ ,

$$\partial_x F = A_x F , \quad A_x \equiv \sum_{k=0}^{\kappa} \epsilon^k A_{x,k} . \quad (5.60)$$

By iterating the algorithm described in the previous section, the solution of the differential equation (5.60) can be expressed in terms of a chain of products of Magnus exponentials,

$$F(\epsilon, x) = B_0(x) B_1(\epsilon, x) \cdots B_\kappa(\epsilon, x) f_\kappa(\epsilon) , \quad B_k(\epsilon, x) \equiv e^{\Omega[\epsilon^k \hat{A}_{x,k}](x, x_0)} , \quad (5.61)$$

where the kernel $\hat{A}_{x,k}$ is defined as

$$\begin{aligned}\hat{A}_{x,k} &= \hat{A}_{x,k}^{(k)}, \\ \hat{A}_{x,k}^{(j)} &= B_{j-1}^{-1} \cdots B_1^{-1} B_0^{-1} A_{x,k} B_0 B_1 \cdots B_{j-1} .\end{aligned}\quad (5.62)$$

It is worth to observe that, within our construction, the solution F is given by repeated transformations. Starting from

$$F(\epsilon, x) = B_0 F^{(0)}(\epsilon, x), \quad (5.63)$$

we iteratively write $F^{(k)}$ as,

$$F^{(k)}(\epsilon, x) = B_{k+1} F^{(k+1)}(\epsilon, x), \quad (0 \leq k \leq \kappa - 1), \quad (5.64)$$

which obeys the system

$$\partial_x F^{(k)} = \epsilon^k \left(\sum_{j=1}^{\kappa-k} \epsilon^j \hat{A}_{k+j,x}^{(k+1)} \right) F^{(k)}. \quad (5.65)$$

The generalization of the canonical system is obtained at the last step of the iteration, when $k = \kappa - 1$,

$$F^{(\kappa-1)}(\epsilon, x) = B_\kappa F^{(\kappa)}(\epsilon), \quad \partial_x F^{(\kappa-1)} = \epsilon^\kappa \hat{A}_{\kappa,x} F^{(\kappa-1)}. \quad (5.66)$$

It is important to remark that the complete factorization of ϵ is achieved only if $\kappa = 1$, i.e. if the system is linear in ϵ , because, although $\hat{A}_{1,x}$ is independent of ϵ , $\hat{A}_{k,x}$ acquires a dependence on ϵ for $k > 1$, *cfr.* Eq. (5.62).

The algorithm described here has a wide range of applicability and can be used to compute generic sets of MI's, provided that the matrix associated to the system of differential equations can be Taylor expanded around $\epsilon = 0$. In this case, the MI's are obtained perturbatively by truncating the ϵ expansion of the matrices associated to the systems of differential equations.

5.3. Canonical Systems and Deflation

Before we describe the deflation algorithm to find a canonical form, let us first discuss how we can deflate the Eigenvalues of a general matrix.

5.3.1. Eigenvalue Deflation

The right eigenvectors u_i are non-zero vectors, which are only rescaled by the eigenvalue λ_i under the linear transformation A

$$A u_i = \lambda_i u_i . \quad (5.67)$$

Equivalently we can define a left eigenvector v_j^\dagger through

$$v_j^\dagger A = \lambda_j v_j^\dagger . \quad (5.68)$$

An important property of left and right eigenvectors is that they are either related to the same eigenvalue or orthogonal to each other.

$$v_j^\dagger u_i = \delta_{i,j} \quad (5.69)$$

Another important ingredient for the Eigenvalue deflation is the decomposition into the Jordan form. Any complex matrix can be brought into a block diagonal form

$$J = \begin{pmatrix} J_1 & & \\ & \ddots & \\ & & J_N \end{pmatrix} \quad \text{with} \quad J_i = \begin{pmatrix} \lambda_i & 1 & & \\ & \lambda_i & \ddots & \\ & & \ddots & 1 \\ & & & \lambda_i \end{pmatrix} , \quad (5.70)$$

where J_i are the Jordan blocks and the empty entries correspond to zeros. Each of the Jordan blocks has a dimension K_i with $\sum_i^N K_i = n$. In the case where we have non-trivial Jordan blocks $K_i > 1$ it is useful to introduce generalized right eigenvectors satisfying

$$(A - \lambda_i) u_i^{(k)} = u_i^{(k-1)}, \quad (A - \lambda_i) u_i^{(1)} = 0 \quad \text{with} \quad 1 \leq k \leq K_i , \quad (5.71)$$

and generalized left eigenvectors satisfying

$$v_i^{(k)\dagger} (A - \lambda_i) = v_i^{(k-1)\dagger}, \quad v_i^{(1)\dagger} (A - \lambda_i) = 0 \quad \text{with} \quad 1 \leq k \leq K_i , \quad (5.72)$$

which define the similarity transformation P to bring our matrix into the Jordan form

$$J = P^{-1} A P \quad \text{with} \quad P = \left(u_1^{(1)}, \dots, u_1^{(K_1)}, \dots, u_N^{(1)}, \dots, u_N^{(K_N)} \right) . \quad (5.73)$$

The generalized eigenvectors satisfy an orthogonality condition similar to the eigenvectors

$$v_j^{(k)\dagger} u_i^{(h)} = \delta_{i,j} \delta_{k+h, K_i} . \quad (5.74)$$

With these definitions we are now able to perform two operations on our matrix A . First we can shift an eigenvalue λ_i by some number a through a transformation

$$\hat{A} = A + a u_i^{(1)} x_i^\dagger , \quad (5.75)$$

build from the corresponding generalized right eigenvector $u_i^{(1)}$ and some vector x_i^\dagger satisfying $x_i^\dagger u_i^{(1)} = 1$. This transformation will act only on the eigenvalue λ_i , while leaving all other eigenvalues unchanged.

Second we can deflate an eigenvalue λ_i , meaning that we will set it to zero by a transformation

$$\hat{A} = \left(\mathbb{1} - u_i^{(1)} x_i^\dagger \right) A, \quad (5.76)$$

using the same vectors as in the previous transformation (5.75). More over this transformation also reduces the rank of A by one. Instead of performing this transformation sequentially we can deflate each Jordan block simultaneously with the transformation

$$\hat{A} = \left(\mathbb{1} - \sum_i^N u_i^{(1)} x_i^\dagger \right) A, \quad (5.77)$$

where $u_i^{(1)}$ are the generalized right eigenvectors and x_i^\dagger are arbitrary vectors satisfying

$$x_i^\dagger u_j^{(1)} = \delta_{i,j}. \quad (5.78)$$

With the help of this transformation we can write down an algorithm which reduces the rank of any matrix A to zero:

- 1. Set

$$A_0 \leftarrow A \quad (5.79)$$

- 2. Construct the projector

$$\mathcal{P} = \sum_i u_i^{(0)} x_i^\dagger \quad (5.80)$$

from the generalized eigenvectors $u_i^{(1)}$ of A and the arbitrary vectors x_i^\dagger satisfying $x_i^\dagger u_j^{(1)} = \delta_{i,j}$

- 3. Transform the matrix with the complementary projector

$$A_0 \leftarrow (\mathbb{1} - \mathcal{P}) A_0 \quad (5.81)$$

- 4. Repeat steps 2 through 4 until A_0 has rank 0 and is therefore a null matrix.

This algorithm will succeed after $\max\{\text{rank}(J_i), 1 \leq i \leq N\}$ iterations, since at each step we lower the rank of each Jordan block by one. These ideas we presented here will be the underlining principle of finding a canonical basis with the help of the deflation algorithm. First we will deflate the eigenvalues of all higher pole matrices in our differential equation until we obtain a Fuchsian form. Second we will shift the eigenvalues of the simple pole matrices to be multiples of ϵ , which brings us to the canonical form up to a constant similarity transformation.

Example

Let us consider an example where we apply the deflation we discussed above. The matrix

$$A = \begin{pmatrix} 5 & 4 & 2 & 1 \\ 0 & 1 & -1 & -1 \\ -1 & -1 & 3 & 0 \\ 1 & 1 & -1 & 2 \end{pmatrix}, \quad (5.82)$$

has the following Jordan decomposition

$$J = \begin{pmatrix} 1 & 0 & 0 & 0 \\ 0 & 2 & 0 & 0 \\ 0 & 0 & 4 & 1 \\ 0 & 0 & 0 & 4 \end{pmatrix}, \quad (5.83)$$

from which we can see that we have three different eigenvalues $\lambda_1 = 1, \lambda_2 = 2$ and $\lambda_3 = 4$, where the latter appears twice and forms a non trivial Jordan block. We have four generalized eigenvectors

$$u_1^{(1)} = \begin{pmatrix} -1 \\ 1 \\ 0 \\ 0 \end{pmatrix}, \quad u_2^{(1)} = \begin{pmatrix} 1 \\ -1 \\ 0 \\ 1 \end{pmatrix}, \quad u_3^{(1)} = \begin{pmatrix} 1 \\ 0 \\ -1 \\ 1 \end{pmatrix}, \quad u_3^{(2)} = \begin{pmatrix} 1 \\ 0 \\ 0 \\ 0 \end{pmatrix}, \quad (5.84)$$

satisfying

$$A u_1^{(1)} = \lambda_1 u_1^{(1)}, \quad A u_2^{(1)} = \lambda_2 u_2^{(1)}, \quad A u_3^{(1)} = \lambda_3 u_3^{(1)}, \quad A u_3^{(2)} = \lambda_3 u_3^{(2)} + u_3^{(1)}, \quad (5.85)$$

and defining the similarity transformation into the Jordan form

$$J = P^{-1} A P \quad \text{with} \quad P = \left(u_1^{(1)}, u_2^{(1)}, u_3^{(1)}, u_3^{(2)} \right). \quad (5.86)$$

First let us raise λ_2 by one with the help of equation (5.75)

$$\hat{A} = A + u_2^{(1)} x_2^\dagger \quad \text{with} \quad x_2^\dagger = (1, 1, 2, 1), \quad (5.87)$$

where x_2^\dagger satisfies the normalization condition $x_2^\dagger u_2^{(1)} = 1$. Indeed after bringing \hat{A} into its Jordan form we find

$$\hat{P}^{-1} \hat{A} \hat{P} = \hat{J} = \begin{pmatrix} 1 & 0 & 0 & 0 \\ 0 & 3 & 0 & 0 \\ 0 & 0 & 4 & 1 \\ 0 & 0 & 0 & 4 \end{pmatrix} \quad (5.88)$$

that λ_2 was shifted by one, while all other eigenvalues remained the same.

If we use the transformation (5.76) to deflate the eigenvalue λ_1

$$\hat{A} = \left(\mathbb{1} - u_1^{(1)} x_1^\dagger \right) A, \quad \text{with} \quad x_1^\dagger = (1, 2, 2, 1), \quad (5.89)$$

and applying the Jordan decomposition we find

$$\hat{P}^{-1}\hat{A}\hat{P} = \hat{J} = \begin{pmatrix} 0 & 0 & 0 & 0 \\ 0 & 2 & 0 & 0 \\ 0 & 0 & 4 & 1 \\ 0 & 0 & 0 & 4 \end{pmatrix}, \quad (5.90)$$

that λ_1 was set to zero as we claimed.

Instead of deflating the eigenvalues sequentially let us use equation (5.77) to deflate each Jordan block simultaneously

$$\hat{A} = \left(\mathbb{1} - u_1^{(1)}x_1^\dagger - u_2^{(1)}x_2^\dagger - u_3^{(1)}x_3^\dagger \right) A, \quad \text{with } x_3^\dagger = (1, 1, 0, 0). \quad (5.91)$$

and the other x_i^\dagger as defined previously. We should note that as required the x_i^\dagger their defining property

$$x_i^\dagger u_j^{(1)} = \delta_{i,j}. \quad (5.92)$$

After the transformation (5.91) and the Jordan decomposition of \hat{A} we find

$$\hat{P}^{-1}\hat{A}\hat{P} = \hat{J} = \begin{pmatrix} 0 & 0 & 0 & 0 \\ 0 & 0 & 0 & 0 \\ 0 & 0 & 0 & 0 \\ 0 & 0 & 0 & 4 \end{pmatrix}, \quad (5.93)$$

where all Jordan blocks were deflated by one. We can now use a second transformation similar to (5.91)

$$\left(\mathbb{1} - \hat{u}_2^{(1)}\hat{x}_2^\dagger \right) \hat{A} = \begin{pmatrix} 0 & 0 & 0 & 0 \\ 0 & 0 & 0 & 0 \\ 0 & 0 & 0 & 0 \\ 0 & 0 & 0 & 0 \end{pmatrix}, \quad (5.94)$$

with $\hat{u}_2^{(1)} = \begin{pmatrix} 0 \\ 0 \\ -1 \\ 2 \end{pmatrix}$ and $\hat{x}_2^\dagger = (0, 0, -1, 0)$ to deflate the last non-zero eigenvalue.

5.3.2. An Algorithm based on Eigenvalue Deflation

A second algorithm for obtaining a canonical form was described by Lee [83]. Here we consider a differential equation in only one dimensionless variable

$$\partial_x F = A_x^{[0]} F, \quad (5.95)$$

which after performing a Laurent expansion in each of the poles $x_{i=1\dots n}$ of $A_x^{[0]}$

$$A_x^{[0]} = \sum_{j=1+p_1} \frac{\mathcal{S}_{1,j}^{[0]}}{(x-x_1)^j}, \quad A_x^{[0]} = \sum_{j=1+p_2} \frac{\mathcal{S}_{2,j}^{[0]}}{(x-x_2)^j} \dots \quad (5.96)$$

exposes the pole's Poincaré rank p_i .

A three step algorithm allows us to transform this system into the canonical one.

1. Reduce all Poincaré ranks to zero by deflating the corresponding pole matrices in order to cast the differential equation into a Fuchsian form

$$A_x^{[1]} = \frac{\mathcal{S}_{1,1}^{[1]}}{x-x_1} + \frac{\mathcal{S}_{2,1}^{[1]}}{x-x_2} \dots \quad (5.97)$$

In the following we will drop the pole order label on the matrices $\mathcal{S}_{i,1}^{[1]} \equiv \mathcal{S}_i^{[1]}$.

2. Shift all Eigenvalues of the matrices $\mathcal{S}_i^{[1]}$ to be multiples of ϵ .

$$A_x^{[2]} = \frac{\mathcal{S}_1^{[2]}}{x-x_1} + \frac{\mathcal{S}_2^{[2]}}{x-x_2} \dots \quad (5.98)$$

3. Find a constant similarity transformation

$$\mathcal{T}^{-1}(\epsilon) \mathcal{S}_1^{[2]}(\epsilon) \mathcal{T}(\epsilon) = \epsilon \mathcal{S}_1^{[3]}, \quad (5.99)$$

$$\mathcal{T}^{-1}(\epsilon) \mathcal{S}_2^{[2]}(\epsilon) \mathcal{T}(\epsilon) = \epsilon \mathcal{S}_2^{[3]}, \quad (5.100)$$

$$\dots, \quad (5.101)$$

which brings all matrices $\mathcal{S}_i^{[2]}$ simultaneously into the canonical form

$$\partial_x I = \epsilon A_x^{[3]} I \quad \text{with} \quad A_x^{[3]} = \frac{\mathcal{S}_1^{[3]}}{x-x_1} + \frac{\mathcal{S}_2^{[3]}}{x-x_2} \dots, \quad (5.102)$$

Step one in the context of a differential equation is a well covered problem in the mathematical literature and is related to the 21st Hilbert problem. The latter was shown to have a negative solution through an explicit counter example [84]. Therefore it is not always possible to reduce all Poincaré ranks to zero. Nevertheless there exists a necessary and sufficient condition for the reduction and an algorithm developed by Moser [125]. This algorithm was later improved by Barkatou and Pflügel [126, 127], which generates a sequence of rational transformations, minimizing the Poincaré ranks of all but one singularity (usually chosen to be inf). Especially if all singularities are regular this algorithm allows us to reduce the system to a Fuchsian form, except for maybe one point. The possibility of reducing all points to a Fuchsian form would correspond to a positive solution to the 21st Hilbert problem. In the following text we will assume that it is possible to reduce the given system

to a Fuchsian form, since otherwise the application of the deflation algorithm is not possible.

The deflation algorithm uses a slight variation of the algorithm by Barkatou and Pflügel, it is based on so-called *balance* transformations between points two points x_1 and x_2

$$\mathcal{B}(\mathcal{P}, x_1, x_2 | x) = \begin{cases} \bar{\mathcal{P}} + \frac{x-x_2}{x-x_1}\mathcal{P} & \text{if } x_1 \neq \infty \neq x_2 \\ \bar{\mathcal{P}} - (x-x_2)\mathcal{P} & \text{if } x_1 = \infty \neq x_2 \\ \bar{\mathcal{P}} - \frac{1}{x-x_1}\mathcal{P} & \text{if } x_1 \neq \infty = x_2 \end{cases}, \quad (5.103)$$

where \mathcal{P} and $\bar{\mathcal{P}}$ are complimentary projectors satisfying $\mathcal{P}^2 = \mathcal{P}$ and $\bar{\mathcal{P}}\mathcal{P} = 0$.

In order to reduce our system to a Fuchsian form we can use the following algorithm:

- 1. Set

$$M_x \leftarrow A_x^{[0]} \quad (5.104)$$

$$T \leftarrow \mathbb{1} \quad (5.105)$$

- 2. Choose a singular point x_1 with a positive Poincaré rank and the corresponding leading pole matrix $\mathcal{S}_{1,j}$ of M_x
- 3. **If** there is a second singular point x_2 with a leading pole matrix, which has a left invariant space spanned by $\{v_1^\dagger, \dots, v_N^\dagger\}$ and where the basis vectors satisfy $v_i^\dagger u_j^{(1)} = \delta_{i,j}$ with $u_j^{(1)}$ being the generalized right eigenvectors of $\mathcal{S}_{1,j}$

– Construct the Projector

$$\mathcal{P} = \sum_{k=1}^N u_k^{(1)} v_k^\dagger \quad (5.106)$$

- **Else** Choose an arbitrary regular point x_2

– Construct the Projector

$$\mathcal{P} = u_{k_0}^{(1)} v_{k_0}^{(K_0)\dagger} + \sum_{k \in \text{trivial Jordan blocks}} u_k^{(1)} v_k^{(1)\dagger} \quad (5.107)$$

where $u_k^{(0)}$ and $v_k^{(j)}$ are the generalized right and left eigenvectors of $\mathcal{S}_{1,j}$ and k_0 is the position corresponding to a non trivial Jordan block of size K_0

- 4. Construct a balance transformation and transform the differential equation

$$T_0 \leftarrow \mathcal{B}(\mathcal{P}, x_1, x_2 | x) \quad (5.108)$$

$$M_x \leftarrow T_0^{-1} M_x T_0 - T_0^{-1} \partial_x T_0 \quad (5.109)$$

$$T \leftarrow T T_0 \quad (5.110)$$

- 5. Repeat steps 2 through 5 until all Poincaré ranks are zero.

After completion this algorithm will provide us a transformation matrix T which removes all non Fuchisan poles from our differential equation

$$A_x^{[1]} = T^{-1} A_x^{[0]} T - T^{-1} \partial_x T \quad (5.111)$$

$$A_x^{[1]} = \frac{\mathcal{S}_1^{[1]}}{x - x_1} + \frac{\mathcal{S}_2^{[1]}}{x - x_2} \dots \quad (5.112)$$

In step two we investigate the eigenvalues of the matrices $\mathcal{S}_i^{[1]}$ sitting on top of the simple poles. In addition we will consider the matrix of the residue at infinity, which is given as the negative sum of all simple pole matrices

$$\mathcal{S}_\infty^{[1]} = - \sum_{i=1}^n \mathcal{S}_i^{[1]} \quad (5.113)$$

If all eigenvalues are not of the form $\lambda = n + k \epsilon$, $k \in \mathcal{N}$, the system can not be transformed into the canonical form at least in the current variables. But if this condition holds we can use a second series of balance transformation in order to shift all eigenvalues to be multiples of ϵ .

- 1. Set

$$M_x \leftarrow A_x^{[1]} \quad (5.114)$$

$$T \leftarrow \mathbb{1} \quad (5.115)$$

- 2. Derive all eigenvalues of the pole matrices of M_x including the pole at ∞ .
- 3. Pick a pair of eigenvalues (λ_1, λ_2) , which are not multiples of ϵ and where $\lambda_1 = n_1 + k_1 \epsilon$, $n_1 > 0$ and $\lambda_2 = n_2 + k_2 \epsilon$, $n_2 < 0$.
- 4. Build the projector \mathcal{P}

$$\mathcal{P} = uv^\dagger \quad (5.116)$$

from the generalized right eigenvector u of λ_1 and the generalized left eigenvector v^\dagger of λ_2 .

- 5. Transform the differential equation and save the transformation matrix

$$T_0 \leftarrow \mathcal{B}(\mathcal{P}, x_1, x_2 | x) \quad (5.117)$$

$$M_x \leftarrow T_0^{-1} M_x T_0 - T_0^{-1} \partial_x T_0 \quad (5.118)$$

$$T \leftarrow T T_0 \quad (5.119)$$

- 6. Repeat steps 2. through 5. until all eigenvalues are multiples of ϵ .

The algorithm provides us a transformation T , which brings our differential equation in the following form

$$A_x^{[2]} = T^{-1} A_x^{[1]} T - T^{-1} \partial_x T \quad (5.120)$$

$$A_x^{[2]} = \frac{\mathcal{S}_1^{[2]}}{x - x_1} + \frac{\mathcal{S}_{2,j}^{[2]}}{x - x_2} \dots, \quad (5.121)$$

where all eigenvalues of the pole matrices $\mathcal{S}_i^{[2]}$ are now multiples of ϵ .

If $A_x^{[2]}$ is not yet in the canonical form, we have to find a constant similarity transformation

$$T^{-1}(\epsilon) \mathcal{S}_i^{[2]} T(\epsilon) = \epsilon \mathcal{S}_i^{[3]}, \quad (5.122)$$

which transforms each of the pole matrices into the canonical ones. The easiest way to find such a similarity transformation is to exploit the fact the the matrices $\mathcal{S}_i^{[3]}$ are independent of ϵ . Therefore if we replace ϵ with another variable μ we can derive a system of equations

$$T^{-1}(\epsilon) \frac{\mathcal{S}_i^{[2]}}{\epsilon} T(\epsilon) = \mathcal{S}_i^{[3]} = T^{-1}(\mu) \frac{\mathcal{S}_i^{[2]}}{\mu} T(\mu) \quad (5.123)$$

$$\Rightarrow \frac{\mathcal{S}_i^{[2]}}{\epsilon} \tilde{T}(\epsilon, \mu) = \mathcal{S}_i^{[3]} = \tilde{T}(\epsilon, \mu) \frac{\mathcal{S}_i^{[2]}}{\mu} \quad (5.124)$$

where we defined $\tilde{T}(\epsilon, \mu) = T(\epsilon) T^{-1}(\mu)$. We can solve the latter system of equations with algebraic methods and set the remaining free parameters if there are any to some convenient value, since we only need to obtain one specific transformation and not the whole class of solutions. The resulting system is then by definition our canonical differential equation

$$A_x^{[3]} = \frac{\epsilon \mathcal{S}_1^{[3]}}{x - x_1} + \frac{\epsilon \mathcal{S}_{2,j}^{[3]}}{x - x_2} \dots \quad (5.125)$$

Even though the steps of this algorithm might sound cumbersome, they can be easily be implemented in a computer code, which can be applied to any problem with only one dimensionless invariant.

5.4. The QED Sunrise

In this section we will consider an example, where both algorithms can be used to obtain the canonical form. The differential equation for such an example has to be linear in ϵ and depend on only one dimensionless invariant. One system that fulfills these requirements, is given by the QED sunrise. The three master integrals in our system are depicted in figure 5.1, where the latter two master integrals actually belong to the same topology. Therefore

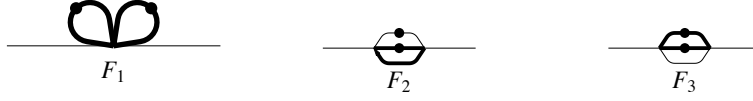


Figure 5.1.: The figure shows the three master integrals of the QED sunrise, where the thick line represent massive propagators and dots squared propagators.

they form a non-trivial block, which is already triangularized by the choice of masters we made. The differential equation for the three master integrals is given by

$$\partial_x F = A_x F \quad (5.126)$$

$$A_x = \begin{pmatrix} 0 & 0 & 0 \\ -\frac{\epsilon}{2(1-x)} - \frac{\epsilon}{2(1+x)} & -\frac{1+6\epsilon}{1+x} + \frac{1+3\epsilon}{x} + \frac{1}{1-x} & -\frac{1-2\epsilon}{2(1-x)} - \frac{\epsilon}{x} - \frac{1-6\epsilon}{2(1+x)} \\ 0 & \frac{2\epsilon}{x} + \frac{4\epsilon}{1-x} & \frac{1}{x} + \frac{2}{1-x} \end{pmatrix}, \quad (5.127)$$

where we choose our dimensionless variable x as $-\frac{s}{m^2} = \frac{(1-x)^2}{x}$. This change of variables removes square roots which occur in the differential equation in s and we will show how to derive the variables in section 5.5.1.

5.4.1. Canonical Form with the Magnus Exponential

Following the algorithm described in section 5.2.3 we first split the ϵ^0 -part into a diagonal and an off-diagonal part

$$A_{x,0} = D_{x,0} + N_{x,0}, \quad (5.128)$$

with

$$D_{x,0} = \begin{pmatrix} 1 & 0 & 0 \\ 0 & \frac{x}{1-x^2} & 0 \\ 0 & 0 & \frac{x}{(1-x)^2} \end{pmatrix} \quad N_{x,0} = \begin{pmatrix} 0 & 0 & 0 \\ 0 & 0 & -\frac{1}{2(1-x)} - \frac{1}{2(1+x)} \\ 0 & 0 & 0 \end{pmatrix}, \quad (5.129)$$

and then build the rotation matrix by the Magnus exponential of the diagonal part

$$B_1 = e^{\int dx D_{x,0}} = \begin{pmatrix} 1 & 0 & 0 \\ 0 & \frac{x}{1-x^2} & 0 \\ 0 & 0 & \frac{x}{(1-x)^2} \end{pmatrix}. \quad (5.130)$$

This rotation matrix transforms our differential equation to

$$A_x^{[1]} = B_1^{-1} A_x B_1 - B_1^{-1} \partial_x B_1 = \begin{pmatrix} 0 & 0 & 0 \\ -\frac{\epsilon}{x} & \frac{3\epsilon}{x} - \frac{6\epsilon}{1+x} & -\frac{1-2\epsilon}{(x-1)^2} - \frac{\epsilon}{x} \\ 0 & \frac{2\epsilon}{x} & 0 \end{pmatrix}, \quad (5.131)$$

where now the diagonal part is ϵ -factorized. For the second transformation we build the Dyson series from the ϵ^0 part of our transformed differential equation $A_x^{[1]}$

$$B_2 = \mathbb{1} + \int dx N_x^{[1]} \quad (5.132)$$

with

$$N_x^{[1]} = \begin{pmatrix} 0 & 0 & 0 \\ 0 & 0 & -\frac{1}{(x-1)^2} \\ 0 & 0 & 0 \end{pmatrix}, \quad (5.133)$$

where the Dyson series stopped after the first integral since $N_x^{[1]}$ is a nilpotent matrix of degree two. The transformed differential equation is given by

$$A_x^{[2]} = B_2^{-1} A_x^{[1]} B_2 - B_2^{-1} \partial_x B_2 = \begin{pmatrix} 0 & 0 & 0 \\ -\frac{\epsilon}{x} & \frac{2\epsilon}{1-x} + \frac{5\epsilon}{x} - \frac{6\epsilon}{1+x} & -\frac{2\epsilon}{1-x} - \frac{6\epsilon}{x} + \frac{3\epsilon}{1+x} \\ 0 & \frac{2\epsilon}{x} & -\frac{2\epsilon}{1-x} - \frac{2\epsilon}{x} \end{pmatrix}, \quad (5.134)$$

where the dependence on ϵ is completely factorized. The master integrals, which obey this canonical equation can be obtained by multiplying the original master integrals by the two rotation matrices

$$B_1 B_2 F = \begin{pmatrix} F_1 \\ \frac{x}{1-x^2} F_2 - \frac{x}{(1-x)(1-x^2)} F_3 \\ \frac{x}{(1-x)^2} F_3 \end{pmatrix}. \quad (5.135)$$

5.4.2. Canonical Form with Eigenvalue Deflation

Since the contributions of the tadpole, which corresponds to the first line and column of the differential equation (5.127), are already completely ϵ -factorized we will only focus on the homogeneous part of the two master integrals belonging to the QED sunrise. The first thing we should note is that the differential equation (5.127) is already in Fuchsian form

$$C_x = \frac{\mathcal{S}_1}{x-1} + \frac{\mathcal{S}_2}{x} + \frac{\mathcal{S}_3}{1+x}, \quad (5.136)$$

with the pole matrices

$$\mathcal{S}_1 = \begin{pmatrix} 1 & -\frac{1-2\epsilon}{2} \\ 4\epsilon & 2 \end{pmatrix} \quad \mathcal{S}_2 = \begin{pmatrix} 1+3\epsilon & -\epsilon \\ 2\epsilon & 1 \end{pmatrix} \quad \mathcal{S}_3 = \begin{pmatrix} -1-6\epsilon & -\frac{1-6\epsilon}{2} \\ 0 & 0 \end{pmatrix}. \quad (5.137)$$

Therefore we can immediately start with the second part of the algorithm, where we shift all eigenvalues of the pole matrices

$$\begin{aligned} \sigma(\mathcal{S}_1) &= \{-1-2\epsilon, -2(1-\epsilon)\} & \sigma(\mathcal{S}_2) &= \{1+\epsilon, 1+2\epsilon\} & \sigma(\mathcal{S}_3) &= \{0, -1-6\epsilon\} \\ & & & & \sigma(\mathcal{S}_\infty) &= \{1+\epsilon, 1+2\epsilon\}, \end{aligned} \quad (5.138)$$

to be multiple of ϵ . Here we also have to consider the pole matrix corresponding to the pole at ∞ , which can be obtained by $\mathcal{S}_\infty = -\mathcal{S}_1 - \mathcal{S}_2 - \mathcal{S}_3$. Before we start shifting the eigenvalues we should note that all our eigenvalues are of the form $n + k\epsilon$ with $n, k \in \mathbb{Z}$ and that their sum vanishes, which were both requirements of the applicability of the algorithm². In the first step we will shift the Eigenvalue $\lambda_1 = -2(1 - \epsilon)$ of the first pole matrix \mathcal{S}_1 by plus one and the Eigenvalue $\lambda_\infty = 1 + \epsilon$ of the last pole matrix \mathcal{S}_∞ by minus one. The projector, which we need for the shift, is build from the right generalized Eigenvector of λ_1 and left generalized Eigenvector of λ_∞

$$\mathcal{P}_1 = u_1 \cdot v_\infty^\dagger = \begin{pmatrix} -\frac{1}{2} \\ 1 \end{pmatrix} \cdot \begin{pmatrix} -\frac{2}{3} & \frac{2}{3} \end{pmatrix} = \begin{pmatrix} \frac{1}{3} & -\frac{1}{3} \\ -\frac{2}{3} & \frac{2}{3} \end{pmatrix}. \quad (5.139)$$

With this projector we can obtain the corresponding balance transformation

$$\mathcal{B}_1(\mathcal{P}_1, -1, \infty | x) = \bar{\mathcal{P}}_1 + \frac{1}{1-x} \mathcal{P} = \begin{pmatrix} \frac{3-2x}{3(1-x)} & -\frac{x}{3(1-x)} \\ -\frac{2x}{3(1-x)} & \frac{3-x}{3(1-x)} \end{pmatrix}, \quad (5.140)$$

which transforms the differential equation to

$$C_x^{[1]} = \mathcal{B}_1^{-1} A_x \mathcal{B}_1 - \mathcal{B}_1^{-1} \partial_x \mathcal{B}_1 \quad (5.141)$$

$$= \begin{pmatrix} \frac{3+2\epsilon}{3(1-x)} + \frac{1+3\epsilon}{x} - \frac{4(1+4\epsilon)}{3(1+x)} & \frac{4\epsilon}{3(1-x)} - \frac{\epsilon}{x} - \frac{2(1-2\epsilon)}{3(1+x)} \\ \frac{8\epsilon}{3(1-x)} + \frac{2\epsilon}{x} + \frac{2(1+4\epsilon)}{3(1+x)} & \frac{1-2\epsilon}{3(1+x)} + \frac{3-2\epsilon}{3(1-x)} + \frac{1}{x} \end{pmatrix}. \quad (5.142)$$

We see that the balance transformation did not alter the pole structure of our matrix, as one would expect. In fact the only thing that changed are the eigenvalues of the first and last pole matrices

$$\begin{aligned} \sigma(\mathcal{S}_1^{[1]}) = \{-1 - 2\epsilon, -1 + 2\epsilon\} \quad \sigma(\mathcal{S}_2^{[1]}) = \{1 + \epsilon, 1 + 2\epsilon\} \quad \sigma(\mathcal{S}_3^{[1]}) = \{0, -1 - 6\epsilon\} \\ \sigma(\mathcal{S}_\infty^{[1]}) = \{\epsilon, 1 + 2\epsilon\}, \end{aligned} \quad (5.143)$$

which got shifted by +1 and -1 respectively. All balance transformations, which have to be performed in order to shift all eigenvalues to be multiples of ϵ have been summarized in table 5.1. After four transformation we arrive at a differential equation of the form

$$C_x^{[4]} = \begin{pmatrix} \frac{2\epsilon}{1-x} + \frac{5\epsilon}{x} - \frac{6\epsilon}{1+x} & \frac{2\epsilon}{1-x} + \frac{6\epsilon}{x} - \frac{3\epsilon}{1+x} \\ -\frac{2\epsilon}{x} & -\frac{2\epsilon}{1-x} - \frac{2\epsilon}{x} \end{pmatrix}, \quad (5.144)$$

which is already completely ϵ -factorized making the last step in the deflation algorithm unnecessary. Embedding the obtained rotation matrices in an 3×3 unit matrix

$$B_D = \begin{pmatrix} 1 & 0 & 0 \\ 0 & \mathcal{B}_1 \mathcal{B}_2 \mathcal{B}_3 \mathcal{B}_4 \\ 0 & & \end{pmatrix} = \begin{pmatrix} 1 & 0 & 0 \\ 0 & \frac{x}{1-x^2} & \frac{x}{(1-x)^2(1+x)} \\ 0 & 0 & -\frac{x}{(1-x)^2} \end{pmatrix}, \quad (5.145)$$

²The condition that the sum of all eigenvalues vanishes is trivially satisfied, but the condition that the eigenvalues have to be integer valued is indeed a limitation. In the case where we have non integer eigenvalues we usually need to perform a change of variables, since non integer eigenvalues point to the appearance of non-rational factors in the differential equation

Step	λ shifted by +1	λ shifted by -1	Balance transformation
1	$\lambda = 2(-1 + \epsilon)$ of \mathcal{S}_1	$\lambda = 1 + \epsilon$ of \mathcal{S}_∞	$\mathcal{B}_1 = \begin{pmatrix} \frac{3-2x}{3(1-x)} & -\frac{x}{3(1-x)} \\ \frac{2x}{3(1-x)} & \frac{3-x}{3(1-x)} \end{pmatrix}$
2	$\lambda = -1 - 2\epsilon$ of $\mathcal{S}_1^{[1]}$	$\lambda = 1 + 2\epsilon$ of $\mathcal{S}_\infty^{[1]}$	$\mathcal{B}_2 = \begin{pmatrix} \frac{3-x}{3(1-x)} & \frac{x}{3(1-x)} \\ \frac{2x}{3(1-x)} & \frac{3-2x}{3(1-x)} \end{pmatrix}$
3	$\lambda = -1 + 2\epsilon$ of $\mathcal{S}_1^{[2]}$	$\lambda = 1 + \epsilon$ of $\mathcal{S}_2^{[2]}$	$\mathcal{B}_3 = \begin{pmatrix} \frac{2-3x}{3(1-x)} & \frac{1}{3(1-x)} \\ \frac{2}{3(1-x)} & \frac{1-3x}{3(1-x)} \end{pmatrix}$
4	$\lambda = -1 - 6\epsilon$ of $\mathcal{S}_3^{[3]}$	$\lambda = 1 + 2\epsilon$ of $\mathcal{S}_2^{[3]}$	$\mathcal{B}_4 = \begin{pmatrix} -\frac{1-3x}{3(1+x)} & -\frac{2}{3(1+x)} \\ \frac{2}{3(1+x)} & \frac{4+3x}{3(1+x)} \end{pmatrix}$

Table 5.1.: We summarize the Balance transformations, which have to be performed in order to shift all eigenvalues to be multiples of ϵ .

gives us the rotation matrix for the complete system including the tadpole

$$A_x^{[4]} = \begin{pmatrix} 0 & 0 & 0 \\ -\frac{\epsilon}{x} & \frac{2\epsilon}{1-x} + \frac{5\epsilon}{x} - \frac{6\epsilon}{1+x} & \frac{2\epsilon}{1-x} + \frac{6\epsilon}{x} - \frac{3\epsilon}{1+x} \\ 0 & -\frac{2\epsilon}{x} & -\frac{2\epsilon}{1-x} - \frac{2\epsilon}{x} \end{pmatrix}. \quad (5.146)$$

The canonical master integrals, which were obtained with the deflation algorithm are given by

$$B_D \mathbf{F} = \begin{pmatrix} F_1 \\ \frac{x}{1-x^2} F_2 + \frac{x}{(1-x)(1-x^2)} F_3 \\ -\frac{x}{(1-x)^2} F_3 \end{pmatrix}. \quad (5.147)$$

Comparing the master integrals from Magnus (5.135) with the ones we obtained with the deflation algorithm we see that both algorithms obtained the same master integrals up to a simple redefinition of the third master integral $F_3 \rightarrow -F_3$. This is of course not a general feature, since both algorithms have completely different limitations. Nevertheless it is interesting to observe that these two algorithms, which are based on completely different ideas, deliver the same canonical master integrals.

5.5. Irrational Terms within Differential Equations

In the process of obtaining a canonical form we might reveal non-rational terms, which were hidden in the homogeneous part of the differential equation. These non-rational terms impede the solution of the differential equation, since we can't express the solution in terms of the well known Goncharov's polylogarithm. Instead we have to rely on the representation in terms of Chen's iterated integrals, which due to the lack of a dedicated code can not be efficiently numerically evaluated at the moment. For this reason it is desirable to remove all

non-rational terms from the differential equation. Unfortunately there is no general strategy to do this, but we will present an algorithm here, which allows us to reformulate the problem of removing non-rational terms from our differential equation in a well defined mathematical framework.

For a system with k invariants and l non-rational terms we should first assign the variables β_1, \dots, β_l to each non-rational term. Then we must be able to write down $l - k$ equations relating the different non-rational terms. Each of these relations defines a subspace of the l dimensional space spanned by β_1, \dots, β_l . The problem can now be reformulated. We want to find a rational parametrization of each subspace or in the case of overlapping subspaces for the intersection region, which are only defined implicitly. If we are able to find such a rational parametrization for the β_i we can simply relate them back to our invariants, to find a rational parametrization, which removes all square roots from our system. Let us summarize the steps we described for a differential equation with k kinematic invariants and l non-rational terms.

- 1. Assign the l non-rational terms a variable β_i
- 2. Find the $l - k$ relations between the β_i
- 3. Find a rational parametrization of the β_i , which solves all relations of step 2.
- 4. Using the definitions of β_i relate the rational parametrization back to our kinematic invariants

Without a doubt step 3. is the problematic part of the algorithm, but nevertheless for some problems we encounter rather easy relations between the β_i , for which we can find rational parametrizations solve. Furthermore this procedure brings the problem into a well defined mathematical framework, where we want to obtain a rational parametric representation of a subspace, which is given implicitly by an equation. Let us illustrate how this algorithm can be applied and derive the well known Landau variables.

5.5.1. Landau Variables

For the QED sunrise, which we discussed previously, we find two square roots $\sqrt{-s} = \beta_1$ and $\sqrt{4m^2 - s} = \beta_2$ in the differential equation. The arguments of the square roots are connected through a simple relation

$$(\sqrt{4m^2 - s})^2 - (\sqrt{-s})^2 = 4m^2 , \quad (5.148)$$

$$\beta_2^2 - \beta_1^2 = 4m^2 . \quad (5.149)$$

The equation above has two free parameters β_1 and β_2 and therefore describes a line in a two dimensional plane. Our goal is to move from this implicit representation of our subspace to a rational parametric representation. In our case we can achieve this by rewriting equation (5.149) into a slightly different form

$$\frac{\beta_2^2}{4m^2} - \frac{\beta_1^2}{4m^2} = 1 , \quad (5.150)$$

and realizing that this equation describes a rectangular hyperbola which in general is given by

$$\frac{x^2}{a^2} - \frac{y^2}{a^2} = 1 . \quad (5.151)$$

The parametrization of this curve is well know

$$x = a \sec(u) \quad (5.152)$$

$$y = a \tan(u) , \quad (5.153)$$

and readily solves eq. (5.151). In order to find a rational parametrization we will use the rational representation of the secant and the tangent

$$x = a \sec(u) = a \frac{1}{\cos(u)} = a \frac{1+t^2}{2t} \quad (5.154)$$

$$y = a \tan(u) = a \frac{\sin(u)}{\cos(u)} = a \frac{1-t^2}{2t} . \quad (5.155)$$

which are based on the rational representation of the sine and cosine

$$\sin(u) = \frac{1-t^2}{1+t^2} \quad (5.156)$$

$$\cos(u) = \frac{2t}{1+t^2} . \quad (5.157)$$

From eq. (5.155) we can now find our variable transformation, which removes all square roots

$$\sqrt{-s} = y = a \frac{1-t^2}{2t} \quad (5.158)$$

$$\Rightarrow -s = a^2 \frac{(1-t^2)^2}{4t^2} \quad (5.159)$$

$$\Rightarrow \frac{-s}{m^2} = \frac{(1-t^2)^2}{t^2} , \quad (5.160)$$

In our case it is possible to send $t \rightarrow \sqrt{v}$ without introducing non-rational terms in our variables, which simplifies our change of variables even further

$$\frac{-s}{m^2} = \frac{(1-v)^2}{v} . \quad (5.161)$$

Through this procedure we arrived at well known Landau variables, which we also used in (5.127).

Iterated Integrals

Our starting point is the differential equation in the canonical basis

$$d\mathbb{I} = \epsilon dA \mathbb{I} , \quad (6.1)$$

with

$$dA = \sum_{i=1}^n \mathbb{M}_i d\log \eta_i , \quad (6.2)$$

where dA is the $d\log$ matrix written in terms of differentials $d\log \eta_i$ (that contain the kinematic dependence) and coefficient matrices \mathbb{M}_i (with rational-number entries). The integrability conditions for eq. (9.16) read

$$\partial_a \partial_b \mathbb{A} - \partial_b \partial_a \mathbb{A} = 0 , \quad [\partial_a \mathbb{A}, \partial_b \mathbb{A}] = 0 . \quad (6.3)$$

6.1. Chen's Iterated Integrals

The general solution of the canonical system of differential equations (9.16) can be compactly written at a point $\vec{x} = (x_1, x_2, \dots, x_n)$ as

$$\mathbb{I}(\epsilon, \vec{x}) = \mathcal{P} \exp \left\{ \epsilon \int_{\gamma} dA \right\} \mathbb{I}(\epsilon, \vec{x}_0) , \quad (6.4)$$

where $\mathbb{I}(\epsilon, \vec{x}_0)$ is a vector of arbitrary constants, depending on ϵ , while dA depends only on the kinematic variables. In the above expression, the *path-ordered* exponential is a short notation for the series

$$\mathcal{P} \exp \left\{ \epsilon \int_{\gamma} dA \right\} = \mathbb{1} + \epsilon \int_{\gamma} dA + \epsilon^2 \int_{\gamma} dA dA + \epsilon^3 \int_{\gamma} dA dA dA \dots , \quad (6.5)$$

in which the line integral of the product of k matrix-valued 1-forms dA is understood in the sense of *Chen's iterated integrals* [128] (see also [129] and the pedagogical lectures [130]) and γ is a piecewise-smooth path

$$\gamma : [0, 1] \ni t \mapsto \gamma(t) = (\gamma_1(t), \gamma_2(t), \dots, \gamma_n(t)), \quad (6.6)$$

such that $\gamma(0) = \vec{x}_0$ and $\gamma(1) = \vec{x}$. It follows from Chen's theorem that the iterated integrals in eq. (6.5) do not depend on the actual choice of the path, provided the curve does not contain any singularity of dA and it does not cross any of its branch cuts, but only on the endpoints. In this sense, if one fixes \vec{x}_0 and lets \vec{x} vary, eq. (6.4) can be thought of as a function of \vec{x} . In the limit $\vec{x} \rightarrow \vec{x}_0$, the line shrinks to a point and all the path integrals in eq.(6.5) vanish, so that $I(\epsilon, \vec{x}) \rightarrow I(\epsilon, \vec{x}_0)$, i.e. the integration constants have a natural interpretation as *initial* values, and the path-ordered exponential as *evolution* operator. We assume that the vector of MI's at any point $I(\vec{x})$ is normalized in such a way that it admits a Taylor series in ϵ :

$$I(\epsilon, \vec{x}) = I^{(0)}(\vec{x}) + \epsilon I^{(1)}(\vec{x}) + \epsilon^2 I^{(2)}(\vec{x}) + \dots \quad (6.7)$$

The solution $I(\epsilon, \vec{x})$ is then in principle determined through (6.4) at any order of the ϵ -expansion, and reads (up to the coefficient of ϵ^4)

$$I^{(0)}(\vec{x}) = I^{(0)}(\vec{x}_0), \quad (6.8)$$

$$I^{(1)}(\vec{x}) = I^{(1)}(\vec{x}_0) + \int_{\gamma} dA I^{(0)}(\vec{x}_0), \quad (6.9)$$

$$I^{(2)}(\vec{x}) = I^{(2)}(\vec{x}_0) + \int_{\gamma} dA I^{(1)}(\vec{x}_0) + \int_{\gamma} dA dA I^{(0)}(\vec{x}_0), \quad (6.10)$$

$$I^{(3)}(\vec{x}) = I^{(3)}(\vec{x}_0) + \int_{\gamma} dA I^{(2)}(\vec{x}_0) + \int_{\gamma} dA dA I^{(1)}(\vec{x}_0) + \int_{\gamma} dA dA dA I^{(0)}(\vec{x}_0), \quad (6.11)$$

$$I^{(4)}(\vec{x}) = I^{(4)}(\vec{x}_0) + \int_{\gamma} dA I^{(3)}(\vec{x}_0) + \int_{\gamma} dA dA I^{(2)}(\vec{x}_0) + \int_{\gamma} dA dA dA I^{(1)}(\vec{x}_0) + \int_{\gamma} dA dA dA dA I^{(0)}(\vec{x}_0). \quad (6.12)$$

The problem of solving (9.16), given a set of initial conditions $I(\vec{x}_0)$, reduces therefore to the evaluation of matrices of the type

$$\int_{\gamma} \underbrace{dA \dots dA}_{k \text{ times}}, \quad (6.13)$$

whose entries, due to (9.17), are linear combinations of Chen's iterated integrals of the form

$$\int_{\gamma} d \log \eta_{i_k} \dots d \log \eta_{i_1} \equiv \int_{0 \leq t_1 \leq \dots \leq t_k \leq 1} g_{i_k}^{\gamma}(t_k) \dots g_{i_1}^{\gamma}(t_1) dt_1 \dots dt_k, \quad (6.14)$$

with

$$g_i^\gamma(t) = \frac{d}{dt} \log \eta_i(\gamma(t)). \quad (6.15)$$

We refer to the number of iterated integrations k as the *weight* of the path-integral. The empty integral (eq. (6.14) for $k = 0$) is defined to be equal to 1. We stress that only the matrices (6.13) do not depend on the explicit choice of the path. The individual summands of the form in eq. (6.14), which contribute to their entries, in general depend on such a choice. To keep the notation compact, we define

$$\mathcal{C}_{i_k, \dots, i_1}^{[\gamma]} \equiv \int_\gamma d\log \eta_{i_k} \dots d\log \eta_{i_1}, \quad (6.16)$$

which also emphasizes that the iterated integrals in (6.14) are in general *functionals* of the path γ .

6.1.1. Properties of Chen's iterated integrals

The general theory of iterated path integrals was developed by Chen [128]. Chen's iterated integrals satisfy a number of properties that we summarize for completeness:

- *Invariance under path reparametrization.* The integral $\mathcal{C}_{i_k, \dots, i_1}^{[\gamma]}$ does not depend on how one chooses to parametrize the path γ .
- *Reverse path formula.* If the path γ^{-1} is the path γ traversed in the opposite direction, then

$$\mathcal{C}_{i_k, \dots, i_1}^{[\gamma^{-1}]} = (-1)^k \mathcal{C}_{i_k, \dots, i_1}^{[\gamma]}. \quad (6.17)$$

- *Recursive structure.* From (6.14) and (6.15) it follows that the line integral of one $d\log$ is defined as usual

$$\int_\gamma d\log \eta \equiv \int_{0 \leq t \leq 1} \frac{d\log \eta(\gamma(t))}{dt} dt, \quad (6.18)$$

and only depends on the endpoints \vec{x}_0, \vec{x}

$$\int_\gamma d\log \eta = \log \eta(\vec{x}) - \log \eta(\vec{x}_0). \quad (6.19)$$

It is convenient to introduce the path integral “up to some point along γ ”: given a path γ and a parameter $s \in [0, 1]$, one can define the 1-parameter family of paths

$$\gamma_s : [0, 1] \ni t \mapsto \vec{x} = (\gamma_1(st), \gamma_2(st), \dots, \gamma_n(st)). \quad (6.20)$$

If $s = 1$, then trivially $\gamma_s = \gamma$. If $s = 0$ the image of the interval $[0, 1]$ is just $\{\vec{x}_0\}$. If $s \in (0, 1)$, then the curve $\gamma_s([0, 1])$ starts at $\gamma(0) = \vec{x}_0$ and overlaps with the curve

$\gamma([0, 1])$ up to the point $\gamma(s)$, where it ends. It is then easy to see that the path integral along γ_s can be written as

$$\mathcal{C}_{i_k, \dots, i_1}^{[\gamma_s]} = \int_{0 \leq t_1 \leq \dots \leq t_k \leq s} g_{i_k}^{\gamma}(t_k) \dots g_{i_1}^{\gamma}(t_1) dt_1 \dots dt_k, \quad (6.21)$$

which differs from eq. (6.14) by the fact that the outer integration (i.e. the one in dt_k) is performed over $[0, s]$ instead of $[0, 1]$. Having introduced γ_s , we can rewrite (6.14) in a recursive manner:

$$\mathcal{C}_{i_k, \dots, i_1}^{[\gamma]} = \int_0^1 g_{i_k}^{\gamma}(s) \mathcal{C}_{i_{k-1}, \dots, i_1}^{[\gamma_s]} ds. \quad (6.22)$$

From eq. (6.21) we can also immediately derive the following identity:

$$\frac{d}{ds} \mathcal{C}_{i_k, \dots, i_1}^{[\gamma_s]} = g_{i_k}^{\gamma}(s) \mathcal{C}_{i_{k-1}, \dots, i_1}^{[\gamma_s]}. \quad (6.23)$$

- *Shuffle algebra.* Chen's iterated integrals fulfil shuffle algebra relations: if $\vec{m} = m_M, \dots, m_1$ and $\vec{n} = n_N, \dots, n_1$ (with M and N natural numbers)

$$\mathcal{C}_{\vec{m}}^{[\gamma]} \mathcal{C}_{\vec{n}}^{[\gamma]} = \sum_{\text{shuffles } \sigma} \mathcal{C}_{\sigma(m_M), \dots, \sigma(m_1), \sigma(n_N), \dots, \sigma(n_1)}^{[\gamma]}, \quad (6.24)$$

where the shuffles are all possible merges of \vec{m} and \vec{n} preserving their respective orderings. Because of shuffle relations, for a given alphabet and a given weight one can identify a minimal basis of Chen's iterated integrals. The number of basis elements depending on the weight n and the alphabet size α is given by the *Witt formula*:

$$N(n, \alpha) = \frac{1}{n} \sum_{d|n} \mu(d) \alpha^{\frac{n}{d}}, \quad (6.25)$$

where μ denotes the Möbius function and the sum is done over all divisors of n . For reference we give some values of $N(n, \alpha)$ in table 6.1.

- *Path composition formula.* If $\alpha, \beta : [0, 1] \rightarrow \mathcal{M}$ are such that $\alpha(0) = \vec{x}_0$, $\alpha(1) = \beta(0)$, and $\beta(1) = \vec{x}$, then the composed path $\gamma \equiv \alpha\beta$ is obtained by first traversing α and then β . One can prove that the integral over such a composed path satisfies

$$\mathcal{C}_{i_k, \dots, i_1}^{[\alpha\beta]} = \sum_{p=0}^k \mathcal{C}_{i_k, \dots, i_{p+1}}^{[\beta]} \mathcal{C}_{i_p, \dots, i_1}^{[\alpha]}. \quad (6.26)$$

The formula arises by splitting the integration regions of the full path $\alpha\beta$ into several pieces. As an example we show how the integration region is split for $k = 2$ in figure 6.1.

weight	$\alpha = 2$	$\alpha = 3$	$\alpha = 4$
1	2	3	4
2	1	3	6
3	2	8	20
4	3	18	60
5	6	48	204
6	9	116	670

Table 6.1.: Size of a basis of Chen's iterated integrals.

- *Integration-by-parts formula.* In order to compute the path ordered integral of k $d\log$ forms using the definition, eq. (6.14) (or, equivalently, eq. (6.22)), in principle one would have to perform k nested integrations. When a full analytical solution cannot be achieved, numerical integration can as well be employed. Therefore one can use an alternative form of the Chen's iterated integral suitable for the combined use of analytic and numerical integrations. In fact, we observe that the innermost integration can always be performed analytically using (6.18), so that only $k - 1$ integrations are left. For instance, in the case $k = 2$,

$$\begin{aligned} \mathcal{C}_{b,a}^{[\gamma]} &= \int_0^1 g_b(t) \mathcal{C}_a^{[\gamma t]} dt \\ &= \int_0^1 g_b(t) (\log \eta_a(\vec{x}(t)) - \log \eta_a(\vec{x}_0)) dt. \end{aligned} \quad (6.27)$$

For $k \geq 3$, one can proceed recursively using eq. (6.22), assuming that the numerical evaluation up to the first $k - 1$ iterations is a solved problem. Using integration by parts, one can show that the numerical integration over the outermost weight g_k can actually be avoided, leaving only $k - 2$ integrations to be performed

$$\mathcal{C}_{i_k, \dots, i_1}^{[\gamma]} = \log \eta_{i_k}(\vec{x}) \mathcal{C}_{i_{k-1}, \dots, i_1}^{[\gamma]} - \int_0^1 \log \eta_{i_k}(\vec{x}(t)) g_{i_{k-1}}(t) \mathcal{C}_{i_{k-2}, \dots, i_1}^{[\gamma t]} dt. \quad (6.28)$$

6.1.2. Path Invariance

We should note that only a combination of Chen's iterated integrals corresponding to a total differential is path invariant. Such a combination is e.g. formed by each master integral in our canonical differential equation, resulting in the path invariance of each individual master integral. In order to illustrate this point let us consider two weight two Chen's iterated integrals

$$\int_{\gamma} d\log(x+y) d\log(1+x) + \int_{\gamma} d\log(1+x) d\log(x+y), \quad (6.29)$$

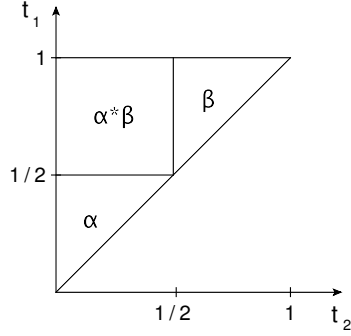


Figure 6.1.: A weight two Chen's iterated integral, where for the full path the inner path parameter t_2 ranges from 0 to t_1 and the outer path parameter t_1 range from 0 to 1. Therefore the integration covers the full triangle, which is shown. If we split the path in half, with α covering the first half and β the second half, the path splitting formula produces three terms: one Chen's iterated integral where we integrate over path α , one where we integrate over path β and one where the inner $d\log$ is integrated over α times another Chen's iterated integral where the outer $d\log$ is integrated over path β . The three terms are represented by the sections in the triangle, namely α, β and $\alpha * \beta$ respectively.

which together form a total differential. Choosing a linear path γ which is shown in figure 6.2 between the start point $\vec{x}_0 = (x_0, y_0) = (1.23, 0.34)$ and end point $\vec{x}_1 = (x_1, y_1) = (0.435, 0.96)$

$$\gamma : \vec{x}(t) = (x_0 + t(x_1 - x_0), y_0 + t(y_1 - y_0)) \quad (6.30)$$

we find the following numerical value for the first integral

$$\begin{aligned} \int_{\gamma} d\log(x+y) d\log(1+x) &= \int_0^1 dt_1 \int_0^{t_1} dt_2 \frac{d\log(x_0 + y_0 + t_1(x_1 + y_1 - x_0 - y_0))}{dt_1} \\ &\quad \times \frac{d\log(1 + x_0 + t_2(x_1 - x_0))}{dt_2} \\ &= 0.0247 . \end{aligned} \quad (6.31)$$

Similarly the second integral evaluates to

$$\int_{\gamma} d\log(1+x) d\log(x+y) = 0.0274 . \quad (6.32)$$

If we combine both results we find a numerical value, which is completely independent of the path choice we have made

$$\int_{\gamma} d\log(x+y) d\log(1+x) + \int_{\gamma} d\log(1+x) d\log(x+y) = 0.0521 . \quad (6.33)$$

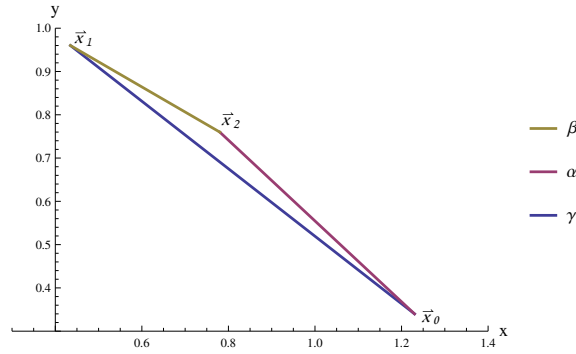


Figure 6.2.: The three paths γ , α and β are shown.

Let us verify this statement by choosing two linear paths α and β such that $\alpha(0) = \gamma(0) = \vec{x}_0$, $\alpha(1) = \beta(0) = \vec{x}_2 = (x_2, y_2) = (0.78, 0.76)$ and $\beta(1) = \gamma(1) = \vec{x}_1$

$$\alpha : \vec{x}(t) = (x_0 + t(x_2 - x_0), y_0 + t(y_2 - y_0)) , \quad (6.34)$$

$$\beta : \vec{x}(t) = (x_2 + t(x_1 - x_2), y_2 + t(y_1 - y_2)) , \quad (6.35)$$

which are also depicted in figure 6.2. Using the path splitting formula in (6.26) we can express our integral over the composed path $\alpha\beta$ as path integrals over α and β , which we can evaluate numerically

$$\begin{aligned} \int_{\alpha\beta} d\log(x+y) d\log(1+y) &= \int_{\alpha} d\log(x+y) d\log(1+x) \\ &+ \int_{\beta} d\log(x+y) d\log(1+x) + \int_{\beta} d\log(x+y) \int_{\alpha} d\log(1+x) \\ &= 0.0348 . \end{aligned} \quad (6.36)$$

Comparing this value to (6.31) we confirm that the individual integral is not path invariant. Repeating the steps for the second integral

$$\begin{aligned} \int_{\alpha\beta} d\log(1+x) d\log(x+y) &= \int_{\alpha} d\log(1+x) d\log(x+y) \\ &+ \int_{\beta} d\log(1+x) d\log(x+y) + \int_{\beta} d\log(1+x) \int_{\alpha} d\log(x+y) \\ &= 0.0173 , \end{aligned} \quad (6.37)$$

and comparing it to equation (6.32) we confirm that also this integral is not path invariant. But if we combine both results together

$$\int_{\alpha\beta} d\log(x+y) d\log(1+x) + \int_{\alpha\beta} d\log(1+x) d\log(x+y) = 0.0521 , \quad (6.38)$$

we obtain the same numerical value as for path γ (6.33), therefore we have shown that our combination of integrals is indeed path invariant.

6.2. Goncharov Polylogarithms

If the alphabet is rational we are able to express our solution in terms of Goncharov's multiple polylogarithms (*GPL* for short) [131–134],

$$G(\vec{w}_n; x) \equiv G(w_1, \vec{w}_{n-1}; x) \equiv \int_0^x dt \frac{1}{t - w_1} G(\vec{w}_{n-1}; t), \quad (6.39)$$

$$G(\vec{0}_n; x) \equiv \frac{1}{n!} \log^n(x), \quad (6.40)$$

with \vec{w}_n being a vector of n arguments. The number n is referred to as the *weight* of $G(\vec{w}_n; x)$ and amounts to the number of iterated integrations needed to define it. Equivalently one has

$$\partial_x G(\vec{w}_n; x) = \partial_x G(w_1, \vec{w}_{n-1}; x) = \frac{1}{x - w_1} G(\vec{w}_{n-1}; x). \quad (6.41)$$

GPLs inherit the shuffle algebra relations from the Chen's iterated integrals

$$G(\vec{m}; x) G(\vec{n}; x) = G(\vec{m}; x) \sqcup \sqcup G(\vec{n}; x) = \sum_{\vec{p} = \vec{m} \sqcup \sqcup \vec{n}} G(\vec{p}; x), \quad (6.42)$$

where shuffle product $\vec{m} \sqcup \sqcup \vec{n}$ denotes all possible merges of \vec{m} and \vec{n} preserving their respective orderings. In the limit, where the argument of the *GPL* approaches the value of the leftmost weight, the *GPL* has a logarithmic divergence which we can make explicit with the help of the shuffle algebra

$$\lim_{x \rightarrow w_1} G(w_1, w_2, \dots, w_n; x) = \lim_{x \rightarrow w_1} (G(w_1; x)G(w_2, \dots, w_n; x) - G(w_2, w_1, w_3, \dots, w_n; x) - \dots - G(w_2, w_3, \dots, w_n, w_1; x)) , \quad (6.43)$$

where all *GPLs* are now finite in the limit except for $G(w_1; x) = \log(1 - \frac{x}{w_1})$ which is logarithmic divergent. In the case, where the first k weights are equal and diverge simultaneously, we can use the above formula recursively.

In the limit $x \rightarrow 0$ we encounter a different behavior. Here only the trailing zeros may develop a logarithmic divergence. But nevertheless we can use the shuffle algebra in the same manner as we did for the previous divergence

$$\lim_{x \rightarrow 0} G(w_1, \dots, w_n, 0; x) = \lim_{x \rightarrow 0} (G(0; x)G(w_1, \dots, w_n; x) - G(w_1, \dots, w_{n-1}, 0, w_n; x) - \dots - G(0, w_1, \dots, w_n; x)) . \quad (6.44)$$

It is important to note that a divergent limit and higher powers of *GPLs* do not necessarily commute

$$\lim_{x \rightarrow w_1} (G(w_1; x))^2 \neq \left(\lim_{x \rightarrow w_1} G(w_1; x) \right)^2 , \quad (6.45)$$

as it was described in [132].

If we have more than two dimensionless kinematic invariants at least one of them will appear in the weights. In certain cases it might be useful to exchange an invariant appearing in the weight with the one in the argument. This can be done by iteratively using the following formula

$$G(\vec{w}(x_2, \dots, x_n), x_1) = G(\vec{w}(x_2 = 0, x_3, \dots, x_n); x_1) + \int_0^{x_2} dt \frac{d}{dt} G(\vec{w}(x_2 = t, x_3, \dots, x_n); x_1) . \quad (6.46)$$

As an example let us consider a *GPL* with two invariants x and y

$$\begin{aligned} G(1, 1 - y; x) &= G(1, 1; x) + \int_0^y dt \frac{d}{dt} G(1, 1 - t; x) \\ &= G(1, 1; x) + \int_0^y dt \frac{d}{dt} \int_0^x \frac{dt_1}{t_1 - 1} \int_0^{t_1} \frac{dt_2}{t_2 - 1 + t} \\ &= G(1, 1; x) - \int_0^y dt \int_0^x \frac{dt_1}{t_1 - 1} \int_0^{t_1} \frac{dt_2}{(t_2 - 1 + t)^2} \\ &= G(1, 1; x) + \int_0^y dt \int_0^x \frac{dt_1}{t_1 - 1} \left(\frac{1}{t_1 - 1 + t} - \frac{1}{t - 1} \right) \\ &= G(1, 1; x) + \int_0^y dt \int_0^x dt_1 \left[\left(\frac{1}{t} - \frac{1}{t - 1} \right) \frac{1}{t_1 - 1} - \frac{1}{t} \frac{1}{t_1 - 1 + t} \right] \\ &= G(1, 1; x) + \int_0^y dt \left[\left(\frac{1}{t} - \frac{1}{t - 1} \right) G(1; x) - \frac{1}{t} G(1 - t; x) \right] \\ &= G(1, 1; x) + G(0; y)G(1; x) - G(1; y)G(1; x) \\ &\quad - \int_0^y \frac{dt}{t} [G(1 - x; t) + G(1; x) - G(1; t)] \\ &= G(1, 1; x) - G(0, 1 - x; y) - G(0, 1; y) - G(1; y)G(1; x) , \end{aligned} \quad (6.47)$$

where we expressed a *GPL* with y in the weight and x as the argument in terms of a *GPL* with x in the weight and y as the argument plus *GPLs* with constant weights and either y or x as the argument. We can use a very similar formula to compute limiting cases of *GPLs*

$$G(\vec{w}(x_2, \dots, x_n), x_1(x_2, \dots, x_n)) = G(\vec{w}(x_2 = 0, x_3, \dots, x_n); x_1(x_2 = 0, \dots, x_n)) + \int_0^{x_2} dt \frac{d}{dt} G(\vec{w}(x_2 = t, x_3, \dots, x_n); x_1(x_2 = t, x_3, \dots, x_n)) , \quad (6.48)$$

where we took the limit of x_1 going to some function of the other invariants $x_1 \rightarrow x_1(x_2, \dots, x_n)$. As an example of how this formula can be used let us consider

$$\begin{aligned}
G(1, 1-x; 1-x) &= G(1, 0; 0) + \int_1^x dt \frac{d}{dt} G(1, 1-t; 1-t) \\
&= \int_1^x dt \frac{d}{dt} \int_0^{1-t} \frac{dt_1}{t_1-1} \int_0^{t_1} \frac{dt_2}{t_2-1+t} \\
&= \int_1^x dt \left[\frac{1}{t} \int_0^{1-t} \frac{dt_2}{t_2-1+t} - \int_0^{1-t} \frac{dt_1}{t_1-1} \int_0^{t_1} \frac{dt_2}{(t_2-1+t)^2} \right] \\
&= \int_1^x dt \left(\frac{1}{t} - \frac{1}{t-1} \right) \int_0^{1-t} \frac{dt_1}{t_1-1} \\
&= \int_1^x dt \left(\frac{1}{t} - \frac{1}{t-1} \right) G(1; 1-t) \\
&= \int_1^x dt \left(\frac{1}{t} - \frac{1}{t-1} \right) G(0; t) \\
&= G(0, 0; x) - G(1, 0; x) + G(1, 0; 1) . \tag{6.49}
\end{aligned}$$

Here we also illustrated a subtlety when using formulas (6.48) and (6.46). We have to avoid using a lower integration bound, which introduces a divergent boundary term $G(\vec{w}(x_2 = 0, x_3, \dots, x_n); x_1(x_2 = 0, \dots, x_n))$ or $G(\vec{w}(x_2 = 0, x_3, \dots, x_n); x_1)$ respectively. A divergence could either be introduced when the leftmost weight matches the argument as it would have happened in the example above if we choose zero as a lower integration bound or when taking the limit introduces an additional trailing zero, while the argument is different from zero. In addition to the methods we discussed here we should also mention the symbol [129, 135–137] and coproduct formalism ([135, 138, 139] and [140] for a pedagogical introduction), which can be used to efficiently treat all relations between *GPLs*.

As a last point let us discuss how we can convert a given Chen's iterated integral with rational weights into *GPLs*. We can achieve this through a three step procedure

- 1) Split the path such that only one kinematic invariant varies linearly at a time using the path splitting formula (6.26)
- 2) Factor all arguments of the d logs over \mathbb{C} , such that the dependence on the varying kinematic invariant is linear
- 3) Use the conversion formula

$$\int_{\gamma} d\log(x_i + w_n) \dots d\log(x_i + w_1) = G\left(\frac{x_{i,0} + w_n}{x_{i,0} - x_{i,1}}, \dots, \frac{x_{i,0} + w_1}{x_{i,0} - x_{i,1}}; 1\right), \tag{6.50}$$

where the path γ only affects the invariant x_i and takes it from the start point $x_{i,0}$ to $x_{i,1}$.

Let us illustrate this procedure on an example. We can convert a weight two Chen's iterated integral depending on two invariants x and y into *GPLs* by splitting γ

$$\gamma : (x(t), y(t)) = (x_0 + t(x_1 - x_0), y_0 + t(y_1 - y_0)) , \quad (6.51)$$

into a path γ_1 , which takes x from x_0 to x_1 and a path γ_2 , which takes y from y_0 to y_1 ,

$$\gamma_1 : (x(t), y(t)) = (x_0 + t(x_1 - x_0), y_0) \quad (6.52)$$

$$\gamma_2 : (x(t), y(t)) = (x_1, y_0 + t(y_1 - y_0)) , \quad (6.53)$$

while leaving the other kinematic invariant constant. Using the path splitting formula we find

$$\begin{aligned} & \int_{\gamma} d\log(y + x^2) d\log(1 + x) = \\ & \int_{\gamma_1} d\log(y + x^2) d\log(1 + x) + \int_{\gamma_2} d\log(y + x^2) d\log(1 + x) + \int_{\gamma_2} d\log(y + x^2) \int_{\gamma_1} d\log(1 + x) , \\ & = \int_{\gamma_1} d\log(y + x^2) d\log(1 + x) + \int_{\gamma_2} d\log(y + x^2) \int_{\gamma_1} d\log(1 + x) , \end{aligned} \quad (6.54)$$

where we used that the path integral $\int_{\gamma_2} d\log(y + x^2) d\log(1 + x)$ vanishes, since path γ_2 only varies y .

In the second step we need to factorize $d\log(y + x^2)$, when we integrate over path γ_1 , since it is not linear in x

$$\begin{aligned} & \int_{\gamma} d\log(y + x^2) d\log(1 + x) = \\ & \int_{\gamma_1} d\log(x + i\sqrt{y}) d\log(1 + x) + \int_{\gamma_1} d\log(x - i\sqrt{y}) d\log(1 + x) + \int_{\gamma_2} d\log(y + x^2) \int_{\gamma_1} d\log(1 + x) . \end{aligned} \quad (6.55)$$

Now we are ready to using the formula (6.50) to convert the Chen's iterated integrals to *GPLs*

$$\begin{aligned} & \int_{\gamma} d\log(y + x^2) d\log(1 + x) = \\ & G\left(\frac{x_0 + i\sqrt{y_0}}{x_0 - x_1}, \frac{x_0 + 1}{x_0 - x_1}; 1\right) + G\left(\frac{x_0 - i\sqrt{y_0}}{x_0 - x_1}, \frac{x_0 + 1}{x_0 - x_1}; 1\right) + G\left(\frac{y_0 + x_1^2}{y_0 - y_1}; 1\right)G\left(\frac{x_0 + 1}{x_0 - x_1}; 1\right) . \end{aligned} \quad (6.56)$$

The steps we outlined above allow us to convert any Chen's iterated integral with rational $d\log$ arguments to *GPLs*.

6.3. Mixed Chen-Goncharov Representation

In principle eq. (6.4) completely determines the solution, which can be written in terms of Chen's iterated integrals along an arbitrary piecewise-smooth path (see the discussion below eq. (6.4)). The initial conditions $I(\vec{x}_0)$ can be computed analytically, if possible, or by means of numerical methods. The number of iterated integrals that have to be evaluated numerically can be minimized by the use of algebraic identities relating them. According to the discussion in section 6.1.1, the evaluation of the solution up to weight 4 requires in general 2 nested numerical integrations. But since numerical integrations can be rather expensive in computing time it is desirable to convert as many Chen's iterated integrals into *GPLs* as possible. In cases, where we have non-rational elements in our alphabet this will lead to a mixed representation, where the integrand is given as *GPLs*, but the integration is done over a path in sense of Chen's iterated integrals.

To reach this mixed representation, we have to exploit the property of path-independence of the coefficients of the ϵ -expansion of the solution eq. (6.4). In particular, eqs. (6.9)-(6.12) can be written in an equivalent alternative form using eq. (6.22):

$$I^{(k)}(\vec{x}) = I^{(k)}(\vec{x}_0) + \int_0^1 \left[\frac{dA(t)}{dt} I^{(k-1)}(\vec{x}_t) \right] dt, \quad (6.57)$$

where \vec{x}_t is the point $(x(t), y(t))$ along the curve identified by γ . We see that, in order to build the weight- k coefficient, one must perform a path integration over the weight- $(k-1)$ coefficient. The choice of such path is independent of the path used to compute the former because, as we have already discussed, each coefficient is a function of the sole endpoints. In other words, as far as the weight- k coefficient of the solution is concerned, we are free to choose the integration path independently for each of the k integrations (for each component of $I(\vec{x})$).

To see how this can be useful in our computation, we note that the letters η_i (in suitable variables, say \vec{x}) can be grouped in two classes. The first contains the letters that are rational in the components of \vec{x} and the second is the class of letters that are non-rational functions of the variables.

Starting from the weight-1 coefficient of the solution, we proceed as follows. As far as the involved η_i 's belong to the first class of letters, we can express the solution in terms of *GPLs*. We keep integrating in this manner until, at some weight k , the solution begins to involve non-rational η_i 's. At this point we proceed with the path integration as in (6.57). Within this approach, the weight $k-1$ solution is not expressed in terms of Chen's iterated integrals over an arbitrary path, but in terms of *GPLs*. We should note that as soon as we have more than two integrations over non-rational letters η_i , we can use the integration-by-parts formula (6.28) again to reduce the number of integrations by 1.

Magnus Series for Master Integrals

In this chapter we will shortly discuss the calculation of the master integrals for several processes with the help of differential equation method. In particular we will consider cases, where we used the algorithm based on the Magnus series to obtain a canonical basis for our process. The canonical differential equation was then solved in terms of *GPLs*, since the considered processes admitted a rational alphabet.

7.1. One-Loop Bhabha Scattering

As a first example let us consider the calculation of one-loop Bhabha scattering within the DE's method, which was already discussed in [141, 142], and more recently in Ref. [143]. A selection of the Feynman diagrams contributing to this process is depicted in Fig. 7.1. In this section, we compute a set of MI's with a slightly different definition from the ones in [143].

The diagrams depend on the invariants $s = (p_1 + p_2)^2$, $t = (p_1 + p_3)^2$, $u = (p_2 + p_3)^2$ and on the fermion mass m . Momentum conservation and the on-shellness of the external legs render these variables not independent as they are related by the condition $s + t + u = 4m^2$. The integrals can be expressed in terms of the Landau auxiliary variables x and y , defined as follows

$$s = -\frac{m^2(1-x)^2}{x}, \quad t = -\frac{m^2(1-y)^2}{y}. \quad (7.1)$$

We identify the following basis f of scalar integrals,

$$\begin{aligned} F_1 &= \epsilon \mathcal{T}_1, & F_2 &= \epsilon \mathcal{T}_2(t), & F_3 &= \epsilon \mathcal{T}_3(s), \\ F_4 &= \epsilon^2 \mathcal{T}_4(t), & F_5 &= \epsilon^2 \mathcal{T}_5(s, t), \end{aligned} \quad (7.2)$$

in terms of the integrals \mathcal{T} in Fig. 7.2. The basis F fulfills the following systems of differential equations ($\sigma = x, y$)

$$\partial_\sigma F(\epsilon, x, y) = A_\sigma(\epsilon, x, y)F(\epsilon, x, y), \quad A_\sigma(\epsilon, x, y) = D_{\sigma,0}(x, y) + \epsilon A_{\sigma,1}(x, y). \quad (7.3)$$

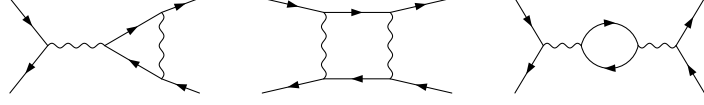


Figure 7.1.: Selection of Feynman diagrams entering Bhabha scattering at one loop.

Both systems are linear in ϵ and in both cases the $\mathcal{O}(\epsilon^0)$ term, $D_{\sigma,0}$, is diagonal. The systems can be brought in the canonical form by performing the transformation

$$F(\epsilon, x, y) = B_0 I(\epsilon, x, y) \quad B_0(x, y) = e^{\int_{x_0}^x d\tau D_{x,0}(\tau, y)} e^{\int_{y_0}^y d\tau D_{y,0}(x, \tau)} . \quad (7.4)$$

The new basis I,

$$\begin{aligned} I_1 &= F_1 , & I_2 &= t F_2 , & I_3 &= \sqrt{(-s)(4m^2 - s)} F_3 \\ I_4 &= \sqrt{(-t)(4m^2 - t)} F_4 , & I_5 &= \sqrt{(-s)(4m^2 - s)} t F_5 . \end{aligned} \quad (7.5)$$

fulfills the canonical systems

$$\partial_x I(\epsilon, x, y) = \epsilon \hat{A}_{x,1}(x, y) I(\epsilon, x, y) , \quad \partial_y I(\epsilon, x, y) = \epsilon \hat{A}_{y,1}(x, y) I(\epsilon, x, y) , \quad (7.6)$$

with

$$\begin{aligned} \hat{A}_{x,1}(x, y) &= \begin{pmatrix} 0 & 0 & 0 & 0 & 0 \\ 0 & 0 & 0 & 0 & 0 \\ \frac{1}{x} & 0 & \frac{1-x}{x(1+x)} & 0 & 0 \\ 0 & 0 & 0 & 0 & 0 \\ 0 & \frac{2}{x} & \frac{2(1-x)(1-y)^2}{(1+x)(x+y)(1+xy)} & -\frac{2(1-y)(1+y)}{(x+y)(1+xy)} & \frac{(1-x)(1-y)^2}{(1+x)(x+y)(1+xy)} \end{pmatrix} , \\ \hat{A}_{y,1}(x, y) &= \begin{pmatrix} 0 & 0 & 0 & 0 & 0 \\ 0 & \frac{1+y}{(1-y)y} & 0 & 0 & 0 \\ 0 & 0 & 0 & 0 & 0 \\ \frac{1}{y} & \frac{1}{y} & 0 & \frac{4}{(1-y)(y+1)} & 0 \\ 0 & 0 & -\frac{2x(1-y)(1+y)}{y(x+y)(1+xy)} & -\frac{2(1-x)(1+x)}{(x+y)(1+xy)} & \frac{(1+x)^2(1+y)}{(1-y)(x+y)(1+xy)} \end{pmatrix} . \end{aligned} \quad (7.7)$$

The two systems of DE's in Eq.(7.6) can be combined in a full differential form, along the lines of Ref. [143],

$$dI(\epsilon, x, y) = \epsilon d\hat{A}_1(x, y) I(\epsilon, x, y) , \quad (7.8)$$

where the matrix $\hat{A}_1(x, y)$ fulfills the relations,

$$\partial_x \hat{A}_1(x, y) = \hat{A}_{x,1}(x, y) , \quad \partial_y \hat{A}_1(x, y) = \hat{A}_{y,1}(x, y) . \quad (7.9)$$

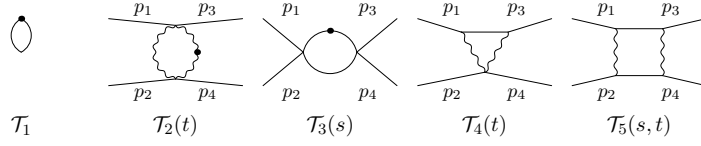


Figure 7.2.: MI's for the one-loop corrections to Bhabha scattering. All the external momenta are incoming. A dot denotes a squared propagator.

and the integrability condition

$$\epsilon \left(\partial_x \partial_y \hat{A}_1(x, y) - \partial_y \partial_x \hat{A}_1(x, y) \right) + \epsilon^2 \left[\partial_x \hat{A}_1(x, y), \partial_y \hat{A}_1(x, y) \right] = 0 . \quad (7.10)$$

The matrix $\hat{A}_1(x, y)$ is logarithmic in the variables x and y ,

$$\begin{aligned} \hat{A}_1(x, y) = & \mathbb{M}_1 \log(x) + \mathbb{M}_2 \log(1+x) + \mathbb{M}_3 \log(y) + \mathbb{M}_4 \log(1+y) + \\ & + \mathbb{M}_5 \log(1-y) + \mathbb{M}_6 \log(x+y) + \mathbb{M}_7 \log(1+xy) , \end{aligned} \quad (7.11)$$

with

$$\begin{aligned} \mathbb{M}_1 = & \begin{pmatrix} 0 & 0 & 0 & 0 & 0 \\ 0 & 0 & 0 & 0 & 0 \\ 1 & 0 & 1 & 0 & 0 \\ 0 & 0 & 0 & 0 & 0 \\ 0 & 2 & 0 & 0 & 0 \end{pmatrix} , & \mathbb{M}_2 = & \begin{pmatrix} 0 & 0 & 0 & 0 & 0 \\ 0 & 0 & 0 & 0 & 0 \\ 0 & 0 & -2 & 0 & 0 \\ 0 & 0 & 0 & 0 & 0 \\ 0 & 0 & -4 & 0 & -2 \end{pmatrix} , \\ \mathbb{M}_3 = & \begin{pmatrix} 0 & 0 & 0 & 0 & 0 \\ 0 & 1 & 0 & 0 & 0 \\ 0 & 0 & 0 & 0 & 0 \\ 1 & 1 & 0 & 0 & 0 \\ 0 & 0 & -2 & 0 & 0 \end{pmatrix} , & \mathbb{M}_4 = & \begin{pmatrix} 0 & 0 & 0 & 0 & 0 \\ 0 & 0 & 0 & 0 & 0 \\ 0 & 0 & 0 & 0 & 0 \\ 0 & 0 & 0 & 2 & 0 \\ 0 & 0 & 0 & 0 & 0 \end{pmatrix} , \\ \mathbb{M}_5 = & \begin{pmatrix} 0 & 0 & 0 & 0 & 0 \\ 0 & -2 & 0 & 0 & 0 \\ 0 & 0 & 0 & 0 & 0 \\ 0 & 0 & 0 & -2 & 0 \\ 0 & 0 & 0 & 0 & 2 \end{pmatrix} , & \mathbb{M}_6 = & \begin{pmatrix} 0 & 0 & 0 & 0 & 0 \\ 0 & 0 & 0 & 0 & 0 \\ 0 & 0 & 0 & 0 & 0 \\ 0 & 0 & 0 & 0 & 0 \\ 0 & 0 & -2 & -2 & -1 \end{pmatrix} , \\ \mathbb{M}_7 = & \begin{pmatrix} 0 & 0 & 0 & 0 & 0 \\ 0 & 0 & 0 & 0 & 0 \\ 0 & 0 & 0 & 0 & 0 \\ 0 & 0 & 0 & 0 & 0 \\ 0 & 0 & 2 & 2 & 1 \end{pmatrix} . \end{aligned} \quad (7.12)$$

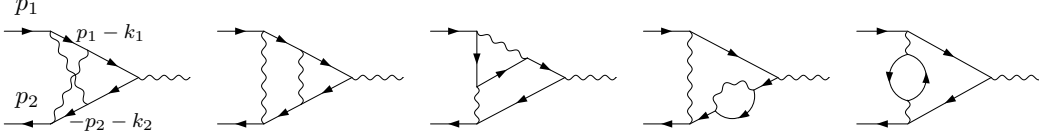


Figure 7.3.: Selection of Feynman diagrams entering the correction of the QED vertex at two loops. The internal momenta in the first diagram are oriented according to the fermion flow, while the external momenta are incoming.

The position of the non-zero entries of the sparse matrices \mathbb{M}_i agrees with the result obtained in Ref. [143]. The actual value of the non-zero entries, however, are different, owing to the different normalization of the elements of the basis of MI's. The solution of the system (7.8) can be computed along the lines of Ref. [143]. In particular, the solution is computed in the Euclidean region $0 < x, y < 1$ by using the analytic structures of the I_i and then extended in the physical region by analytic continuation [142].

7.2. Two-Loop QED Vertices

A basis of MI's for the electron form factor at two loops in QED [144] was computed in Ref. [145], for arbitrary kinematics and finite electron mass. The diagrams contributing to such corrections are depicted in Fig. 7.3 and depend on $s = (p_1 + p_2)^2$ and $p_1^2 = p_2^2 = m^2$. In this example we start from an alternative set of MI's,

$$\begin{aligned}
F_1 &= \epsilon^2 \mathcal{T}_1, & F_2 &= \epsilon^2 \mathcal{T}_2, & F_3 &= \epsilon^2 \mathcal{T}_3, & F_4 &= \epsilon^2 \mathcal{T}_4, & F_5 &= \epsilon^2 \mathcal{T}_5, \\
F_6 &= \epsilon^2 \mathcal{T}_6, & F_7 &= \epsilon^2 \mathcal{T}_7, & F_8 &= \epsilon^3 \mathcal{T}_8, & F_9 &= \epsilon^3 \mathcal{T}_9, & F_{10} &= \epsilon^2 \mathcal{T}_{10}, \\
F_{11} &= \epsilon^3 \mathcal{T}_{11}, & F_{12} &= \epsilon^3 \mathcal{T}_{12}, & F_{13} &= \epsilon^2 \mathcal{T}_{13}, & F_{14} &= \epsilon^3 \mathcal{T}_{14}, & F_{15} &= \epsilon^4 \mathcal{T}_{15}, \\
F_{16} &= \epsilon^4 \mathcal{T}_{16}, & F_{17} &= \epsilon^4 \mathcal{T}_{17}, & & & & & &
\end{aligned} \tag{7.13}$$

where the integrals \mathcal{T}_i are collected in Fig. 7.4. The system of differential equation for f , in the auxiliary variable x , defined through

$$s = -\frac{m^2(1-x)^2}{x}, \tag{7.14}$$

is linear in ϵ ,

$$\partial_x F(\epsilon, x) = A(\epsilon, x) F(\epsilon, x), \quad A(\epsilon, x) = A_0(x) + \epsilon A_1(x). \tag{7.15}$$

The canonical form can be obtained performing the transformation described in Section 5.2.3,

$$F(\epsilon, x) = B_0(x) I(\epsilon, x), \quad B_0(x) = e^{\Omega[A_0](x)}. \tag{7.16}$$

The new basis I is given by

$$\begin{aligned}
I_1 &= F_1, & g_2 &= \lambda_1 F_2, \\
I_3 &= (-s)\lambda_2 F_3, & g_4 &= m^2 F_4, \\
I_5 &= \lambda_1 \left(F_5 + \frac{F_6}{2} \right) - \frac{s}{2} F_6, & g_6 &= (-s)F_6, \\
I_7 &= m^2 F_7, & g_8 &= \lambda_1 F_8, \\
I_9 &= \lambda_1 F_9, & I_{10} &= \lambda_3 (2F_5 + F_6) + m^2 \lambda_2 F_{10}, \\
I_{11} &= \lambda_1 F_{11}, & g_{12} &= \lambda_1 F_{12}, \\
I_{13} &= 3 \left(m^2 - \frac{s}{2} \right) F_7 - s \lambda_2 F_{13}, & g_{14} &= (-s)\lambda_2 F_{14}, \\
I_{15} &= \lambda_1 F_{15}, & g_{16} &= \lambda_1 F_{16}, \\
I_{17} &= (-s)\lambda_2 F_{17}, & &
\end{aligned} \tag{7.17}$$

where

$$\lambda_1 = \sqrt{-s} \sqrt{4m^2 - s}, \quad \lambda_2 = (4m^2 - s), \quad \lambda_3 = \frac{\lambda_1 + \lambda_2}{4}. \tag{7.18}$$

The new basis of MI's obeys a system of DE's in the canonical form,

$$\partial_x I(\epsilon, x) = \epsilon \hat{A}_1(x) I(\epsilon, x), \quad \hat{A}_1(x) = \frac{\mathbb{M}_1}{x} + \frac{\mathbb{M}_2}{1+x} + \frac{\mathbb{M}_3}{1-x}, \tag{7.19}$$

with

$$\mathbb{M}_1 = \begin{pmatrix} 0 & 0 & 0 & 0 & 0 & 0 & 0 & 0 & 0 & 0 & 0 & 0 & 0 & 0 & 0 & 0 \\ 1 & 1 & 0 & 0 & 0 & 0 & 0 & 0 & 0 & 0 & 0 & 0 & 0 & 0 & 0 & 0 \\ 0 & 2 & 2 & 0 & 0 & 0 & 0 & 0 & 0 & 0 & 0 & 0 & 0 & 0 & 0 & 0 \\ 0 & 0 & 0 & 0 & 0 & 0 & 0 & 0 & 0 & 0 & 0 & 0 & 0 & 0 & 0 & 0 \\ -1 & 0 & 0 & 0 & 5 & -6 & 0 & 0 & 0 & 0 & 0 & 0 & 0 & 0 & 0 & 0 \\ 0 & 0 & 0 & 0 & 2 & -2 & 0 & 0 & 0 & 0 & 0 & 0 & 0 & 0 & 0 & 0 \\ 0 & 0 & 0 & 0 & 0 & 0 & 0 & 0 & 0 & 0 & 0 & 0 & 0 & 0 & 0 & 0 \\ -1 & 0 & 0 & -4 & 0 & -2 & 0 & -2 & 0 & 0 & 0 & 0 & 0 & 0 & 0 & 0 \\ 0 & 0 & 0 & -2 & 0 & 0 & 0 & 0 & 2 & 0 & 0 & 0 & 0 & 0 & 0 & 0 \\ -\frac{1}{2} & 0 & 0 & 0 & 1 & -2 & -3 & 0 & 0 & 3 & 3 & 0 & 0 & 0 & 0 & 0 \\ 0 & 0 & 0 & 0 & 1 & -1 & 2 & 0 & 0 & -2 & -2 & 0 & 0 & 0 & 0 & 0 \\ 0 & 0 & 0 & 0 & 0 & 0 & 1 & 0 & 0 & 0 & 0 & -1 & -1 & 0 & 0 & 0 \\ 0 & -1 & 0 & 0 & 0 & 0 & -3 & 0 & 0 & 0 & 0 & 3 & 3 & 0 & 0 & 0 \\ 0 & -1 & 0 & 0 & 1 & -\frac{1}{2} & 0 & 2 & 2 & 0 & 0 & 0 & 0 & 2 & 2 & 0 \\ 0 & 0 & 0 & 0 & 0 & \frac{1}{2} & 0 & -\frac{1}{2} & 0 & 0 & 0 & 0 & 0 & -1 & -1 & 0 \\ -\frac{1}{2} & 0 & 0 & -2 & -1 & 0 & -2 & 1 & 0 & 2 & 0 & -2 & 0 & 0 & -2 & -2 \\ 0 & 0 & 0 & 0 & -1 & \frac{1}{2} & 0 & 3 & -2 & 0 & -6 & -2 & 0 & 0 & -4 & -4 \end{pmatrix},$$

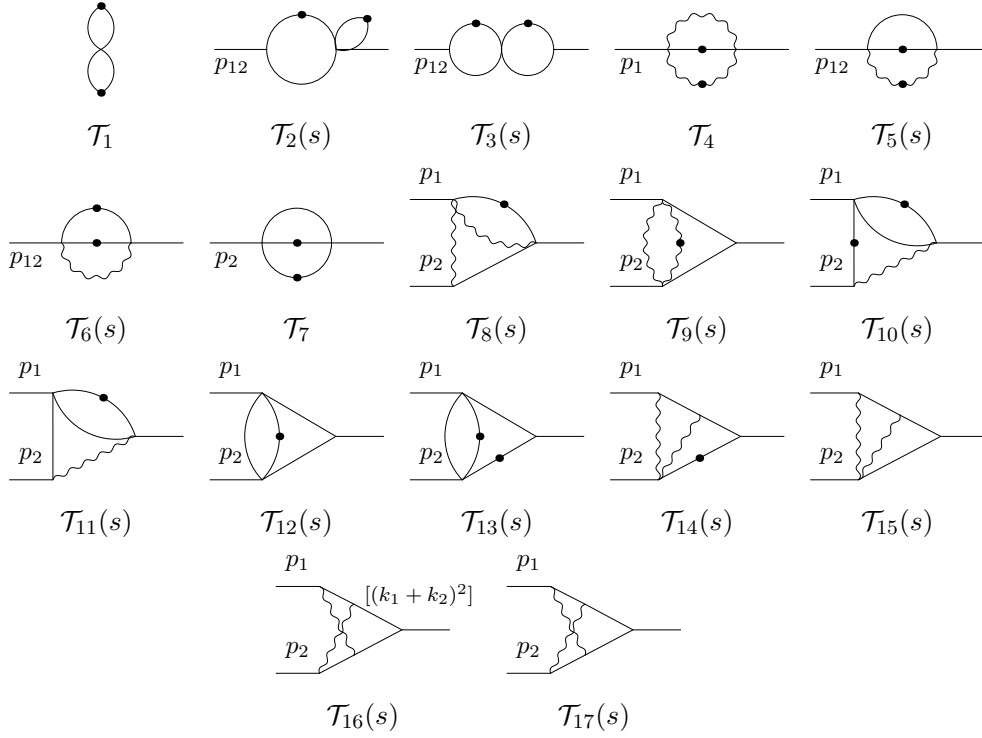


Figure 7.4.: MI's for the two-loop corrections to the QED vertex. All the external momenta depicted are incoming. In the integral \mathcal{T}_{16} the loop momenta k_1, k_2 are fixed according to the first diagram of Fig. 7.3 and a term $(k_1+k_2)^2$ has to be included in the numerator of the integrand. A dot indicates a squared propagator.

$$\mathbb{M}_2 = \begin{pmatrix}
 0 & 0 & 0 & 0 & 0 & 0 & 0 & 0 & 0 & 0 & 0 & 0 & 0 & 0 & 0 & 0 & 0 & 0 \\
 0 & -2 & 0 & 0 & 0 & 0 & 0 & 0 & 0 & 0 & 0 & 0 & 0 & 0 & 0 & 0 & 0 & 0 \\
 0 & 0 & -4 & 0 & 0 & 0 & 0 & 0 & 0 & 0 & 0 & 0 & 0 & 0 & 0 & 0 & 0 & 0 \\
 0 & 0 & 0 & 0 & 0 & 0 & 0 & 0 & 0 & 0 & 0 & 0 & 0 & 0 & 0 & 0 & 0 & 0 \\
 0 & 0 & 0 & 0 & -6 & 3 & 0 & 0 & 0 & 0 & 0 & 0 & 0 & 0 & 0 & 0 & 0 & 0 \\
 0 & 0 & 0 & 0 & 0 & 0 & 0 & 0 & 0 & 0 & 0 & 0 & 0 & 0 & 0 & 0 & 0 & 0 \\
 0 & 0 & 0 & 0 & 0 & 0 & 0 & 0 & 0 & 0 & 0 & 0 & 0 & 0 & 0 & 0 & 0 & 0 \\
 0 & 0 & 0 & 0 & 0 & 0 & 0 & 0 & 2 & 0 & 0 & 0 & 0 & 0 & 0 & 0 & 0 & 0 \\
 0 & 0 & 0 & 0 & 0 & 0 & 0 & 0 & 0 & -4 & 0 & 0 & 0 & 0 & 0 & 0 & 0 & 0 \\
 0 & 0 & 0 & 0 & 0 & -1 & \frac{1}{2} & 0 & 0 & 0 & -4 & 0 & 0 & 0 & 0 & 0 & 0 & 0 \\
 0 & 0 & 0 & 0 & 0 & 0 & 0 & 0 & 0 & 0 & 0 & 2 & 0 & 0 & 0 & 0 & 0 & 0 \\
 0 & 0 & 0 & 0 & 0 & 0 & 0 & 0 & 0 & 0 & 0 & 2 & 0 & 0 & 0 & 0 & 0 & 0 \\
 0 & 0 & 0 & 0 & 0 & 0 & 0 & -6 & 0 & 0 & 0 & 0 & 0 & -2 & 0 & 0 & 0 & 0 \\
 0 & 0 & 0 & 0 & 0 & 0 & 0 & 0 & 0 & 0 & 0 & 0 & 0 & 0 & -4 & 0 & 0 & 0 \\
 0 & 0 & 0 & 0 & 0 & 0 & 0 & 0 & 0 & 0 & 0 & 0 & 0 & 0 & 0 & 2 & 0 & 0 \\
 0 & 0 & 0 & 0 & 0 & 0 & 0 & 0 & 0 & 0 & 0 & 0 & 0 & 0 & 0 & 0 & 0 & 2 \\
 0 & 0 & 0 & 0 & 0 & 0 & 0 & 0 & 0 & 0 & 0 & 0 & 0 & 0 & 0 & 0 & 0 & -4
 \end{pmatrix},$$

$$\mathbb{M}_3 = \begin{pmatrix} 0 & 0 & 0 & 0 & 0 & 0 & 0 & 0 & 0 & 0 & 0 & 0 & 0 & 0 & 0 & 0 & 0 \\ 0 & 0 & 0 & 0 & 0 & 0 & 0 & 0 & 0 & 0 & 0 & 0 & 0 & 0 & 0 & 0 & 0 \\ 0 & 0 & 0 & 0 & 0 & 0 & 0 & 0 & 0 & 0 & 0 & 0 & 0 & 0 & 0 & 0 & 0 \\ 0 & 0 & 0 & 0 & 0 & 0 & 0 & 0 & 0 & 0 & 0 & 0 & 0 & 0 & 0 & 0 & 0 \\ 0 & 0 & 0 & 0 & 2 & -2 & 0 & 0 & 0 & 0 & 0 & 0 & 0 & 0 & 0 & 0 & 0 \\ 0 & 0 & 0 & 0 & 0 & -2 & 0 & 0 & 0 & 0 & 0 & 0 & 0 & 0 & 0 & 0 & 0 \\ 0 & 0 & 0 & 0 & 0 & 0 & 0 & 0 & 0 & 0 & 0 & 0 & 0 & 0 & 0 & 0 & 0 \\ 0 & 0 & 0 & 0 & 0 & 0 & 0 & -2 & 0 & 0 & 0 & 0 & 0 & 0 & 0 & 0 & 0 \\ 0 & 0 & 0 & 0 & 0 & 0 & 0 & 0 & 0 & 0 & 0 & 0 & 0 & 0 & 0 & 0 & 0 \\ 0 & 0 & 0 & 0 & 0 & 0 & -6 & 0 & 0 & 2 & 0 & 0 & 0 & 0 & 0 & 0 & 0 \\ 0 & 0 & 0 & 0 & 0 & 0 & 0 & 0 & 0 & 0 & -2 & 0 & 0 & 0 & 0 & 0 & 0 \\ 0 & 0 & 0 & 0 & 0 & 0 & 0 & 0 & 0 & 0 & 0 & 0 & 0 & 0 & 0 & 0 & 0 \\ 0 & 0 & 0 & 0 & 0 & 0 & -12 & 0 & 0 & 0 & 0 & 0 & 4 & 0 & 0 & 0 & 0 \\ 0 & 0 & 0 & 0 & 0 & 0 & 0 & 0 & 0 & 0 & 0 & 0 & 0 & 0 & 0 & 0 & 0 \\ 0 & 0 & 0 & 0 & 0 & 0 & 0 & -1 & 0 & 0 & 0 & 0 & 0 & 0 & 0 & 0 & 0 \\ 0 & 0 & 0 & 0 & 0 & 0 & 0 & 2 & 0 & 0 & 0 & -4 & 0 & 0 & -4 & -2 & 0 \\ 0 & 0 & 0 & 0 & 0 & 0 & 0 & 0 & 0 & 0 & 0 & 0 & 0 & 0 & 0 & 0 & 4 \end{pmatrix}. \quad (7.20)$$

The solution of the system can be expressed as Dyson series, as well as Magnus series, in terms of one-dimensional Harmonic Polylogarithms (HPL's) [132], which are a special case of the discussed *GPL's*. The requirements that the MI's are real-valued in the Euclidean region and regular in $x = 1$ ($s = 0$), or simply the matching against the known integrals at $x = 1$, fix all but three boundary conditions, corresponding to the *constant* MI's I_1 , I_4 and I_7 (that do not depend on x). The integrals I_1 and I_4 can be easily computed by direct integration, while I_7 can be determined from the results of Ref. [146]. Our results were checked analytically, using the code HPL [147, 148], against the results available in the literature [145]. The expressions of the transcendentially homogenous MI's I are shown in Appendix B.

7.3. Massless $2 \rightarrow 2$ Scattering at Two-Loop

The evaluation of the two-loop MIs for $2 \rightarrow 2$ scattering has already been considered in the literature [65, 66, 74, 149] and more recently a set of MI's obeying a canonical differential equations was presented in [1, 77]. Here we will present a slightly different choice of master integrals, which is motivated by the leading singularity of the non-planar box as described in section 5.1.1.

The routings for planar and non-planar two-loop diagrams can be defined in terms of the following sets of denominators D_n , where k_i ($i = 1, 2$) are the loop momenta, and p_i ($i = 1, \dots, 4$) are the external momenta:

- For the planar topology (figure 7.5 *a*), we have:

$$\begin{aligned} D_1 &= k_1^2, & D_2 &= k_2^2, & D_3 &= (k_1 + p_1)^2, & D_4 &= (k_1 - k_2)^2, \\ D_5 &= (k_1 + p_1 + p_2)^2, & D_6 &= (k_2 + p_1 + p_2)^2, & D_7 &= (k_2 - p_3)^2, \\ D_8 &= (k_2 + p_1)^2, & D_9 &= (k_1 - p_3)^2. \end{aligned} \quad (7.21)$$

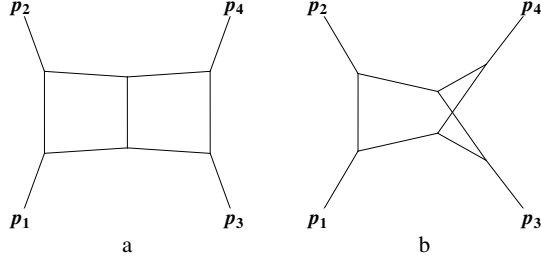


Figure 7.5.: The two parent topologies for massless $2 \rightarrow 2$ scattering.

- For the non-planar topology (figure 7.5 b), we have:

$$\begin{aligned}
 D_1 &= k_1^2, & D_2 &= k_2^2, & D_3 &= (k_1 + p_1)^2, & D_4 &= (k_2 - p_3)^2, \\
 D_5 &= (k_1 - k_2)^2, & D_6 &= (k_1 + p_1 + p_2)^2, & D_7 &= (k_1 - k_2 - p_4)^2, \\
 D_8 &= (k_2 + p_1)^2, & D_9 &= (k_1 - p_3)^2.
 \end{aligned} \tag{7.22}$$

The integrals, in this case, are functions of the invariants $s = (p_1 + p_2)^2$, $t = (p_1 + p_3)^2$, and $u = (p_2 + p_3)^2$, with $p_i^2 = 0$, and $s + t + u = 0$.

We adopt the following initial choice of MI's,

$$\begin{aligned}
 F_1 &= \epsilon^2 \mathcal{T}_1, & F_2 &= \epsilon^2 \mathcal{T}_2, & F_3 &= \epsilon^2 \mathcal{T}_3, \\
 F_4 &= \epsilon^2 \mathcal{T}_4, & F_5 &= \epsilon^3 \mathcal{T}_5, & F_6 &= \epsilon^4 \mathcal{T}_6, \\
 F_7 &= \epsilon^4 \mathcal{T}_7, & F_8 &= \epsilon^4 \mathcal{T}_8, & F_9 &= \epsilon^3 \mathcal{T}_9, \\
 F_{10} &= \epsilon^3 \mathcal{T}_{10}, & F_{11} &= \epsilon^4 \mathcal{T}_{11}, & F_{12} &= \epsilon^4 \mathcal{T}_{12}, \\
 F_{13} &= \epsilon^4 \mathcal{T}_{13}, & F_{14} &= \epsilon^4 \mathcal{T}_{14}, & F_{15} &= \epsilon^4 u \mathcal{T}_{15},
 \end{aligned} \tag{7.23}$$

where the integrals \mathcal{T}_i correspond to the diagrams in Fig. 7.6. The set F of MI's obeys a system of differential equations the variable x , defined as,

$$x = -\frac{t}{s}, \tag{7.24}$$

which is linear in ϵ . According to the procedure in Section 5.2.3, we can build the matrix

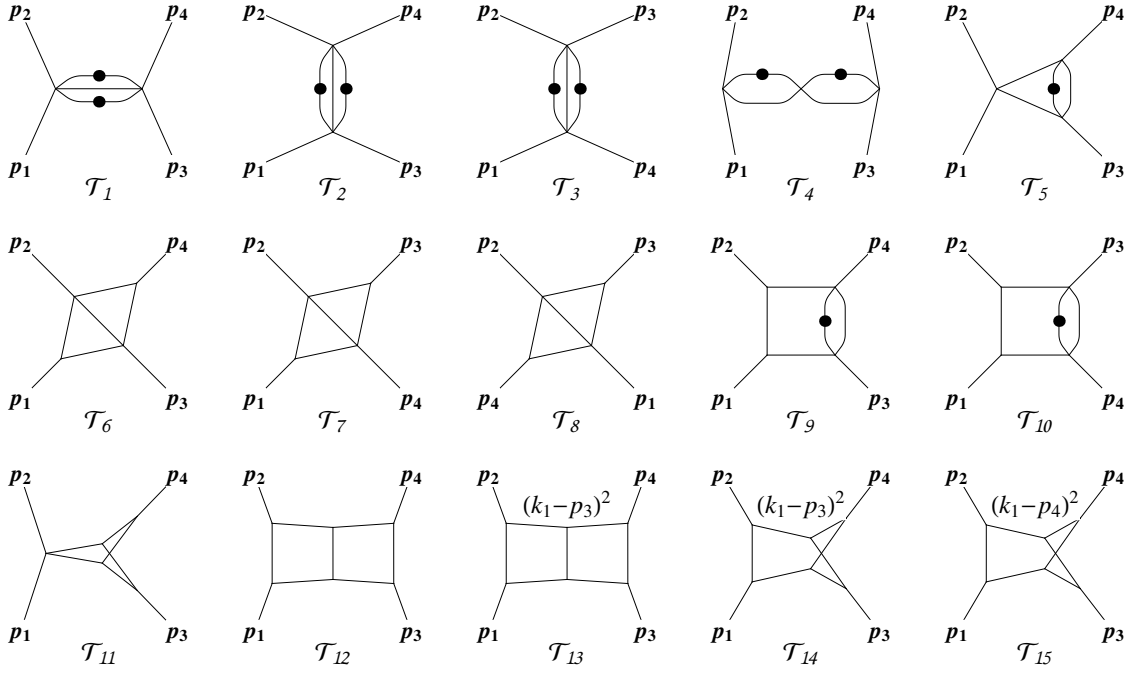


Figure 7.6.: MI's for the two-loop $2 \rightarrow 2$ scattering. All the external momenta depicted are incoming. A dot indicates a squared propagator.

$B_0(x)$ ruling the change of basis $F(\epsilon, x) = B_0(x)I(\epsilon, x)$, so that the new MI's,

$$\begin{aligned}
 I_1 &= s F_1, & I_2 &= -t F_2, & I_3 &= u F_3, \\
 I_4 &= s^2 F_4, & I_5 &= s F_5, & I_6 &= u F_6, \\
 I_7 &= -t F_7, & I_8 &= s F_8, & I_9 &= -s t F_9, \\
 I_{10} &= s u F_{10}, & I_{11} &= s^2 F_{11}, & I_{12} &= -s^2 t F_{12}, \\
 I_{13} &= s^2 F_{13}, & I_{14} &= s u F_{14}, & I_{15} &= -s t F_{15},
 \end{aligned} \tag{7.25}$$

obey the canonical system,

$$dI = \epsilon dA_x I, \quad dA_x = M_1 d\log(x) + M_2 d\log(1-x), \tag{7.26}$$

with

$$\begin{aligned}
\mathbb{M}_1 = & \begin{pmatrix} 0 & 0 & 0 & 0 & 0 & 0 & 0 & 0 & 0 & 0 & 0 & 0 & 0 & 0 \\ 0 & -2 & 0 & 0 & 0 & 0 & 0 & 0 & 0 & 0 & 0 & 0 & 0 & 0 \\ 0 & 0 & 0 & 0 & 0 & 0 & 0 & 0 & 0 & 0 & 0 & 0 & 0 & 0 \\ 0 & 0 & 0 & 0 & 0 & 0 & 0 & 0 & 0 & 0 & 0 & 0 & 0 & 0 \\ 0 & 0 & 0 & 0 & 0 & 0 & 0 & 0 & 0 & 0 & 0 & 0 & 0 & 0 \\ \frac{1}{2} & 0 & 0 & 0 & 0 & 0 & -2 & 0 & 0 & 0 & 0 & 0 & 0 & 0 \\ 0 & 0 & 0 & 0 & 0 & 0 & 0 & 2 & 0 & 0 & 0 & 0 & 0 & 0 \\ 0 & 0 & 0 & 0 & 0 & 0 & 0 & 0 & -2 & 0 & 0 & 0 & 0 & 0 \\ 0 & 0 & 0 & 0 & 0 & 0 & 0 & 0 & 0 & -2 & 0 & 0 & 0 & 0 \\ 0 & 0 & 0 & 0 & 0 & 0 & 0 & 0 & 0 & 0 & 1 & 0 & 0 & 0 \\ 0 & 0 & 0 & 0 & 0 & 0 & 0 & 0 & 0 & 0 & 0 & 0 & 0 & 0 \\ 3 & -3 & 0 & 0 & 0 & -12 & 0 & 0 & -4 & 0 & 0 & -2 & 0 & 0 \\ -3 & 3 & 0 & -1 & 3 & 18 & 0 & 0 & 4 & 0 & 0 & 1 & 1 & 0 \\ 3 & 3 & 0 & 0 & 0 & -12 & 0 & 6 & -2 & 0 & -1 & 0 & 0 & 1 \\ 3 & 3 & 0 & 0 & 0 & -12 & 0 & -6 & -2 & 0 & 0 & 0 & 0 & -2 \end{pmatrix}, \\
\mathbb{M}_2 = & \begin{pmatrix} 0 & 0 & 0 & 0 & 0 & 0 & 0 & 0 & 0 & 0 & 0 & 0 & 0 & 0 \\ 0 & 0 & 0 & 0 & 0 & 0 & 0 & 0 & 0 & 0 & 0 & 0 & 0 & 0 \\ 0 & 0 & 2 & 0 & 0 & 0 & 0 & 0 & 0 & 0 & 0 & 0 & 0 & 0 \\ 0 & 0 & 0 & 0 & 0 & 0 & 0 & 0 & 0 & 0 & 0 & 0 & 0 & 0 \\ 0 & 0 & 0 & 0 & 0 & 0 & 0 & 0 & 0 & 0 & 0 & 0 & 0 & 0 \\ 0 & 0 & 0 & 0 & 0 & -2 & 0 & 0 & 0 & 0 & 0 & 0 & 0 & 0 \\ -\frac{1}{2} & 0 & 0 & 0 & 0 & 0 & 2 & 0 & 0 & 0 & 0 & 0 & 0 & 0 \\ 0 & 0 & 0 & 0 & 0 & 0 & 0 & 2 & 0 & 0 & 0 & 0 & 0 & 0 \\ 0 & 0 & 0 & 0 & -3 & 0 & 0 & 0 & -1 & 0 & 0 & 0 & 0 & 0 \\ 0 & 0 & 0 & 0 & 0 & 0 & 0 & 0 & 0 & 2 & 0 & 0 & 0 & 0 \\ 0 & 0 & 0 & 0 & 0 & 0 & 0 & 0 & 0 & 0 & 0 & 0 & 0 & 0 \\ 6 & -3 & 0 & -2 & 6 & -12 & 0 & 0 & -4 & 0 & 0 & -2 & -2 & 0 \\ -3 & 3 & 0 & 1 & 3 & 18 & 0 & 0 & 4 & 0 & 0 & 1 & 1 & 0 \\ -3 & 3 & 0 & 0 & 0 & 0 & 12 & 6 & 0 & 2 & 0 & 0 & 0 & 2 \\ -3 & 3 & 0 & 0 & 0 & 0 & 12 & -6 & 0 & 2 & 1 & 0 & 0 & 1 \end{pmatrix}. \quad (7.27)
\end{aligned}$$

The solution of the system can be expressed as Dyson series, as well as Magnus series, in terms of one-dimensional HPL's [132]. All MI's have been computed in the scattering kinematics, i.e. $s > 0$, $t < 0$, $u < 0$ with $|s| > |t|$, which gives $0 < x < 1$. As long as the planar sub topologies are concerned, one can fix the boundary conditions using the regularity properties of the integrals in some special kinematical points. On the other hand, the analyticity structure of the crossed box is more complicated, since it involves at the same time cuts in all three Mandelstam variables s , t , u . Nevertheless, in this particular case, the boundaries can be fixed by direct comparison with the results presented in [66, 149].

Associated Higgs plus One Jet Production

8.1. Introduction

In this chapter, we apply Magnus exponential method to solve the system of differential equations fulfilled by 85 MI's required for the determination of the three-loop ladder box integrals with one massive leg, shown in figure 8.2b, and of the tower of integrals associated to their subtopologies, depicted in figures 8.7–8.9. All propagators are massless. The solution of the system is finally determined after fixing the values of the otherwise arbitrary constants that naturally arise from solving differential equations. In the considered case, boundary conditions are obtained by imposing the *regularity* of the MI's around unphysical singularities, ruling out the divergent behavior of the general solution of the systems.

Among the evaluated 85 MI's, there are 16 vertex-like integrals with two off-shell legs not yet considered in the literature, and 10 one-scale vertex- and bubble-like integrals, which had already been computed by means of Mellin-Barnes integral representation [150–153]. In general, homogeneous differential equations for single scale integrals carry only information on the scaling behavior of the solution. The determination of the boundary constants for such differential equations amounts to the evaluation of the integrals themselves by other means. Within a multi-scale problem, where integrals may depend on more than one external invariant, single-scale integrals enter the regularity conditions (or equivalently could be the limit) of the multi-scale ones [146, 154]. These relations, entangling single- and multi-scale functions, can be exploited to determine the arbitrary constants of the single-scale integrals, or at least to reduce the number of independent single-scale integrals that needs to be computed by alternative methods, other than differential equations. Therefore, solving multi-scale systems of differential equations yields the simultaneous determination of single- and multi-scale MI's, which are finally expressed in terms of a few single-scale MI's, to be independently provided. In fact, the considered case of 85 MI's requires only 2 one-scale integrals as external *input*.

The MI's hereby computed can be considered the first contributions to the next-to-next-to-next-to-leading order (N^3 LO) virtual corrections to scattering processes like the three-jet

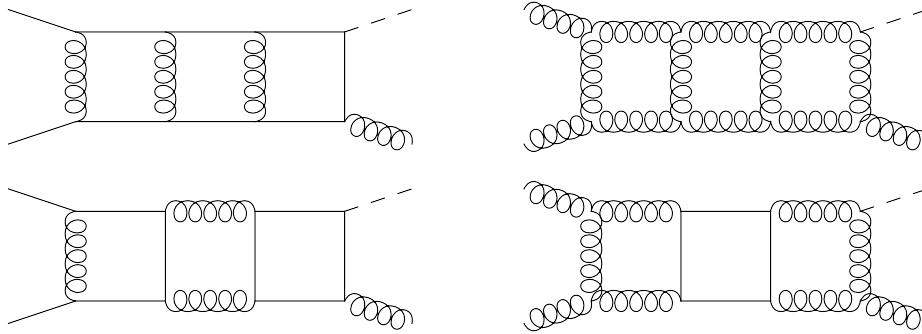


Figure 8.1.: This figure shows some Feynman diagrams, which contribute to the three-loop virtual corrections to Higgs production associated with one jet in the heavy top limit. solid lines represent massless quark propagators; curly lines stand for the gluon propagators; dashed external lines represent the Higgs boson.

production from vector boson decay, $V^* \rightarrow jjj$, as well as the Higgs plus one-jet production in gluon fusion, $pp \rightarrow Hj$, currently computed at NNLO accuracy in refs. [155–158] and refs. [159,160] respectively. The collinear limits of the MI’s we present enter the computation of the three-loop one-particle splitting amplitudes, currently known at two-loop order [161]. Such amplitudes also serve as an ingredient for the derivation, following the procedure of ref. [162], of the N³LO Altarelli-Parisi splitting kernel.

The results of the considered box-type integrals and of the tower of vertex- and bubble-type integrals associated to subtopologies are given as a Taylor series expansion in ϵ . The coefficients of the series are expressed in terms of uniform weight combinations of transcendental constants and generalised harmonic polylogarithms [132,133,163] up to weight 6.

We also present the calculation of the two-loop one-mass planar box diagram in figure 8.2a, giving the result for the corresponding MI’s, whose topologies are depicted in figure 8.7. We provide higher orders ϵ -expansions w.r.t. the expressions available in the literature [74,164].

We used the computer code `Reduze 2` [106,165] for solving the system of integration-by-parts relations and generating the system of differential equations. The analytic results of the MI’s at two- and three-loop can be numerically evaluated by means of `GiNaC` [134,166] and are found in agreement with the outcome of the direct numerical integrations carried out by `FIESTA 3` [60,167] (within per-mille level of accuracy).

8.2. Differential Equations and Magnus Exponential

All Feynman integrals belonging to the topologies which we consider for this process can be defined in terms of the following sets of denominators \mathcal{D}_n (k_i are the loop momenta). For

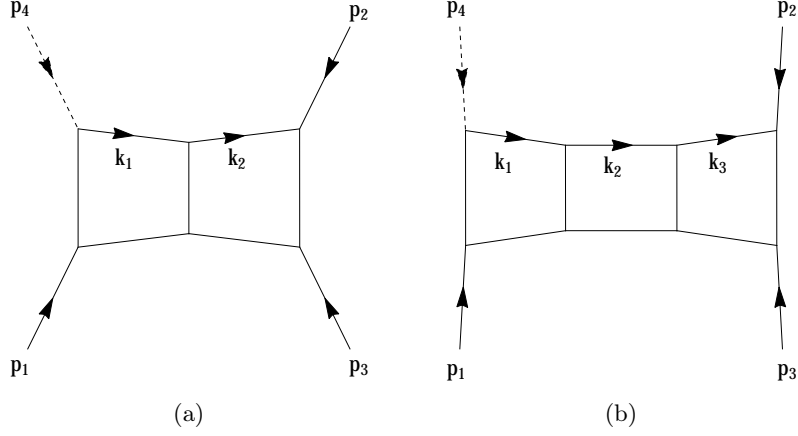


Figure 8.2.: The two-loop and three-loop ladder box diagram, with one off-shell leg: the solid lines stand for massless particles; the dashed line represents a massive particle. Momentum conservation is $\sum_{i=1}^4 p_i = 0$, with $p_i^2 = 0$ ($i = 1, 2, 3$) and $p_4^2 = m^2$.

the planar two-loop ladder diagram in figure 8.2a, one has

$$\begin{aligned} \mathcal{D}_1 &= k_1^2, & \mathcal{D}_2 &= k_2^2, & \mathcal{D}_3 &= (k_1 - k_2)^2, & \mathcal{D}_4 &= (k_2 + p_2)^2, \\ \mathcal{D}_5 &= (k_1 + p_2 + p_3)^2, & \mathcal{D}_6 &= (k_2 + p_2 + p_3)^2, & \mathcal{D}_7 &= (k_1 + p_1 + p_2 + p_3)^2, \end{aligned} \quad (8.1)$$

supplemented by the auxiliary denominators

$$\mathcal{D}_8 = (k_1 + p_2)^2, \quad \mathcal{D}_9 = (k_2 + p_1 + p_2 + p_3)^2. \quad (8.2)$$

For the first non-planar graph in figure 8.3a, we have

$$\begin{aligned} \mathcal{D}_1 &= k_1^2, & \mathcal{D}_2 &= k_2^2, & \mathcal{D}_3 &= (k_1 - k_2)^2, & \mathcal{D}_4 &= (k_2 + p_2)^2, \\ \mathcal{D}_5 &= (k_1 + p_1 + p_2)^2, & \mathcal{D}_6 &= (k_1 - k_2 + p_1)^2, & \mathcal{D}_7 &= (k_1 + p_1 + p_2 + p_3)^2, \end{aligned} \quad (8.3)$$

supplemented by the auxiliary denominators

$$\mathcal{D}_8 = (k_1 + p_2)^2, \quad \mathcal{D}_9 = (k_2 + p_1 + p_2 + p_3)^2. \quad (8.4)$$

For the second non-planar graph in figure 8.3b, we have

$$\begin{aligned} \mathcal{D}_1 &= k_1^2, & \mathcal{D}_2 &= k_2^2, & \mathcal{D}_3 &= (k_1 - k_2)^2, & \mathcal{D}_4 &= (k_2 + p_2)^2, \\ \mathcal{D}_5 &= (k_1 - k_2 + p_3)^2, & \mathcal{D}_6 &= (k_2 + p_1 + p_2)^2, & \mathcal{D}_7 &= (k_1 + p_1 + p_2 + p_3)^2, \end{aligned} \quad (8.5)$$

supplemented by the auxiliary denominators

$$\mathcal{D}_8 = (k_1 + p_2)^2, \quad \mathcal{D}_9 = (k_2 + p_1 + p_2 + p_3)^2. \quad (8.6)$$

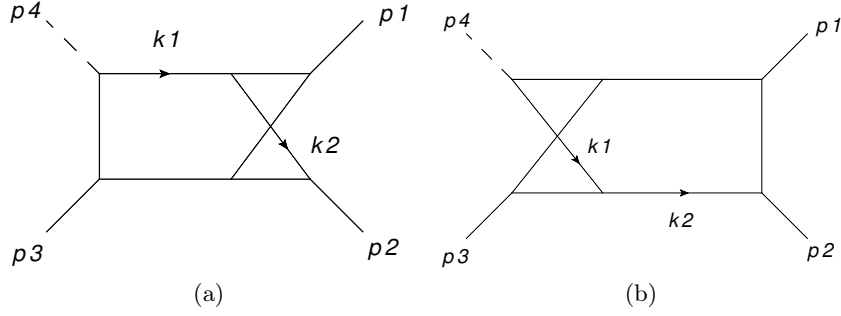


Figure 8.3.: The two non-planar topologies at two-loop, with one off-shell leg: the solid lines stand for massless particles; the dashed line represents a massive particle. Momentum conservation is $\sum_{i=1}^4 p_i = 0$, with $p_i^2 = 0$ ($i = 1, 2, 3$) and $p_4^2 = m^2$.

For the three-loop ladder diagram in figure 8.2b one has instead

$$\begin{aligned} \mathcal{D}_1 &= k_1^2, & \mathcal{D}_2 &= k_2^2, & \mathcal{D}_3 &= k_3^2, & \mathcal{D}_4 &= (k_1 - k_2)^2, \\ \mathcal{D}_5 &= (k_2 - k_3)^2, & \mathcal{D}_6 &= (k_3 + p_2)^2, & \mathcal{D}_7 &= (k_1 + p_2 + p_3)^2, \\ \mathcal{D}_8 &= (k_2 + p_2 + p_3)^2, & \mathcal{D}_9 &= (k_3 + p_2 + p_3)^2, & \mathcal{D}_{10} &= (k_1 + p_1 + p_2 + p_3)^2, \end{aligned} \quad (8.7)$$

supplemented by the auxiliary denominators

$$\begin{aligned} \mathcal{D}_{11} &= (k_1 + p_2)^2, & \mathcal{D}_{12} &= (k_2 + p_2)^2, & \mathcal{D}_{13} &= (k_2 + p_1 + p_2 + p_3)^2, \\ \mathcal{D}_{14} &= (k_3 + p_1 + p_2 + p_3)^2, & \mathcal{D}_{15} &= (k_3 - k_1)^2. \end{aligned} \quad (8.8)$$

In the following we consider ℓ -loop Feynman integrals built out of p of the above denominators, each raised to some integer power, of the form

$$\int \widetilde{d^d k_1} \dots \widetilde{d^d k_\ell} \frac{1}{\mathcal{D}_{a_1}^{n_1} \dots \mathcal{D}_{a_p}^{n_p}}, \quad (8.9)$$

where the integration measure is defined as

$$\widetilde{d^d k_i} \equiv \frac{d^d k_i}{(2\pi)^d} \left(\frac{i S_\epsilon}{16\pi^2} \right)^{-1} (-m^2)^\epsilon, \quad \text{with } S_\epsilon \equiv (4\pi)^\epsilon \frac{\Gamma(1+\epsilon)\Gamma^2(1-\epsilon)}{\Gamma(1-2\epsilon)}. \quad (8.10)$$

The two- and three-loop MI's, respectively depicted in figure 8.4–8.6 and figures. 8.7–8.9, are functions of the kinematic variables

$$s = (p_2 + p_3)^2, \quad t = (p_1 + p_3)^2, \quad u = (p_1 + p_2)^2, \quad m^2 = (p_1 + p_2 + p_3)^2, \quad (8.11)$$

with $p_i^2 = 0$ ($i = 1, 2, 3$) and $p_4^2 = (p_1 + p_2 + p_3)^2$, fulfilling $s + t + u = m^2$. For convenience, we define the dimensionless ratios

$$x \equiv \frac{s}{m^2}, \quad y \equiv \frac{t}{m^2}, \quad z \equiv \frac{u}{m^2}, \quad \text{with } x + y + z = 1. \quad (8.12)$$

For planar topologies, like the ones we consider, one can always choose the Euclidean kinematic region $m^2, s, t, u < 0$ such that the MI's are real. For definiteness, we work in the region $0 < y < 1, 0 < x < 1 - y$ (or equivalently $0 < x < 1, 0 < y < 1 - x$). The analytic continuation of our results to regions of physical interests can be performed by generalizing to higher weights the procedure of ref. [168].

The sets of MI's we choose to work with (see sections 8.4 and 8.5) obey ϵ -linear systems of first order differential equations in the kinematic variables ($\sigma = x, y$),

$$\partial_\sigma F(\epsilon, m^2, x, y) = A_\sigma(\epsilon, m^2, x, y) F(\epsilon, m^2, x, y), \quad (8.13)$$

$$\text{with } A_\sigma(\epsilon, m^2, x, y) = A_{\sigma,0}(m^2, x, y) + \epsilon A_{\sigma,1}(m^2, x, y). \quad (8.14)$$

Given that m^2 is the only dimensionful variable, the differential equation in m^2 is related to the scaling equation. A factor $(-m^2)^{-\ell\epsilon}$ is already included in integration measure (8.10), therefore for each F_i we simply have

$$\partial_{m^2} F_i(m^2, x, y, \epsilon) = -\frac{n_i}{m^2} F_i(\epsilon, m^2, x, y), \quad (8.15)$$

where n_i is the dimension of the integral F_i in units of a squared mass.

8.3. Canonical System

With the help of the Magnus expansion we can find a transformation, which rotates our differential equation (8.14) into the canonical form

$$\partial_\sigma I(\epsilon, m^2, x, y) = \epsilon \hat{A}_\sigma(m^2, x, y) I(\epsilon, m^2, x, y). \quad (8.16)$$

This two partial-derivative systems satisfied by the new set of MI's, $I = B^{-1}F$, can be conveniently combined in an exact differential form,

$$dI(\epsilon, x, y) = \epsilon d\hat{A}(x, y) I(\epsilon, x, y), \quad d\hat{A} \equiv \hat{A}_x dx + \hat{A}_y dy, \quad (8.17)$$

where $\hat{A}(x, y)$ is logarithmic in the variables x and y ,

$$\begin{aligned} \hat{A}(x, y) = & \mathbb{M}_1 \log(x) + \mathbb{M}_2 \log(1-x) + \mathbb{M}_3 \log(y) + \mathbb{M}_4 \log(1-y) + \\ & + \mathbb{M}_5 \log\left(\frac{x+y}{x}\right) + \mathbb{M}_6 \log\left(\frac{1-x-y}{1-x}\right). \end{aligned} \quad (8.18)$$

The matrices \mathbb{M}_i are $n \times n$ sparse matrices with purely rational entries, where n is the number of MI's. The value of n depends on the number of loops, and it amounts to $n = 4, 18, 85$, respectively at one-, two- and three-loop. The arguments of the logarithms are defined as *letters*, and the set of letters

$$\{x, 1-x, y, 1-y, x+y, 1-x-y\} \quad (8.19)$$

constitutes the *alphabet*. We observe that this alphabet is common both to the two- and the three loop cases. At one-loop [74], although not shown here, \mathbb{M}_5 is absent, while at two-loop \mathbb{M}_5 has only one non-vanishing entry.

The solution of (8.16, 8.17) can be expressed as a Dyson series in ϵ ,

$$I(x, y, \epsilon) = \left(1 + \sum_{n=1}^{\infty} \epsilon^n Y_n(x, y) \right) I_0(\epsilon), \quad (8.20)$$

where the (matrix) coefficients of the series can be written as the iterated line integral,

$$Y_n(x, y) \equiv \int_{\gamma} d\hat{A}_1 d\hat{A}_2 \cdots d\hat{A}_n, \quad (8.21)$$

where $d\hat{A}_i \equiv d\hat{A}(x_i, y_i)$. Equivalently, the solution admits a representation in terms of the Magnus exponential

$$I(x, y, \epsilon) = e^{\Omega[\epsilon d\hat{A}](x, y)} I_0(\epsilon), \quad (8.22)$$

where the vector $I_0(\epsilon) \equiv I(x_0, y_0, \epsilon)$ corresponds to the boundary values of the MI's. This form is very suggestive, as Magnus exponential can be considered as an *evolution* operator, like in the unitary formalism, that brings the MI's g from their initial, boundary values to the considered point in the (x, y) -plane.¹

For definiteness, we integrate the exact differential form (8.17) from an arbitrary point (x_0, y_0) to (x, y) , along the broken path composed of the two segments in which one of the variables is kept constant. The integration is performed order by order in ϵ , up to a multiplicative vector of unknown constants. The latter are fixed by requiring the regularity of $g(x, y, \epsilon)$ at the pseudothresholds (see section 8.6).

8.4. Two-Loop Master Integrals

8.4.1. Planar Topology

A set of 18 two-loop MI's for the planar massless box integrals with one massive leg of figure 8.2a was first computed in refs. [74, 164]. We present the calculation of an alternative,

¹In this case, the evolution has to be understood like the variation w.r.t. the kinematic invariants that are the variables of the system of differential equations obeyed by MI's, rather than the quantum-mechanical time-evolution. Moreover, the matrices representing the systems of differential equations for MI's are not unitary.

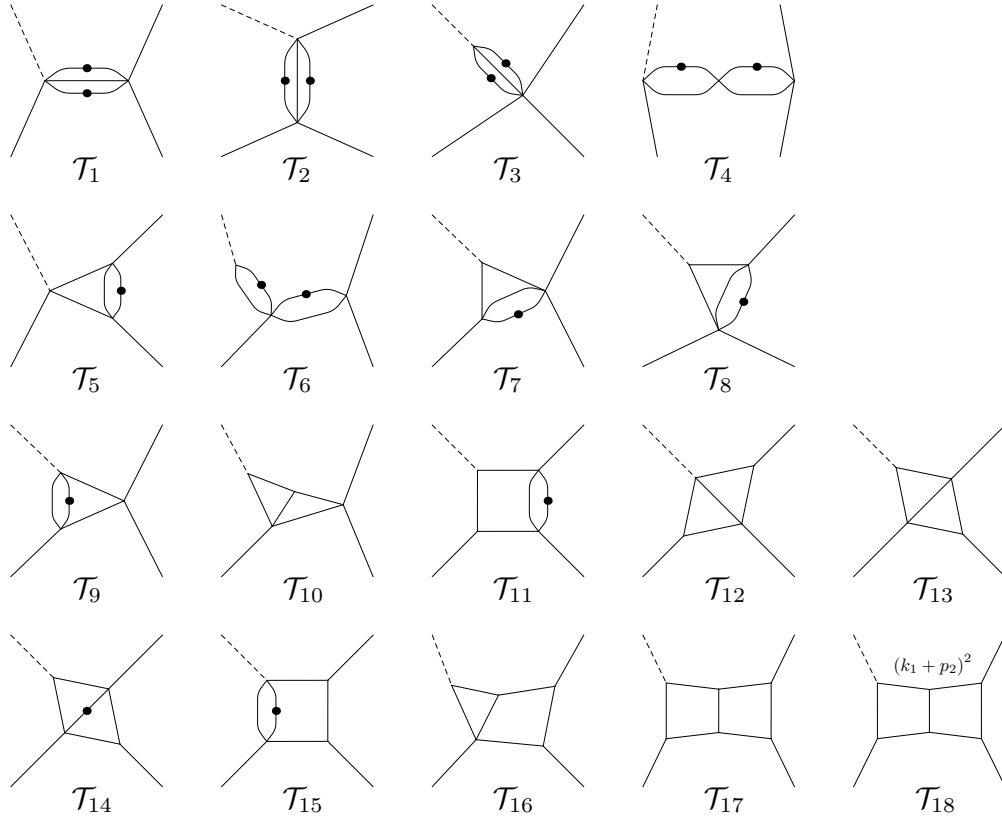


Figure 8.4.: Two-loop Master Integrals $\{\mathcal{T}_i\}_{i=1,\dots,18}$. The solid lines stand for massless particles; the dashed line represents a massive particle; dots indicate squared propagators; numerators may appear as indicated ($p_{ij} \equiv p_i + p_j$).

yet compatible set of MI's. We begin by choosing the following basis

$$\begin{aligned}
 F_1 &= \epsilon^2 \mathcal{T}_1 & F_2 &= \epsilon^2 \mathcal{T}_2 & F_3 &= \epsilon^2 \mathcal{T}_3 \\
 F_4 &= \epsilon^2 \mathcal{T}_4 & F_5 &= \epsilon^3 \mathcal{T}_5 & F_6 &= \epsilon^2 \mathcal{T}_6 \\
 F_7 &= \epsilon^3 \mathcal{T}_7 & F_8 &= \epsilon^3 \mathcal{T}_8 & F_9 &= \epsilon^3 \mathcal{T}_9 \\
 F_{10} &= \epsilon^4 \mathcal{T}_{10} & F_{11} &= \epsilon^3 \mathcal{T}_{11} & F_{12} &= \epsilon^4 \mathcal{T}_{12} \\
 F_{13} &= \epsilon^4 \mathcal{T}_{13} & F_{14} &= \epsilon^3 \mathcal{T}_{14} & F_{15} &= \epsilon^3 \mathcal{T}_{15} \\
 F_{16} &= \epsilon^4 \mathcal{T}_{16} & F_{17} &= \epsilon^4 \mathcal{T}_{17} & F_{18} &= \epsilon^4 \mathcal{T}_{18}
 \end{aligned} \tag{8.23}$$

where the integrals \mathcal{T}_i are depicted in figure 8.4. The set $\{F\}_{i=1,\dots,18}$ is chosen to obey a ϵ -linear system of differential equations in x and y , which, as previously described, can be cast in canonical form by means of Magnus exponentials. In this case, the canonical

transformation B , generically defined in (5.53), reduces to $B \equiv e^{\Omega[A_{m^2,0}]} e^{\Omega[D_{x,0}^{[0]}]} e^{\Omega[D_{y,0}^{[1]}]}$, because after the first three transformations $N_{x,0}^{[2]} = N_{y,0}^{[2]} = 0$. The canonical basis $\{I\}_{i=1,\dots,18}$ reads,

$$\begin{aligned}
I_1 &= s F_1 & I_2 &= t F_2 & I_3 &= m^2 F_3 \\
I_4 &= s^2 F_4 & I_5 &= s F_5 & I_6 &= m^2 s F_6 \\
I_7 &= \lambda_s F_7 & I_8 &= \lambda_t F_8 & I_9 &= \lambda_s F_9 \\
I_{10} &= \lambda_s F_{10} & I_{11} &= s t F_{11} & I_{12} &= u F_{12} \\
I_{13} &= \lambda_u F_{13} & I_{14} &= s t F_{14} & I_{15} &= s t F_{15} \\
I_{16} &= s \lambda_t F_{16} & I_{17} &= s^2 t F_{17} & I_{18} &= s \lambda_s F_{18}
\end{aligned} \tag{8.24}$$

where $\lambda_a = (m^2 - a)$. The sparse matrices M_i ($i = 1, \dots, 6$) appearing in the corresponding canonical system in (8.17) and (8.18) are given in appendix C.1.

8.4.2. Easy non-planar Topology

There are two non-planar topologies for our process at two-loop, which were both previously computed in [169]. First let us consider the topology where the off-shell leg is attached to the planar part of the diagram. In this computation we will consider an alternative set of MI's in respect to [169], which satisfies a canonical differential equation. Our starting point is a set of MIs, which is depicted in figure 8.5 and which obeys a linear differential equation

$$\begin{aligned}
F_1 &= \epsilon^2 \mathcal{T}_1 & F_2 &= \epsilon^2 \mathcal{T}_2 & F_3 &= \epsilon^2 \mathcal{T}_3 \\
F_4 &= \epsilon^2 \mathcal{T}_4 & F_5 &= \epsilon^3 \mathcal{T}_5 & F_6 &= \epsilon^3 \mathcal{T}_6 \\
F_7 &= \epsilon^3 \mathcal{T}_7 & F_8 &= \epsilon^3 \mathcal{T}_8 & F_9 &= \epsilon^3 \mathcal{T}_9 \\
F_{10} &= \epsilon^3 \mathcal{T}_{10} & F_{11} &= \epsilon^4 \mathcal{T}_{11} & F_{12} &= \epsilon^4 \mathcal{T}_{12} \\
F_{13} &= \epsilon^4 \mathcal{T}_{13} & F_{14} &= \epsilon^4 \mathcal{T}_{14} & F_{15} &= \epsilon^3 \mathcal{T}_{15} \\
F_{16} &= \epsilon^4 \mathcal{T}_{16} & F_{17} &= \epsilon^3 \mathcal{T}_{17} & F_{18} &= \epsilon^4 \mathcal{T}_{18} \\
F_{19} &= \epsilon^4 \mathcal{T}_{19} & F_{20} &= \epsilon^4 \mathcal{T}_{20} & F_{21} &= \epsilon^4 \mathcal{T}_{21} \\
F_{22} &= \epsilon^4 \mathcal{T}_{22} .
\end{aligned} \tag{8.25}$$

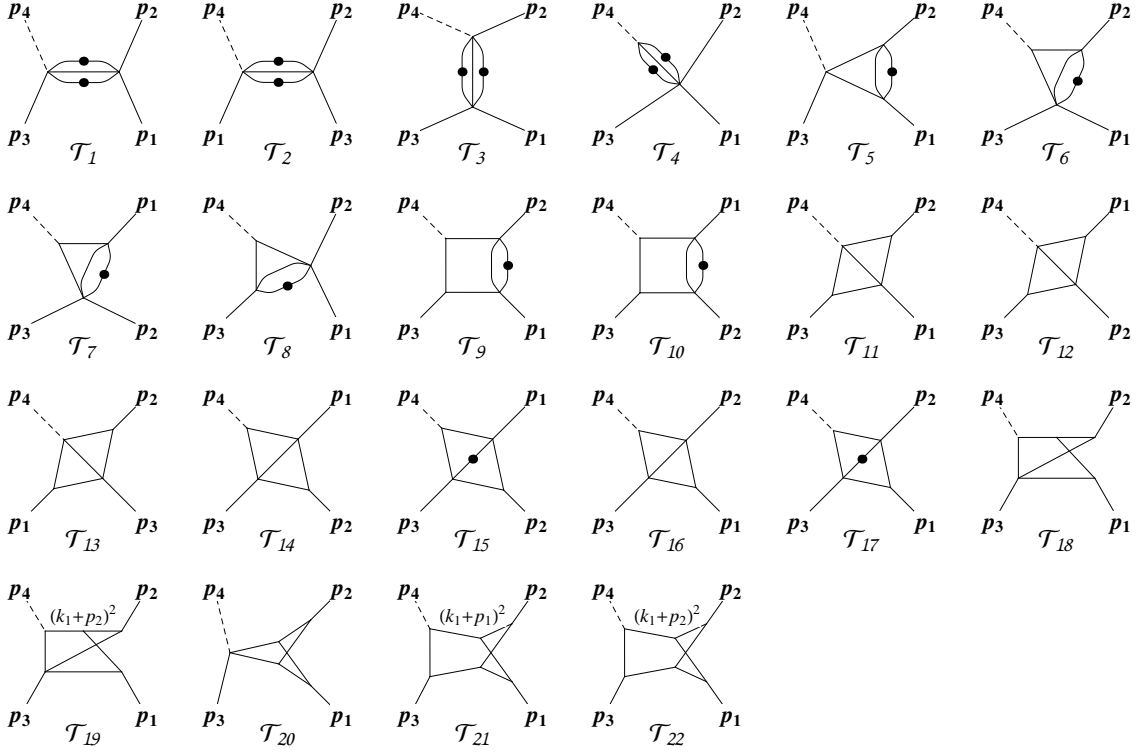


Figure 8.5.: Two-loop Master Integrals $\{\mathcal{T}_i\}_{i=1,\dots,22}$. The solid lines stand for massless particles; the dashed line represents a massive particle; dots indicate squared propagators.

After applying the Magnus transformation we obtain the following set of MIs

$$\begin{aligned}
I_1 &= u F_1 & I_2 &= s F_2 & I_3 &= t F_3 \\
I_4 &= m^2 F_4 & I_5 &= u F_5 & I_6 &= \lambda_t F_6 \\
I_7 &= \lambda_s F_7 & I_8 &= \lambda_u F_8 & I_9 &= u t F_9 \\
I_{10} &= u s F_{10} & I_{11} &= s F_{11} & I_{12} &= t F_{12} \\
I_{13} &= u F_{13} & I_{14} &= \lambda_t F_{14} & I_{15} &= u s F_{15} \\
I_{16} &= \lambda_s F_{16} & I_{17} &= u t F_{17} & I_{18} &= u m^2 F_{18} \\
I_{19} &= -u F_{13} - \lambda_s (F_{13} - F_{19}) & I_{20} &= u^2 F_{20} & I_{21} &= u t F_{21} \\
I_{22} &= u s F_{22} & & & &
\end{aligned} \tag{8.26}$$

which satisfy a canonical differential equation (8.17) with same alphabet as the planar topology.

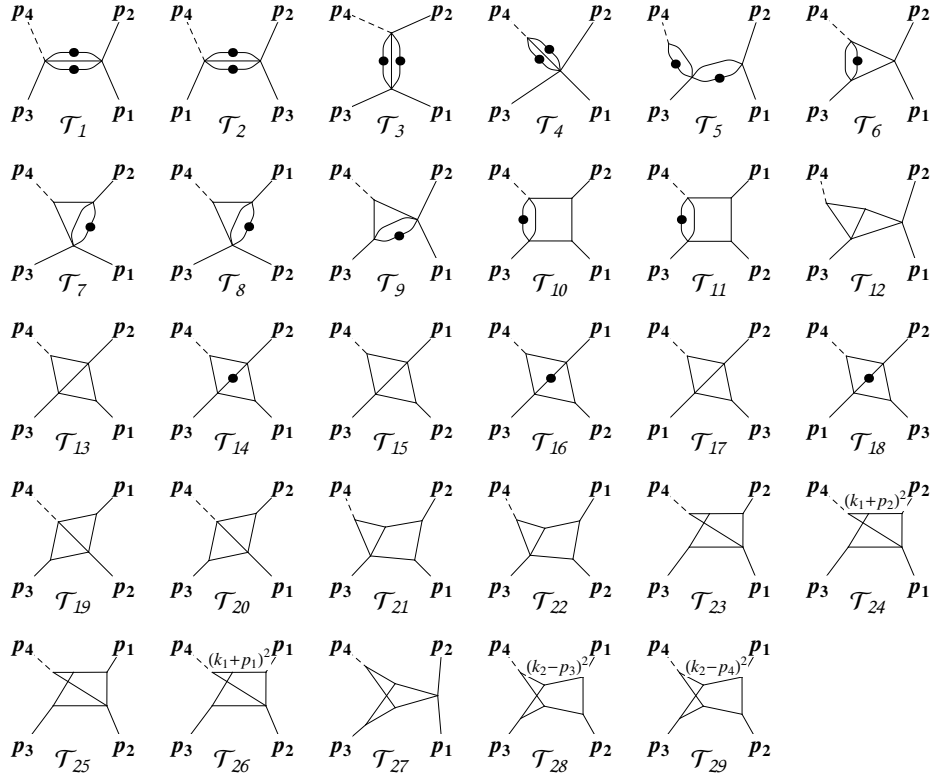


Figure 8.6.: Two-loop Master Integrals $\{\mathcal{T}_i\}_{i=1,\dots,29}$. The solid lines stand for massless particles; the dashed line represents a massive particle; dots indicate squared propagators.

8.4.3. Hard non-planar Topology

In the second non-planar topology the off-shell leg is attached to non-planar part of the diagram. We start from a set of master integrals, which are shown in figure 8.6 and obey a

linear differential equation

$$\begin{aligned}
F_1 &= \epsilon^2 \mathcal{T}_1 & F_2 &= \epsilon^2 \mathcal{T}_2 & F_3 &= \epsilon^2 \mathcal{T}_3 \\
F_4 &= \epsilon^2 \mathcal{T}_4 & F_5 &= \epsilon^2 \mathcal{T}_5 & F_6 &= \epsilon^3 \mathcal{T}_6 \\
F_7 &= \epsilon^3 \mathcal{T}_7 & F_8 &= \epsilon^3 \mathcal{T}_8 & F_9 &= \epsilon^3 \mathcal{T}_9 \\
F_{10} &= \epsilon^3 \mathcal{T}_{10} & F_{11} &= \epsilon^3 \mathcal{T}_{11} & F_{12} &= \epsilon^4 \mathcal{T}_{12} \\
F_{13} &= \epsilon^4 \mathcal{T}_{13} & F_{14} &= \epsilon^3 \mathcal{T}_{14} & F_{15} &= \epsilon^4 \mathcal{T}_{15} \\
F_{16} &= \epsilon^3 \mathcal{T}_{16} & F_{17} &= \epsilon^4 \mathcal{T}_{17} & F_{18} &= \epsilon^3 \mathcal{T}_{18} \\
F_{19} &= \epsilon^4 \mathcal{T}_{19} & F_{20} &= \epsilon^4 \mathcal{T}_{20} & F_{21} &= \epsilon^4 \mathcal{T}_{21} \\
F_{22} &= \epsilon^4 \mathcal{T}_{22} & F_{23} &= \epsilon^4 \mathcal{T}_{23} & F_{24} &= \epsilon^4 \mathcal{T}_{24} \\
F_{25} &= \epsilon^4 \mathcal{T}_{25} & F_{26} &= \epsilon^4 \mathcal{T}_{26} & F_{27} &= \epsilon^4 \mathcal{T}_{27} \\
F_{28} &= \epsilon^4 \mathcal{T}_{28} & F_{29} &= \epsilon^4 \mathcal{T}_{29} .
\end{aligned} \tag{8.27}$$

With the help of the Magnus expansion we are able to remove the constant part in respect to ϵ and obtain a set of master integrals

$$\begin{aligned}
I_1 &= u F_1 & I_2 &= s F_2 & I_3 &= t F_3 \\
I_4 &= m^2 F_4 & I_5 &= u m^2 F_5 & I_6 &= \lambda_u F_6 \\
I_7 &= \lambda_t F_7 & I_8 &= \lambda_s F_8 & I_9 &= \lambda_u F_9 \\
I_{10} &= u t F_{10} & I_{11} &= u s F_{11} & I_{12} &= \lambda_u F_{12} \\
I_{13} &= \lambda_s F_{13} & I_{14} &= u t F_{14} & I_{15} &= \lambda_t F_{15} \\
I_{16} &= u s F_{16} & I_{17} &= \lambda_u F_{17} & I_{18} &= s t F_{18} \\
I_{19} &= t F_{19} & I_{20} &= s F_{20} & I_{21} &= u \lambda_t F_{21} \\
I_{22} &= u \lambda_s F_{22} & I_{23} &= s m^2 F_{23} & I_{24} &= -t F_{20} + \lambda_u F_{24} \\
I_{25} &= t m^2 F_{25} & I_{26} &= -s F_{19} + \lambda_u F_{26} & I_{27} &= \lambda_u^2 F_{27} \\
I_{28} &= u t F_{28} & I_{29} &= u s F_{29}
\end{aligned} \tag{8.28}$$

which satisfy a canonical differential equation of the form (8.17).

8.5. Three-Loop Master Integrals

After performing the automatic reduction by means of the computer code REDUZE2 [106, 165], we identify a set of 85 MI's,

$$\begin{aligned}
F_1 &= \epsilon^3 \mathcal{T}_1 & F_2 &= \epsilon^3 \mathcal{T}_2 & F_3 &= \epsilon^3 \mathcal{T}_3 \\
F_4 &= \epsilon^3 \mathcal{T}_4 & F_5 &= \epsilon^3 (1 + 2\epsilon) \mathcal{T}_5 & F_6 &= \epsilon^4 \mathcal{T}_6 \\
F_7 &= \epsilon^4 \mathcal{T}_7 & F_8 &= \epsilon^4 \mathcal{T}_8 & F_9 &= \epsilon^3 \mathcal{T}_9 \\
F_{10} &= \epsilon^3 \mathcal{T}_{10} & F_{11} &= \epsilon^4 \mathcal{T}_{11} & F_{12} &= \epsilon^4 \mathcal{T}_{12}
\end{aligned}$$

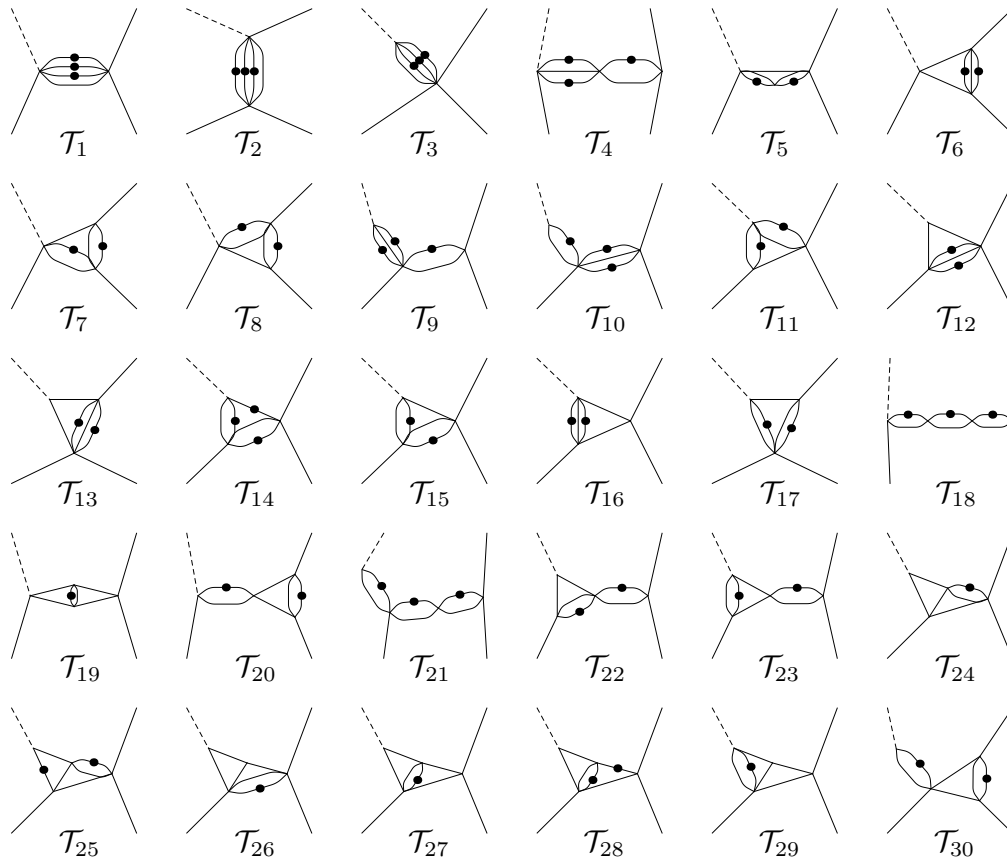


Figure 8.7.: Three-loop Master Integrals $\{\mathcal{T}_i\}_{i=1,\dots,30}$. The solid lines stand for massless particles; the dashed line represents a massive particle; dots indicate squared propagators; numerators may appear as indicated ($p_{ij} \equiv p_i + p_j$). See also figures 8.8 and 8.9.

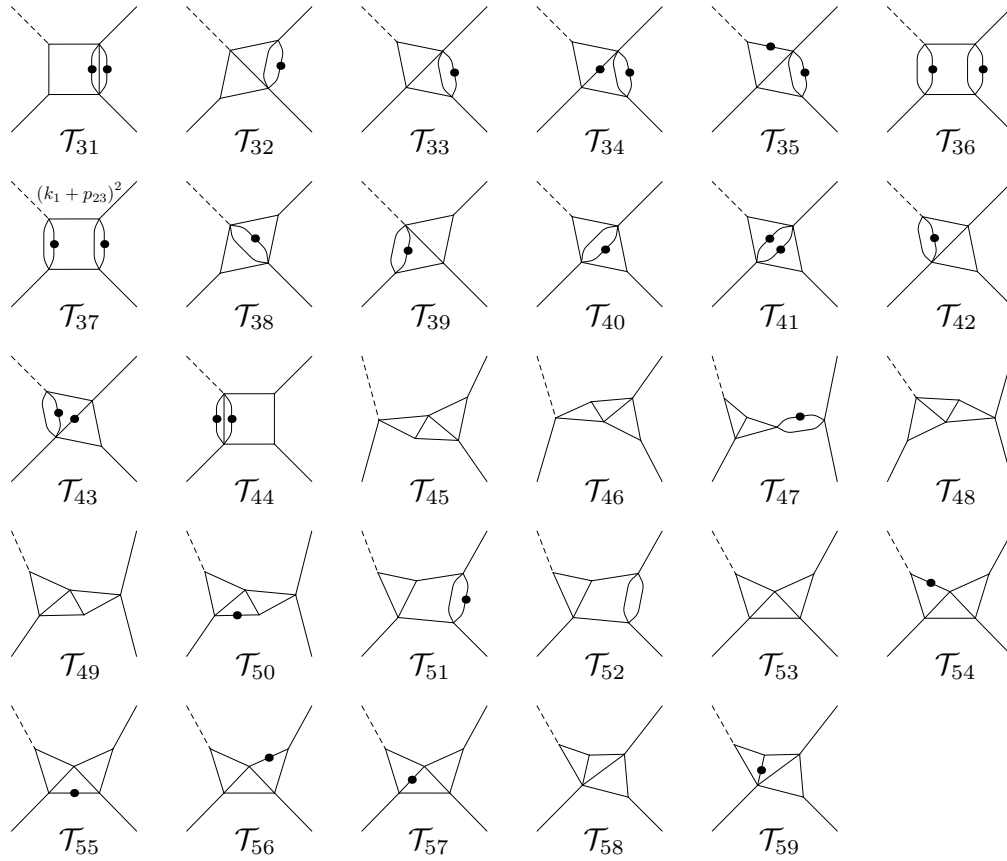


Figure 8.8.: Three-loop Master Integrals $\{\mathcal{T}_i\}_{i=31,\dots,59}$. The solid lines stand for massless particles; the dashed line represents a massive particle; dots indicate squared propagators; numerators may appear as indicated ($p_{ij} \equiv p_i + p_j$). See also figures 8.7 and 8.9.

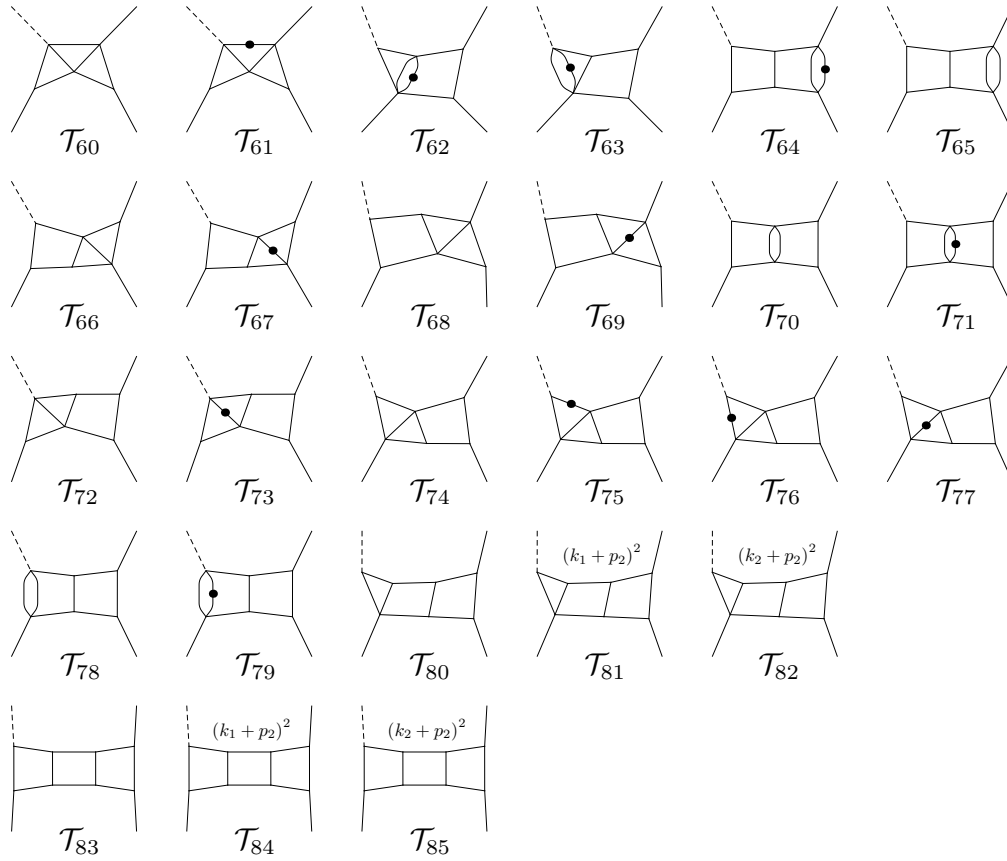


Figure 8.9.: Three-loop Master Integrals $\{\mathcal{T}_i\}_{i=60,\dots,85}$. The solid lines stand for massless particles; the dashed line represents a massive particle; dots indicate squared propagators; numerators may appear as indicated ($p_{ij} \equiv p_i + p_j$). See also figures 8.7 and 8.8.

$$\begin{aligned}
F_{13} &= \epsilon^4 \mathcal{T}_{13} & F_{14} &= \epsilon^3 \mathcal{T}_{14} & F_{15} &= \epsilon^4 \mathcal{T}_{15} \\
F_{16} &= \epsilon^4 \mathcal{T}_{16} & F_{17} &= \epsilon^4 \mathcal{T}_{17} & F_{18} &= \epsilon^3 \mathcal{T}_{18} \\
F_{19} &= \epsilon^4 (1 - 2\epsilon) \mathcal{T}_{19} & F_{20} &= \epsilon^4 \mathcal{T}_{20} & F_{21} &= \epsilon^3 \mathcal{T}_{21} \\
F_{22} &= \epsilon^4 \mathcal{T}_{22} & F_{23} &= \epsilon^4 \mathcal{T}_{23} & F_{24} &= \epsilon^5 \mathcal{T}_{24} \\
F_{25} &= \epsilon^4 \mathcal{T}_{25} & F_{26} &= \epsilon^5 \mathcal{T}_{26} & F_{27} &= \epsilon^5 \mathcal{T}_{27} \\
F_{28} &= \epsilon^3 (1 + 2\epsilon) \mathcal{T}_{28} & F_{29} &= \epsilon^5 \mathcal{T}_{29} & F_{30} &= \epsilon^4 \mathcal{T}_{30} \\
F_{31} &= \epsilon^4 \mathcal{T}_{31} & F_{32} &= \epsilon^5 \mathcal{T}_{32} & F_{33} &= \epsilon^5 \mathcal{T}_{33} \\
F_{34} &= \epsilon^4 \mathcal{T}_{34} & F_{35} &= \epsilon^4 \mathcal{T}_{35} & F_{36} &= \epsilon^4 \mathcal{T}_{36} \\
F_{37} &= \epsilon^4 \frac{(1 - 2\epsilon)}{1 - \epsilon} \mathcal{T}_{37} & F_{38} &= \epsilon^5 \mathcal{T}_{38} & F_{39} &= \epsilon^5 \mathcal{T}_{39} \\
F_{40} &= \epsilon^5 \mathcal{T}_{40} & F_{41} &= \epsilon^4 \mathcal{T}_{41} & F_{42} &= \epsilon^5 \mathcal{T}_{42} \\
F_{43} &= \epsilon^4 \mathcal{T}_{43} & F_{44} &= \epsilon^4 \mathcal{T}_{44} & F_{45} &= \epsilon^6 \mathcal{T}_{45} \\
F_{46} &= \epsilon^6 \mathcal{T}_{46} & F_{47} &= \epsilon^5 \mathcal{T}_{47} & F_{48} &= \epsilon^6 \mathcal{T}_{48} \\
F_{49} &= \epsilon^6 \mathcal{T}_{49} & F_{50} &= \epsilon^4 (1 + \epsilon) \mathcal{T}_{50} & F_{51} &= \epsilon^5 \mathcal{T}_{51} \\
F_{52} &= \epsilon^5 (1 - 2\epsilon) \mathcal{T}_{52} & F_{53} &= \epsilon^6 \mathcal{T}_{53} & F_{54} &= \epsilon^5 \mathcal{T}_{54} \\
F_{55} &= \epsilon^5 \mathcal{T}_{55} & F_{56} &= \epsilon^4 (1 + \epsilon) \mathcal{T}_{56} & F_{57} &= \epsilon^5 \mathcal{T}_{57} \\
F_{58} &= \epsilon^6 \mathcal{T}_{58} & F_{59} &= \epsilon^4 (1 + \epsilon) \mathcal{T}_{59} & F_{60} &= \epsilon^6 \mathcal{T}_{60} \\
F_{61} &= \epsilon^5 \mathcal{T}_{61} & F_{62} &= \epsilon^5 \mathcal{T}_{62} & F_{63} &= \epsilon^5 \mathcal{T}_{63} \\
F_{64} &= \epsilon^5 \mathcal{T}_{64} & F_{65} &= \epsilon^5 (1 - 2\epsilon) \mathcal{T}_{65} & F_{66} &= \epsilon^6 \mathcal{T}_{66} \\
F_{67} &= \epsilon^5 \mathcal{T}_{67} & F_{68} &= \epsilon^6 \mathcal{T}_{68} & F_{69} &= \epsilon^5 \mathcal{T}_{69} \\
F_{70} &= \epsilon^5 (1 - 2\epsilon) \mathcal{T}_{70} & F_{71} &= \epsilon^5 \mathcal{T}_{71} & F_{72} &= \epsilon^6 \mathcal{T}_{72} \\
F_{73} &= \epsilon^5 \mathcal{T}_{73} & F_{74} &= \epsilon^6 \mathcal{T}_{74} & F_{75} &= \epsilon^5 \mathcal{T}_{75} \\
F_{76} &= \epsilon^5 \mathcal{T}_{76} & F_{77} &= \epsilon^5 \mathcal{T}_{77} & F_{78} &= \epsilon^5 (1 - 2\epsilon) \mathcal{T}_{78} \\
F_{79} &= \epsilon^5 \mathcal{T}_{79} & F_{80} &= \epsilon^6 \mathcal{T}_{80} & F_{81} &= \epsilon^5 (1 - 2\epsilon) \mathcal{T}_{81} \\
F_{82} &= \epsilon^6 \mathcal{T}_{82} & F_{83} &= \epsilon^6 \mathcal{T}_{83} & F_{84} &= \epsilon^6 \mathcal{T}_{84} \\
F_{85} &= \epsilon^6 \mathcal{T}_{85} & & & &
\end{aligned} \tag{8.29}$$

where the integrals \mathcal{T}_i are depicted in figures 8.7–8.9. As before, the choice of $\{F\}_{i=1,\dots,85}$ is motivated by them obeying a ϵ -linear system of differential equations in x and y .

In this case, the canonical transformation B , generically defined in (5.53), reduces to $B \equiv e^{\Omega[A_{m^2,0}]} e^{\Omega[D_{x,0}^{[0]}]} e^{\Omega[D_{y,0}^{[1]}]} e^{\Omega[N_{x,0}^{[2]}]}$, yielding the canonical basis $\{I\}_{i=1,\dots,85}$

$$\begin{aligned}
I_1 &= s F_1 & I_2 &= t F_2 & I_3 &= m^2 F_3 & I_4 &= s^2 F_4 \\
I_5 &= s F_5 & I_6 &= s F_6 & I_7 &= s F_7 & I_8 &= s F_8 \\
I_9 &= m^2 s F_9 & I_{10} &= m^2 s F_{10} & I_{11} &= \lambda_s F_{11} & I_{12} &= \lambda_s F_{12}
\end{aligned}$$

$$\begin{aligned}
I_{13} &= \lambda_t F_{13} & I_{14} &= m^2 (s F_{14} - 4F_{15}) & I_{15} &= \lambda_s F_{15} & I_{16} &= \lambda_s F_{16} \\
I_{17} &= \lambda_t F_{17} & I_{18} &= s^3 F_{18} & I_{19} &= s F_{19} & I_{20} &= s^2 F_{20} \\
I_{21} &= m^2 s^2 F_{21} & I_{22} &= s \lambda_s F_{22} & I_{23} &= s \lambda_s F_{23} & I_{24} &= \lambda_s F_{24} \\
I_{25} &= m^2 \lambda_s F_{25} & I_{26} &= \lambda_s F_{26} & I_{27} &= \lambda_s F_{27} & I_{28} &= m^2 (s F_{28} - 12F_{27}) \\
I_{29} &= \lambda_s F_{29} & I_{30} &= m^2 s F_{30} & I_{31} &= s t F_{31} & I_{32} &= u F_{32} \\
I_{33} &= \lambda_u F_{33} & I_{34} &= s t F_{34} & I_{35} &= m^2 s F_{35} & I_{36} &= s t F_{36} \\
I_{37} &= s (F_{37} - F_{17}) & I_{38} &= u F_{38} & I_{39} &= u F_{39} & I_{40} &= \lambda_u F_{40} \\
I_{41} &= s t F_{41} & I_{42} &= \lambda_u F_{42} & I_{43} &= s t F_{43} & I_{44} &= s t F_{44} \\
I_{45} &= s F_{45} & I_{46} &= s F_{46} & I_{47} &= s \lambda_s F_{47} & I_{48} &= \lambda_s F_{48} \\
I_{49} &= \lambda_s F_{49} & I_{50} &= s \lambda_s F_{50} & I_{51} &= s \lambda_t F_{51} & I_{52} &= \lambda_s F_{52} \\
I_{53} &= \lambda_t F_{53} & I_{54} &= m^2 s F_{54} & I_{55} &= s \lambda_s F_{55} & I_{56} &= s \lambda_t F_{56} \\
I_{57} &= s t F_{57} & I_{58} &= \lambda_u F_{58} & I_{59} &= m^2 s F_{59} & I_{60} &= t F_{60} \\
I_{61} &= s \lambda_s F_{61} & I_{62} &= s \lambda_t F_{62} & I_{63} &= s \lambda_t F_{63} & I_{64} &= s^2 t F_{64} \\
I_{65} &= s \lambda_s F_{65} & I_{66} &= s u F_{66} & I_{67} &= s^2 t F_{67} & I_{68} &= s u F_{68} \\
I_{69} &= s^2 t F_{69} & I_{70} &= s \lambda_s F_{70} & I_{71} &= s^2 t F_{71} & I_{72} &= s u F_{72} \\
I_{73} &= s^2 t F_{73} & I_{74} &= s \lambda_u F_{74} & I_{75} &= m^2 s^2 F_{75} & I_{76} &= m^2 s t F_{76} \\
I_{77} &= s^2 t F_{77} & I_{78} &= s^2 F_{78} & I_{79} &= s^2 t F_{79} & I_{80} &= s^2 \lambda_t F_{80} \\
I_{81} &= m^2 \left(-2F_{24} - 3F_{26} + 4F_{27} - F_{29} + 2s F_{47} - 2F_{49} - 2\frac{st}{m^2} F_{74} + \frac{s^2}{m^2} F_{81} - 2s F_{82} \right) \\
I_{82} &= s \lambda_s F_{82} & I_{83} &= s^3 t F_{83} & I_{84} &= s^2 \lambda_s F_{84} & I_{85} &= s^2 \lambda_s F_{85} \quad (8.30)
\end{aligned}$$

with λ_a defined below (8.28). The sparse matrices \mathbb{M}_i ($i = 1, \dots, 6$) appearing in the corresponding canonical system (8.17) and (8.18) are given in appendix C.2.

8.6. Boundary Conditions

The generic solutions (8.20) of the canonical systems at two- and three-loop are written in terms of G -polylogarithms and constants to be fixed by boundary conditions. The alphabet (8.19) determines the thresholds which appear in the final result. For the planar two- and three-loop integrals only two out of the six thresholds are physical, since they correspond to the production of massless particles in s - and t -channels at $x = 0$ and $y = 0$. Imposing the regularity of the generic solutions at the unphysical thresholds, namely $x = 1$, $y = 1$, $y = -x$, $y = 1 - x$, amounts to ruling out the terms that give rise to divergent behaviors, hence enforcing conditions that unequivocally fix the arbitrary constants.

For the non-planar graphs we have $y = 1 - x$ ($u = 0$) as an additional physical threshold. Therefore we are left with more non-trivial boundary constants, which we fixed by matching our results to the planar ones and by matching them against the known expressions from [169].

Relations for one-scale Integrals

In general, homogeneous differential equations for single scale integrals carry only information on the scaling behaviour of the solution. Boundary constants for such differential equations require the evaluation of the integrals themselves by independent methods. Within a multi-scale problem, such as the one we are considering, integrals may depend on more than one external invariant, and single-scale integrals participate in the regularity conditions of the multi-scale ones. Therefore, these relations can be exploited to determine the arbitrary constants of the single-scale integrals. Alternatively, they can reduce the number of independent single-scale integrals that needs to be independently provided. Therefore, solving multi-scale systems of differential equations yields the simultaneous determination of single- and multi-scale MI's, which are finally expressed in terms of a few single-scale MI's, to be considered as external *input*.

Let us discuss, as a pedagogical example, the systems of DE's for the two-loop master integrals I_2 , I_5 , I_8 and I_{11} , represented by the corresponding topologies in figure 8.4, which

read,

$$\partial_x \left(\text{diagram} \right) = 0, \quad (8.31)$$

$$\partial_x \left(\text{diagram} \right) = -\frac{2}{x} \left(\text{diagram} \right), \quad (8.32)$$

$$\partial_x \left(\text{diagram} \right) = 0, \quad (8.33)$$

$$\begin{aligned} \partial_x \left(\text{diagram} \right) = & -\frac{3}{2} \frac{1}{1-x} \left(\text{diagram} \right) + 3 \left(-\frac{1}{1-x} + \frac{1}{1-x-y} \right) \left(\text{diagram} \right) \\ & + 3 \left(\frac{1}{1-x} - \frac{1}{1-x-y} \right) \left(\text{diagram} \right) - \left(\frac{1}{1-x} + \frac{2}{x} + \frac{1}{1-x-y} \right) \left(\text{diagram} \right), \end{aligned} \quad (8.34)$$

$$\partial_y \left(\text{diagram} \right) = -\frac{2}{y} \left(\text{diagram} \right), \quad (8.35)$$

$$\partial_y \left(\text{diagram} \right) = 0, \quad (8.36)$$

$$\partial_y \left(\text{diagram} \right) = -\frac{1}{2y} \left(\text{diagram} \right) + \frac{1}{1-y} \left(\text{diagram} \right), \quad (8.37)$$

$$\begin{aligned} \partial_y \left(\text{diagram} \right) = & \frac{3}{1-x-y} \left(\text{diagram} \right) + 3 \left(\frac{1}{1-y} - \frac{1}{1-x-y} \right) \left(\text{diagram} \right) \\ & + \left(-\frac{2}{y} - \frac{1}{1-x-y} \right) \left(\text{diagram} \right). \end{aligned} \quad (8.38)$$

From the regular behavior of (8.34) and (8.38) at $(1-x) \rightarrow 0$, $(1-y) \rightarrow 0$ and $(1-x-y) \rightarrow 0$, the following relations can be established:

$$\left(-\frac{3}{2} \left(\text{diagram} \right) - 3 \left(\text{diagram} \right) + 3 \left(\text{diagram} \right) - \left(\text{diagram} \right) \right) \Big|_{x \rightarrow 1} = 0 \quad (8.39)$$

$$\left(\text{diagram} \right) \Big|_{y \rightarrow 1} = 0 \quad (8.40)$$

$$\left(3 \left(\text{diagram} \right) - 3 \left(\text{diagram} \right) - \left(\text{diagram} \right) \right) \Big|_{y \rightarrow 1-x} = 0 \quad (8.41)$$

The zeroth order term of the ϵ -expansion is independent of x and y . Therefore, we can combine the equations above in order to find a relation between (the constant terms of) two one-scale integrals,

$$\left. \text{Diagram 1} \right|_{\epsilon^0, \text{const.}} = -\frac{1}{4} \left. \text{Diagram 2} \right|_{\epsilon^0, \text{const.}} \quad (8.42)$$

At higher order in ϵ , these equations acquire a richer structure, because constants coming from the limiting values of the G -polylogarithms appear. For the considered example, the relation at the first order in ϵ is unaltered (the only constant which could appear being imaginary, hence not allowed in the Euclidean region),

$$\left. \text{Diagram 1} \right|_{\epsilon^1, \text{const.}} = -\frac{1}{4} \left. \text{Diagram 2} \right|_{\epsilon^1, \text{const.}}, \quad (8.43)$$

but at the second order in ϵ the relation becomes,

$$\left. \text{Diagram 1} \right|_{\epsilon^2, \text{const.}} = -\frac{1}{4} \left. \text{Diagram 2} \right|_{\epsilon^2, \text{const.}} - \frac{\zeta_2}{2} \left. \text{Diagram 3} \right|_{\epsilon^2, \text{const.}}. \quad (8.44)$$

Similar relations are systematically established, so that all MI's can be finally determined by providing few simple integrals as external inputs. At two-loop, the only external input is I_3 in (8.28), which can be independently computed and is given by,

$$I_3 = \epsilon^2 \frac{\Gamma^2(1-2\epsilon) \Gamma^2(-\epsilon) \Gamma(1+2\epsilon)}{\Gamma(1-3\epsilon) \Gamma^3(1-\epsilon) \Gamma^2(1+\epsilon)}, \quad (8.45)$$

while I_3 and I_9 in (8.30) are the input integrals for the three-loop MI's, amounting to

$$I_3 = \epsilon^3 \frac{\Gamma^3(1-2\epsilon) \Gamma^3(-\epsilon) \Gamma(1+3\epsilon)}{\Gamma(1-4\epsilon) \Gamma^5(1-\epsilon) \Gamma^3(1+\epsilon)}, \quad (8.46)$$

$$I_9 = \epsilon^3 \frac{\Gamma^2(1-2\epsilon) \Gamma^3(-\epsilon) \Gamma(1+2\epsilon)}{\Gamma(1-3\epsilon) \Gamma^4(1-\epsilon) \Gamma^2(1+\epsilon)} x^{-\epsilon}, \quad (8.47)$$

where we omit the common normalization factors (8.10).

We would like to observe that the relations between single-scale integrals, coming from the regularity conditions of multi-scale ones, seem not to belong to the set of IBP identities needed to derive the considered systems of differential equations. In the future, it is worth to investigate whether such relations are truly independent from IBP identities, or if they would arise when considering larger sets of identities for increasing powers of denominators and irreducible scalar products.

8.7. Conclusions

In this chapter we presented the analytic expressions of the 85 master integrals (MI's) of the three-loop ladder-box topology with one massive leg. Their calculation was performed with the method of differential equations, namely by solving a system of first order differential equations fulfilled by the MI's. The generic solution of the system was obtained in a purely algebraic way, by means of Magnus exponential method, and cast in terms of repeated integrations, according to Dyson series expansion, as recently proposed in ref. [1]. The boundary conditions were provided by the regularity of the solutions at pseudothresholds.

The results of the considered four-leg integrals, as well as of the tower of three- and two-leg master integrals associated to subtopologies (including previously unknown two-scale vertex diagrams), were written as a Taylor expansion in the dimensional regulator parameter $\epsilon = (4 - d)/2$. The coefficients of the series are expressed in terms of uniform weight combinations of multiple polylogarithms and transcendental constants up to weight six.

The considered integrals contribute to the N³LO virtual corrections to scattering processes like the three-jet production mediated by vector boson decay, $V^* \rightarrow jjj$, as well as the Higgs plus one-jet production in gluon fusion, $pp \rightarrow Hj$, and to the three-loop one-particle splitting amplitudes.

Mixed EW and QCD Corrections to Drell-Yan Scattering

9.1. Introduction

The Drell-Yan production of Z and W bosons [170] is one of the standard candles for physical studies at the LHC. Due to the large cross section and clean experimental signature, Drell-Yan processes can be measured with small experimental uncertainty and, therefore, allow for very precise tests of the Standard Model of fundamental interactions (SM). They give access to the determination of important parameters of the weak sector, as for instance the sine of the weak mixing angle and the W boson mass, that together with the top and the Higgs masses provides stringent constraints on the validity of the SM at the TeV energy scale. Furthermore, Drell-Yan processes constitute the SM background in searches of New Physics, involving for instance new vector boson resonances, Z' and W' , originating from GUT extensions of the SM. Finally, the Drell-Yan mechanism is used for constraining parton distribution functions, for detector calibration and determination of the collider luminosity. For all these reasons, an accurate and reliable experimental and theoretical control on Drell-Yan processes would be of the maximum importance for future physics studies at colliders.

The theoretical description of Drell-Yan processes currently includes NNLO QCD and NLO EW radiative corrections, implemented in flexible tools able to provide predictions for inclusive observables as well as kinematic distributions. Current theoretical predictions are in good agreement with the experimental measurements. However, higher theoretical accuracy is needed in order to match the future experimental requirements, in particular in view of the run II of the LHC. A consistent part of an increasing theoretical accuracy regards higher-order perturbative corrections.

Very recently, NNNLO QCD corrections were calculated for the Higgs total production cross section in gluon-gluon fusion [26, 171]. The residual factorization/renormalization scales variation moved from about 10-15% of the NNLO calculation (supplemented by NNLL resummation) to about 5% of the current result. These results will be applied to Drell-Yan as well, since they involve the evaluation of the same topologies for the calculation of the corresponding Feynman diagrams [150–153, 172, 173].

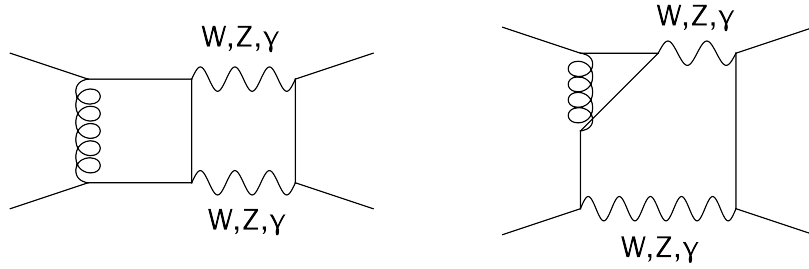


Figure 9.1.: This figure shows some Feynman diagrams for the mixed EW-QCD correction to Drell-Yan scattering. solid lines represent either the massless quark or lepton propagators; curly lines stand for the gluon propagators; wavy lines represent the vector boson propagators.

At the same order of accuracy (one can roughly think to exchange two powers of α_S with one power of α), the mixed QCD-EW corrections have to be taken into account. As in the case of QCD NNLO with EW NLO perturbative corrections, the mixed QCD-EW corrections are expected to become of similar size with respect to QCD NNNLO at high leptonic invariant mass [174].

At LO, the partonic process in the SM is mediated by the exchange of a photon or a Z/W vector boson, in the s annihilation channel: $q\bar{q} \rightarrow \gamma, Z \rightarrow l^-l^+$ and $q\bar{q}' \rightarrow W \rightarrow l\nu$.

At higher orders in the coupling constants, we can distinguish between QCD and electroweak (EW) or mixed (EW-QCD) corrections to the LO process. In the first case, only the initial state receives quantum corrections, since the leptonic final state does not couple to gluons.

The NLO QCD corrections to the total cross section were calculated in [175, 176] and revealed a sizable increase of the cross section with respect to the LO result. The NNLO QCD corrections [177, 178] stabilized, then, the convergence of the perturbative series.

QCD fixed-order corrections to the total production cross section are supplemented by the resummation of soft-gluon logarithmically enhanced terms, up to NNNLL approximation [179–182].

EW quantum corrections allow exchanges of quanta between initial and final states. Therefore, already at the NLO, massive four-point functions have to be evaluated. Since the bulk of the corrections for inclusive observables comes from the resonant region, in which the exchanged vector boson is nearly on-shell, electroweak NLO corrections to the total cross section were calculated for the W [183] and Z [184] in narrow-width approximation.

More exclusive observables are known in the literature. The Z and W production at non-zero transverse momentum p_T is known at the NLO in QCD [185–190] and in the full SM [191]. The two-loop QCD helicity amplitudes for the production of a Z or a W with a photon have also been calculated [192]. For small p_T ($p_T \ll m_W, m_Z$) the convergence of the fixed-order calculation is spoiled by the large logarithmic terms $\alpha_S^n \log^m(m_W^2/p_T^2)$ that

have to be resummed [193–203]. Finally, the rapidity distribution of a vector boson is known at the NNLO in QCD [204].

The NLO corrections are available in a fully differential description. They are implemented in flexible NLO Monte Carlo programs, and merged with QCD parton shower in `MC@NLO` [205] and `POWHEG` [206]. In [207], the NLO EW and the QED multiple photon corrections are combined with NLO QCD corrections and parton shower. Pure QED generators are also available [208–211]. Although these implementations provide an accurate description of the process and allow for realistic phenomenological studies at the hadronic level, they are not accurate enough for the performances of the run II at the LHC. The NNLO results mentioned above, however, are widely inclusive and they cannot provide realistic descriptions, that necessarily have to include experimental cuts. Therefore, a fully differential description of the Drell-Yan process at the NNLO is needed. With this respect, the state of the art is represented by the two programs `FEWZ` [212], that includes also EW NLO corrections [213], and `DYNNLO` [214, 215]. In these two programs, the decay products of the vector boson, the spin correlations and the finite-width effects are also taken into account. .

A sizable impact on the $pp(\bar{p}) \rightarrow W \rightarrow l\nu$ distributions, and therefore on the determination of the W mass, comes from the QCD initial state radiation (ISR) with QED final state radiation (FSR) or from the real-virtual (factorisable) corrections. However, at the level of precision required ($\Delta m_W \sim 10$ MeV), the complete set of mixed QCD-EW corrections may be important and have to be considered.

The NNLO mixed QCD-EW corrections to the production of a leptonic pair, i.e. order $\alpha\alpha_S$ corrections to the LO partonic amplitude, consist on two-loop $2 \rightarrow 2$ processes, in which the quark-antiquark initial state goes in the final leptonic pair (l^+l^- or $l\nu$), one-loop $2 \rightarrow 3$ processes, in which the final leptonic pair is produced together with an unresolved photon or gluon, and tree-level $2 \rightarrow 4$ processes in which the leptonic pair is produced together with an unresolved photon and an unresolved gluon.

The QCD \times QED perturbative corrections were considered in [216]. In [217], the mixed two-loop corrections to the form factors for the production of a Z boson were calculated analytically, expressing the result in terms of harmonic polylogarithms and related generalizations. In [218], the authors calculated the mixed corrections in pole approximation near the resonance region. In particular, they worked out contributions coming from the QCD corrections to the production and soft-photon exchange between production and decay process, which cause distortions in the shape of the distributions. In [219], the factorisable mixed corrections were included in the analysis.

In this chapter, we present the calculation of the master integrals (MIs) needed for the virtual corrections to the two-loop $2 \rightarrow 2$ processes:

$$q + \bar{q} \rightarrow l^- + l^+ , \quad \text{and} \quad q + \bar{q}' \rightarrow l^- + \bar{\nu} ,$$

for massless external particles. The masses of the W and Z bosons are numerically close to each other, in fact $\Delta m^2 \equiv m_Z^2 - m_W^2 \ll m_Z^2$. Therefore, in the diagrams containing both Z and W propagators at the same time, one can perform a series expansion in $\xi \equiv$

$\Delta m^2/m_Z^2 \sim 0.25$. Within this approximation, all topologies appearing in the two-loop QCD \times EW virtual corrections to Drell-Yan scattering shall contain either no internal massive line, or one massive propagator with mass m_W , or two massive propagators with the same mass m_W [220]. Should they be needed for achieving higher accuracy within the virtual amplitudes, the coefficients of the series in ξ correspond to scalar integrals with higher powers of the denominators.

Using the code `Reduze 2` [106, 165], the dimensionally regulated integrals involved in the calculation are reduced to a set of 49 MIs, which are later determined by means of the differential equations method [72–74], reviewed in [80, 221]. Of those 49 MIs, 8 contain only massless internal lines, 24 involve one massive line and 17 involve two massive lines. The system of differential equations obeyed by the MIs is cast in a canonical form [77], following the algorithm based on the use of the Magnus exponential, introduced in [1, 2]¹. Boundary conditions are retrieved either from the knowledge of simpler integrals emerging from the limiting kinematics, or by requiring the regularity of the solution at pseudo-thresholds.

Finally, the canonical MIs are given as Taylor series in ϵ ($= (4 - d)/2$), up to order ϵ^4 , being d the dimensional regularization parameter. The coefficients of the series are pure functions, represented as iterated integrals with rational and irrational kernels, up to weight four. The solution could be expressed in terms of Chen’s iterated integrals. Alternatively, we adopt a *mixed representation*, where, when possible, we make explicit the presence of Goncharov polylogarithms (*GPLs*) [131, 138], also within the nested integration structure. This representation is suitable for the numerical evaluation of our solution.

While the two-loop four-point integrals with massless internal lines are well known in the literature [65, 66, 74, 149], the four point integrals with one and two massive internal lines considered here are new and represent the main result of this communication.

We verified the numerical agreement of the MI’s in the unphysical region against the results of `SecDec` [61–63]. In particular, because of the presence of irreducible irrational weight functions, we found it convenient to cast 5 of the 17 MI’s with two massive internal lines as one-dimensional integral formulas [222], involving *GPLs* in the integrands. The numerical evaluation of our solutions can, therefore, be performed with the help of the `GiNaC` library [134] for the evaluation of *GPLs*.

9.2. Notations and Conventions

In this chapter we study the two-loop corrections to the following partonic scattering processes:

$$q(p_1) + \bar{q}(p_2) \rightarrow l^-(p_3) + l^+(p_4), \quad (9.1)$$

$$q(p_1) + \bar{q}'(p_2) \rightarrow l^-(p_3) + \bar{\nu}(p_4). \quad (9.2)$$

¹Other related studies can be found in [81, 83, 154]

The external particles are considered mass-less and they are on their mass-shell, $p_1^2 = p_2^2 = p_3^2 = p_4^2 = 0$. The scattering can be described in terms of the Mandelstam variables

$$s = (p_1 + p_2)^2, \quad t = (p_1 - p_3)^2, \quad u = (p_1 - p_4)^2, \quad (9.3)$$

in such a way that, for momentum conservation, we have $s + t + u = 0$. The physical region is defined by

$$s > 0, \quad t = -\frac{s}{2}(1 - \cos(\theta)), \quad (9.4)$$

where θ is the scattering angle in the partonic center of mass frame, lying in the range $0 < \theta < \pi$. Therefore, while $s > 0$, t is always negative and $-s < t < 0$.

The quantum corrections to the processes (9.1) and (9.2) can be expanded in power series of the coupling constants. At one loop, the QCD corrections consist on the exchange of a virtual gluon between the initial-state quarks. The final state is not affected, and at most mass-less three-point functions have to be evaluated. The EW corrections, instead, consist on the exchange of photons, Z and W bosons. Moreover, these quanta can be exchanged between the quarks in the initial state as well as the leptons in the final state, but they can also be exchanged between a quark in the initial state and a lepton in the final state. Consequently, in the calculation of the one-loop corrections one has to evaluate massive box and vertex diagrams. In the process of $q\bar{q} \rightarrow l\nu$ one has to evaluate diagrams in which a Z and a W bosons are exchanged simultaneously. In order to reduce the number of scales present in the calculation, we expand the Z propagators around m_W :

$$\frac{1}{p^2 - m_Z^2} = \frac{1}{p^2 - m_W^2 - \Delta m^2} \approx \frac{1}{p^2 - m_W^2} + \frac{m_Z^2}{(p^2 - m_W^2)^2} \xi + \dots \quad (9.5)$$

where

$$\xi = \frac{\Delta m^2}{m_Z^2} = \frac{m_Z^2 - m_W^2}{m_Z^2} \sim \frac{1}{4} \quad (9.6)$$

is the effective parameter of the expansion. The coefficients of the series in ξ are Feynman diagrams with the same masses, and eventually with increased powers in the expanded denominator. Such diagrams depend only on s, t , and one mass $m = m_W$.

However, this does not cause any problem in the calculation, since diagrams with higher powers of the propagators are in any case reduced to the same set of MI's. For phenomenological purposes the first order in ξ might be sufficient, but in principle any order in ξ can be calculated without effort, just relying on the reduction procedure. We apply the same approximation to the two-loop diagrams as well.

We calculate the quantum corrections to the processes (9.1,9.2) using a Feynman diagrams approach. After considering the interference with the leading order, and summing over the spins and colors, we express the squared absolute value of the amplitude in terms of dimensionally regularized scalar integrals. These integrals are reduced to a set of MI's by means of integration-by-parts identities [98, 223] and Lorentz-invariance identities [74], implemented in the computer program² `Reduze 2` [106, 165].

²Other public programs are available for the reduction to the MI's [104, 105, 107, 224–226].

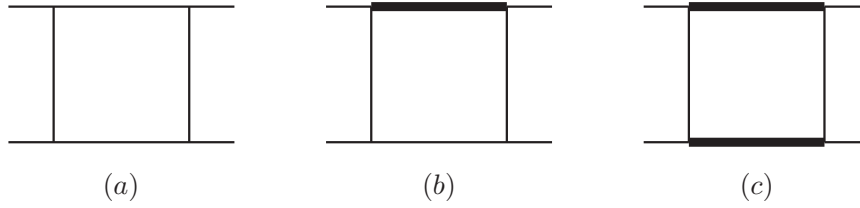


Figure 9.2.: One-loop topologies. Thin lines represent massless external particles and propagators, while thick lines represent massive propagators.

At one-loop, the topologies involved in the QCD and EW corrections are shown in figure 9.2, where we distinguish: *a*) the mass-less case; *b*) the exchange of one massive particle; and *c*) the exchange of two massive particles.

At two-loop, the topologies required by the $\mathcal{O}(\alpha\alpha_S)$ corrections are only planar. They are shown in figure 9.3. As for the one-loop case, we consider three classes of diagrams, according to the presence of massive particles.

Topologies *a*₁) and *a*₂) belong to the same 9-denominators mass-less topology. They reduce to 8 MIs, that were already known in the literature [65, 66, 74, 149]. Topologies *b*₁)–*b*₃) have one massive propagator. They reduce to 31 MI's out of which 24 contain one massive propagator and 7 are part of the MI's for topologies *a*₁) and *a*₂). The three-point functions were already known in the literature [227–229]. The four-point functions are calculated and presented here for the first time. Topologies *c*₁) and *c*₂) have two massive propagators and they reduce to 36 MI's, out of which 17 contain two massive propagators, 15 contain one massive propagator (and they are included in the set of MI's for topologies *b*₁)–*b*₃) and 4 contain only massless propagators. The three-point functions were known in the literature [230, 231] and the four-point functions are presented here for the first time.

The routings for one- and two-mass topologies, at the one- and two-loop level, can be defined in terms of the following sets of denominators D_n , where k_i ($i = 1, 2$) are the loop momenta, and p_i ($i = 1, \dots, 4$) are the external momenta:

- *One-mass topologies.* For the one-loop one-mass integrals (figure 9.2 *b*), we have:

$$D_1 = k_1^2, \quad D_2 = (k_1 - p_1)^2, \quad D_3 = (k_1 + p_2)^2 - m^2, \quad D_4 = (k_1 - p_1 + p_3)^2.$$

At two loops (figure 9.3 *b*₁–*b*₃), instead, we have:

$$\begin{aligned} D_1 &= k_1^2, & D_2 &= k_2^2, & D_3 &= (k_1 + k_2)^2, & D_4 &= (k_1 - p_1)^2, \\ D_5 &= (k_1 + p_2)^2, & D_6 &= (k_1 + k_2 - p_1)^2 - m^2, & D_7 &= (k_1 + k_2 + p_2)^2, \\ D_8 &= (k_1 + k_2 - p_1 + p_3)^2, & D_9 &= (k_1 - p_1 + p_3)^2. \end{aligned} \quad (9.7)$$

- *Two-mass topologies.* For the one-loop two-mass integrals (figure 9.2 *c*), we have:

$$D_1 = k_1^2, \quad D_2 = (k_1 - p_1)^2 - m^2, \quad D_3 = (k_1 + p_2)^2 - m^2, \quad D_4 = (k_1 - p_1 + p_3)^2.$$

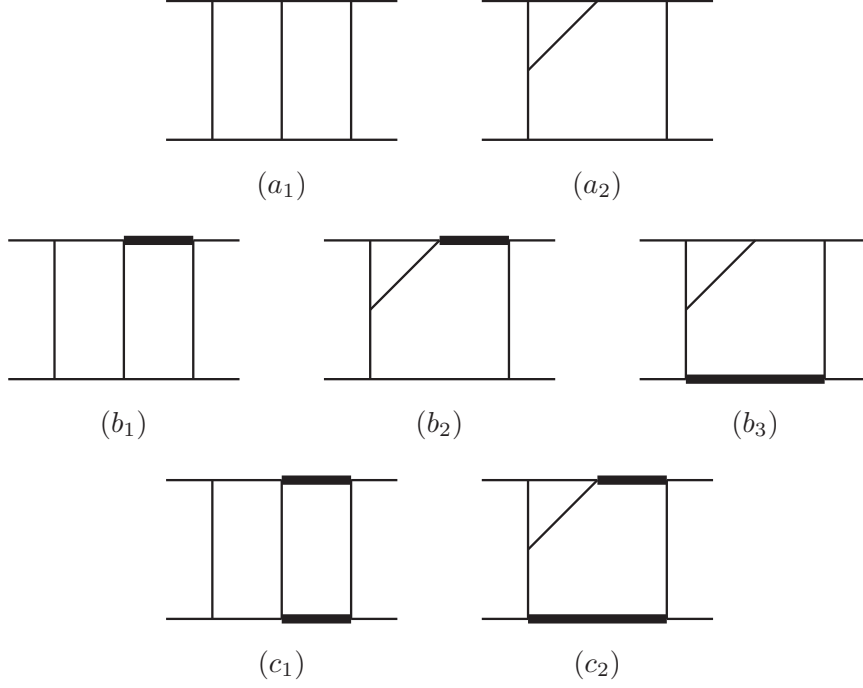


Figure 9.3.: Two-loop topologies. Thin lines represent massless external particles and propagators, while thick lines represent massive propagators.

At two loops (figure 9.3 c_1 and c_2), instead, we have:

$$\begin{aligned}
D_1 &= k_1^2, & D_2 &= k_2^2, & D_3 &= (k_1 + k_2)^2, & D_4 &= (k_1 - p_1)^2, \\
D_5 &= (k_1 + p_2)^2, & D_6 &= (k_1 + k_2 - p_1)^2 - m^2, & D_7 &= (k_1 + k_2 + p_2)^2 - m^2, \\
D_8 &= (k_1 + k_2 - p_1 + p_3)^2, & D_9 &= (k_1 - p_1 + p_3)^2.
\end{aligned} \tag{9.8}$$

In the following we consider ℓ -loop Feynman integrals in d dimensions, built out of p of the above denominators, each raised to some integer power, of the form

$$\int \widetilde{d^d k_1} \dots \widetilde{d^d k_\ell} \frac{1}{D_{a_1}^{n_1} \dots D_{a_p}^{n_p}}, \tag{9.9}$$

where the integration measure is defined as

$$\widetilde{d^d k_i} \equiv \frac{d^d k_i}{(2\pi)^d} \left(\frac{i S_\epsilon}{16\pi^2} \right)^{-1} \left(\frac{m^2}{\mu^2} \right)^\epsilon, \tag{9.10}$$

with μ the 't Hooft scale of dimensional regularization, and

$$S_\epsilon \equiv (4\pi)^\epsilon \frac{\Gamma(1 + \epsilon) \Gamma^2(1 - \epsilon)}{\Gamma(1 - 2\epsilon)}. \tag{9.11}$$

In eqs. (9.10), (9.11) we used $\epsilon = (4 - d)/2$.

9.3. System of Differential Equations for Master Integrals

In this section, we describe the general structure of the systems of differential equations obeyed by the MI's, and the corresponding solutions. Sections dedicated to the one-mass and two-mass MIs will follow, where the details of their complete determination will be provided.

The b - and c -type MI's are functions of the Mandelstam invariants defined in eq. (9.3) and of the mass m . For their evaluation it is convenient to define the dimensionless ratios

$$x \equiv -\frac{s}{m^2}, \quad y \equiv -\frac{t}{m^2}, \quad z \equiv -\frac{u}{m^2}, \quad \text{with } x + y + z = 0. \quad (9.12)$$

In the unphysical region $s < 0$, x is real and positive. Correspondingly, y can be either positive or negative.

The analytic continuation to the physical region requires the Feynman prescription on the invariants. There, s becomes positive, with a positive vanishing imaginary part, $s + i0^+$. Accordingly, x is negative:

$$x \rightarrow -x' - i0^+, \quad (9.13)$$

with

$$x' = \frac{s}{m^2} > 0. \quad (9.14)$$

On the other hand, t is negative (with a positive vanishing imaginary part) and ranges between 0 and $-s$, $-s < t < 0$.

The numeric evaluation of the MI's expressed in terms of GPLs of the variables x and y can be done in the whole s, t plain using the routines in [134] expressing our analytic formulas in terms of $GPLs$ evaluated in 1 and giving the explicit imaginary part to the Mandelstam variables (see for instance [232]).

The b -type and c -type MI's obey systems of partial differential equations in x and y , which can be combined into matrix equations for their total differentials. In general, the vector of MIs F is solution of the following system of differential equation,

$$dF = d\mathbb{K} F, \quad (9.15)$$

where the matrix \mathbb{K} depends *both* on the kinematic variables and on the spacetime dimension $d = 4 - 2\epsilon$.

By means of a suitable basis transformation, built with the help of the *Magnus exponential* [1, 115] following the procedure outlined in Sec. 2 of [2], we obtain a *canonical* set of MIs [77]. Such a basis obeys a system of differential equation where the dependence on ϵ is factorized from the kinematics. Moreover, the coefficient matrices can be assembled in a (logarithmic) differential form, referred to as canonical $d\log$ -form. Hence, the canonical basis I obeys the following system of equations,

$$dI = \epsilon dAI, \quad (9.16)$$

with

$$dA = \sum_{i=1}^n \mathbb{M}_i d\log \eta_i, \quad (9.17)$$

where dA is the $d\log$ matrix written in terms of differentials $d\log \eta_i$ (that contain the kinematic dependence) and coefficient matrices \mathbb{M}_i (with rational-number entries). The integrability conditions for eq. (9.16) read

$$\partial_a \partial_b \mathbb{A} - \partial_b \partial_a \mathbb{A} = 0, \quad [\partial_a \mathbb{A}, \partial_b \mathbb{A}] = 0. \quad (9.18)$$

9.3.1. Constant $GPLs$

In the determination of the boundary values of the MI's we encountered constant $GPLs$ of argument 1 with weights drawn from three sets. For the one-mass MI's there is only one relevant set, with four weights,

- $\{-1, 0, \frac{1}{2}, 1\}$.

For the two-mass MI's we encountered the following two sets, with seven weights each

- $\{-1, 0, -i, i, 1, (-1)^{\frac{1}{3}}, -(-1)^{\frac{2}{3}}\}$,
- $\{-1, 0, -i, i, 1, -(-1)^{\frac{1}{6}}, -(-1)^{\frac{5}{6}}\}$,

where the former includes the third roots of -1 and the latter involves a subset of the sixth roots of -1 . With the help of **GiNaC**, we verified that, at order ϵ^k , the Taylor coefficient of each MI $I_i^{(k)}$ contains a combinations of constant $GPLs$ that turns out to be proportional to ζ_k , namely amounting to $q_{i,k} \zeta_k$, with $q_{i,k} \in \mathbb{Q}$. The resulting identities were verified at high numerical accuracy. As examples, we show,

$$0 = G_r + G_{-r^2}, \quad (9.19)$$

$$\begin{aligned} \zeta_2 = & 3G_{0,-r^2} + 4G_{r,-r^2} + 4G_{-r^2,0} - 2G_{-r^2,1} + 4G_{-r^2,r} \\ & + 4G_{-r^2,-r^2} + 3G_{0,r} + 4G_{r,0} - 2G_{r,1} + 4G_{r,r}, \end{aligned} \quad (9.20)$$

$$\begin{aligned} -\frac{77}{8}\zeta_3 = & G_{-1,-1,\frac{1}{2}} + G_{-1,\frac{1}{2},-1} + G_{-1,\frac{1}{2},1} + 3G_{0,0,\frac{1}{2}} + 3G_{0,\frac{1}{2},1} + G_{\frac{1}{2},-1,-1} \\ & + G_{\frac{1}{2},-1,1} - G_{\frac{1}{2},0,\frac{1}{2}} + 4G_{\frac{1}{2},0,1} + G_{\frac{1}{2},1,-1} + \frac{3}{2}\zeta_2 G_{\frac{1}{2}}, \end{aligned} \quad (9.21)$$

where for simplicity we omitted the argument ($x = 1$) of the $GPLs$ and we defined the weight $r \equiv (-1)^{1/3}$. For related studies see also [233–236].

9.4. One-Mass Master Integrals

In this section we describe the computation of the MI's with one internal massive line, namely topology (b) of figure 9.2 and topologies (b₁)-(b₃) of figure 9.3.

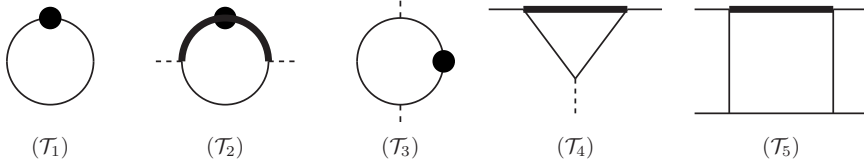


Figure 9.4.: One-loop one-mass MI's $\mathcal{T}_{1,\dots,5}$. Thin lines represent massless external particles and propagators; thick lines stand for massive propagators; an horizontal (vertical) dashed external line represents an off-shell leg with squared momentum equal to s (t); dots indicate squared propagators.

9.4.1. One-Loop

The following set of MI's for the one-loop one-mass box obeys a differential equation in x and y , defined in eq. (9.12), which is linear in ϵ :

$$\begin{aligned} F_1 &= \epsilon \mathcal{T}_1, & F_2 &= \epsilon \mathcal{T}_2, & F_3 &= \epsilon \mathcal{T}_3, \\ F_4 &= \epsilon^2 \mathcal{T}_4, & F_5 &= \epsilon^2 \mathcal{T}_5. \end{aligned} \quad (9.22)$$

where the \mathcal{T}_i are depicted in figure 9.4. By means of the Magnus exponential [1, 115], according to the procedure outlined in Sec. 2 of [2], we obtain the canonical MI's

$$\begin{aligned} I_1 &= F_1, & I_2 &= -s F_2, & I_3 &= -t F_3, \\ I_4 &= -t F_4, & I_5 &= (s - m^2) t F_5. \end{aligned} \quad (9.23)$$

The alphabet of the corresponding $d\log$ -form, eq (9.17), is

$$\begin{aligned} \eta_1 &= x, & \eta_2 &= 1 + x, & \eta_3 &= y, \\ \eta_4 &= 1 - y, & \eta_5 &= x + y, \end{aligned} \quad (9.24)$$

and the coefficient matrices read

$$\begin{aligned} \mathbb{M}_1 &= \begin{pmatrix} 0 & 0 & 0 & 0 & 0 \\ 0 & 1 & 0 & 0 & 0 \\ 0 & 0 & 0 & 0 & 0 \\ 0 & 0 & 0 & 0 & 0 \\ 0 & 2 & -1 & -1 & 1 \end{pmatrix}, & \mathbb{M}_2 &= \begin{pmatrix} 0 & 0 & 0 & 0 & 0 \\ -1 & -2 & 0 & 0 & 0 \\ 0 & 0 & 0 & 0 & 0 \\ 0 & 0 & 0 & 0 & 0 \\ 0 & 0 & 0 & 0 & -2 \end{pmatrix}, & \mathbb{M}_3 &= \begin{pmatrix} 0 & 0 & 0 & 0 & 0 \\ 0 & 0 & 0 & 0 & 0 \\ 0 & 0 & -1 & 0 & 0 \\ 0 & 0 & 0 & 1 & 0 \\ 0 & 0 & 0 & 0 & -1 \end{pmatrix}, \\ \mathbb{M}_4 &= \begin{pmatrix} 0 & 0 & 0 & 0 & 0 \\ 0 & 0 & 0 & 0 & 0 \\ 0 & 0 & 0 & 0 & 0 \\ -1 & 0 & 1 & -1 & 0 \\ -1 & 0 & 1 & -1 & 0 \end{pmatrix}, & \mathbb{M}_5 &= \begin{pmatrix} 0 & 0 & 0 & 0 & 0 \\ 0 & 0 & 0 & 0 & 0 \\ 0 & 0 & 0 & 0 & 0 \\ 0 & 0 & 0 & 0 & 0 \\ 0 & -2 & -1 & 1 & 1 \end{pmatrix}. \end{aligned} \quad (9.25)$$

If $x > 0$ and $0 < y < 1$ all the letters η_i are positive. Since the alphabet is linear in x and y , according to the discussion in section 6.3, the solution can be conveniently cast in terms of *GPLs*.

Instead of choosing a particular basepoint \vec{x}_0 , the integration constants of $I_{2\dots 5}$ can be easily fixed by demanding regularity at the pseudothresholds $t \rightarrow -m^2$, $u \rightarrow 0$, $s \rightarrow 0$

and their reality in the euclidean region. On the other hand, I_1 is a constant and must be determined by direct integration:

$$I_1 = \frac{\Gamma(1 - 2\epsilon)}{\Gamma(1 - \epsilon)^2}. \quad (9.26)$$

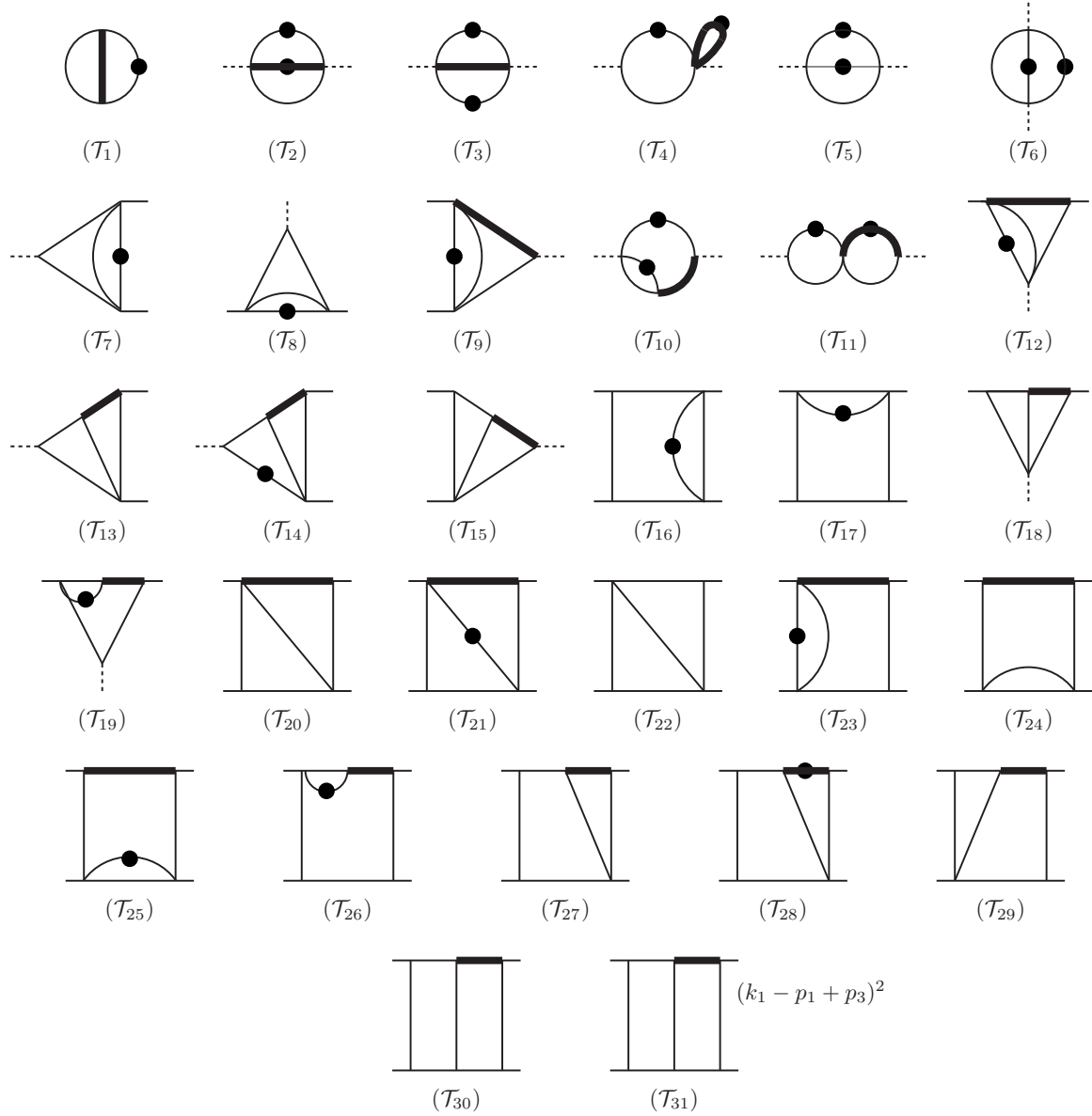


Figure 9.5.: Two-loop one-mass MI's $\mathcal{T}_{1,\dots,31}$. The conventions are as in figure 9.4.

9.4.2. Two-Loop

At the two-loop order, the following set of MI's admits ϵ -linear differential equations in x and y (defined in eq. (9.12)):

$$\begin{aligned}
F_1 &= (1 - \epsilon)\epsilon^2 \mathcal{T}_1, & F_2 &= \epsilon^2 \mathcal{T}_2, & F_3 &= \epsilon^2 \mathcal{T}_3, \\
F_4 &= \epsilon^2 \mathcal{T}_4, & F_5 &= \epsilon^2 \mathcal{T}_5, & F_6 &= \epsilon^2 \mathcal{T}_6, \\
F_7 &= \epsilon^3 \mathcal{T}_7, & F_8 &= \epsilon^3 \mathcal{T}_8, & F_9 &= \epsilon^3 \mathcal{T}_9, \\
F_{10} &= \epsilon^2 \mathcal{T}_{10}, & F_{11} &= \epsilon^2 \mathcal{T}_{11}, & F_{12} &= \epsilon^3 \mathcal{T}_{12}, \\
F_{13} &= \epsilon^4 \mathcal{T}_{13}, & F_{14} &= \epsilon^3 \mathcal{T}_{14}, & F_{15} &= \epsilon^4 \mathcal{T}_{15}, \\
F_{16} &= \epsilon^3 \mathcal{T}_{16}, & F_{17} &= \epsilon^3 \mathcal{T}_{17}, & F_{18} &= \epsilon^4 \mathcal{T}_{18}, \\
F_{19} &= \epsilon^3 \mathcal{T}_{19}, & F_{20} &= \epsilon^4 \mathcal{T}_{20}, & F_{21} &= \epsilon^3 \mathcal{T}_{21}, \\
F_{22} &= \epsilon^4 \mathcal{T}_{22}, & F_{23} &= \epsilon^3 \mathcal{T}_{23}, & F_{24} &= (1 - 2\epsilon)\epsilon^3 \mathcal{T}_{24}, \\
F_{25} &= \epsilon^3 \mathcal{T}_{25}, & F_{26} &= \epsilon^3 \mathcal{T}_{26}, & F_{27} &= \epsilon^4 \mathcal{T}_{27}, \\
F_{28} &= \epsilon^3 \mathcal{T}_{28}, & F_{29} &= \epsilon^4 \mathcal{T}_{29}, & F_{30} &= \epsilon^4 \mathcal{T}_{30}, \\
F_{31} &= \epsilon^4 \mathcal{T}_{31}, & & & &
\end{aligned} \tag{9.27}$$

where the \mathcal{T}_i are depicted in figure 9.5.

Once again, by means of Magnus exponentials, we are able to obtain a canonical basis:

$$\begin{aligned}
I_1 &= F_1, & I_2 &= -s F_2, & I_3 &= 2m^2 F_2 + \lambda_- F_3, \\
I_4 &= -s F_4, & I_5 &= -s F_5, & I_6 &= -t F_6, \\
I_7 &= -s F_7, & I_8 &= -t F_8, & I_9 &= -s F_9, \\
I_{10} &= \frac{m^2}{2\lambda_+} (2s\lambda_- F_{10} - 2F_1 - 3s F_5), & I_{11} &= s^2 F_{11}, & I_{12} &= -t F_{12}, \\
I_{13} &= -s F_{13}, & I_{14} &= s^2 F_{14}, & I_{15} &= -s F_{15}, \\
I_{16} &= s t F_{16}, & I_{17} &= s t F_{17}, & I_{18} &= -t F_{18}, \\
I_{19} &= -m^2 t F_{19}, & I_{20} &= u F_{20}, & I_{21} &= -t \lambda_- F_{21}, \\
I_{22} &= u F_{22}, & I_{23} &= -t \lambda_- F_{23}, & I_{24} &= -t F_{24}, \\
I_{25} &= -t \lambda_- F_{25}, & I_{26} &= -t m^2 (F_{17} + \lambda_- F_{26}), & I_{27} &= s t F_{27}, \\
I_{28} &= m^2 s ((m^2 + t) F_{28} - 2F_{27}), & I_{29} &= (s t + m^2 u) F_{29}, & I_{30} &= s t \lambda_- F_{30}, \\
I_{31} &= m^2 s F_{29} - s \lambda_- F_{31}, & & & &
\end{aligned} \tag{9.28}$$

where $\lambda_{\pm} = (m^2 \pm s)$. After combining the two differential equations into one total differential, we find a $d\log$ -form (9.17) with the alphabet

$$\begin{aligned}
\eta_1 &= x, & \eta_2 &= 1 + x, & \eta_3 &= y, \\
\eta_4 &= 1 - y, & \eta_5 &= x + y, & \eta_6 &= x + y + xy,
\end{aligned} \tag{9.29}$$

which includes the additional letter η_6 as compared to one-loop (9.24). If $x > 0$ and $0 < y < 1$ all the letters η_i are positive. The coefficient matrices are given in the appendix (D.1). Since the additional letter is multilinear in x and y , also at the two-loop order we are able to obtain the solution in terms of *GPLs* (see the discussion in section 6.3).

We hereby list the conditions imposed to which integrals for determining their boundary constants;

- regularity at $t \rightarrow -m^2$ and $u \rightarrow 0$ and imposing reality on the resulting boundary constants: $I_{2,\dots,5,7\dots10,12,14\dots17,19\dots31}$,
- limit $s \rightarrow 0$: $I_{11,13}$,
- limit $t \rightarrow 0$: I_{18} .

This leaves us with $I_{1,6}$, to be determined by direct integration:

$$I_1 = -\frac{1}{2} \frac{\Gamma(1-2\epsilon)^2 \Gamma(1+2\epsilon)}{\Gamma(1-\epsilon)^3 \Gamma(1+\epsilon)}, \quad (9.30)$$

$$I_6 = -\frac{y^{-2\epsilon}}{\pi} \frac{\Gamma(\frac{1}{2}-\epsilon) \Gamma(\frac{1}{2}+\epsilon) \Gamma(1-2\epsilon)}{\Gamma(1-3\epsilon) \Gamma(1+\epsilon)}. \quad (9.31)$$

Owing to the explicit representation in terms of *GPLs*, all the one-mass MI's can be computed in the whole (s, t) domain. Our results have been successfully checked against *SecDec*.

9.5. Two-Mass Master Integrals

In this section we describe the computation of the MI's with two internal massive lines, namely topology (c) of figure 9.2 and topologies (c_1) - (c_2) of figure 9.3.

9.5.1. Variables for the two-mass Integrals

For the evaluation of the two-mass MI's, we find it convenient to introduce the reduced variables w and z defined by

$$-\frac{s}{m^2} = \frac{(1-w)^2}{w}, \quad -\frac{t}{m^2} = \frac{w(1+z)^2}{z(1+w)^2}. \quad (9.32)$$

We note that the above mapping allows the evaluation of our results everywhere in the (s, t) plane, with the exception of the value $w = -1$ (corresponding to $s = 4m^2$). For that specific value of w , the t dependence in z gets lost by construction, and $z = -1$ independently on t .

The evaluation of the solution at $s = 4m^2$ requires further investigations and it will be addressed in a forthcoming publication.

Range of values for w

For w , defined by the first of eqs. (9.32), we choose the following root:

$$w = \frac{\sqrt{4m^2 - s - i0^+} - \sqrt{-s - i0^+}}{\sqrt{4m^2 - s - i0^+} + \sqrt{-s - i0^+}}, \quad (9.33)$$

where we explicitly used the Feynman prescription $s + i0^+$.

1. If $s < 0$, we have positive w and $0 < w < 1$. In particular, when $s \rightarrow -\infty$, $w \rightarrow 0$, while for $s \rightarrow 0$, $w \rightarrow 1$.
2. If $0 < s < 4m^2$, w becomes a phase. In fact

$$w = \frac{\sqrt{4m^2 - s} + i\sqrt{s}}{\sqrt{4m^2 - s} - i\sqrt{s}} = e^{i\phi}, \quad (9.34)$$

where

$$\phi = 2 \arctan \sqrt{\frac{s}{4m^2 - s}} \quad (9.35)$$

and $0 < \phi < \pi$.

3. If $s > 4m^2$, w becomes negative (with a positive vanishing imaginary part)

$$w = -\frac{\sqrt{s} - \sqrt{s - 4m^2}}{\sqrt{s} + \sqrt{s - 4m^2}} = -w' + i0^+, \quad (9.36)$$

and $1 > w' > 0$ when $4m^2 < s < +\infty$.

Range of values for z

The variable z depends both on s and t . In order to study the different regimes, we define the following function of s

$$\begin{aligned} t_* &\equiv -m^2 \frac{w}{(1+w)^2} \\ &= -\frac{m^4}{4m^2 - s}. \end{aligned} \quad (9.37)$$

where the second equality follows from eq. (9.33). We also define the ratio

$$K \equiv \frac{t}{t_*}, \quad (9.38)$$

so that the second of eqs. (9.32) reads

$$K = \frac{(1+z)^2}{z}. \quad (9.39)$$

We choose the following root of the above equation

$$z = \frac{\sqrt{K} - \sqrt{K-4}}{\sqrt{K} + \sqrt{K-4}}. \quad (9.40)$$

Note that eq. (9.40) contains square-roots of K . Therefore, in order to compute z when $K < 4$, we have to keep track of the vanishing imaginary parts of the quantities entering eq. (9.38). Region by region in the (s, t) plane, the correct sign of the vanishing imaginary part (if present) is determined by the Feynman prescription on s, t, u , i.e. $s + i0^+$ when $s > 0$, and likewise for t and u .

Depending on the value of K , we distinguish three cases (here we keep the prescription for the vanishing imaginary part of K arbitrary):

1. $K > 4$

All the square roots in eq. (9.40) are real, so z is real with $0 < z < 1$.

2. $0 < K < 4$

For a given prescription $K \pm i0^+$, one obtains from eq. (9.40)

$$z = \frac{\sqrt{K} \mp i\sqrt{4-K}}{\sqrt{K} \pm i\sqrt{4-K}}, \quad (9.41)$$

which is solved by

$$z = e^{\mp i\psi}, \quad \psi = 2 \arctan \sqrt{\frac{4-K}{K}}, \quad 0 < \psi < \pi. \quad (9.42)$$

3. $K < 0$

For a given prescription $K \pm i0^+$, one obtains from eq. (9.40)

$$\begin{aligned} z &= \frac{\sqrt{-|K| \pm i0^+} - \sqrt{-|K| - 4 \pm i0^+}}{\sqrt{-|K| \pm i0^+} + \sqrt{-|K| - 4 \pm i0^+}} \\ &= \frac{\sqrt{|K|} - \sqrt{|K| + 4}}{\sqrt{|K|} + \sqrt{|K| + 4}} \mp i0^+ \\ &\equiv -z' \mp i0^+, \end{aligned} \quad (9.43)$$

with $0 < z' < 1$.

Note that, since K is a function of s and t , each case can arise from multiple regions in the (s, t) plane. In table 9.1 we summarize the solution for z in the different regions of the (s, t) plane, by displaying also the appropriate sign for the $i0^+$ prescription (if a vanishing imaginary part is present).

	$t < -4 t_* $	$-4 t_* < t < 0$	$0 < t < t_* $	$ t_* < t < 4 t_* $	$t > 4 t_* $
$s < 0$	z	$e^{-i\psi}$	$-z' + i0^+$	$-z' + i0^+$	$-z' + i0^+$
$0 < s < 4m^2$	z	$e^{i\psi}$	$-z' + i0^+$	$-z' - i0^+$	$-z' - i0^+$
$s > 4m^2$	$-z' + i0^+$	$-z' + i0^+$	$e^{-i\psi}$	$e^{-i\psi}$	z

Table 9.1.: We show the solution for z in each region of the (s, t) plane, as in eqs. (9.40), (9.42), and (9.43). The boldface entries are the solutions in the regions that contain a part of the physical s -channel scattering region, $s > 0$ with $-s < t < 0$.

9.5.2. One-Loop

We choose the following set of MI's, admitting a differential equation linear in ϵ

$$\begin{aligned}
F_1 &= \epsilon \mathcal{T}_1, & F_2 &= \epsilon \mathcal{T}_2, & F_3 &= \epsilon \mathcal{T}_3, \\
F_4 &= \epsilon^2 \mathcal{T}_4, & F_5 &= \epsilon^2 \mathcal{T}_5, & F_6 &= \epsilon^2 \mathcal{T}_6,
\end{aligned} \tag{9.44}$$

where the \mathcal{T}_i are shown in figure 9.6. After applying the Magnus transformation we obtain the following canonical basis

$$\begin{aligned}
I_1 &= F_1, & I_2 &= -s \sqrt{1 - \frac{4m^2}{s}} F_2, & I_3 &= -t F_3, \\
I_4 &= -s F_4, & I_5 &= -t F_5, & I_6 &= st \sqrt{1 - 4 \frac{m^2}{s} \left(1 + \frac{m^2}{t}\right)} F_6,
\end{aligned} \tag{9.45}$$

The alphabet of the corresponding canonical $d\log$ -form, (9.17), is non-rational in s, t and m . In particular four square roots appear

$$\sqrt{-s}, \sqrt{4m^2 - s}, \sqrt{-t}, \text{ and } \sqrt{1 - \frac{4m^2}{s} \left(1 + \frac{m^2}{t}\right)}. \tag{9.46}$$

We can rationalize the $d\log$ -form with the help of the variable transformation (9.32). In terms of w and z , the alphabet reads

$$\begin{aligned}
\eta_1 &= z, & \eta_2 &= 1 + z, & \eta_3 &= 1 - z, \\
\eta_4 &= w, & \eta_5 &= 1 + w, & \eta_6 &= 1 - w, \\
\eta_7 &= z - w, & \eta_8 &= z + w^2, & \eta_9 &= 1 - wz, \\
\eta_{10} &= 1 + w^2 z,
\end{aligned} \tag{9.47}$$

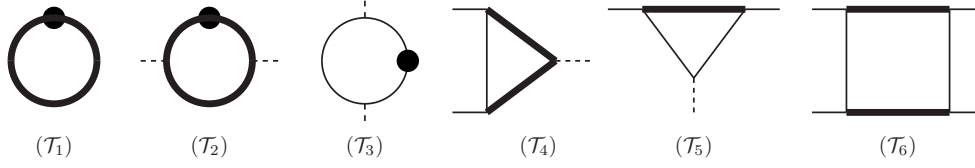


Figure 9.6.: One-loop two-mass MIs $\mathcal{T}_{1,\dots,6}$. The conventions are as in figure 9.4.

and the coefficient matrices are

$$\begin{aligned}
\mathbb{M}_1 &= \begin{pmatrix} 0 & 0 & 0 & 0 & 0 & 0 \\ 0 & 0 & 0 & 0 & 0 & 0 \\ 0 & 0 & 1 & 0 & 0 & 0 \\ 0 & 0 & 0 & 0 & 0 & 0 \\ 1 & 0 & -1 & 0 & 0 & 0 \\ 0 & 2 & 0 & 0 & 0 & 0 \end{pmatrix}, & \mathbb{M}_4 &= \begin{pmatrix} 0 & 0 & 0 & 0 & 0 & 0 \\ 1 & 1 & 0 & 0 & 0 & 0 \\ 0 & 0 & -1 & 0 & 0 & 0 \\ 0 & -2 & 0 & -1 & 0 & 0 \\ 0 & 0 & 0 & 0 & 1 & 0 \\ 0 & 0 & 0 & 0 & 0 & -1 \end{pmatrix}, & \mathbb{M}_5 &= \begin{pmatrix} 0 & 0 & 0 & 0 & 0 & 0 \\ 0 & -2 & 0 & 0 & 0 & 0 \\ 0 & 0 & 2 & 0 & 0 & 0 \\ 0 & 0 & 0 & 0 & 0 & 0 \\ 2 & 0 & -2 & 0 & 0 & 0 \\ 0 & 0 & 0 & 0 & 0 & -2 \end{pmatrix}, \\
\mathbb{M}_7 &= \begin{pmatrix} 0 & 0 & 0 & 0 & 0 & 0 \\ 0 & 0 & 0 & 0 & 0 & 0 \\ 0 & 0 & 0 & 0 & 0 & 0 \\ 0 & 0 & 0 & 0 & 0 & 0 \\ -1 & 0 & 1 & 0 & -1 & 0 \\ -2 & 0 & 2 & 0 & -2 & 0 \end{pmatrix}, & \mathbb{M}_8 &= \begin{pmatrix} 0 & 0 & 0 & 0 & 0 & 0 \\ 0 & 0 & 0 & 0 & 0 & 0 \\ 0 & 0 & 0 & 0 & 0 & 0 \\ 0 & 0 & 0 & 0 & 0 & 0 \\ 0 & 0 & 0 & 0 & 0 & 0 \\ 0 & 0 & 0 & 2 & 2 & 1 \end{pmatrix}, \\
\mathbb{M}_9 &= \begin{pmatrix} 0 & 0 & 0 & 0 & 0 & 0 \\ 0 & 0 & 0 & 0 & 0 & 0 \\ 0 & 0 & 0 & 0 & 0 & 0 \\ 0 & 0 & 0 & 0 & 0 & 0 \\ -1 & 0 & 1 & 0 & -1 & 0 \\ 2 & 0 & -2 & 0 & 2 & 0 \end{pmatrix}, & \mathbb{M}_{10} &= \begin{pmatrix} 0 & 0 & 0 & 0 & 0 & 0 \\ 0 & 0 & 0 & 0 & 0 & 0 \\ 0 & 0 & 0 & 0 & 0 & 0 \\ 0 & 0 & 0 & 0 & 0 & 0 \\ 0 & 0 & 0 & 0 & 0 & 0 \\ 0 & 0 & 0 & -2 & -2 & 1 \end{pmatrix}, & & (9.48)
\end{aligned}$$

and $(\mathbb{M}_2)_{3,3} = -2$ and $(\mathbb{M}_2)_{5,5} = 2$ are the only non-vanishing entries in \mathbb{M}_2 , $(\mathbb{M}_3)_{6,6} = -2$ is the only non-vanishing entry in \mathbb{M}_3 , and $(\mathbb{M}_6)_{4,4} = 2$ is the only non-vanishing entry in \mathbb{M}_6 . In the region $0 < w < z < 1$ all the letters η_i are positive. For a detailed discussion of how the interesting regions in the s, t plane are mapped to the $\mathbb{C} \times \mathbb{C}$ space of the w, z variables. The alphabet in (9.47) is linear in z but contains letters quadratic in w . As the latter can be linearized by factorization over the complex numbers, we are once again able to express the solution in terms of *GPLs* (see the discussion in section 6.3).

The integration constants of $I_{4,5,6}$ can be fixed by requiring their regularity at the pseudothresholds $s \rightarrow 0$, $t \rightarrow -m^2$ and $u \rightarrow 0$. The boundary constant of I_2 can be fixed by taking the $s \rightarrow 0$ limit. This leaves us with two integrals, $I_{1,3}$, to be determined by direct integration:

$$I_1 = \frac{\Gamma(1 - 2\epsilon)}{\Gamma(1 - \epsilon)^2}, \quad (9.49)$$

$$I_3 = \left[\frac{z(1+w)^2}{w(1+z)^2} \right]^\epsilon. \quad (9.50)$$

9.5.3. Two-Loop

At the two-loop order we start with the set of MIs

$$\begin{aligned}
F_1 &= (1 - \epsilon) \epsilon^2 \mathcal{T}_1, & F_2 &= \epsilon^2 \mathcal{T}_2, & F_3 &= \epsilon^2 \mathcal{T}_3, \\
F_4 &= \epsilon^2 \mathcal{T}_4, & F_5 &= \epsilon^2 \mathcal{T}_5, & F_6 &= \epsilon^3 \mathcal{T}_6, \\
F_7 &= \epsilon^3 \mathcal{T}_7, & F_8 &= \epsilon^3 \mathcal{T}_8, & F_9 &= \epsilon^2 \mathcal{T}_9, \\
F_{10} &= (1 - 2\epsilon) \epsilon^2 \mathcal{T}_{10}, & F_{11} &= \epsilon^2 \mathcal{T}_{11}, & F_{12} &= \epsilon^3 \mathcal{T}_{12}, \\
F_{13} &= \epsilon^4 \mathcal{T}_{13}, & F_{14} &= \epsilon^3 \mathcal{T}_{14}, & F_{15} &= \epsilon^4 \mathcal{T}_{15}, \\
F_{16} &= \epsilon^3 \mathcal{T}_{16}, & F_{17} &= (1 - 2\epsilon) \epsilon^3 \mathcal{T}_{17}, & F_{18} &= \epsilon^3 \mathcal{T}_{18}, \\
F_{19} &= \epsilon^3 \mathcal{T}_{19}, & F_{20} &= \epsilon^4 \mathcal{T}_{20}, & F_{21} &= \epsilon^3 \mathcal{T}_{21}, \\
F_{22} &= \epsilon^4 \mathcal{T}_{22}, & F_{23} &= \epsilon^3 \mathcal{T}_{23}, & F_{24} &= (1 - 2\epsilon) \epsilon^3 \mathcal{T}_{24}, \\
F_{25} &= \epsilon^3 \mathcal{T}_{25}, & F_{26} &= (1 - 2\epsilon) \epsilon^3 \mathcal{T}_{26}, & F_{27} &= \epsilon^3 \mathcal{T}_{27}, \\
F_{28} &= \epsilon^3 \mathcal{T}_{28}, & F_{29} &= \epsilon^4 \mathcal{T}_{29}, & F_{30} &= \epsilon^4 \mathcal{T}_{30}, \\
F_{31} &= \epsilon^3 \mathcal{T}_{31}, & F_{32} &= \epsilon^4 \mathcal{T}_{32}, & F_{33} &= \epsilon^4 \mathcal{T}_{33}, \\
F_{34} &= \epsilon^4 \mathcal{T}_{34}, & F_{35} &= \epsilon^4 \mathcal{T}_{35}, & F_{36} &= \epsilon^4 \mathcal{T}_{36},
\end{aligned} \tag{9.51}$$

where the \mathcal{T}_i are shown in figure 9.7. The MIs \mathbf{F} admit ϵ -linear differential equations, except for one of them. We have indeed

$$d\mathbf{F} = d\mathbb{K} \mathbf{F}, \quad \mathbb{K} = \mathbb{K}_0 + \epsilon \mathbb{K}_1 + \frac{1}{1 - 2\epsilon} \mathbb{K}_2, \tag{9.52}$$

where $\mathbb{K}_0, \mathbb{K}_1$ and \mathbb{K}_2 do not depend on ϵ , and \mathbb{K}_2 is non-vanishing only in the inhomogeneous part of the differential equation for F_{36} . In a first step we apply the Magnus algorithm on $\mathbb{K}_0 + \epsilon \mathbb{K}_1$ in order to remove \mathbb{K}_0 , and in a second step we apply an ad-hoc transformation in order to remove the remaining non-linear piece.

The corresponding canonical basis reads

$$\begin{aligned}
I_1 &= F_1, & I_2 &= -s F_2, & I_3 &= m^2 (2 F_2 + F_3) - s F_3, & I_4 &= -s F_4, \\
I_5 &= -t F_5, & I_6 &= -s F_6, & I_7 &= -t F_7, & I_8 &= -s F_8, \\
I_9 &= -\sqrt{1 - \frac{4m^2}{s}} \left(\frac{3}{2} F_8 + m^2 F_9 \right) - \frac{3}{2} s F_8, \\
I_{10} &= \frac{1}{4} \left(1 + \sqrt{\frac{-s}{4m^2 - s}} \right) \left(-2F_1 + (m^2 - s) (F_2 + F_3) + m^2 F_2 \right. \\
&\quad \left. + s F_{10} - s \sqrt{1 - \frac{4m^2}{s}} (F_2 + F_{10}) \right),
\end{aligned}$$

$$\begin{aligned}
I_{11} &= s^2 \sqrt{1 - \frac{4m^2}{s}} F_{11}, & I_{12} &= -t F_{12}, & I_{13} &= -s F_{13}, \\
I_{14} &= s^2 F_{14}, & I_{15} &= -s F_{15}, & I_{16} &= -m^2 s F_{16}, \\
I_{17} &= -s F_{17}, & I_{18} &= s^2 F_{18}, & I_{19} &= s t F_{19}, \\
I_{20} &= -t F_{20}, & I_{21} &= -m^2 t F_{21}, & I_{22} &= u F_{22}, \\
I_{23} &= (s - m^2) t F_{23}, & I_{24} &= -t F_{24}, & I_{25} &= (s - m^2) t F_{25}, \\
I_{26} &= -s F_{26}, & I_{27} &= s t \sqrt{1 - \frac{4m^2}{s} \left(1 + \frac{m^2}{t}\right)} F_{27}, \\
I_{28} &= s t \sqrt{1 - \frac{4m^2}{s} \left(1 + \frac{m^2}{t}\right)} (F_{25} + m^2 F_{28}) + t(m^2 - s) F_{25}, \\
I_{29} &= s^2 \sqrt{1 - \frac{4m^2}{s}} F_{29}, & I_{30} &= s t F_{30}, \\
I_{31} &= -m^2 s (2F_{30} + (m^2 + t) F_{31}), & I_{32} &= s t \sqrt{1 + \frac{m^4}{t^2} - \frac{2m^2}{s} \left(1 - \frac{u}{t}\right)} F_{32}, \\
I_{33} &= -s^2 t \sqrt{1 - \frac{4m^2}{s} \left(1 + \frac{m^2}{t}\right)} F_{33}, & I_{34} &= s^2 F_{34}, \\
I_{35} &= s \sqrt{1 - \frac{4m^2}{s}} (2t F_{32} - s t F_{33} + s F_{35}) - s^2 t \sqrt{1 + \frac{4m^2}{s} \left(1 + \frac{m^2}{t}\right)} F_{33}, \\
I_{36} &= \frac{s}{2(1 - 2\epsilon)} F_{17} - s t \left(1 - \sqrt{1 - \frac{4m^2}{s}}\right) F_{32} - s t F_{18} - 2 t F_{22} \\
&\quad - \frac{2m^2 s}{2 - \frac{s}{m^2} (1 - \sqrt{1 - \frac{4m^2}{s}})} (F_{29} + t F_{33} - F_{35}) - s F_{36}.
\end{aligned} \tag{9.53}$$

As compared to the one-loop case (9.46) we encounter one additional square root in the canonical $d\log$ -form

$$\sqrt{1 + \frac{m^4}{t^2} - \frac{2m^2}{s} \left(1 - \frac{u}{t}\right)}, \tag{9.54}$$

which is not rationalized by the change of variables in eq. (9.32). In terms of w and z , the

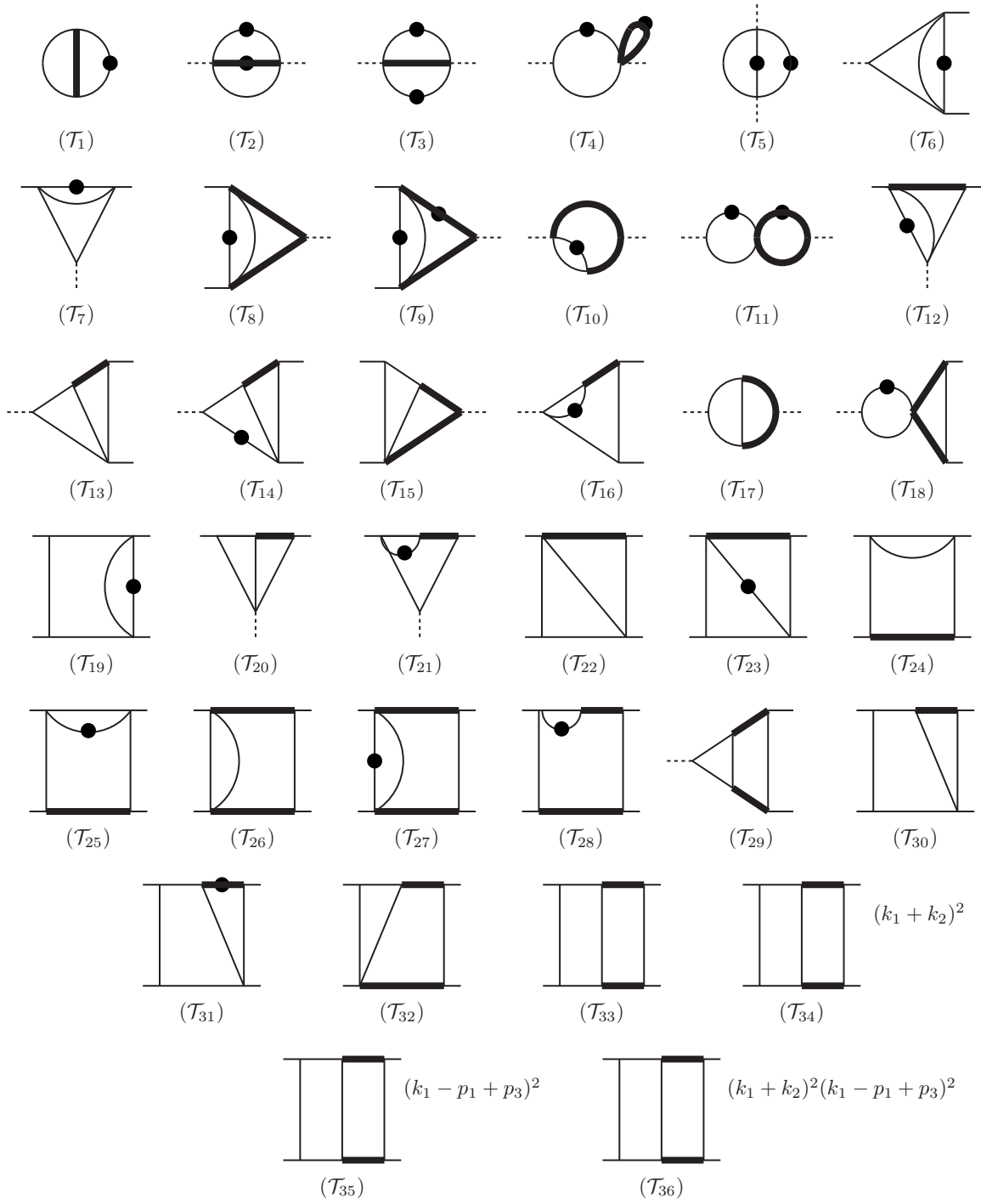


Figure 9.7.: Two-loop two-mass MI's $\mathcal{T}_{1,\dots,36}$. The conventions are as in figure 9.4.

alphabet reads

$$\begin{aligned}
\eta_1 &= z, & \eta_2 &= 1 + z, & \eta_3 &= 1 - z, \\
\eta_4 &= w, & \eta_5 &= 1 + w, & \eta_6 &= 1 - w, \\
\eta_7 &= 1 - w + w^2, & \eta_8 &= 1 - wz, & \eta_9 &= z - w, \\
\eta_{10} &= 1 + w^2 z, & \eta_{11} &= z + w^2, \\
\eta_{12} &= 4(1 + z)^4 w^3 + (1 - w)^2 \kappa_+^2(w, z), & \eta_{13} &= (1 + w)\sqrt{\rho} + (1 - w)\kappa_-(w, z), \\
\eta_{14} &= (1 + w)\sqrt{\rho} - (1 - w)\kappa_-(w, z), & \eta_{15} &= (1 + w)\sqrt{\rho} + (1 - w)\kappa_+(w, z), \\
\eta_{16} &= \frac{c_1 + c_2 \sqrt{\rho}}{c_3 + c_4 \sqrt{\rho}}, \\
\eta_{17} &= 2(1 - w)^2 w z^2 + \kappa_-^2(-w, z) + (z + w)(1 + wz)\sqrt{\rho},
\end{aligned} \tag{9.55}$$

where

$$\kappa_{\pm}(a, b) \equiv a(1 + b)^2 \pm b(1 + a)^2, \tag{9.56}$$

the argument of the square root entering $\eta_{13, \dots, 17}$ is

$$\rho = 4wz^2(1 + w)^2 - \kappa_+(w, z)\kappa_+(-w, -z), \tag{9.57}$$

and the four coefficients in η_{16} are given by

$$c_1 = (1 + w)^2 (1 - 4w + w^2) z^2 (1 + z)^2 + w^2 (1 + z)^6 + 2w (1 - w + w^2) z (1 + z)^4 - 2(1 + w)^4 z^3, \tag{9.58}$$

$$c_2 = (1 - z^2) \kappa_+(w, z), \tag{9.59}$$

$$\begin{aligned}
c_3 &= 2w^8 z^4 + 2w^7 z^3 (z^2 + 6z + 1) - w^6 (z - 1)^2 z^2 (z^2 + 4z + 1) \\
&\quad - 2w^5 z (z^6 - z^5 - 8z^4 - 8z^3 - 8z^2 - z + 1) \\
&\quad + w^4 (z^8 - 2z^7 - 2z^6 + 6z^5 - 10z^4 + 6z^3 - 2z^2 - 2z + 1) \\
&\quad - 2w^3 z (z^6 - z^5 - 8z^4 - 8z^3 - 8z^2 - z + 1) \\
&\quad - w^2 (z - 1)^2 z^2 (z^2 + 4z + 1) + 2wz^3 (z^2 + 6z + 1) + 2z^4,
\end{aligned} \tag{9.60}$$

$$c_4 = -w(1 - z^2)(z - w)(1 - wz) \left(\kappa_-(-w, -z) + (1 + w)^2 z \right). \tag{9.61}$$

In the region $0 < w < z < 1$ all the letters η_i are positive.

As already stressed, the alphabet is not rational in w and z . This prevents us from expressing the complete solution in terms of *GPLs*. In particular, the structure of the coefficient matrices \mathbb{M}_i is such that the solution for $I_{32}^{(3)}$ and for $I_{32, \dots, 36}^{(4)}$, see eqs. (6.11), (6.12), involves path integration over *dlog*'s with non rational arguments. Nevertheless, the MI's $I_{1, \dots, 31}$ admit a representation in terms of *GPLs* which is convenient for their numerical evaluation. As for the remaining MI's, we followed the procedure outlined in section 6.3: we express the solution up to weight 2 for I_{32} and up to weight 3 for $I_{33, \dots, 36}$ in terms of *GPLs*

and then obtain an 1-fold integral representation for the higher weights (for $I_{32,\dots,36}^{(4)}$ we use eq. (6.28)).

We hereby list the conditions imposed to integrals $I_{1,\dots,31}$ for determining their boundary constants;

- independent input: $I_{1,4,\dots,7,13,14,20,25}$,
- regularity at $s \rightarrow 0$: I_{24} ,
- regularity at $t \rightarrow -m^2$: $I_{12,21}$,
- regularity at $u \rightarrow 0$: $I_{19,30,31}$,
- limit $s \rightarrow 0$: $I_{2,3,6,\dots,10,15\dots 18,29}$,
- limit $t \rightarrow -m^2$ and $s \rightarrow 0$: I_{28} ,
- regularity at $s \rightarrow 0$ and matching to independent input: $I_{22,23}$.

For the MI's $I_{32,\dots,36}$ we observe that regularity at $u = s = t = 0$, corresponding to $\vec{x}_0 = (w_0, z_0) = (1, -1)$, implies

$$I_{32,\dots,36}(\epsilon, \vec{x}_0) = 0, \quad (9.62)$$

that we choose as initial condition of our solution in terms of iterated integrals.

The MI's $I_{1,\dots,31}$ are represented in terms of *GPLs*, and can be computed on the whole (s, t) plane (except for the line $s = 4m^2$).

The explicit evaluation of $I_{32,\dots,36}$ requires a careful choice of the integration path, in such a way that no branch cuts are crossed. We successfully checked our results in the unphysical region $s < 0$ against the numerical values obtained with **SecDec**. The evaluation of our analytic result relies on the use of **GiNaC** for the computation of the *GPLs* and on a one-dimensional integration for the cases where non-rational weights appear in the most external iteration, according to the eq. (6.28). As for the latter, we exploited the propriety of path-independence to choose simple paths (that avoid the singularities on the way from the basepoint to the chosen endpoints). Let us remark that in this work we did not focus on the the computing performances of the numerical evaluation of the mixed Chen-Goncharov iterated integrals appearing in our analytic expression. This aspect, together with a study of the analytic properties of our solutions in the whole phase-space, requires a dedicated future investigation.

9.6. Conclusions

In this chapter, we presented the calculation of the master integrals (MI's) needed for the virtual QCD×EW two-loop corrections to the Drell-Yan scattering processes,

$$q + \bar{q} \rightarrow l^- + l^+ , \quad q + \bar{q}' \rightarrow l^- + \bar{\nu},$$

for massless external particles. Besides the exchange of massless gauge bosons, such as gluons and photons, the relevant Feynman diagrams involve also the presence of W and Z propagators. Given the small difference between the masses of the W and Z bosons, in the diagrams containing both virtual particles at the same time, we performed a series expansion in the difference of the squared masses. Owing to this approximation, we distinguished three types of diagrams, according to the presence of massive internal lines: the no-mass type, the one-mass type, and the two-mass type, where all massive propagators, when occurring, contain the same mass value. The evaluations of the four point functions with one and two internal massive propagators are the main novel results of this communication.

To achieve it, we identified a basis of 49 MI's and evaluated them with the method of the differential equations. With the help of the Magnus exponential, the MI's were found to obey a canonical system of differential equations. Boundary conditions were imposed either by matching the solutions onto simpler integrals in special kinematic configurations, or by requiring the regularity of the solution at pseudo-thresholds. The canonical MI's were given as Taylor series around $d = 4$ space-time dimensions, up to order four, whose coefficients were given in terms of iterated integrals up to weight four. The solution could be expressed in terms of Chen's iterated integrals, yet, we adopted a mixed representation in terms of Chen-Goncharov iterated integrals, suitable for their numerical evaluation. Further studies concerning the analytic properties of the presented MI's in the whole phase-space, and the optimization of their numerical evaluation will be the subject of a forthcoming publication.

Higgs Boson Pair Production in Gluon Fusion at NLO

10.1. Introduction

The couplings of the Higgs boson to electroweak bosons and heavy fermions are being established as Standard-Model-like at an impressive rate. In contrast, the measurement of the Higgs boson self-coupling, which is vital in order to confirm the mechanism of electroweak symmetry breaking, is still outstanding, and will have to wait until the LHC high-luminosity upgrade. However, the Higgs boson self-coupling(s) could be enhanced by physics Beyond the Standard Model (BSM), and it is an important task to be able to distinguish BSM effects from effects due to higher order corrections in perturbation theory.

Gluon fusion is the dominant production channel for Higgs boson pair production. However, as this process proceeds via a heavy quark loop already at the leading order (LO), the next-to-leading order corrections involve two-loop four-point diagrams with two masses, m_h and m_t , and the analytic calculation of two-loop four-point integrals with different internal and external mass scales has not been achieved so far.

The leading order (one-loop) calculation of Higgs boson pair production in gluon fusion has been performed in Refs. [88, 237]. NLO corrections in the $m_t \rightarrow \infty$ limit for both the Standard Model and the MSSM have been performed in Ref. [89]. Finite top-quark mass corrections to the NLO result have been calculated in Refs. [92–97]. The NNLO QCD corrections in the $m_t \rightarrow \infty$ effective field theory also have been computed [93, 238, 239], and they have been supplemented by an expansion in $1/m_t^2$ in Ref. [96]. In the effective field theory, resummation at NLO+NNLL has been considered in Ref. [240], and recently, even matched NNLO+NNLL resummed results became available [241]. The dominant uncertainty therefore is given by the unknown top-quark mass effects at NLO.

The top-quark mass effects have been included in various approximations in the literature:

- (i) The “Born-improved HEFT (Higgs Effective Field Theory)” approximation, which is the one employed in the program HPAIR [88, 89]. It uses the heavy top-quark limit throughout the NLO calculation, in combination with a re-weighting factor B/B_{HEFT} , where B denotes the leading order result in the full theory. In HPAIR the re-weighting

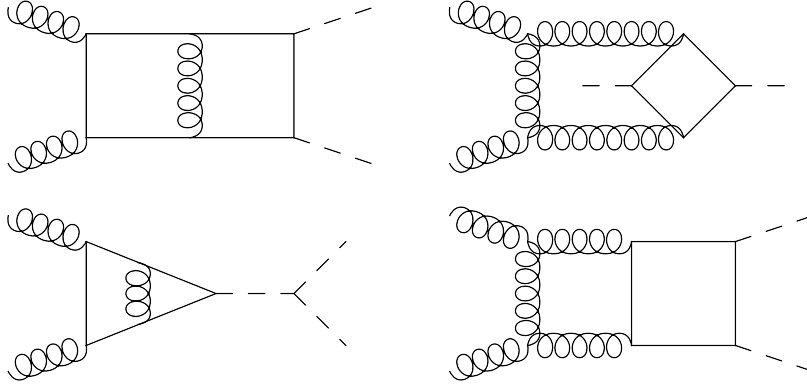


Figure 10.1.: This figure shows some Feynman diagrams, which contribute to the virtual two-loop amplitude for Higgs pair production through gluon fusion at NLO. solid lines represent massive top propagators; curly lines stand for the gluon propagators; dashed external lines represent the Higgs bosons.

is done at matrix element level, but after the angular integration of the phase space, while in Ref. [95] it is done on an event-by-event basis.

- (ii) The “FT_{approx}” result of Refs. [94, 95] contains the full top-quark mass dependence in the real radiation, while the virtual part is rescaled by the re-weighting factor mentioned above.

It was found that (ii) leads to a total cross section which is about 10% smaller than the one obtained using Born-improved HEFT.

- (iii) The “FT’_{approx}” result [95] is as in (ii) for the real radiation part, while it uses partial NLO results for the virtual part, specifically, the exact results for the two-loop triangle diagrams as far as they are known from single Higgs boson production [86, 87, 90, 91].
- (iv) HEFT results at NLO and NNLO have been improved by an expansion in $1/m_t^{2\rho}$ in Refs. [92, 93, 96, 97], where Ref. [96] contains corrections up to $\rho^{\max} = 6$ at NLO, and $\rho^{\max} = 2$ for the soft-virtual part at NNLO. In Ref. [96] it is also demonstrated that the sign of the finite top-quark mass corrections depends on whether the re-weighting factor is applied at differential level, i.e. before the integration over the partonic center of mass energy, or at total cross section level.

All these results suggest that the uncertainty on the cross section due to top-quark mass effects is $\pm 10\%$ at NLO.

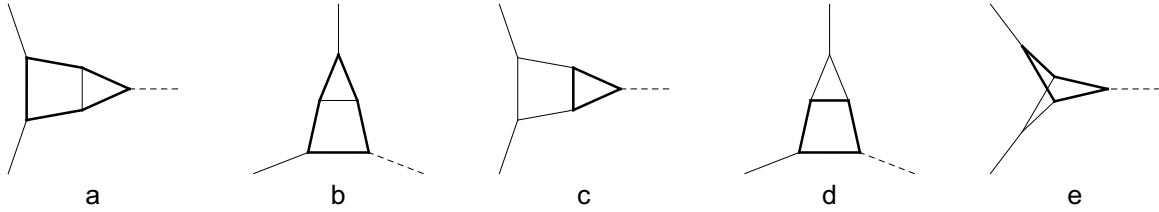


Figure 10.2.: Examples of Feynman diagrams appearing in the two-loop amplitude for Higgs production via gluon fusion. Thick lines represent massive propagators and dashed external lines represent an off-shell leg with squared momentum equal to s

10.2. Analytic Computation of Master Integrals

As a first step towards the two-loop virtual amplitude for double Higgs production we recomputed the two-loop virtual amplitude for gluon fusion into a single Higgs [85]. The amplitude was generated with QGRAF [242] and then parsed to REDUZE [106] in order to perform the IBP-reduction. The latter enabled us to express our amplitude in terms of 18 MI's. The computation of these integrals will be discussed in the following.

10.2.1. Notations and Conventions

The process of gluon fusion into a single Higgs via a top-loop depends on two kinematic invariants: the top mass m and the squared momentum of the Higgs, which we denote by s . It is convenient to work with the dimensionless variable x defined as

$$-\frac{s}{m^2} = \frac{(1-x)^2}{x}. \quad (10.1)$$

This variable transformation is motivated by appearance of non-rational terms in the differential equations for s and m , which are absent in the differential equation for x (see section 5.5.1 for a derivation).

The Feynman integrals, which appear in our amplitude can be expressed in terms of the following three integral families, where $k_{1,2}$ are loop momenta and $p_{1,2}$ are the gluon momenta:

- *full top-loop topologies.* For the integrals with a full top-loop (figure 10.2 *a, b*), we have:

$$\begin{aligned} D_1 &= k_1^2 - m^2, & D_2 &= k_2^2 - m^2, & D_3 &= (k_1 - k_2)^2, & D_4 &= (k_1 - p_1)^2 - m^2, \\ D_5 &= (k_2 - p_1)^2 - m^2, & D_6 &= (k_1 - p_1 - p_2)^2 - m^2, & D_7 &= (k_2 - p_1 - p_2)^2 - m^2. \end{aligned} \quad (10.2)$$

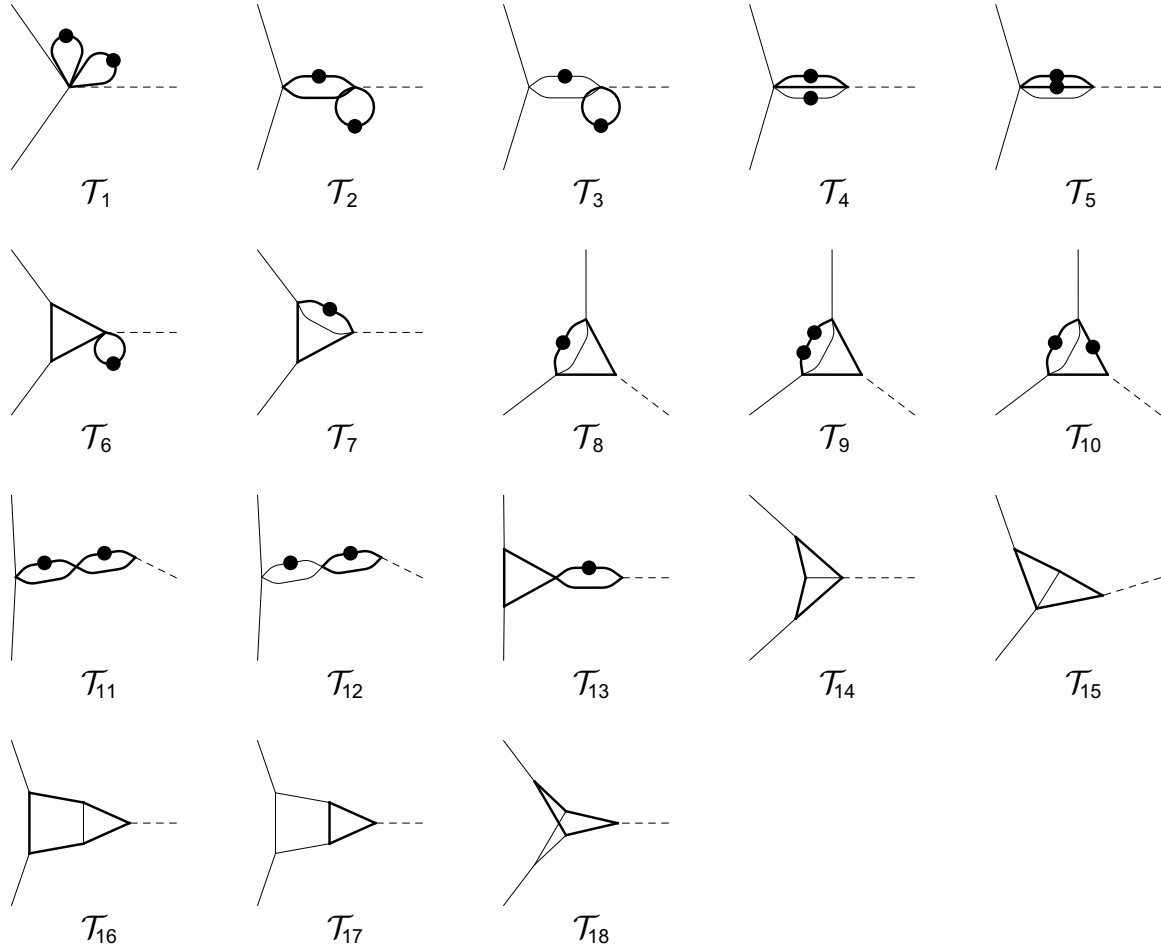


Figure 10.3.: Two-loop MI's for gluon fusion into Higgs $\mathcal{T}_{1,\dots,18}$. Thin lines represent massless external particles and propagators; thick lines stand for massive propagators; dashed external line represents an off-shell leg with squared momentum equal to s ; dots indicate squared propagators.

- *partial top-loop topologies*. For the integrals with a partial top-loop (figure 10.2 c, d), we have:

$$\begin{aligned}
 D_1 &= k_1^2, & D_2 &= k_2^2 - m^2, & D_3 &= (k_1 - k_2)^2 - m^2, & D_4 &= (k_1 - p_1)^2, \\
 D_5 &= (k_2 - p_1)^2 - m^2, & D_6 &= (k_1 - p_1 - p_2)^2, & D_7 &= (k_2 - p_1 - p_2)^2 - m^2.
 \end{aligned}
 \tag{10.3}$$

- *non-planar topology.* For the non-planar integrals (figure 10.2 e), we have:

$$\begin{aligned}
D_1 &= k_1^2, & D_2 &= k_2^2, & D_3 &= (k_1 - k_2)^2 - m^2, & D_4 &= (k_1 - p_1)^2 - m^2, \\
D_5 &= (k_2 - p_1)^2, & D_6 &= (k_1 - p_1 - p_2)^2 - m^2, & D_7 &= (k_1 - k_2 - p_1 - p_2)^2 - m^2.
\end{aligned}
\tag{10.4}$$

In the following we consider ℓ -loop Feynman integrals in d dimensions, built out of p of the above denominators, each raised to some integer power, of the form

$$\int \widetilde{d^d k_1} \dots \widetilde{d^d k_\ell} \frac{1}{D_{a_1}^{n_1} \dots D_{a_p}^{n_p}},
\tag{10.5}$$

where the integration measure is defined as

$$\widetilde{d^d k_i} \equiv \frac{d^d k_i}{(\pi)^{\frac{d}{2}}} e^{-\epsilon \gamma_E} \left(\frac{m^2}{\mu^2} \right)^\epsilon,
\tag{10.6}$$

with μ the 't Hooft scale of dimensional regularization, and $\epsilon = (4 - d)/2$.

10.2.2. Canonical System and Boundary Conditions

We consider the following set of master integrals, which admits an ϵ -linear differential equation in x :

$$\begin{aligned}
F_1 &= \epsilon^2 \mathcal{T}_1, & F_2 &= \epsilon^2 \mathcal{T}_2, & F_3 &= \epsilon^2 \mathcal{T}_3, \\
F_4 &= \epsilon^2 \mathcal{T}_4, & F_5 &= \epsilon^2 \mathcal{T}_5, & F_6 &= \epsilon^3 \mathcal{T}_6, \\
F_7 &= \epsilon^3 \mathcal{T}_7, & F_8 &= \epsilon^3 \mathcal{T}_8, & F_9 &= \epsilon^2 \mathcal{T}_9, \\
F_{10} &= \epsilon^2 \mathcal{T}_{10}, & F_{11} &= \epsilon^2 \mathcal{T}_{11}, & F_{12} &= \epsilon^2 \mathcal{T}_{12}, \\
F_{13} &= \epsilon^4 \mathcal{T}_{13}, & F_{14} &= \epsilon^4 \mathcal{T}_{14}, & F_{15} &= \epsilon^3 \mathcal{T}_{15}, \\
F_{16} &= \epsilon^4 \mathcal{T}_{16}, & F_{17} &= \epsilon^4 \mathcal{T}_{17}, & F_{18} &= \epsilon^4 \mathcal{T}_{18},
\end{aligned}
\tag{10.7}$$

where the \mathcal{T}_i are depicted in figure 10.3. We can use the Magnus exponentials to find a rotation matrix, which removes the ϵ^0 -part of our differential equation and therefore transforms

our set of master integrals to the corresponding canonical set of master integrals

$$\begin{aligned}
I_1 &= F_1, & I_2 &= -\sqrt{-s(4m^2 - s)} F_2, \\
I_3 &= -s F_3, & I_4 &= -\sqrt{-s(4m^2 - s)} \left(F_3 + \frac{1}{2} F_4 \right) - \frac{s}{2} F_4, \\
I_5 &= -s F_5, & I_6 &= -s F_6, & I_7 &= -s F_7, \\
I_8 &= -s F_8, & I_9 &= -s m^2 F_9, \\
I_{10} &= -\sqrt{-s(4m^2 - s)} \left(\frac{3}{2m^2} F_8 + m^2 F_9 + m^2 F_{10} \right) - \frac{s}{2m^2} (3 F_8 + 2m^4 F_9) \\
I_{11} &= -s (4m^2 - s) F_{11}, & I_{12} &= -s \sqrt{-s(4m^2 - s)} F_{12}, & I_{13} &= -s F_{13}, \\
I_{14} &= s \sqrt{-s(4m^2 - s)} F_{14}, & I_{15} &= s \sqrt{-s(4m^2 - s)} F_{15}, & I_{16} &= -s F_{16}, \\
I_{17} &= s^2 F_{17}, & I_{18} &= s^2 F_{18}.
\end{aligned}$$

These canonical master integrals satisfy a canonical differential equation

$$dI = \sum_i^3 \mathfrak{M}_i d\log(\eta_i) I, \quad (10.8)$$

with the following alphabet

$$\eta_1 = x, \quad \eta_2 = 1 + x, \quad \eta_3 = 1 - x. \quad (10.9)$$

Since the alphabet is completely linear in x we can express our solutions in terms of *GPLs*. After the integration of the differential equations we have to fix the boundary constants of our master integrals. We hereby list the conditions we have imposed on each integrals;

- regularity at $s \rightarrow 0$: $I_{4,5,7\dots 10}$,
- limit $s \rightarrow 0$: $I_{2,6,11,14,15,16,18}$,

This leaves us with $I_{1,3}$, which can be obtained by direct integration and $I_{12,17}$, which we fixed by comparing to the known expressions in [229]. Our results have been successfully checked against *SecDec*.

10.2.3. Outlook for the Double Higgs Master Integrals

The master integrals we presented are a subset of the integrals needed for the full NLO corrections to double Higgs production. Despite the additional subset of three-point integrals, which has been computed in [243, 244] most integrals are out of reach for current analytic computational methods. This is especially true for the integrals in the non-planar sector, where we could not even obtain the IBP-ids needed for the derivation of the differential equations. Even if this reduction could be achieved, we expect that at least one three-point topology, depicted in 10.4, contains elliptic integrals. This suspicion was raised, since the

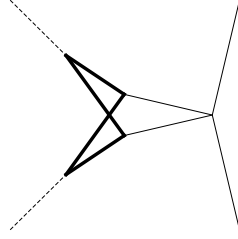


Figure 10.4.: This figure shows the presumably elliptic topology. Thin lines represent massless external particles and propagators; thick lines stand for massive propagators; dashed external lines represent a massive external particle.

boundary point, where the mass of the Higgs is set to zero, contains elliptic integrals as it was shown in [245]. Even for much simpler topologies like the two-loop massive sunrise the computation of elliptic master integrals is still under thorough investigation [246–255], putting our more involved topology beyond the current analytic technologies. In addition the suspected elliptic integral will appear in the inhomogeneous part of the differential equation of several other master integrals, impeding their computations as well. For these reasons we concluded that the analytic computation of all master integrals is beyond the current technology and therefore embody numerical techniques for their evaluation.

10.3. Numerical Integration via Sector Decomposition

In this section we will give an introduction to the method of sector decomposition for the numerical integration of Feynman integrals, based on the discussion in [256].

The major obstruction for the numerical integration of a Feynman integral is its singularity structure, which is best understood in the Feynman parameter representation of an integral. A scalar L -loop Feynman integral in d dimensions can be written as

$$F = \int \prod_{i=1}^L d^d k_i \frac{1}{D_1^{\alpha_1} \dots D_N^{\alpha_N}}. \quad (10.10)$$

We can bring all propagators under a common exponent by introducing additional integrations over the Feynman parameters x_i

$$F = \Gamma(N_\alpha) \int \prod_{i=1}^N dx_i x_i^{\alpha_i-1} \delta\left(1 - \sum_{i=1}^N x_i\right) \int \prod_{i=1}^L d^d k_i \left[\sum_{j,l} k_j \cdot k_l M_{jl} - 2 \sum_{j=1}^L k_j \cdot Q_j + J \right]^{-N_\alpha} \quad (10.11)$$

where $N_\alpha = \sum_{i=1}^N \alpha_i$. After completing the square for the loop momenta by a shift in the loop momenta we can perform all loop integrals and are only left with the integrations over

the Feynman parameters

$$F = (-1)^{N_\alpha} \frac{\Gamma(N_\alpha - \frac{Ld}{2})}{\prod_{i=1}^N \Gamma(\alpha_i)} \int_0^\infty \prod_{i=1}^N dx_i x_i^{\alpha_i - 1} \delta\left(1 - \sum_{i=1}^N x_i\right) \frac{\mathcal{U}^{N_\alpha - (L+1)d/2}}{\mathcal{F}^{N_\alpha - Ld/2}}, \quad (10.12)$$

where \mathcal{U} and \mathcal{F} are the first and second Symanzik polynomials and given by

$$\mathcal{U} = \det(M) \quad \mathcal{F} = \det(M) \left[\sum_{j,l=1}^L Q_j M_{j,l} Q_l - J - i\delta \right]. \quad (10.13)$$

We should note that the two Symanzik polynomials can also be directly obtained by considering all possible topological cuts of the corresponding Feynman integrals, where for the first Symanzik polynomial \mathcal{U} we cut L lines and for the second Symanzik polynomial \mathcal{F} we cut $L + 1$ lines [59, 124, 257].

In the euclidean region we have three possible singularities: The factor $\Gamma(N_\alpha - \frac{Ld}{2})$ may produce an overall UV divergence, the vanishing of the first Symanzik polynomial \mathcal{U} indicates a UV subdivergence and the vanishing of the second Symanzik polynomial may point towards an infrared singularity. In order to be able to numerically integrate over the Feynman parameters x_i we have to regularize the divergences of the two Symanzik polynomials. This regularization requires that all singularities are of the form

$$F \propto \int_0^1 \prod_{i=1}^{N-1} dx_i x_i^{a_i - b_i \epsilon} \frac{\mathcal{U}^{e_u(\epsilon)}}{\mathcal{F}^{e_f(\epsilon)}}, \quad (10.14)$$

which for $a_i < 0$ is singular as $x_i \rightarrow 0$ and where e_u and e_f are some functions of the dimensional regularization parameter ϵ . Note we demanded that all singularities are explicit, hence the two Symanzik polynomials have the form

$$\mathcal{U} = 1 + u(x) \quad (10.15)$$

$$\mathcal{F} = -s_0 + f(x), \quad (10.16)$$

where $u(x)$ and $f(x)$ are some polynomials in the Feynman parameters x_i without a constant term.

We can achieve this required form (10.14) by sector decomposition, which splits our integration regions such that all overlapping singularities are resolved. The basic idea of sector decomposition is best illustrated through a simple example

$$\int_0^1 dx_1 \int_0^1 dx_2 \frac{1}{(x_1 + x_2)^{2+\epsilon}}, \quad (10.17)$$

which has an overlapping singularity at $x_1, x_2 \rightarrow 0$, but if we triangularize the integration region we can separate the two divergences

$$\begin{aligned}
& \int_0^1 dx_1 \int_0^1 dx_2 \frac{1}{(x_1 + x_2)^{2+\epsilon}} \\
&= \int_0^1 dx_1 \int_0^{x_1} dx_2 \frac{1}{(x_1 + x_2)^{2+\epsilon}} + \int_0^1 dx_2 \int_0^{x_2} dx_1 \frac{1}{(x_1 + x_2)^{2+\epsilon}} \\
&= \int_0^1 dx_1 \int_0^1 d\tilde{x}_2 \frac{x_1}{(x_1 + \tilde{x}_2 x_1)^{2+\epsilon}} + \int_0^1 dx_2 \int_0^1 d\tilde{x}_1 \frac{x_2}{(\tilde{x}_1 x_2 + x_2)^{2+\epsilon}} \\
&= \int_0^1 dx_1 \int_0^1 d\tilde{x}_2 \frac{1}{x_1^{1+\epsilon}} \frac{1}{(1 + \tilde{x}_2)^{2+\epsilon}} + \int_0^1 dx_2 \int_0^1 d\tilde{x}_1 \frac{1}{x_2^{1+\epsilon}} \frac{1}{(1 + \tilde{x}_1)^{2+\epsilon}}, \quad (10.18)
\end{aligned}$$

where we performed a change of variables in order to make the singularity explicit. The sector decomposition algorithm will iteratively resolve all overlapping singularities until we achieved the form (10.14), where all singularities are explicit. We can regularize these singularities by a simple trick, which is best shown in a simple example

$$\int_0^1 dx x^{-1-b\epsilon} f(x) = \int_0^1 dx x^{-1+b\epsilon} (f(x) - f(0) + f(0)) \quad (10.19)$$

$$= \int_0^1 dx \frac{f(0)}{x^{1+b\epsilon}} + \int_0^1 dx x^{-1-b\epsilon} (f(x) - f(0)) \quad (10.20)$$

$$= \frac{f(0)}{-b\epsilon} + \int_0^1 dx x^{-b\epsilon} \frac{(f(x) - f(0))}{x}, \quad (10.21)$$

where the integral in the last line is now completely finite.

After all poles of the integral are regularized we can perform a series expansion around $\epsilon = 0$ and integrate each order in ϵ numerically, since all integrands are now finite.

We should note that the sector decomposition in this form only works for integrals in the euclidean region. In the physical region the Mandelstam invariants may have different signs and therefore allow for additional singularities in the second Symanzik polynomial. Therefore an integral in the physical region is usually first sector decomposed as it would be in the euclidean region and later the additional poles are avoided by contour deformation [62]. The strategies we discussed here have been implemented into the two computer codes **SecDec** [63] and **FIESTA** [64], which allow for the numerical evaluation of any Feynman integral.

10.4. NLO Calculation

In the following I will give a short overview of the calculation of the Higgs pair production at NLO, including the full top mass. For a more detailed description we refer to [4].

10.4.1. Amplitude Structure

At any loop order, the amplitude for the process $g(p_1) + g(p_2) \rightarrow h(p_3) + h(p_4)$ can be decomposed into form factors as

$$\mathcal{M}_{ab} = \delta_{ab} \epsilon_1^\mu \epsilon_2^\nu \mathcal{M}_{\mu\nu} \quad (10.22)$$

$$\mathcal{M}^{\mu\nu} = F_1(\hat{s}, \hat{t}, m_h^2, m_t^2, D) T_1^{\mu\nu} + F_2(\hat{s}, \hat{t}, m_h^2, m_t^2, D) T_2^{\mu\nu}, \quad (10.23)$$

where $\epsilon_1^\mu, \epsilon_2^\nu$ are the gluon polarization vectors, a, b are color indices, and

$$\hat{s} = (p_1 + p_2)^2, \quad \hat{t} = (p_1 - p_3)^2, \quad \hat{u} = (p_2 - p_3)^2. \quad (10.24)$$

The decomposition into tensors carrying the Lorentz structure is not unique. With the following definitions

$$T_1^{\mu\nu} = g^{\mu\nu} - \frac{p_1^\nu p_2^\mu}{p_1 \cdot p_2}, \quad (10.25)$$

$$T_2^{\mu\nu} = g^{\mu\nu} + \frac{1}{p_T^2 (p_1 \cdot p_2)} \tilde{T}_2^{\mu\nu}, \quad (10.26)$$

$$\tilde{T}_2^{\mu\nu} = \{ m_h^2 p_1^\nu p_2^\mu - 2(p_1 \cdot p_3) p_3^\nu p_2^\mu - 2(p_2 \cdot p_3) p_3^\mu p_1^\nu \} \quad (10.27)$$

$$+ 2(p_1 \cdot p_2) p_3^\nu p_3^\mu \}, \quad (10.28)$$

$$\text{where } p_T^2 = (\hat{t}\hat{u} - m_h^4)/\hat{s}, \quad (10.29)$$

$$T_1 \cdot T_2 = D - 4, \quad T_1 \cdot T_1 = T_2 \cdot T_2 = D - 2, \quad (10.30)$$

we have [237]

$$\mathcal{M}^{++} = \mathcal{M}^{--} = -F_1, \quad \mathcal{M}^{+-} = \mathcal{M}^{-+} = -F_2. \quad (10.31)$$

At leading order, we can further split F_1 into a triangle diagram and a box diagram contribution, $F_1 = F_\Delta + F_\square$. As the form factor F_Δ only contains the triangle diagrams, which have no angular momentum dependence, it can be attributed entirely to an s-wave contribution. The form factor F_2 contains only box contributions. At NLO in QCD, the feature persists that only F_1 contains diagrams involving the triple Higgs coupling. The form factors F_1 and F_2 can be attributed to the spin-0 and spin-2 states of the scattering amplitude, respectively.

We construct projectors $P_j^{\mu\nu}$ such that

$$\begin{aligned} P_1^{\mu\nu} \mathcal{M}_{\mu\nu} &= F_1(\hat{s}, \hat{t}, m_h^2, m_t^2, D), \\ P_2^{\mu\nu} \mathcal{M}_{\mu\nu} &= F_2(\hat{s}, \hat{t}, m_h^2, m_t^2, D). \end{aligned}$$

For the projectors in D dimensions we can use as a basis the tensors $T_i^{\mu\nu}$ defined in Eqs. (10.25). The projectors can be written as

$$P_1^{\mu\nu} = \frac{1}{4} \frac{D-2}{D-3} T_1^{\mu\nu} - \frac{1}{4} \frac{D-4}{D-3} T_2^{\mu\nu}, \quad (10.32)$$

$$P_2^{\mu\nu} = -\frac{1}{4} \frac{D-4}{D-3} T_1^{\mu\nu} + \frac{1}{4} \frac{D-2}{D-3} T_2^{\mu\nu}. \quad (10.33)$$

LO Cross Section

The partonic leading order cross section can be written as

$$\hat{\sigma}^{\text{LO}} = \frac{1}{2^9 \pi \hat{s}^2} \int_{\hat{t}_-}^{\hat{t}_+} d\hat{t} \left\{ |F_1|^2 + |F_2|^2 \right\}, \quad (10.34)$$

where

$$\hat{t}^\pm = m_h^2 - \frac{\hat{s}}{2} (1 \mp \beta_h), \quad \beta_h^2 = 1 - 4 \frac{m_h^2}{\hat{s}}. \quad (10.35)$$

The leading order form factors F_i with full mass dependence can be found e.g. in Refs. [88, 237].

For the total cross section, we also have to integrate over the parton distribution functions, so we have

$$\sigma^{\text{LO}} = \int_{\tau_0}^1 d\tau \frac{d\mathcal{L}_{gg}}{d\tau} \hat{\sigma}^{\text{LO}}(\hat{s} = \tau s). \quad (10.36)$$

The luminosity function is defined as

$$\frac{d\mathcal{L}_{ij}}{d\tau} = \sum_{ij} \int_{\tau}^1 \frac{dx}{x} f_i(x, \mu_F) f_j\left(\frac{\tau}{x}, \mu_F\right), \quad (10.37)$$

where s is the square of the hadronic center of mass energy, $\tau_0 = 4m_h^2/s$, μ_F is the factorization scale and f_i are the parton distribution functions (PDFs) for parton type i .

NLO Cross Section

The NLO cross section is composed of various parts, which we will discuss separately in the following:

$$\sigma^{\text{NLO}}(pp \rightarrow hh) = \sigma^{\text{LO}} + \sigma^{\text{virt}} + \sum_{i,j \in \{g, q, \bar{q}\}} \sigma_{ij}^{\text{real}} \quad (10.38)$$

10.4.2. The virtual two-loop Amplitude

For the virtual two-loop amplitude, we use the projectors defined in Eqs. (10.32),(10.33) to express the amplitude in terms of the scalar form factors F_1 and F_2 .

The virtual amplitude has been generated with an extension of the program GOSAM [43, 258], where the diagrams are generated using QGRAF [242] and then further processed using FORM [259, 260]. This leads to about 10000 integrals, before any symmetries are taken into account. The two-loop extension of GOSAM contains an interface to REDUZE [106], which we used for the reduction to master integrals. We have defined 8 integral families with 9 propagators each. For the 6 and 7 propagator non-planar topologies we could not achieve a complete reduction with our available computing resources using the reduction programs REDUZE [106], FIRE [105] or LITERED [107]. In this case we evaluated the tensor integrals directly, exploiting the fact that SECDEC can calculate integrals with (contracted) loop momenta in the numerator.

After the partial reduction, we end up with 145 planar master integrals plus 70 non-planar integrals and a further 112 integrals that differ by a crossing. As the master integrals contain up to four independent mass scales, \hat{s} , \hat{t} , m_t^2 , m_h^2 , only a small subset is known analytically. Therefore we have calculated all the integrals numerically using the program SECDEC-3.0 [63]. We partially used a finite basis [261] for the planar master integrals, as far as it turned out to be beneficial for the numerical integration.

The interface to SECDEC has been constructed such that the coefficients of the master integrals as they occur in the amplitude are taken into account when evaluating the integrals numerically. For each integral, once a relative accuracy of 0.2 is reached, the number of sampling points is then set dynamically according to two criteria: (i) the contribution of the integral including its coefficient to the error estimate of the amplitude and (ii) the time per sampling point spent on the integral. The numerical integration is continued until the desired precision for the full amplitude is reached. This procedure allows for a precise evaluation of the amplitude, without spending an unnecessary amount of time on individual integrals which are suppressed in the full amplitude.

We use conventional dimensional regularization (CDR) with $D = 4 - 2\epsilon$. The top-quark mass is renormalized in the on-shell scheme and the QCD coupling in the $\overline{\text{MS}}$ scheme with $N_f = 5$. The top-quark mass counterterm is obtained by insertion of the mass counterterm into the heavy quark propagators. Alternatively, the mass counterterm can be calculated by taking the derivative of the one-loop amplitude with respect to m_t . We have used both methods as a cross-check.

10.4.3. Real Radiation

The contributions from the real radiation, $\sigma_{ij}^{\text{real}}$, can be divided into four channels, according to the partonic subprocesses $gg \rightarrow hh + g$, $gq \rightarrow hh + q$, $g\bar{q} \rightarrow hh + \bar{q}$, $q\bar{q} \rightarrow hh + g$. The $q\bar{q}$ channel is infrared finite.

We have generated the one-loop amplitudes for all subprocesses with the program GOSAM [43, 258]. For the subtraction of the infrared poles, we use the Catani-Seymour dipole formal-

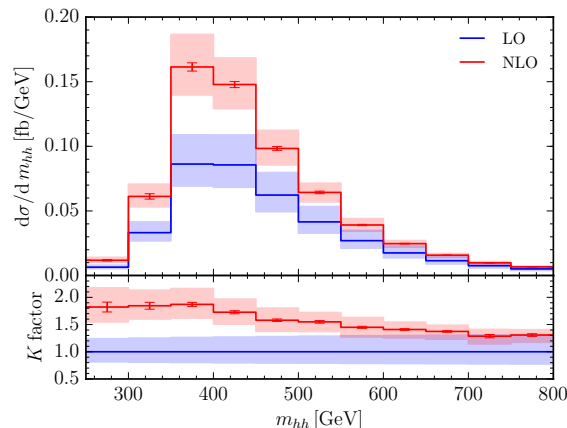


Figure 10.5.: Comparison of the NLO result to the LO result for the Higgs pair invariant mass distribution.

ism [262]. We have retained the full top-quark mass dependence throughout the calculation of the $2 \rightarrow 3$ matrix elements and IR subtraction terms. For the phase-space integration we use the VEGAS algorithm [263] as implemented in the CUBA library [264].

The infrared poles of the virtual contribution $d\hat{\sigma}^{\text{virt}}$ cancel in the combination $(d\hat{\sigma}^{\text{virt}} + d\hat{\sigma}^{\text{LO}} \otimes \mathbf{I})$, where the \mathbf{I} -operator is given by

$$\mathbf{I} = \frac{\alpha_s}{2\pi} \frac{(4\pi)^\epsilon}{\Gamma(1-\epsilon)} \left(\frac{\mu^2}{\hat{s}} \right)^\epsilon \left\{ \frac{2C_A}{\epsilon^2} + \frac{\beta_0}{\epsilon} + \text{finite} \right\}. \quad (10.39)$$

We have checked that for all calculated phase space points the numerical cancellations of the poles in ϵ are within the numerical uncertainties. For a randomly chosen sample of phase-space points we calculated the poles with higher accuracy and obtained a median cancellation of five digits.

10.5. Numerical Results

In our numerical computation we set $\mu_R = \mu_F = \mu = m_{hh}/2$, where m_{hh} is the invariant mass of the Higgs boson pair. We use the PDF4LHC15_nlo_100_pdfas [265–268] parton distribution functions, along with the corresponding value for α_s . The masses have been set to $m_b = 125$ GeV, $m_t = 173$ GeV, and the top-quark width has been set to zero. We use a center-of-mass energy of $\sqrt{s} = 14$ TeV and no cuts except a technical cut in the real radiation of $p_T^{\text{min}} = 10^{-4} \cdot \sqrt{\hat{s}}$, which we varied in the range $10^{-2} \leq p_T^{\text{min}}/\sqrt{\hat{s}} \leq 10^{-6}$ to verify that the contribution to the total cross section is stable and independent of the cut within the numerical accuracy.

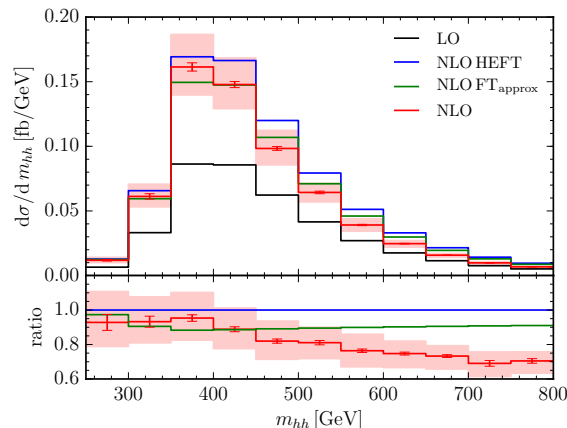


Figure 10.6.: Comparison of the full calculation to various approximations for the Higgs pair invariant mass distribution. “NLO HEFT” denotes the effective field theory result, i.e. approximation (i) above, while “FT_{approx}” stands for approximation (ii), where the top-quark mass is taken into account in the real radiation part only. The band results from scale variations by a factor of two around the central scale $\mu = m_{hh}/2$.

Including the top-mass dependence, we obtain the total cross section

$$\sigma^{NLO} = 32.80^{+13\%}_{-12\%} \text{ fb} \pm 0.4\% (\text{stat.}) \pm 0.1\% (\text{int.}). \quad (10.40)$$

In addition to the dependence of the result on the variation of the scales by a factor of two around the central scale, we state the statistical error coming from the limited number of phase-space points evaluated and the error stemming from the numerical integration of the amplitude. The latter value has been obtained using error propagation and assuming Gaussian distributed errors and no correlation between the amplitude-level results. The value of the cross section is 14% smaller than the Born-improved HEFT result, $\sigma_{HEFT}^{NLO} = 38.32^{+18\%}_{-15\%} \text{ fb}$.

In Fig. 10.5 we compare the LO result with the full NLO calculation. We observe that the LO result gets rather large corrections, which even lay outside the estimated error band. This underlines the importance of NLO calculations for a reliable prediction of an observable.

The results for the m_{hh} distribution are shown in Fig. 10.6. We can see that for m_{hh} beyond $\sim 450 \text{ GeV}$, the top-quark mass effects lead to a reduction of the m_{hh} distribution by about 20-30% as compared to the Born-improved HEFT approximation. We also observe that the central value of the Born-improved HEFT result lies outside the NLO scale uncertainty band of the full result for $m_{hh} \gtrsim 450 \text{ GeV}$, while the FT_{approx} result, where the real radiation contains the full mass dependence, lies outside the scale uncertainty band for m_{hh} beyond $\sim 550 \text{ GeV}$. The scale uncertainty of the Born-improved HEFT and FT_{approx} does not enclose the central value of the full result in the tail of the m_{hh} distribution.

10.6. Conclusions

In this chapter we have presented the analytic calculation for the master integrals of Higgs production through gluon fusion at NLO. These MI's are a subset of the MI's needed for the calculation of the virtual corrections to Higgs boson pair production in gluon fusion at NLO. Due to the expected appearance of elliptic integrals a full analytic computation of the complete set of master integrals is currently not feasible. Therefore we embodied a numerical strategy for evaluation of the MI's entering the virtual amplitude. This virtual amplitude was used to compute the total cross section and the m_{hh} distribution for Higgs boson pair production in gluon fusion at NLO, including the full top-quark mass dependence. We observe that the total cross section including the full top-quark mass dependence is about 14% smaller than the one obtained within the Born-improved HEFT approximation. The m_{hh} distribution shows that for m_{hh} values beyond ~ 500 GeV, the top quark mass effects lead to a reduction of the differential cross section by about 20-30% as compared to the Born-improved HEFT approximation, and by about 10-20% as compared to the FT_{approx} result. Our results demonstrate that the calculation of the full top-quark mass dependence is vital in order to get reliable predictions for Higgs boson pair production over the full invariant mass range.

The close cooperation between Theory and Experiment has allowed for spectacular results in Run I at the LHC, including competitive measurements of standard model parameters, precision Higgs physics and stringent constraints on the parameter space of several BSM physics models. The Run II at the LHC will provide us with even more precise measurements, which have to be met with better theoretical predictions, in order to repeat the success of the first Run. Higher order corrections to the underlying hard scattering event are an important ingredient to improve the theoretical description, but their calculation poses several theoretical challenges. We are approaching an accuracy level, where the mass corrections stemming from electroweak bosons and top quarks becomes increasingly important. Including mass effects impede the calculation of virtual corrections, not only by increasing the number of scales involved, but also due to the absence of symmetries, which facilitated the calculations for massless theories.

In this work we focused on the development of novel techniques for the computation of scattering amplitudes, by understanding their underlying algebraic structure. A special emphasis was given to the generality of our techniques, which allow us to treat the aforementioned mass effects. We explored the wealth of relations obeyed by dimensional regulated integrals, which allowed us to find a process dependent basis of integrals. The space of integrals, spanned by these integrals, includes their derivative in respect to kinematical invariants, hence allowing us to derive a set of differential equations for the basis integrals. The complexity of the latter varies significantly for different choices of basis integrals. A particular well suited form seems to be reached, when the dimensional regularization parameter is factorized from the kinematics, which is known as the canonical form. A differential equation in canonical form can be readily solved algebraically and the analytic structure is evidently determined from the associated matrix.

We focused on master integrals, obeying a differential equation, which is linear in the dimensional regularization parameter. The Magnus theory for differential equations allows

us to readily solve such systems in terms of a kinematical evolution operator, which evolves our integrals from some boundary point to any point in the kinematic space. The evolution operator is most conveniently built by a product of two Magnus exponentials, where the first exponential can be interpreted as a rotation in the space of master integrals transforming the differential equation into a canonical form and where the second exponential describes the solution of this canonical form. We embodied this strategy to compute MIs for a wide range of processes.

Especially we have computed the three-loop ladder-box integrals with one off-shell leg, which contribute to the N^3LO virtual corrections to scattering processes like the three-jet production mediated by vector boson decay, $V^* \rightarrow jjj$, as well as Higgs plus one-jet production in gluon fusion, $pp \rightarrow Hj$, and to the three-loop one-particle splitting amplitudes. Furthermore we computed the master integrals belonging to the mixed QCD-EW corrections to Drell-Yan scattering, which are characterized by the exchange of two electroweak vector bosons. After series expanding in the mass difference of the W and Z boson, we are left with three types of diagrams, according to the presence of massive internal lines: the no-mass type, the one-mass type and the two-mass type with equal masses. We obtained the solution of the latter two as Chen's iterated integrals, but whenever it was possible we transformed them into $GPLs$, which are better suited for numerical evaluation.

Finally we presented the calculation of the cross section and invariant mass distribution for Higgs boson pair production in gluon fusion at NLO . In contrast to the previous examples the occurring MI's were computed numerically using the sector decomposition algorithm implemented in SECDEC. This computation demonstrates for the first time that a cross section can be obtained from a virtual correction, where the majority of master integrals have been computed numerically. This approach opens a new direction for the computation of virtual corrections and will help us to further push the limits of what is feasible and possible.

Acknowledgements

First and foremost I want to thank my supervisor Pierpaolo Mastrolia for guiding and patiently supporting me through my studies. It is a great pleasure to work with such an inspiring and motivating person. He never failed to come up with interesting new ideas, which provided me with a new perspective on problems and therefore deepened my understanding of the subject. I also want to thank Stefano Di Vita for collaborating on many interesting projects with me and for patiently helping me with Mathematica. I would also like to thank all my other collaborators for their help and insights they shared with me. I'm also grateful for the members of the Pheno group at the Max-Planck Institut für Physik for providing me with such a welcoming and inspiring atmosphere during my time here.

I would also like to say thank you to the Max-Planck Institut für Physik (Werner-Heisenberg-Institut) for providing such a great environment for studies, including the computing power that was needed to finish some of the projects described within this thesis. Especially I want to thank Thomas Hahn for the excellent support he provided with any computer related problem.

Finally I want to thank my whole family for supporting me throughout my studies. Especially I'm grateful to my wife Kate and my daughter Enna, who always help me to recharge after a long day at work by creating such a loving and supportive atmosphere.

The work presented in this dissertation was supported by the Alexander von Humboldt Foundation, in the framework of the Sofia Kovalevskaja Award Project *Advanced Mathematical Methods for Particle Physics*, endowed by the German Federal Ministry of Education and Research.

Appendices

Computing Leading Singularities

In this appendix we will show explicitly how the leading singularity can be computed by cutting the corresponding propagators. For convenience we will restrict ourselves to four dimensional integrals.

A.1. One-Loop massless Box

Let us consider the one-loop massless box

$$\int d^4k \frac{1}{k^2(k-p_2)^2(k+p_1)^2(k+p_1+p_3)^2} \quad (\text{A.1})$$

where all external momenta are massless $p_i^2 = 0$ and we have three Mandelstam invariants

$$s = (p_1 + p_2)^2 = 2p_1 \cdot p_2, \quad t = (p_1 + p_3)^2 = 2p_1 \cdot p_3, \quad u = (p_2 + p_3)^2 = 2p_2 \cdot p_3, \quad (\text{A.2})$$

satisfying

$$s + t + u = 0 \quad (\text{A.3})$$

In order to compute the leading singularity of the box we replace all propagators with delta functions

$$\begin{array}{c} \diagup \quad \diagdown \\ | \quad | \\ \diagdown \quad \diagup \\ | \quad | \\ \diagup \quad \diagdown \end{array} = \int d^4k \delta(k^2) \delta((k-p_2)^2) \delta((k+p_1)^2) \delta((k+p_1+p_3)^2) \quad (\text{A.4})$$

To solve these delta functions we will perform a variable change to a more convenient basis

$$k^\mu = \alpha_1 p_1^\mu + \alpha_2 p_2^\mu + \alpha_3 \epsilon_{12}^\mu + \alpha_4 \epsilon_{21}^\mu, \quad (\text{A.5})$$

where α_i are our new integration variables and ϵ_{ij} is the polarization vector associated with p_i and with reference momenta p_j . Note that here we will choose an unusual normalization, namely

$$\epsilon_{12} \cdot \epsilon_{21} = s . \quad (\text{A.6})$$

We can express our propagators in terms of our new basis

$$k^2 = (\alpha_1 \alpha_2 - \alpha_3 \alpha_4) s \quad (\text{A.7})$$

$$(k - p_2)^2 = (\alpha_1 \alpha_2 - \alpha_3 \alpha_4 - \alpha_1) s \quad (\text{A.8})$$

$$(k + p_1)^2 = (\alpha_1 \alpha_2 - \alpha_3 \alpha_4 + \alpha_2) s \quad (\text{A.9})$$

$$(k + p_1 + p_3)^2 = (\alpha_1 \alpha_2 - \alpha_3 \alpha_4) s + (1 + \alpha_1 - \alpha_2) t + \alpha_3 \epsilon_{12} \cdot p_3 + \alpha_4 \epsilon_{21} \cdot p_3 \quad (\text{A.10})$$

The delta functions set all propagators to zero, which will uniquely determine all parameters α_i . Setting the first three propagators to zero we arrive at the solution

$$\alpha_1 \alpha_2 = \alpha_3 \alpha_4, \quad \alpha_1 = 0, \quad \alpha_2 = 0, \quad (\text{A.11})$$

This means we have two solutions S_1 and S_2 where $\alpha_3 = 0$ or $\alpha_4 = 0$ respectively. After taking into account also the last in order to fix the remaining parameter we find

$$S_1 = \begin{cases} \alpha_1 = 0 \\ \alpha_2 = 0 \\ \alpha_3 = 0 \\ \alpha_4 = -\frac{t}{\epsilon_{21} \cdot p_3} \end{cases}, \quad S_2 = \begin{cases} \alpha_1 = 0 \\ \alpha_2 = 0 \\ \alpha_3 = -\frac{t}{\epsilon_{12} \cdot p_3} \\ \alpha_4 = 0 \end{cases}, \quad (\text{A.12})$$

Let us now consider the Jacobian, which is generated by the variable transformation (A.5)

$$J = \sqrt{\left| \det \left(\frac{\partial k^\mu}{\partial \alpha_i} \frac{\partial k_\mu}{\partial \alpha_j} \right) \right|}. \quad (\text{A.13})$$

From

$$\left(\frac{\partial k^\mu}{\partial \alpha_i} \frac{\partial k_\mu}{\partial \alpha_j} \right) = \begin{pmatrix} 0 & \frac{s}{2} & 0 & 0 \\ \frac{s}{2} & 0 & 0 & 0 \\ 0 & 0 & 0 & -\frac{s}{2} \\ 0 & 0 & -\frac{s}{2} & 0 \end{pmatrix}, \quad (\text{A.14})$$

we find

$$J = \frac{s^2}{4}. \quad (\text{A.15})$$

This allows us to write our integral (A.4) as

$$\text{Diagram} = \left(\frac{1}{|\det K(\alpha)|_{S_1}} + \frac{1}{|\det K(\alpha)|_{S_2}} \right) \frac{s^2}{4}, \quad (\text{A.16})$$

with

$$K(\alpha) = \frac{\partial D_i}{\partial \alpha_j} = \begin{pmatrix} \alpha_2 s & \alpha_1 s & -\alpha_4 s & -\alpha_3 s \\ -(1 - \alpha_2) s & \alpha_1 s & -\alpha_4 s & -\alpha_3 s \\ \alpha_2 s & (1 + \alpha_1) s & -\alpha_4 s & -\alpha_3 s \\ t + \alpha_2 s & -t + \alpha_1 s & -\alpha_4 s + \epsilon_{12} \cdot p_3 & -\alpha_3 s + \epsilon_{21} \cdot p_3 \end{pmatrix} \quad (\text{A.17})$$

Evaluating this matrix at the two cut solutions we find

$$[K(\alpha)]_{S_1} = \begin{pmatrix} 0 & 0 & \frac{t s}{\epsilon_{21} \cdot p_3} & 0 \\ -s & 0 & \frac{t s}{\epsilon_{21} \cdot p_3} & 0 \\ 0 & s & \frac{t s}{\epsilon_{21} \cdot p_3} & 0 \\ t & -t & \frac{t s}{\epsilon_{21} \cdot p_3} + \epsilon_{12} \cdot p_3 & \epsilon_{21} \cdot p_3 \end{pmatrix} \quad (\text{A.18})$$

$$[K(\alpha)]_{S_2} = \begin{pmatrix} 0 & 0 & 0 & \frac{t s}{\epsilon_{12} \cdot p_3} \\ -s & 0 & 0 & \frac{t s}{\epsilon_{12} \cdot p_3} \\ 0 & s & 0 & \frac{t s}{\epsilon_{12} \cdot p_3} \\ t & -t & \epsilon_{12} \cdot p_3 & \frac{t s}{\epsilon_{12} \cdot p_3} + \epsilon_{21} \cdot p_3 \end{pmatrix} \quad (\text{A.19})$$

$$[\det K(\alpha)]_{S_1} = -s^3 t \quad [\det K(\alpha)]_{S_2} = s^3 t \quad (\text{A.20})$$

Putting all the pieces together we find the leading singularity of our massless box

$$\begin{array}{c} \diagup \quad \diagdown \\ | \quad | \\ \diagdown \quad \diagup \end{array} = \left(\frac{1}{s^3 t} + \frac{1}{s^3 t} \right) \frac{s^2}{4} = \frac{1}{2} \frac{1}{s t}. \quad (\text{A.21})$$

A.2. One-Loop massless Bubble in two Dimensions

Let us now consider the one-loop massless bubble in two dimensions

$$\int d^2 k \frac{1}{k^2 (k + p_1 + p_2)^2} \quad (\text{A.22})$$

where traded the off-shell leg for two massless momenta $p_i^2 = 0$ with $p^2 = (p_1 + p_2)^2 = s$. For convenience we will again perform a variable transformation

$$k^\mu = \alpha_1 p_1^\mu + \alpha_2 p_2^\mu \quad (\text{A.23})$$

We can express our propagators in terms of our new basis

$$k^2 = \alpha_1 \alpha_2 s \quad (\text{A.24})$$

$$(k + p_1 + p_2)^2 = (\alpha_1 \alpha_2 + \alpha_1 + \alpha_2 + 1) s \quad (\text{A.25})$$

The delta functions set all propagators to zero, which will uniquely determine all parameters α_i .

$$S_1 = \left\{ \begin{array}{l} \alpha_1 = 0 \\ \alpha_2 = -1 \end{array} \right. , \quad S_2 = \left\{ \begin{array}{l} \alpha_1 = -1 \\ \alpha_2 = 0 \end{array} \right. , \quad (\text{A.26})$$

Next we will compute the Jacobian, which is generated by the variable transformation (A.23)

$$J = \sqrt{\left| \det \begin{pmatrix} \frac{\partial k^\mu}{\partial \alpha_i} & \frac{\partial k_\mu}{\partial \alpha_j} \end{pmatrix} \right|} \quad (\text{A.27})$$

$$\begin{pmatrix} \frac{\partial k^\mu}{\partial \alpha_i} & \frac{\partial k_\mu}{\partial \alpha_j} \end{pmatrix} = \begin{pmatrix} 0 & \frac{s}{2} \\ \frac{s}{2} & 0 \end{pmatrix} \quad (\text{A.28})$$

$$J = \frac{s}{2}. \quad (\text{A.29})$$

Using this we find the following expression for our cut two-dimensional massless bubble

$$\text{---} \text{---} \overset{\text{D}=2}{\text{---}} \text{---} = \left(\frac{1}{|\det K(\alpha)|_{S_1}} + \frac{1}{|\det K(\alpha)|_{S_2}} \right) \frac{s}{2}, \quad (\text{A.30})$$

with

$$K(\alpha) = \frac{\partial D_i}{\partial \alpha_j} = \begin{pmatrix} \alpha_2 s & \alpha_1 s \\ (1 + \alpha_2) s & (1 + \alpha_1) s \end{pmatrix} \quad (\text{A.31})$$

Evaluating this matrix at the two cut solutions we find

$$[K(\alpha)]_{S_1} = \begin{pmatrix} -s & 0 \\ 0 & s \end{pmatrix} \quad (\text{A.32})$$

$$[K(\alpha)]_{S_2} = \begin{pmatrix} 0 & -s \\ s & 0 \end{pmatrix} \quad (\text{A.33})$$

$$[\det K(\alpha)]_{S_1} = s^2 \quad [\det K(\alpha)]_{S_2} = s^2 \quad (\text{A.34})$$

Putting all the pieces together we find the leading singularity of our two-dimensional massless bubble

$$\text{---} \text{---} \overset{\text{D}=2}{\text{---}} \text{---} = \left(\frac{1}{s^2} + \frac{1}{s^2} \right) \frac{s}{2} = \frac{1}{s}. \quad (\text{A.35})$$

A.3. Two-Loop non-planar massless Box

The two-loop non-planar box is a good example how we can make use of the one-loop result at higher loops. If we cut only the non-planar diamond we have the following integral

$$\text{---} \text{---} \text{---} \text{---} = \int d^4 k_1 d^4 k_2 \frac{\delta(k_2^2) \delta((k_1 - k_2)^2) \delta((k_2 - p_3)^2) \delta((k_1 - k_2 - p_4)^2)}{k_1^2 (k_1 + p_1)^2 (k_1 + p_1 + p_2)^2}. \quad (\text{A.36})$$

We see that we can use the four delta functions to completely fix the value of the second loop momenta k_2 . Instead of performing the full calculation we went through for the one-loop box we will carefully recycle the result. In our case the external legs of the box will not only

depend on the external legs but also the uncut loop momenta k_1 . In particular if we closer investigate the cut box we can determine s and t from the momentum flow

$$\begin{array}{c}
 \begin{array}{c}
 \text{---} k_1 + p_1 + p_2 \text{---} \\
 \diagup \quad \diagdown \\
 \text{---} p_3 \text{---} \\
 \diagdown \quad \diagup \\
 \text{---} p_4 \text{---} \\
 \diagup \quad \diagdown \\
 \text{---} k_1 \text{---}
 \end{array}
 \end{array}
 = \frac{1}{2} \frac{1}{st} = \frac{1}{2} \frac{1}{(k_1 - p_3)^2 (k_1 - p_4)^2} , \tag{A.37}$$

Therefore cutting the non-planar part of the full two-loop integral leads to

$$\begin{array}{c}
 \text{---} \text{---} \text{---} \\
 | \quad | \quad | \\
 \text{---} \text{---} \text{---} \\
 \diagup \quad \diagdown \\
 \text{---} p_3 \text{---} \\
 \diagdown \quad \diagup \\
 \text{---} p_4 \text{---} \\
 \diagup \quad \diagdown \\
 \text{---} k_1 \text{---}
 \end{array}
 = \frac{1}{2} \int d^4 k_1 \frac{1}{k_1^2 (k_1 + p_1)^2 (k_1 + p_1 + p_2)^2 (k_1 - p_4)^2 (k_1 - p_3)^2} , \tag{A.38}$$

Master Integrals for the two-loop QED vertices

In this Appendix we collect the 17 MI's of the two-loop QED vertices introduced in Eq. (7.17). In Section 7.2, we have obtained them starting from the integrals \mathcal{T}_i depicted in Fig. 7.4, which are normalized according to the integration measure (Minkowskian metric is understood)

$$\left(\frac{m^{2\epsilon}}{\Gamma(1+\epsilon)} \right)^2 \int \frac{d^D k_1}{\pi^{D/2}} \int \frac{d^D k_2}{\pi^{D/2}}.$$

The MI's exhibit uniform transcendentality. In the following we present the expression of the coefficients of their expansion around $\epsilon = 0$ up to $\mathcal{O}(\epsilon^4)$. The coefficients $g_i^{(a)}$ are defined as follows:

$$g_i = \sum_{a=0}^4 \epsilon^a g_i^{(a)}, \quad i = 1, \dots, 17.$$

$$g_1^{(0)} = -1, \tag{B.1a}$$

$$g_1^{(1)} = 0, \tag{B.1b}$$

$$g_1^{(2)} = 0, \tag{B.1c}$$

$$g_1^{(3)} = 0, \tag{B.1d}$$

$$g_1^{(4)} = 0, \tag{B.1e}$$

$$g_2^{(0)} = 0, \quad (\text{B.2a})$$

$$g_2^{(1)} = -H(0; x), \quad (\text{B.2b})$$

$$g_2^{(2)} = 2H(-1, 0; x) - H(0, 0; x) + \zeta_2, \quad (\text{B.2c})$$

$$g_2^{(3)} = -4H(-1, -1, 0; x) + 2H(-1, 0, 0; x) + 2H(0, -1, 0; x) \\ - H(0, 0, 0; x) + \zeta_2(H(0; x) - 2H(-1; x)) + 2\zeta_3, \quad (\text{B.2d})$$

$$g_2^{(4)} = 8H(-1, -1, -1, 0; x) - 4H(-1, -1, 0, 0; x) - 4H(-1, 0, -1, 0; x) \\ + 2H(-1, 0, 0, 0; x) - 4H(0, -1, -1, 0; x) + 2H(0, -1, 0, 0; x) \\ + 2H(0, 0, -1, 0; x) - H(0, 0, 0, 0; x) + \zeta_2(4H(-1, -1; x) \\ - 2H(-1, 0; x) - 2H(0, -1; x) + H(0, 0; x)) \\ - 2\zeta_3(2H(-1; x) - H(0; x)) + \frac{9\zeta_4}{4}, \quad (\text{B.2e})$$

$$g_3^{(0)} = 0, \quad (\text{B.3a})$$

$$g_3^{(1)} = 0, \quad (\text{B.3b})$$

$$g_3^{(2)} = -2H(0, 0; x), \quad (\text{B.3c})$$

$$g_3^{(3)} = 8H(-1, 0, 0; x) + 4H(0, -1, 0; x) - 6H(0, 0, 0; x) + 2\zeta_2 H(0; x), \quad (\text{B.3d})$$

$$g_3^{(4)} = -32H(-1, -1, 0, 0; x) - 16H(-1, 0, -1, 0; x) + 24H(-1, 0, 0, 0; x) \\ - 8H(0, -1, -1, 0; x) + 20H(0, -1, 0, 0; x) + 12H(0, 0, -1, 0; x) \\ - 14H(0, 0, 0, 0; x) - 2\zeta_2(4H(-1, 0; x) + 2H(0, -1; x) - 3H(0, 0; x)) \\ + 4\zeta_3 H(0; x) - \frac{5\zeta_4}{2}, \quad (\text{B.3e})$$

$$g_4^{(0)} = \frac{1}{4}, \quad (\text{B.4a})$$

$$g_4^{(1)} = 0, \quad (\text{B.4b})$$

$$g_4^{(2)} = \zeta_2, \quad (\text{B.4c})$$

$$g_4^{(3)} = 2\zeta_3, \quad (\text{B.4d})$$

$$g_4^{(4)} = 16\zeta_4, \quad (\text{B.4e})$$

$$g_5^{(0)} = 0, \tag{B.5a}$$

$$g_5^{(1)} = H(0; x), \tag{B.5b}$$

$$g_5^{(2)} = -6 H(-1, 0; x) + 5 H(0, 0; x) + 2 H(1, 0; x) - \zeta_2, \tag{B.5c}$$

$$\begin{aligned} g_5^{(3)} = & 36 H(-1, -1, 0; x) - 24 H(-1, 0, 0; x) - 12 H(-1, 1, 0; x) \\ & - 30 H(0, -1, 0; x) + 13 H(0, 0, 0; x) + 10 H(0, 1, 0; x) \\ & - 12 H(1, -1, 0; x) + 6 H(1, 0, 0; x) + 4 H(1, 1, 0; x) \\ & + \zeta_2(6 H(-1; x) - 5 H(0; x) - 2 H(1; x)) - 14 \zeta_3, \end{aligned} \tag{B.5d}$$

$$\begin{aligned} g_5^{(4)} = & -216 H(-1, -1, -1, 0; x) + 144 H(-1, -1, 0, 0; x) \\ & + 72 H(-1, -1, 1, 0; x) + 144 H(-1, 0, -1, 0; x) - 60 H(-1, 0, 0, 0; x) \\ & - 48 H(-1, 0, 1, 0; x) + 72 H(-1, 1, -1, 0; x) - 48 H(-1, 1, 0, 0; x) \\ & - 24 H(-1, 1, 1, 0; x) + 180 H(0, -1, -1, 0; x) - 120 H(0, -1, 0, 0; x) \\ & - 60 H(0, -1, 1, 0; x) - 78 H(0, 0, -1, 0; x) + 29 H(0, 0, 0, 0; x) \\ & + 26 H(0, 0, 1, 0; x) - 60 H(0, 1, -1, 0; x) + 54 H(0, 1, 0, 0; x) \\ & + 20 H(0, 1, 1, 0; x) + 72 H(1, -1, -1, 0; x) - 48 H(1, -1, 0, 0; x) \\ & - 24 H(1, -1, 1, 0; x) - 36 H(1, 0, -1, 0; x) + 14 H(1, 0, 0, 0; x) \\ & + 12 H(1, 0, 1, 0; x) - 24 H(1, 1, -1, 0; x) + 20 H(1, 1, 0, 0; x) \\ & + 8 H(1, 1, 1, 0; x) + \zeta_2(-36 H(-1, -1; x) + 24 H(-1, 0; x) \\ & + 12 H(-1, 1; x) + 30 H(0, -1; x) - 13 H(0, 0; x) - 10 H(0, 1; x) \\ & + 12 H(1, -1; x) - 6 H(1, 0; x) - 4 H(1, 1; x)) + 2 \zeta_3(33 H(-1; x) \\ & - 17 H(0; x) - 8 H(1; x)) - \frac{61 \zeta_4}{4}, \end{aligned} \tag{B.5e}$$

$$g_6^{(0)} = 0, \quad (\text{B.6a})$$

$$g_6^{(1)} = 0, \quad (\text{B.6b})$$

$$g_6^{(2)} = 2 \text{H}(0, 0; x), \quad (\text{B.6c})$$

$$g_6^{(3)} = -12 \text{H}(0, -1, 0; x) + 6 \text{H}(0, 0, 0; x) + 4 \text{H}(0, 1, 0; x) - 4 \text{H}(1, 0, 0; x) \\ - 2 \zeta_2 \text{H}(0; x) + \\ - 6 \zeta_3, \quad (\text{B.6d})$$

$$g_6^{(4)} = 72 \text{H}(0, -1, -1, 0; x) - 48 \text{H}(0, -1, 0, 0; x) - 24 \text{H}(0, -1, 1, 0; x) \\ - 36 \text{H}(0, 0, -1, 0; x) + 14 \text{H}(0, 0, 0, 0; x) + 12 \text{H}(0, 0, 1, 0; x) \\ - 24 \text{H}(0, 1, -1, 0; x) + 20 \text{H}(0, 1, 0, 0; x) + 8 \text{H}(0, 1, 1, 0; x) \\ + 24 \text{H}(1, 0, -1, 0; x) - 12 \text{H}(1, 0, 0, 0; x) - 8 \text{H}(1, 0, 1, 0; x) \\ + 8 \text{H}(1, 1, 0, 0; x) + 2 \zeta_2 (6 \text{H}(0, -1; x) - 3 \text{H}(0, 0; x)) \\ - 2 \text{H}(0, 1; x) + 2 \text{H}(1, 0; x) - 4 \zeta_3 (4 \text{H}(0; x) - 3 \text{H}(1; x)) - \frac{13 \zeta_4}{2}, \quad (\text{B.6e})$$

$$g_7^{(0)} = 0, \quad (\text{B.7a})$$

$$g_7^{(1)} = 0, \quad (\text{B.7b})$$

$$g_7^{(2)} = \frac{\zeta_2}{2}, \quad (\text{B.7c})$$

$$g_7^{(3)} = -3 \zeta_2 \log 2 + \frac{7 \zeta_3}{4}, \quad (\text{B.7d})$$

$$g_7^{(4)} = \frac{1}{2} \left(24 \text{Li}_4 \frac{1}{2} + \log^4 2 \right) + 6 \zeta_2 \log^2 2 - \frac{31 \zeta_4}{4}, \quad (\text{B.7e})$$

$$g_8^{(0)} = 0, \quad (\text{B.8a})$$

$$g_8^{(1)} = 0, \quad (\text{B.8b})$$

$$g_8^{(2)} = 0, \quad (\text{B.8c})$$

$$g_8^{(3)} = -4 \text{H}(0, 0, 0; x) - 4 \zeta_2 \text{H}(0; x), \quad (\text{B.8d})$$

$$g_8^{(4)} = -8 \text{H}(-1, 0, 0, 0; x) + 24 \text{H}(0, 0, -1, 0; x) - 4 \text{H}(0, 0, 0, 0; x) \\ - 8 \text{H}(0, 0, 1, 0; x) + 8 \text{H}(0, 1, 0, 0; x) + 8 \text{H}(1, 0, 0, 0; x) \\ - 4 \zeta_2 (2 \text{H}(-1, 0; x) - 3 \text{H}(0, 0; x) - 2 \text{H}(1, 0; x)) \\ + 4 \zeta_3 \text{H}(0; x) + 26 \zeta_4, \quad (\text{B.8e})$$

$$g_9^{(0)} = 0, \tag{B.9a}$$

$$g_9^{(1)} = -\frac{1}{2} H(0; x), \tag{B.9b}$$

$$g_9^{(2)} = 2 H(-1, 0; x) - H(0, 0; x) + \zeta_2, \tag{B.9c}$$

$$g_9^{(3)} = -8 H(-1, -1, 0; x) + 4 H(-1, 0, 0; x) + 4 H(0, -1, 0; x) \\ - 2 H(0, 0, 0; x) - 4 \zeta_2 H(-1; x) + 4 \zeta_3, \tag{B.9d}$$

$$g_9^{(4)} = 32 H(-1, -1, -1, 0; x) - 16 H(-1, -1, 0, 0; x) - 16 H(-1, 0, -1, 0; x) \\ + 8 H(-1, 0, 0, 0; x) - 16 H(0, -1, -1, 0; x) + 8 H(0, -1, 0, 0; x) \\ + 8 H(0, 0, -1, 0; x) - 4 H(0, 0, 0, 0; x) + 8 \zeta_2 (2 H(-1, -1; x) \\ - H(0, -1; x)) - 4 \zeta_3 (4 H(-1; x) - H(0; x)) + 19 \zeta_4, \tag{B.9e}$$

$$g_{10}^{(0)} = 0, \quad (\text{B.10a})$$

$$g_{10}^{(1)} = \frac{1}{2} \text{H}(0; x), \quad (\text{B.10b})$$

$$g_{10}^{(2)} = -3 \text{H}(-1, 0; x) + \frac{5}{2} \text{H}(0, 0; x) + \text{H}(1, 0; x) + \zeta_2, \quad (\text{B.10c})$$

$$\begin{aligned} g_{10}^{(3)} = & 18 \text{H}(-1, -1, 0; x) - 14 \text{H}(-1, 0, 0; x) - 6 \text{H}(-1, 1, 0; x) \\ & - 15 \text{H}(0, -1, 0; x) + \frac{17}{2} \text{H}(0, 0, 0; x) + 5 \text{H}(0, 1, 0; x) \\ & - 6 \text{H}(1, -1, 0; x) + 5 \text{H}(1, 0, 0; x) + 2 \text{H}(1, 1, 0; x) \\ & + \frac{1}{2} \zeta_2 (-6 \text{H}(-1; x) + \text{H}(0; x) - 2 \text{H}(1; x) - 6 \log 2) - \frac{9 \zeta_3}{4}, \end{aligned} \quad (\text{B.10d})$$

$$\begin{aligned} g_{10}^{(4)} = & -108 \text{H}(-1, -1, -1, 0; x) + 80 \text{H}(-1, -1, 0, 0; x) \\ & + 36 \text{H}(-1, -1, 1, 0; x) + 84 \text{H}(-1, 0, -1, 0; x) - 44 \text{H}(-1, 0, 0, 0; x) \\ & - 28 \text{H}(-1, 0, 1, 0; x) + 36 \text{H}(-1, 1, -1, 0; x) - 28 \text{H}(-1, 1, 0, 0; x) \\ & - 12 \text{H}(-1, 1, 1, 0; x) + 90 \text{H}(0, -1, -1, 0; x) - 66 \text{H}(0, -1, 0, 0; x) \\ & - 30 \text{H}(0, -1, 1, 0; x) - 51 \text{H}(0, 0, -1, 0; x) + \frac{41}{2} \text{H}(0, 0, 0, 0; x) \\ & + 17 \text{H}(0, 0, 1, 0; x) - 30 \text{H}(0, 1, -1, 0; x) + 29 \text{H}(0, 1, 0, 0; x) \\ & + 10 \text{H}(0, 1, 1, 0; x) + 36 \text{H}(1, -1, -1, 0; x) - 28 \text{H}(1, -1, 0, 0; x) \\ & - 12 \text{H}(1, -1, 1, 0; x) - 30 \text{H}(1, 0, -1, 0; x) + 17 \text{H}(1, 0, 0, 0; x) \\ & + 10 \text{H}(1, 0, 1, 0; x) - 12 \text{H}(1, 1, -1, 0; x) + 10 \text{H}(1, 1, 0, 0; x) \\ & + 4 \text{H}(1, 1, 1, 0; x) + 12 \text{Li}_4 \frac{1}{2} + \frac{\log^4 2}{2} + \frac{1}{2} \zeta_2 (24 \log 2 \text{H}(-1; x) \\ & + 24 \log 2 \text{H}(1; x) + 12 \text{H}(-1, -1; x) + 4 \text{H}(-1, 0; x) + 12 \text{H}(-1, 1; x) \\ & - 6 \text{H}(0, -1; x) - 11 \text{H}(0, 0; x) - 10 \text{H}(0, 1; x) - 12 \text{H}(1, -1; x) \\ & + 2 \text{H}(1, 0; x) - 4 \text{H}(1, 1; x) + 12 \log^2 2) + \zeta_3 (20 \text{H}(-1; x) \\ & - 14 \text{H}(0; x) - 15 \text{H}(1; x)) - \frac{95 \zeta_4}{8}, \end{aligned} \quad (\text{B.10e})$$

$$g_{11}^{(0)} = 0, \quad (\text{B.11a})$$

$$g_{11}^{(1)} = 0, \quad (\text{B.11b})$$

$$g_{11}^{(2)} = 0, \quad (\text{B.11c})$$

$$g_{11}^{(3)} = -2 \text{H}(0, 0, 0; x) - 2 \zeta_2 \text{H}(0; x), \quad (\text{B.11d})$$

$$\begin{aligned} g_{11}^{(4)} = & -4 \text{H}(-1, 0, 0, 0; x) + 4 \text{H}(0, -1, 0, 0; x) + 12 \text{H}(0, 0, -1, 0; x) \\ & - 6 \text{H}(0, 0, 0, 0; x) - 4 \text{H}(0, 0, 1, 0; x) + 4 \text{H}(1, 0, 0, 0; x) \\ & - 4 \zeta_2 (\text{H}(-1, 0; x) - 3 \text{H}(0, -1; x) - \text{H}(1, 0; x)) - \frac{\zeta_4}{2}, \end{aligned} \quad (\text{B.11e})$$

$$g_{12}^{(0)} = 0, \quad (\text{B.12a})$$

$$g_{12}^{(1)} = 0, \quad (\text{B.12b})$$

$$g_{12}^{(2)} = 0, \quad (\text{B.12c})$$

$$g_{12}^{(3)} = -\text{H}(0, 0, 0; x) - \zeta_2 \text{H}(0; x), \quad (\text{B.12d})$$

$$\begin{aligned} g_{12}^{(4)} = & -2 \text{H}(-1, 0, 0, 0; x) + 2 \text{H}(0, -1, 0, 0; x) + 2 \text{H}(0, 0, -1, 0; x) \\ & - 3 \text{H}(0, 0, 0, 0; x) - 4 \text{H}(0, 1, 0, 0; x) + \zeta_2 (-2 \text{H}(-1, 0; x) \\ & + 6 \text{H}(0, -1; x) - \text{H}(0, 0; x)) + 2 \zeta_3 \text{H}(0; x) + \frac{\zeta_4}{4}, \end{aligned} \quad (\text{B.12e})$$

$$g_{13}^{(0)} = 0, \quad (\text{B.13a})$$

$$g_{13}^{(1)} = 0, \quad (\text{B.13b})$$

$$g_{13}^{(2)} = \text{H}(0, 0; x) + \frac{3\zeta_2}{2}, \quad (\text{B.13c})$$

$$g_{13}^{(3)} = -2\text{H}(-1, 0, 0; x) - 2\text{H}(0, -1, 0; x) + 4\text{H}(0, 0, 0; x) + 4\text{H}(1, 0, 0; x) \\ + \zeta_2(-6\text{H}(-1; x) + 2\text{H}(0; x) - 3\log 2) - \frac{\zeta_3}{4}, \quad (\text{B.13d})$$

$$g_{13}^{(4)} = 4\text{H}(-1, -1, 0, 0; x) + 4\text{H}(-1, 0, -1, 0; x) - 8\text{H}(-1, 0, 0, 0; x) \\ - 8\text{H}(-1, 1, 0, 0; x) + 4\text{H}(0, -1, -1, 0; x) - 8\text{H}(0, -1, 0, 0; x) \\ - 8\text{H}(0, 0, -1, 0; x) + 10\text{H}(0, 0, 0, 0; x) + 12\text{H}(0, 1, 0, 0; x) \\ - 8\text{H}(1, -1, 0, 0; x) - 8\text{H}(1, 0, -1, 0; x) + 16\text{H}(1, 0, 0, 0; x) \\ + 16\text{H}(1, 1, 0, 0; x) + 12\text{Li}_4\frac{1}{2} + \frac{\log^4 2}{2} + 2\zeta_2(12\log 2\text{H}(-1; x) \\ + 12\log 2\text{H}(1; x) + 6\text{H}(-1, -1; x) - 2\text{H}(-1, 0; x) - 8\text{H}(0, -1; x) \\ + \text{H}(0, 0; x) - 12\text{H}(1, -1; x) + 4\text{H}(1, 0; x) + 3\log^2 2) \\ - 2\zeta_3(5\text{H}(-1; x) + 4\text{H}(0; x) + 11\text{H}(1; x)) - \frac{47\zeta_4}{4}, \quad (\text{B.13e})$$

$$g_{14}^{(0)} = 0, \quad (\text{B.14a})$$

$$g_{14}^{(1)} = 0, \quad (\text{B.14b})$$

$$g_{14}^{(2)} = \text{H}(0, 0; x), \quad (\text{B.14c})$$

$$g_{14}^{(3)} = -4\text{H}(-1, 0, 0; x) - 4\text{H}(0, -1, 0; x) + 5\text{H}(0, 0, 0; x) \\ + 2\text{H}(0, 1, 0; x) + \zeta_3, \quad (\text{B.14d})$$

$$g_{14}^{(4)} = 16\text{H}(-1, -1, 0, 0; x) + 16\text{H}(-1, 0, -1, 0; x) - 20\text{H}(-1, 0, 0, 0; x) \\ - 8\text{H}(-1, 0, 1, 0; x) + 24\text{H}(0, -1, -1, 0; x) - 26\text{H}(0, -1, 0, 0; x) \\ - 12\text{H}(0, -1, 1, 0; x) - 26\text{H}(0, 0, -1, 0; x) + 9\text{H}(0, 0, 0, 0; x) \\ + 12\text{H}(0, 0, 1, 0; x) - 12\text{H}(0, 1, -1, 0; x) + 8\text{H}(0, 1, 0, 0; x) \\ + 4\text{H}(0, 1, 1, 0; x) - \zeta_2(13\text{H}(0, 0; x) + 2\text{H}(0, 1; x)) \\ - \zeta_3(4\text{H}(-1; x) + 3\text{H}(0; x)) - \frac{7\zeta_4}{2}, \quad (\text{B.14e})$$

$$g_{15}^{(0)} = 0, \quad (\text{B.15a})$$

$$g_{15}^{(1)} = 0, \quad (\text{B.15b})$$

$$g_{15}^{(2)} = 0, \quad (\text{B.15c})$$

$$g_{15}^{(3)} = 0, \quad (\text{B.15d})$$

$$\begin{aligned} g_{15}^{(4)} &= 4 \text{H}(0, -1, 0, 0; x) - 2 \text{H}(0, 0, -1, 0; x) - 2 \text{H}(0, 1, 0, 0; x) \\ &\quad + 4 \text{H}(1, 0, 0, 0; x) + \zeta_2 (\text{H}(0, 0; x) + 4 \text{H}(1, 0; x)) \\ &\quad - 4 \zeta_3 \text{H}(0; x) + \frac{17 \zeta_4}{4}, \end{aligned} \quad (\text{B.15e})$$

$$g_{16}^{(0)} = 0, \quad (\text{B.16a})$$

$$g_{16}^{(1)} = 0, \quad (\text{B.16b})$$

$$g_{16}^{(2)} = 0, \quad (\text{B.16c})$$

$$g_{16}^{(3)} = 0, \quad (\text{B.16d})$$

$$\begin{aligned} g_{16}^{(4)} &= -4 \text{H}(0, -1, 0, 0; x) + 4 \text{H}(0, 0, -1, 0; x) - 2 \text{H}(0, 0, 0, 0; x) \\ &\quad - 4 \text{H}(0, 0, 1, 0; x) + 4 \text{H}(0, 1, 0, 0; x) - 4 \text{H}(1, 0, 0, 0; x) \\ &\quad - 2 \zeta_2 (6 \text{H}(0, -1; x) - \text{H}(0, 0; x) + 2 \text{H}(1, 0; x)) - 2 \zeta_4, \end{aligned} \quad (\text{B.16e})$$

$$g_{17}^{(0)} = 0, \quad (\text{B.17a})$$

$$g_{17}^{(1)} = 0, \quad (\text{B.17b})$$

$$g_{17}^{(2)} = 0, \quad (\text{B.17c})$$

$$g_{17}^{(3)} = 2 (\text{H}(0, -1, 0; x) - \text{H}(0, 0, 0; x) - \text{H}(0, 1, 0; x)) - \zeta_2 \text{H}(0; x) - \zeta_3, \quad (\text{B.17d})$$

$$\begin{aligned} g_{17}^{(4)} &= -8 \text{H}(-1, 0, -1, 0; x) + 8 \text{H}(-1, 0, 0, 0; x) + 8 \text{H}(-1, 0, 1, 0; x) \\ &\quad - 20 \text{H}(0, -1, -1, 0; x) + 16 \text{H}(0, -1, 0, 0; x) + 12 \text{H}(0, -1, 1, 0; x) \\ &\quad + 24 \text{H}(0, 0, -1, 0; x) - 12 \text{H}(0, 0, 0, 0; x) - 16 \text{H}(0, 0, 1, 0; x) \\ &\quad + 12 \text{H}(0, 1, -1, 0; x) - 8 \text{H}(0, 1, 0, 0; x) - 4 \text{H}(0, 1, 1, 0; x) \\ &\quad + 8 \text{H}(1, 0, -1, 0; x) - 8 \text{H}(1, 0, 0, 0; x) - 8 \text{H}(1, 0, 1, 0; x) \\ &\quad + 2 \zeta_2 (2 \text{H}(-1, 0; x) + \text{H}(0, -1; x) + \text{H}(0, 0; x) + \text{H}(0, 1; x) \\ &\quad - 2 \text{H}(1, 0; x)) + \zeta_3 (4 \text{H}(-1; x) - \text{H}(0; x) - 4 \text{H}(1; x)) - \frac{37 \zeta_4}{4}, \end{aligned} \quad (\text{B.17e})$$



Matrices for Associated Higgs plus One Jet Production

C.1. Canonical Matrices at Two-Loop

Here we present the sparse matrices M_i ($i = 1, \dots, 6$) appearing in the canonical system defined in (8.17) and (8.18) obeyed by the MI's (8.28):

$$M_1 = \begin{pmatrix} -2 & 0 & 0 & 0 & 0 & 0 & 0 & 0 & 0 & 0 & 0 & 0 & 0 & 0 & 0 & 0 & 0 & 0 \\ 0 & 0 & 0 & 0 & 0 & 0 & 0 & 0 & 0 & 0 & 0 & 0 & 0 & 0 & 0 & 0 & 0 & 0 \\ 0 & 0 & 0 & 0 & 0 & 0 & 0 & 0 & 0 & 0 & 0 & 0 & 0 & 0 & 0 & 0 & 0 & 0 \\ 0 & 0 & 0 & -2 & 0 & 0 & 0 & 0 & 0 & 0 & 0 & 0 & 0 & 0 & 0 & 0 & 0 & 0 \\ 0 & 0 & 0 & 0 & -2 & 0 & 0 & 0 & 0 & 0 & 0 & 0 & 0 & 0 & 0 & 0 & 0 & 0 \\ -\frac{1}{2} & 0 & 0 & 0 & 0 & -1 & 0 & 0 & 0 & 0 & 0 & 0 & 0 & 0 & 0 & 0 & 0 & 0 \\ 0 & 0 & 0 & 0 & 0 & 0 & 0 & 0 & 0 & 0 & 0 & 0 & 0 & 0 & 0 & 0 & 0 & 0 \\ 0 & 0 & -\frac{1}{2} & 0 & 0 & 0 & 0 & -1 & 0 & 0 & 0 & 0 & 0 & 0 & 0 & 0 & 0 & 0 \\ \frac{1}{2} & 0 & \frac{1}{2} & 0 & 0 & -1 & -2 & 0 & 2 & -2 & 0 & 0 & 0 & 0 & 0 & 0 & 0 & 0 \\ 0 & 0 & 0 & 0 & 0 & 0 & 0 & 0 & 0 & 0 & -2 & 0 & 0 & 0 & 0 & 0 & 0 & 0 \\ 0 & -\frac{1}{2} & \frac{1}{2} & 0 & 0 & 0 & 0 & 0 & 0 & 0 & 0 & -2 & 0 & 0 & 0 & 0 & 0 & 0 \\ \frac{1}{2} & -\frac{1}{2} & 0 & 0 & 0 & 0 & -2 & 2 & 0 & 0 & 0 & 0 & 2 & 0 & 0 & 0 & 0 & 0 \\ 0 & 0 & 0 & 0 & 0 & 0 & 0 & 0 & 0 & 0 & 0 & 0 & 0 & -2 & 0 & 0 & 0 & 0 \\ 0 & 0 & 0 & 0 & 0 & 0 & 0 & 0 & 0 & 0 & 0 & 0 & 0 & 0 & -1 & 0 & 0 & 0 \\ -\frac{3}{8} & \frac{3}{8} & -\frac{3}{4} & 0 & 0 & 1 & \frac{5}{2} & -\frac{3}{2} & -2 & 1 & 0 & 0 & \frac{3}{2} & \frac{1}{4} & 0 & -1 & 0 & 0 \\ 0 & 0 & 0 & 0 & 0 & 0 & 0 & 0 & 0 & 0 & 0 & 0 & 0 & 0 & 0 & 0 & -2 & 0 \\ -\frac{3}{8} & \frac{3}{8} & -\frac{3}{4} & 0 & 0 & 1 & \frac{5}{2} & -\frac{3}{2} & -2 & 1 & 0 & 0 & \frac{3}{2} & \frac{1}{4} & -1 & 1 & 0 & -2 \end{pmatrix} \quad (C.1)$$

(C.9)

$$\left(\begin{array}{c} \text{[A large block of mathematical symbols and operators, including various subscripts and superscripts, arranged in a grid-like structure.]} \end{array} \right)$$

$M_I^{(c)} =$



Two-Loop $d\log$ -forms

In this appendix we give explicitly the coefficient matrices of the $d\log$ -forms, eq. (9.17), for the one-mass and the two-mass two-loop MIs, discussed respectively in sections 9.4 and 9.5.

D.1. One-mass

For the one-mass case at the two-loop order, the $d\log$ -form is

$$\begin{aligned} dA = & \mathbb{M}_1 d\log(1+x) + \mathbb{M}_2 d\log(x) + \mathbb{M}_3 d\log(y) \\ & + \mathbb{M}_4 d\log(1-y) + \mathbb{M}_5 d\log(x+y) + \mathbb{M}_6 d\log(x+y+xy) \end{aligned} \quad (\text{D.1})$$

with

Bibliography

- [1] M. Argeri, S. Di Vita, P. Mastrolia, E. Mirabella, J. Schlenk, U. Schubert, and L. Tancredi, *Magnus and Dyson Series for Master Integrals*, *JHEP* **1403** (2014) 082, [[arXiv:1401.2979](#)].
- [2] S. Di Vita, P. Mastrolia, U. Schubert, and V. Yundin, *Three-loop master integrals for ladder-box diagrams with one massive leg*, *JHEP* **09** (2014) 148, [[arXiv:1408.3107](#)].
- [3] P. Mastrolia, A. Primo, U. Schubert, and W. J. Torres Bobadilla, *Off-shell currents and color-kinematics duality*, *Phys. Lett.* **B753** (2016) 242–262, [[arXiv:1507.0753](#)].
- [4] S. Borowka, N. Greiner, G. Heinrich, S. P. Jones, M. Kerner, J. Schlenk, U. Schubert, and T. Zirke, *Higgs boson pair production in gluon fusion at NLO with full top-quark mass dependence*, [arXiv:1604.0644](#) .
- [5] R. Bonciani, S. Di Vita, P. Mastrolia, and U. Schubert, *Two-Loop Master Integrals for the mixed EW-QCD virtual corrections to Drell-Yan scattering*, [arXiv:1604.0858](#) .
- [6] H. van Deurzen, G. Luisoni, P. Mastrolia, E. Mirabella, G. Ossola, T. Peraro, and U. Schubert, *Multi-loop Integrand Reduction via Multivariate Polynomial Division*, *PoS RADCOR2013* (2013) 012, [[arXiv:1312.1627](#)].
- [7] T. Peraro, H. van Deurzen, G. Luisoni, P. Mastrolia, E. Mirabella, G. Ossola, and U. Schubert, *Integrand reduction at NLO and beyond*, *PoS EPS-HEP2013* (2013) 449.
- [8] P. Mastrolia, M. Argeri, S. Di Vita, E. Mirabella, J. Schlenk, U. Schubert, and L. Tancredi, *Magnus and Dyson Series for Master Integrals*, *PoS LL2014* (2014) 007.

- [9] **UA1** Collaboration, G. Arnison et al., *Experimental Observation of Isolated Large Transverse Energy Electrons with Associated Missing Energy at $s^{**}(1/2) = 540\text{-GeV}$* , *Phys. Lett.* **B122** (1983) 103–116. [[611\(1983\)](#)].
- [10] **UA1** Collaboration, G. Arnison et al., *Experimental Observation of Lepton Pairs of Invariant Mass Around $95\text{-GeV}/c^{**2}$ at the CERN SPS Collider*, *Phys. Lett.* **B126** (1983) 398–410.
- [11] **UA2** Collaboration, M. Banner et al., *Observation of Single Isolated Electrons of High Transverse Momentum in Events with Missing Transverse Energy at the CERN anti-p p Collider*, *Phys. Lett.* **B122** (1983) 476–485.
- [12] **CDF** Collaboration, F. Abe et al., *Observation of top quark production in $\bar{p}p$ collisions*, *Phys. Rev. Lett.* **74** (1995) 2626–2631, [[hep-ex/9503002](#)].
- [13] **D0** Collaboration, S. Abachi et al., *Search for high mass top quark production in $p\bar{p}$ collisions at $\sqrt{s} = 1.8\text{ TeV}$* , *Phys. Rev. Lett.* **74** (1995) 2422–2426, [[hep-ex/9411001](#)].
- [14] **DONUT** Collaboration, K. Kodama et al., *Observation of tau neutrino interactions*, *Phys. Lett.* **B504** (2001) 218–224, [[hep-ex/0012035](#)].
- [15] **ATLAS** Collaboration, G. Aad et al., *Observation of a new particle in the search for the Standard Model Higgs boson with the ATLAS detector at the LHC*, *Phys. Lett.* **B716** (2012) 1–29, [[arXiv:1207.7214](#)].
- [16] **CMS** Collaboration, S. Chatrchyan et al., *Observation of a new boson at a mass of 125 GeV with the CMS experiment at the LHC*, *Phys. Lett.* **B716** (2012) 30–61, [[arXiv:1207.7235](#)].
- [17] **Super-Kamiokande** Collaboration, Y. Fukuda et al., *Evidence for oscillation of atmospheric neutrinos*, *Phys. Rev. Lett.* **81** (1998) 1562–1567, [[hep-ex/9807003](#)].
- [18] **SNO** Collaboration, Q. R. Ahmad et al., *Direct evidence for neutrino flavor transformation from neutral current interactions in the Sudbury Neutrino Observatory*, *Phys. Rev. Lett.* **89** (2002) 011301, [[nucl-ex/0204008](#)].
- [19] **Planck** Collaboration, P. A. R. Ade et al., *Planck 2015 results. xiii. cosmological parameters*, [arXiv:1502.0158](#).
- [20] G. T. Bodwin, *Factorization of the Drell-Yan Cross-Section in Perturbation Theory*, *Phys. Rev.* **D31** (1985) 2616. [Erratum: *Phys. Rev.*D34,3932(1986)].
- [21] J. C. Collins, D. E. Soper, and G. F. Sterman, *Factorization for Short Distance Hadron - Hadron Scattering*, *Nucl. Phys.* **B261** (1985) 104–142.
- [22] J. C. Collins, D. E. Soper, and G. F. Sterman, *Soft Gluons and Factorization*, *Nucl. Phys.* **B308** (1988) 833–856.

- [23] V. N. Gribov and L. N. Lipatov, *Deep inelastic $e p$ scattering in perturbation theory*, *Sov. J. Nucl. Phys.* **15** (1972) 438–450. [*Yad. Fiz.*15,781(1972)].
- [24] G. Altarelli and G. Parisi, *Asymptotic Freedom in Parton Language*, *Nucl. Phys.* **B126** (1977) 298–318.
- [25] Y. L. Dokshitzer, *Calculation of the Structure Functions for Deep Inelastic Scattering and $e^+ e^-$ Annihilation by Perturbation Theory in Quantum Chromodynamics.*, *Sov. Phys. JETP* **46** (1977) 641–653. [*Zh. Eksp. Teor. Fiz.*73,1216(1977)].
- [26] C. Anastasiou, C. Duhr, F. Dulat, F. Herzog, and B. Mistlberger, *Higgs Boson Gluon-Fusion Production in QCD at Three Loops*, *Phys. Rev. Lett.* **114** (2015) 212001, [[arXiv:1503.0605](#)].
- [27] G. Passarino and M. J. G. Veltman, *One Loop Corrections for $e^+ e^-$ Annihilation Into $\mu^+ \mu^-$ in the Weinberg Model*, *Nucl. Phys.* **B160** (1979) 151.
- [28] R. E. Cutkosky, *Singularities and discontinuities of Feynman amplitudes*, *J. Math. Phys.* **1** (1960) 429–433.
- [29] Z. Bern, L. J. Dixon, D. C. Dunbar, and D. A. Kosower, *One-Loop n -Point Gauge Theory Amplitudes, Unitarity and Collinear Limits*, *Nucl. Phys.* **B425** (1994) 217–260, [[hep-ph/9403226](#)].
- [30] R. Britto, F. Cachazo, and B. Feng, *Generalized unitarity and one-loop amplitudes in $N=4$ super-Yang-Mills*, *Nucl.Phys.* **B725** (2005) 275–305, [[hep-th/0412103](#)].
- [31] F. Cachazo, P. Svrcek, and E. Witten, *MHV vertices and tree amplitudes in gauge theory*, *JHEP* **09** (2004) 006, [[hep-th/0403047](#)].
- [32] R. Britto, F. Cachazo, and B. Feng, *New Recursion Relations for Tree Amplitudes of Gluons*, *Nucl. Phys.* **B715** (2005) 499–522, [[hep-th/0412308](#)].
- [33] G. Ossola, C. G. Papadopoulos, and R. Pittau, *Reducing full one-loop amplitudes to scalar integrals at the integrand level*, *Nucl.Phys.* **B763** (2007) 147–169, [[hep-ph/0609007](#)].
- [34] R. K. Ellis, W. T. Giele, and Z. Kunszt, *A Numerical Unitarity Formalism for Evaluating One-Loop Amplitudes*, *JHEP* **03** (2008) 003, [[arXiv:0708.2398](#)].
- [35] G. Ossola, C. G. Papadopoulos, and R. Pittau, *CutTools: a program implementing the OPP reduction method to compute one-loop amplitudes*, *JHEP* **03** (2008) 042, [[arXiv:0711.3596](#)].
- [36] P. Mastrolia, G. Ossola, T. Reiter, and F. Tramontano, *Scattering AMplitudes from Unitarity-based Reduction Algorithm at the Integrand-level*, *JHEP* **1008** (2010) 080, [[arXiv:1006.0710](#)].

- [37] T. Peraro, *Ninja: Automated Integrand Reduction via Laurent Expansion for One-Loop Amplitudes*, *Comput. Phys. Commun.* **185** (2014) 2771–2797, [[arXiv:1403.1229](#)].
- [38] T. Hahn and M. Perez-Victoria, *Automatized one loop calculations in four-dimensions and D-dimensions*, *Comput.Phys.Commun.* **118** (1999) 153–165, [[hep-ph/9807565](#)].
- [39] A. van Hameren, C. Papadopoulos, and R. Pittau, *Automated one-loop calculations: A Proof of concept*, *JHEP* **0909** (2009) 106, [[arXiv:0903.4665](#)].
- [40] G. Bevilacqua, M. Czakon, M. Garzelli, A. van Hameren, A. Kardos, et al., *HELAC-NLO*, [arXiv:1110.1499](#).
- [41] C. Berger, Z. Bern, L. Dixon, F. Febres Cordero, D. Forde, et al., *An Automated Implementation of On-Shell Methods for One-Loop Amplitudes*, *Phys.Rev.* **D78** (2008) 036003, [[arXiv:0803.4180](#)].
- [42] V. Hirschi, R. Frederix, S. Frixione, M. V. Garzelli, F. Maltoni, et al., *Automation of one-loop QCD corrections*, *JHEP* **1105** (2011) 044, [[arXiv:1103.0621](#)].
- [43] G. Cullen, N. Greiner, G. Heinrich, G. Luisoni, P. Mastrolia, et al., *Automated One-Loop Calculations with GoSam*, [arXiv:1111.2034](#).
- [44] F. Cascioli, P. Maierhofer, and S. Pozzorini, *Scattering Amplitudes with Open Loops*, [arXiv:1111.5206](#).
- [45] S. Badger, B. Biedermann, and P. Uwer, *NGLuon: A Package to Calculate One-loop Multi-gluon Amplitudes*, *Comput.Phys.Commun.* **182** (2011) 1674–1692, [[arXiv:1011.2900](#)].
- [46] S. Badger, B. Biedermann, P. Uwer, and V. Yundin, *Numerical evaluation of virtual corrections to multi-jet production in massless QCD*, *Comput. Phys. Commun.* **184** (2013) 1981–1998, [[arXiv:1209.0100](#)].
- [47] P. Mastrolia and G. Ossola, *On the Integrand-Reduction Method for Two-Loop Scattering Amplitudes*, *JHEP* **1111** (2011) 014, [[arXiv:1107.6041](#)].
- [48] P. Mastrolia, E. Mirabella, G. Ossola, and T. Peraro, *Scattering Amplitudes from Multivariate Polynomial Division*, *Phys.Lett.* **B718** (2012) 173–177, [[arXiv:1205.7087](#)].
- [49] S. Badger, H. Frellesvig, and Y. Zhang, *Hepta-Cuts of Two-Loop Scattering Amplitudes*, *JHEP* **1204** (2012) 055, [[arXiv:1202.2019](#)].
- [50] Y. Zhang, *Integrand-Level Reduction of Loop Amplitudes by Computational Algebraic Geometry Methods*, *JHEP* **1209** (2012) 042, [[arXiv:1205.5707](#)].

- [51] P. Mastrolia, T. Peraro, and A. Primo, *Adaptive Integrand Decomposition in parallel and orthogonal space*, [arXiv:1605.0315](#).
- [52] D. A. Kosower and K. J. Larsen, *Maximal Unitarity at Two Loops*, *Phys.Rev.* **D85** (2012) 045017, [[arXiv:1108.1180](#)].
- [53] K. J. Larsen, *Global Poles of the Two-Loop Six-Point $N=4$ SYM integrand*, *Phys. Rev.* **D86** (2012) 085032, [[arXiv:1205.0297](#)].
- [54] S. Caron-Huot and K. J. Larsen, *Uniqueness of two-loop master contours*, *JHEP* **10** (2012) 026, [[arXiv:1205.0801](#)].
- [55] H. Johansson, D. A. Kosower, and K. J. Larsen, *Two-Loop Maximal Unitarity with External Masses*, *Phys. Rev.* **D87** (2013), no. 2 025030, [[arXiv:1208.1754](#)].
- [56] T. Binoth and G. Heinrich, *An automatized algorithm to compute infrared divergent multiloop integrals*, *Nucl. Phys.* **B585** (2000) 741–759, [[hep-ph/0004013](#)].
- [57] T. Binoth and G. Heinrich, *Numerical evaluation of multiloop integrals by sector decomposition*, *Nucl. Phys.* **B680** (2004) 375–388, [[hep-ph/0305234](#)].
- [58] C. Bogner and S. Weinzierl, *Resolution of singularities for multi-loop integrals*, *Comput. Phys. Commun.* **178** (2008) 596–610, [[arXiv:0709.4092](#)].
- [59] G. Heinrich, *Sector Decomposition*, *Int. J. Mod. Phys.* **A23** (2008) 1457–1486, [[arXiv:0803.4177](#)].
- [60] A. Smirnov and M. Tentyukov, *Feynman Integral Evaluation by a Sector decomposition Approach (FIESTA)*, *Comput.Phys.Commun.* **180** (2009) 735–746, [[arXiv:0807.4129](#)].
- [61] J. Carter and G. Heinrich, *SecDec: A general program for sector decomposition*, *Comput. Phys. Commun.* **182** (2011) 1566–1581, [[arXiv:1011.5493](#)].
- [62] S. Borowka, J. Carter, and G. Heinrich, *Numerical Evaluation of Multi-Loop Integrals for Arbitrary Kinematics with SecDec 2.0*, *Comput. Phys. Commun.* **184** (2013) 396–408, [[arXiv:1204.4152](#)].
- [63] S. Borowka, G. Heinrich, S. P. Jones, M. Kerner, J. Schlenk, and T. Zirke, *SecDec-3.0: numerical evaluation of multi-scale integrals beyond one loop*, *Comput. Phys. Commun.* **196** (2015) 470–491, [[arXiv:1502.0659](#)].
- [64] A. V. Smirnov, *FIESTA4: Optimized Feynman integral calculations with GPU support*, *Comput. Phys. Commun.* **204** (2016) 189–199, [[arXiv:1511.0361](#)].
- [65] V. A. Smirnov, *Analytical result for dimensionally regularized massless on shell double box*, *Phys. Lett.* **B460** (1999) 397–404, [[hep-ph/9905323](#)].

- [66] J. Tausk, *Nonplanar massless two loop Feynman diagrams with four on-shell legs*, *Phys.Lett.* **B469** (1999) 225–234, [[hep-ph/9909506](#)].
- [67] M. Czakon, *Automatized analytic continuation of Mellin-Barnes integrals*, *Comput. Phys. Commun.* **175** (2006) 559–571, [[hep-ph/0511200](#)].
- [68] A. V. Smirnov and V. A. Smirnov, *On the Resolution of Singularities of Multiple Mellin-Barnes Integrals*, *Eur. Phys. J.* **C62** (2009) 445–449, [[arXiv:0901.0386](#)].
- [69] S. Laporta, *High precision calculation of multiloop Feynman integrals by difference equations*, *Int.J.Mod.Phys.* **A15** (2000) 5087–5159, [[hep-ph/0102033](#)].
- [70] S. Laporta, *Calculation of master integrals by difference equations*, *Phys. Lett.* **B504** (2001) 188–194, [[hep-ph/0102032](#)].
- [71] R. N. Lee, A. V. Smirnov, and V. A. Smirnov, *Dimensional recurrence relations: an easy way to evaluate higher orders of expansion in ϵ* , *Nucl. Phys. Proc. Suppl.* **205-206** (2010) 308–313, [[arXiv:1005.0362](#)].
- [72] A. Kotikov, *Differential equations method: New technique for massive Feynman diagrams calculation*, *Phys.Lett.* **B254** (1991) 158–164.
- [73] E. Remiddi, *Differential equations for Feynman graph amplitudes*, *Nuovo Cim.* **A110** (1997) 1435–1452, [[hep-th/9711188](#)].
- [74] T. Gehrmann and E. Remiddi, *Differential equations for two loop four point functions*, *Nucl.Phys.* **B580** (2000) 485–518, [[hep-ph/9912329](#)].
- [75] C. G. Papadopoulos, *Simplified differential equations approach for Master Integrals*, [arXiv:1401.6057](#) .
- [76] C. G. Papadopoulos, D. Tommasini, and C. Wever, *The Pentabox Master Integrals with the Simplified Differential Equations approach*, *JHEP* **04** (2016) 078, [[arXiv:1511.0940](#)].
- [77] J. M. Henn, *Multiloop integrals in dimensional regularization made simple*, *Phys.Rev.Lett.* **110** (2013) 251601, [[arXiv:1304.1806](#)].
- [78] T. Gehrmann, J. M. Henn, and T. Huber, *The three-loop form factor in $n=4$ super yang-mills*, [arXiv:1112.4524](#) .
- [79] J. M. Henn, A. V. Smirnov, and V. A. Smirnov, *Analytic results for planar three-loop four-point integrals from a Knizhnik-Zamolodchikov equation*, *JHEP* **1307** (2013) 128, [[arXiv:1306.2799](#)].
- [80] J. M. Henn, *Lectures on differential equations for Feynman integrals*, *J. Phys.* **A48** (2015) 153001, [[arXiv:1412.2296](#)].

- [81] T. Gehrmann, A. von Manteuffel, L. Tancredi, and E. Weihs, *The two-loop master integrals for $q\bar{q} \rightarrow VV$* , *JHEP* **1406** (2014) 032, [[arXiv:1404.4853](#)].
- [82] M. Höschele, J. Hoff, and T. Ueda, *Adequate bases of phase space master integrals for $gg \rightarrow h$ at NNLO and beyond*, *JHEP* **09** (2014) 116, [[arXiv:1407.4049](#)].
- [83] R. N. Lee, *Reducing differential equations for multiloop master integrals*, *JHEP* **04** (2015) 108, [[arXiv:1411.0911](#)].
- [84] A. A. Bolibrukh, *The riemann-hilbert problem on the complex projective line*, .
- [85] C. Anastasiou, S. Beerli, S. Bucherer, A. Daleo, and Z. Kunszt, *Two-loop amplitudes and master integrals for the production of a Higgs boson via a massive quark and a scalar-quark loop*, *JHEP* **01** (2007) 082, [[hep-ph/0611236](#)].
- [86] D. Graudenz, M. Spira, and P. M. Zerwas, *QCD corrections to Higgs boson production at proton proton colliders*, *Phys. Rev. Lett.* **70** (1993) 1372–1375.
- [87] M. Spira, A. Djouadi, D. Graudenz, and P. M. Zerwas, *Higgs boson production at the LHC*, *Nucl. Phys.* **B453** (1995) 17–82, [[hep-ph/9504378](#)].
- [88] T. Plehn, M. Spira, and P. M. Zerwas, *Pair production of neutral Higgs particles in gluon-gluon collisions*, *Nucl. Phys.* **B479** (1996) 46–64, [[hep-ph/9603205](#)]. [Erratum: *Nucl. Phys.*B531,655(1998)].
- [89] S. Dawson, S. Dittmaier, and M. Spira, *Neutral Higgs boson pair production at hadron colliders: QCD corrections*, *Phys. Rev.* **D58** (1998) 115012, [[hep-ph/9805244](#)].
- [90] R. Harlander and P. Kant, *Higgs production and decay: Analytic results at next-to-leading order QCD*, *JHEP* **0512** (2005) 015, [[hep-ph/0509189](#)].
- [91] R. V. Harlander, S. Liebler, and H. Mantler, *SusHi: A program for the calculation of Higgs production in gluon fusion and bottom-quark annihilation in the Standard Model and the MSSM*, *Comput. Phys. Commun.* **184** (2013) 1605–1617, [[arXiv:1212.3249](#)].
- [92] J. Grigo, J. Hoff, K. Melnikov, and M. Steinhauser, *On the Higgs boson pair production at the LHC*, *Nucl. Phys.* **B875** (2013) 1–17, [[arXiv:1305.7340](#)].
- [93] J. Grigo, K. Melnikov, and M. Steinhauser, *Virtual corrections to Higgs boson pair production in the large top quark mass limit*, *Nucl. Phys.* **B888** (2014) 17–29, [[arXiv:1408.2422](#)].
- [94] R. Frederix, S. Frixione, V. Hirschi, F. Maltoni, O. Mattelaer, P. Torrielli, E. Vryonidou, and M. Zaro, *Higgs pair production at the LHC with NLO and parton-shower effects*, *Phys. Lett.* **B732** (2014) 142–149, [[arXiv:1401.7340](#)].

- [95] F. Maltoni, E. Vryonidou, and M. Zaro, *Top-quark mass effects in double and triple Higgs production in gluon-gluon fusion at NLO*, *JHEP* **11** (2014) 079, [[arXiv:1408.6542](#)].
- [96] J. Grigo, J. Hoff, and M. Steinhauser, *Higgs boson pair production: top quark mass effects at NLO and NNLO*, *Nucl. Phys.* **B900** (2015) 412–430, [[arXiv:1508.0090](#)].
- [97] G. Degrossi, P. P. Giardino, and R. Gröber, *On the two-loop virtual QCD corrections to Higgs boson pair production in the Standard Model*, [arXiv:1603.0038](#) .
- [98] F. Tkachov, *A Theorem on Analytical Calculability of Four Loop Renormalization Group Functions*, *Phys.Lett.* **B100** (1981) 65–68.
- [99] K. Chetyrkin and F. Tkachov, *Integration by parts: The algorithm to calculate β -functions in 4 loops*, *Nuclear Physics B* **192** (nov, 1981) 159–204.
- [100] R. N. Lee, *Group structure of the integration-by-part identities and its application to the reduction of multiloop integrals*, *JHEP* **0807:031,2008** (Apr., 2008) [[arXiv:0804.3008](#)].
- [101] A. G. Grozin, *Integration by parts: An introduction*, *Int.J.Mod.Phys.A* **26:2807-2854,2011** (Apr., 2011) [[arXiv:1104.3993](#)].
- [102] S. Laporta and E. Remiddi, *The analytical value of the electron ($g-2$) at order α^3 in qed*, *Phys.Lett. B* **379** (1996) 283–291, [[hep-ph/9602417](#)].
- [103] A. V. Smirnov and A. V. Petukhov, *The number of master integrals is finite*, [arXiv:1004.4199](#) .
- [104] C. Anastasiou and A. Lazopoulos, *Automatic integral reduction for higher order perturbative calculations*, *JHEP* **07** (2004) 046, [[hep-ph/0404258](#)].
- [105] A. V. Smirnov, *FIRE5: a C++ implementation of Feynman Integral REduction*, *Comput. Phys. Commun.* **189** (2014) 182–191, [[arXiv:1408.2372](#)].
- [106] A. von Manteuffel and C. Studerus, *Reduze 2 - Distributed Feynman Integral Reduction*, [arXiv:1201.4330](#) .
- [107] R. N. Lee, *LiteRed 1.4: a powerful tool for reduction of multiloop integrals*, *J. Phys. Conf. Ser.* **523** (2014) 012059, [[arXiv:1310.1145](#)].
- [108] J. M. Henn, A. V. Smirnov, and V. A. Smirnov, *Evaluating single-scale and/or non-planar diagrams by differential equations*, [arXiv:1312.2588](#) .
- [109] J. Gluza, K. Kajda, and D. A. Kosower, *Towards a basis for planar two-loop integrals*, *Phys.Rev.D* **83:045012,2011** (Sept., 2010) [[arXiv:1009.0472](#)].

- [127] M. A. Barkatou and E. Pfister, *On the Moser- and super-reduction algorithms of systems of linear differential equations and their complexity*, .
- [128] K.-T. Chen, *Iterated path integrals*, *Bull. Am. Math. Soc.* **83** (1977) 831–879.
- [129] F. C. S. Brown, *Multiple zeta values and periods of moduli spaces $\overline{\mathcal{M}}_{0,n}(\mathbb{R})$* , *Annales Sci. Ecole Norm. Sup.* **42** (2009) 371, [[math/0606419](#)].
- [130] F. C. S. Brown, *Iterated integrals in quantum field theory*, *IHES*, .
- [131] A. Goncharov, *Polylogarithms in arithmetic and geometry*, *Proceedings of the International Congress of Mathematicians* **1,2** (1995) 374–387.
- [132] E. Remiddi and J. Vermaseren, *Harmonic polylogarithms*, *Int.J.Mod.Phys.* **A15** (2000) 725–754, [[hep-ph/9905237](#)].
- [133] T. Gehrmann and E. Remiddi, *Numerical evaluation of harmonic polylogarithms*, *Comput.Phys.Commun.* **141** (2001) 296–312, [[hep-ph/0107173](#)].
- [134] J. Vollinga and S. Weinzierl, *Numerical evaluation of multiple polylogarithms*, *Comput.Phys.Commun.* **167** (2005) 177, [[hep-ph/0410259](#)].
- [135] A. B. Goncharov, *Galois symmetries of fundamental groupoids and noncommutative geometry*, *Duke Math. J.* **128** (2005) 209, [[math/0208144](#)].
- [136] A. B. Goncharov, M. Spradlin, C. Vergu, and A. Volovich, *Classical Polylogarithms for Amplitudes and Wilson Loops*, *Phys. Rev. Lett.* **105** (2010) 151605, [[arXiv:1006.5703](#)].
- [137] C. Duhr, H. Gangl, and J. R. Rhodes, *From polygons and symbols to polylogarithmic functions*, *JHEP* **10** (2012) 075, [[arXiv:1110.0458](#)].
- [138] A. Goncharov, *Multiple polylogarithms and mixed Tate motives*, [math/0103059](#) .
- [139] F. Brown, *On the decomposition of motivic multiple zeta values*, [arXiv:1102.1310](#) .
- [140] C. Duhr, *Mathematical aspects of scattering amplitudes*, in *Theoretical Advanced Study Institute in Elementary Particle Physics: Journeys Through the Precision Frontier: Amplitudes for Colliders (TASI 2014) Boulder, Colorado, June 2-27, 2014*, 2014. [arXiv:1411.7538](#) .
- [141] R. Bonciani, *Phd thesis, University of Bologna, Italy* (2001).
- [142] R. Bonciani, A. Ferroglia, P. Mastrolia, E. Remiddi, and J. van der Bij, *Planar box diagram for the $(N(F) = 1)$ two loop QED virtual corrections to Bhabha scattering*, *Nucl.Phys.* **B681** (2004) 261–291, [[hep-ph/0310333](#)].
- [143] J. M. Henn and V. A. Smirnov, *Analytic results for two-loop master integrals for Bhabha scattering I*, *JHEP* **1311** (2013) 041, [[arXiv:1307.4083](#)].

- [144] R. Bonciani, P. Mastrolia, and E. Remiddi, *QED vertex form-factors at two loops*, *Nucl.Phys.* **B676** (2004) 399–452, [[hep-ph/0307295](#)].
- [145] R. Bonciani, P. Mastrolia, and E. Remiddi, *Vertex diagrams for the QED form-factors at the two loop level*, *Nucl.Phys.* **B661** (2003) 289–343, [[hep-ph/0301170](#)].
- [146] M. Argeri, P. Mastrolia, and E. Remiddi, *The Analytic value of the sunrise selfmass with two equal masses and the external invariant equal to the third squared mass*, *Nucl.Phys.* **B631** (2002) 388–400, [[hep-ph/0202123](#)].
- [147] D. Maitre, *HPL, a mathematica implementation of the harmonic polylogarithms*, *Comput.Phys.Commun.* **174** (2006) 222–240, [[hep-ph/0507152](#)].
- [148] D. Maitre, *Extension of HPL to complex arguments*, *Comput.Phys.Commun.* **183** (2012) 846, [[hep-ph/0703052](#)].
- [149] C. Anastasiou, T. Gehrmann, C. Oleari, E. Remiddi, and J. Tausk, *The Tensor reduction and master integrals of the two loop massless crossed box with lightlike legs*, *Nucl.Phys.* **B580** (2000) 577–601, [[hep-ph/0003261](#)].
- [150] G. Heinrich, T. Huber, D. Kosower, and V. Smirnov, *Nine-Propagator Master Integrals for Massless Three-Loop Form Factors*, *Phys.Lett.* **B678** (2009) 359–366, [[arXiv:0902.3512](#)].
- [151] G. Heinrich, T. Huber, and D. Maitre, *Master integrals for fermionic contributions to massless three-loop form-factors*, *Phys.Lett.* **B662** (2008) 344–352, [[arXiv:0711.3590](#)].
- [152] T. Gehrmann, G. Heinrich, T. Huber, and C. Studerus, *Master integrals for massless three-loop form-factors: One-loop and two-loop insertions*, *Phys.Lett.* **B640** (2006) 252–259, [[hep-ph/0607185](#)].
- [153] R. Lee, A. Smirnov, and V. Smirnov, *Analytic Results for Massless Three-Loop Form Factors*, *JHEP* **1004** (2010) 020, [[arXiv:1001.2887](#)].
- [154] J. M. Henn, A. V. Smirnov, and V. A. Smirnov, *Evaluating single-scale and/or non-planar diagrams by differential equations*, *JHEP* **1403** (2014) 088, [[arXiv:1312.2588](#)].
- [155] L. Garland, T. Gehrmann, E. N. Glover, A. Koukoutsakis, and E. Remiddi, *The Two loop QCD matrix element for $e^+e^- \rightarrow 3$ jets*, *Nucl.Phys.* **B627** (2002) 107–188, [[hep-ph/0112081](#)].
- [156] L. Garland, T. Gehrmann, E. N. Glover, A. Koukoutsakis, and E. Remiddi, *Two loop QCD helicity amplitudes for $e^+e^- \rightarrow$ three jets*, *Nucl.Phys.* **B642** (2002) 227–262, [[hep-ph/0206067](#)].

- [157] A. Gehrmann-De Ridder, T. Gehrmann, E. Glover, and G. Heinrich, *NNLO moments of event shapes in e^+e^- annihilation*, *JHEP* **0905** (2009) 106, [[arXiv:0903.4658](#)].
- [158] S. Weinzierl, *Event shapes and jet rates in electron-positron annihilation at NNLO*, *JHEP* **0906** (2009) 041, [[arXiv:0904.1077](#)].
- [159] T. Gehrmann, M. Jaquier, E. Glover, and A. Koukoutsakis, *Two-Loop QCD Corrections to the Helicity Amplitudes for $H \rightarrow 3$ partons*, *JHEP* **1202** (2012) 056, [[arXiv:1112.3554](#)].
- [160] R. Boughezal, F. Caola, K. Melnikov, F. Petriello, and M. Schulze, *Higgs boson production in association with a jet at next-to-next-to-leading order in perturbative QCD*, *JHEP* **1306** (2013) 072, [[arXiv:1302.6216](#)].
- [161] S. Badger and E. N. Glover, *Two loop splitting functions in QCD*, *JHEP* **0407** (2004) 040, [[hep-ph/0405236](#)].
- [162] D. A. Kosower and P. Uwer, *Evolution kernels from splitting amplitudes*, *Nucl.Phys.* **B674** (2003) 365–400, [[hep-ph/0307031](#)].
- [163] T. Gehrmann and E. Remiddi, *Numerical evaluation of two-dimensional harmonic polylogarithms*, *Comput.Phys.Commun.* **144** (2002) 200–223, [[hep-ph/0111255](#)].
- [164] T. Gehrmann and E. Remiddi, *Two loop master integrals for $\gamma^* \rightarrow 3$ jets: The Planar topologies*, *Nucl.Phys.* **B601** (2001) 248–286, [[hep-ph/0008287](#)].
- [165] C. Studerus, *Reduze-Feynman Integral Reduction in C++*, *Comput.Phys.Commun.* **181** (2010) 1293–1300, [[arXiv:0912.2546](#)].
- [166] C. W. Bauer, A. Frink, and R. Kreckel, *Introduction to the GiNaC framework for symbolic computation within the C++ programming language*, [cs/0004015](#) .
- [167] A. V. Smirnov, *FIESTA 3: cluster-parallelizable multiloop numerical calculations in physical regions*, *Comput.Phys.Commun.* **185** (2014) 2090–2100, [[arXiv:1312.3186](#)].
- [168] T. Gehrmann and E. Remiddi, *Analytic continuation of massless two loop four point functions*, *Nucl.Phys.* **B640** (2002) 379–411, [[hep-ph/0207020](#)].
- [169] T. Gehrmann and E. Remiddi, *Two loop master integrals for $\gamma^* \rightarrow 3$ jets: The Nonplanar topologies*, *Nucl. Phys.* **B601** (2001) 287–317, [[hep-ph/0101124](#)].
- [170] S. D. Drell and T.-M. Yan, *Massive Lepton Pair Production in Hadron-Hadron Collisions at High-Energies*, *Phys. Rev. Lett.* **25** (1970) 316–320. [Erratum: *Phys. Rev. Lett.*25,902(1970)].

- [171] C. Anastasiou, C. Duhr, F. Dulat, E. Furlan, T. Gehrmann, F. Herzog, A. Lazopoulos, and B. Mistlberger, *High precision determination of the gluon fusion Higgs boson cross-section at the LHC*, [arXiv:1602.0069](#) .
- [172] P. Baikov, K. Chetyrkin, A. Smirnov, V. Smirnov, and M. Steinhauser, *Quark and gluon form factors to three loops*, *Phys.Rev.Lett.* **102** (2009) 212002, [[arXiv:0902.3519](#)].
- [173] T. Gehrmann, E. W. N. Glover, T. Huber, N. Ikizlerli, and C. Studerus, *Calculation of the quark and gluon form factors to three loops in QCD*, *JHEP* **06** (2010) 094, [[arXiv:1004.3653](#)].
- [174] J. R. Andersen et al., *Les Houches 2013: Physics at TeV Colliders: Standard Model Working Group Report*, [arXiv:1405.1067](#) .
- [175] G. Altarelli, R. K. Ellis, and G. Martinelli, *Large Perturbative Corrections to the Drell-Yan Process in QCD*, *Nucl. Phys.* **B157** (1979) 461.
- [176] G. Altarelli, R. K. Ellis, M. Greco, and G. Martinelli, *Vector Boson Production at Colliders: A Theoretical Reappraisal*, *Nucl. Phys.* **B246** (1984) 12.
- [177] T. Matsuura, S. C. van der Marck, and W. L. van Neerven, *The Calculation of the Second Order Soft and Virtual Contributions to the Drell-Yan Cross-Section*, *Nucl. Phys.* **B319** (1989) 570.
- [178] R. Hamberg, W. L. van Neerven, and T. Matsuura, *A Complete calculation of the order $\alpha - s^2$ correction to the Drell-Yan K factor*, *Nucl. Phys.* **B359** (1991) 343–405. [Erratum: *Nucl. Phys.*B644,403(2002)].
- [179] G. F. Sterman, *Summation of Large Corrections to Short Distance Hadronic Cross-Sections*, *Nucl. Phys.* **B281** (1987) 310.
- [180] S. Catani and L. Trentadue, *Resummation of the QCD Perturbative Series for Hard Processes*, *Nucl. Phys.* **B327** (1989) 323.
- [181] S. Catani and L. Trentadue, *Comment on QCD exponentiation at large x*, *Nucl. Phys.* **B353** (1991) 183–186.
- [182] S. Moch and A. Vogt, *Higher-order soft corrections to lepton pair and Higgs boson production*, *Phys. Lett.* **B631** (2005) 48–57, [[hep-ph/0508265](#)].
- [183] D. Wackerroth and W. Hollik, *Electroweak radiative corrections to resonant charged gauge boson production*, *Phys. Rev.* **D55** (1997) 6788–6818, [[hep-ph/9606398](#)].
- [184] U. Baur, S. Keller, and W. K. Sakumoto, *QED radiative corrections to Z boson production and the forward backward asymmetry at hadron colliders*, *Phys. Rev.* **D57** (1998) 199–215, [[hep-ph/9707301](#)].

- [185] R. K. Ellis, G. Martinelli, and R. Petronzio, *Lepton Pair Production at Large Transverse Momentum in Second Order QCD*, *Nucl. Phys.* **B211** (1983) 106.
- [186] P. B. Arnold and M. H. Reno, *The Complete Computation of High $p(t)$ W and Z Production in 2nd Order QCD*, *Nucl. Phys.* **B319** (1989) 37. [Erratum: *Nucl. Phys.* **B330**, 284(1990)].
- [187] R. J. Gonsalves, J. Pawlowski, and C.-F. Wai, *QCD Radiative Corrections to Electroweak Boson Production at Large Transverse Momentum in Hadron Collisions*, *Phys. Rev.* **D40** (1989) 2245.
- [188] F. T. Brandt, G. Kramer, and S.-L. Nyeo, *W , Z plus jet production at p anti- p colliders*, *Int. J. Mod. Phys.* **A6** (1991) 3973–3987.
- [189] W. T. Giele, E. W. N. Glover, and D. A. Kosower, *Higher order corrections to jet cross-sections in hadron colliders*, *Nucl. Phys.* **B403** (1993) 633–670, [[hep-ph/9302225](#)].
- [190] L. J. Dixon, Z. Kunszt, and A. Signer, *Helicity amplitudes for $O(\alpha_s)$ production of W^+W^- , $W^\pm Z$, ZZ , $W^\pm\gamma$, or $Z\gamma$ pairs at hadron colliders*, *Nucl. Phys.* **B531** (1998) 3–23, [[hep-ph/9803250](#)].
- [191] J. H. Kuhn, A. Kulesza, S. Pozzorini, and M. Schulze, *Logarithmic electroweak corrections to hadronic $Z+1$ jet production at large transverse momentum*, *Phys. Lett.* **B609** (2005) 277–285, [[hep-ph/0408308](#)].
- [192] T. Gehrmann and L. Tancredi, *Two-loop QCD helicity amplitudes for $q\bar{q} \rightarrow W^\pm\gamma$ and $q\bar{q} \rightarrow Z^0\gamma$* , *JHEP* **02** (2012) 004, [[arXiv:1112.1531](#)].
- [193] P. B. Arnold and R. P. Kauffman, *W and Z production at next-to-leading order: From large $q(t)$ to small*, *Nucl. Phys.* **B349** (1991) 381–413.
- [194] C. Balazs, J.-w. Qiu, and C. P. Yuan, *Effects of QCD resummation on distributions of leptons from the decay of electroweak vector bosons*, *Phys. Lett.* **B355** (1995) 548–554, [[hep-ph/9505203](#)].
- [195] C. Balazs and C. P. Yuan, *Soft gluon effects on lepton pairs at hadron colliders*, *Phys. Rev.* **D56** (1997) 5558–5583, [[hep-ph/9704258](#)].
- [196] R. K. Ellis, D. A. Ross, and S. Veseli, *Vector boson production in hadronic collisions*, *Nucl. Phys.* **B503** (1997) 309–338, [[hep-ph/9704239](#)].
- [197] R. K. Ellis and S. Veseli, *W and Z transverse momentum distributions: Resummation in q_T space*, *Nucl. Phys.* **B511** (1998) 649–669, [[hep-ph/9706526](#)].
- [198] J.-w. Qiu and X.-f. Zhang, *QCD prediction for heavy boson transverse momentum distributions*, *Phys. Rev. Lett.* **86** (2001) 2724–2727, [[hep-ph/0012058](#)].

- [199] J.-w. Qiu and X.-f. Zhang, *Role of the nonperturbative input in QCD resummed Drell-Yan Q_T distributions*, *Phys. Rev.* **D63** (2001) 114011, [[hep-ph/0012348](#)].
- [200] A. Kulesza and W. J. Stirling, *Soft gluon resummation in transverse momentum space for electroweak boson production at hadron colliders*, *Eur. Phys. J.* **C20** (2001) 349–356, [[hep-ph/0103089](#)].
- [201] A. Kulesza, G. F. Sterman, and W. Vogelsang, *Joint resummation in electroweak boson production*, *Phys. Rev.* **D66** (2002) 014011, [[hep-ph/0202251](#)].
- [202] F. Landry, R. Brock, P. M. Nadolsky, and C. P. Yuan, *Tevatron Run-1 Z boson data and Collins-Soper-Sterman resummation formalism*, *Phys. Rev.* **D67** (2003) 073016, [[hep-ph/0212159](#)].
- [203] G. Bozzi, S. Catani, G. Ferrera, D. de Florian, and M. Grazzini, *Production of Drell-Yan lepton pairs in hadron collisions: Transverse-momentum resummation at next-to-next-to-leading logarithmic accuracy*, *Phys. Lett.* **B696** (2011) 207–213, [[arXiv:1007.2351](#)].
- [204] C. Anastasiou, L. J. Dixon, K. Melnikov, and F. Petriello, *Dilepton rapidity distribution in the Drell-Yan process at NNLO in QCD*, *Phys. Rev. Lett.* **91** (2003) 182002, [[hep-ph/0306192](#)].
- [205] S. Frixione and B. R. Webber, *Matching NLO QCD computations and parton shower simulations*, *JHEP* **0206** (2002) 029, [[hep-ph/0204244](#)].
- [206] S. Frixione, P. Nason, and C. Oleari, *Matching NLO QCD computations with Parton Shower simulations: the POWHEG method*, *JHEP* **0711** (2007) 070, [[arXiv:0709.2092](#)].
- [207] L. Barze, G. Montagna, P. Nason, O. Nicrosini, F. Piccinini, and A. Vicini, *Neutral current Drell-Yan with combined QCD and electroweak corrections in the POWHEG BOX*, *Eur. Phys. J.* **C73** (2013), no. 6 2474, [[arXiv:1302.4606](#)].
- [208] C. M. Carloni Calame, G. Montagna, O. Nicrosini, and M. Treccani, *Higher order QED corrections to W boson mass determination at hadron colliders*, *Phys. Rev.* **D69** (2004) 037301, [[hep-ph/0303102](#)].
- [209] C. M. Carloni Calame, S. Jadach, G. Montagna, O. Nicrosini, and W. Placzek, *Comparisons of the Monte Carlo programs HORACE and WINHAC for single W boson production at hadron colliders*, *Acta Phys. Polon.* **B35** (2004) 1643–1674, [[hep-ph/0402235](#)].
- [210] D. Bardin, S. Bondarenko, S. Jadach, L. Kalinovskaya, and W. Placzek, *Implementation of SANC EW corrections in WINHAC Monte Carlo generator*, *Acta Phys. Polon.* **B40** (2009) 75–92, [[arXiv:0806.3822](#)].

- [211] W. Placzek, S. Jadach, and M. W. Krasny, *Drell-Yan processes with WINHAC*, *Acta Phys. Polon.* **B44** (2013), no. 11 2171–2178, [[arXiv:1310.5994](#)].
- [212] K. Melnikov and F. Petriello, *The W boson production cross section at the LHC through $O(\alpha_s^2)$* , *Phys. Rev. Lett.* **96** (2006) 231803, [[hep-ph/0603182](#)].
- [213] Y. Li and F. Petriello, *Combining QCD and electroweak corrections to dilepton production in FEWZ*, *Phys. Rev.* **D86** (2012) 094034, [[arXiv:1208.5967](#)].
- [214] S. Catani and M. Grazzini, *An NNLO subtraction formalism in hadron collisions and its application to Higgs boson production at the LHC*, *Phys. Rev. Lett.* **98** (2007) 222002, [[hep-ph/0703012](#)].
- [215] S. Catani, L. Cieri, G. Ferrera, D. de Florian, and M. Grazzini, *Vector boson production at hadron colliders: a fully exclusive QCD calculation at NNLO*, *Phys. Rev. Lett.* **103** (2009) 082001, [[arXiv:0903.2120](#)].
- [216] W. B. Kilgore and C. Sturm, *Two-Loop Virtual Corrections to Drell-Yan Production at order $\alpha_s\alpha^3$* , *Phys. Rev.* **D85** (2012) 033005, [[arXiv:1107.4798](#)].
- [217] A. Kotikov, J. H. Kuhn, and O. Veretin, *Two-Loop Formfactors in Theories with Mass Gap and Z-Boson Production*, *Nucl. Phys.* **B788** (2008) 47–62, [[hep-ph/0703013](#)].
- [218] S. Dittmaier, A. Huss, and C. Schwinn, *Mixed QCD-electroweak $O(\alpha_s\alpha)$ corrections to Drell-Yan processes in the resonance region: pole approximation and non-factorizable corrections*, *Nucl. Phys.* **B885** (2014) 318–372, [[arXiv:1403.3216](#)].
- [219] S. Dittmaier, A. Huss, and C. Schwinn, *Dominant mixed QCD-electroweak $O(\alpha_s\alpha)$ corrections to Drell-Yan processes in the resonance region*, *Nucl. Phys.* **B904** (2016) 216–252, [[arXiv:1511.0801](#)].
- [220] R. Bonciani, *Two-loop mixed QCD-EW virtual corrections to the Drell-Yan production of Z and W bosons*, *PoS EPS-HEP2011* (2011) 365.
- [221] M. Argeri and P. Mastrolia, *Feynman Diagrams and Differential Equations*, *Int.J.Mod.Phys.* **A22** (2007) 4375–4436, [[arXiv:0707.4037](#)].
- [222] S. Caron-Huot and J. M. Henn, *Iterative structure of finite loop integrals*, *JHEP* **1406** (2014) 114, [[arXiv:1404.2922](#)].
- [223] K. Chetyrkin and F. Tkachov, *Integration by parts: The algorithm to calculate beta functions in 4 loops*, *Nucl.Phys.* **B192** (1981) 159–204.
- [224] A. V. Smirnov, *Algorithm FIRE – Feynman Integral REduction*, *JHEP* **10** (2008) 107, [[arXiv:0807.3243](#)].

- [225] A. V. Smirnov and V. A. Smirnov, *FIRE4, LiteRed and accompanying tools to solve integration by parts relations*, *Comput. Phys. Commun.* **184** (2013) 2820–2827, [[arXiv:1302.5885](#)].
- [226] R. N. Lee, *Presenting LiteRed: a tool for the Loop InTEgrals REDuction*, [arXiv:1212.2685](#) .
- [227] J. Fleischer, A. V. Kotikov, and O. L. Veretin, *Analytic two loop results for selfenergy type and vertex type diagrams with one nonzero mass*, *Nucl. Phys.* **B547** (1999) 343–374, [[hep-ph/9808242](#)].
- [228] U. Aglietti and R. Bonciani, *Master integrals with one massive propagator for the two loop electroweak form-factor*, *Nucl. Phys.* **B668** (2003) 3–76, [[hep-ph/0304028](#)].
- [229] R. Bonciani, P. Mastrolia, and E. Remiddi, *Master integrals for the two loop QCD virtual corrections to the forward backward asymmetry*, *Nucl. Phys.* **B690** (2004) 138–176, [[hep-ph/0311145](#)].
- [230] U. Aglietti and R. Bonciani, *Master integrals with 2 and 3 massive propagators for the 2 loop electroweak form-factor - planar case*, *Nucl. Phys.* **B698** (2004) 277–318, [[hep-ph/0401193](#)].
- [231] U. Aglietti, R. Bonciani, G. Degrassi, and A. Vicini, *Master integrals for the two-loop light fermion contributions to $gg \rightarrow H$ and $H \rightarrow \gamma\gamma$* , *Phys. Lett.* **B600** (2004) 57–64, [[hep-ph/0407162](#)].
- [232] R. Bonciani, G. Degrassi, and A. Vicini, *On the Generalized Harmonic Polylogarithms of One Complex Variable*, *Comput. Phys. Commun.* **182** (2011) 1253–1264, [[arXiv:1007.1891](#)].
- [233] D. J. Broadhurst, *Massive three - loop Feynman diagrams reducible to SC^* primitives of algebras of the sixth root of unity*, *Eur. Phys. J.* **C8** (1999) 311–333, [[hep-th/9803091](#)].
- [234] J. Zhao, *Standard Relations of Multiple Polylogarithm Values at Roots of Unity*, *ArXiv e-prints* (July, 2007) [[arXiv:0707.1459](#)].
- [235] F. Moriello, *Linearization and symmetrization of generalized harmonic polylogarithms*, *Master Thesis, University of Rome “La Sapienza”* (April 2013).
- [236] J. M. Henn, A. V. Smirnov, and V. A. Smirnov, *Evaluating Multiple Polylogarithm Values at Sixth Roots of Unity up to Weight Six*, [arXiv:1512.0838](#) .
- [237] E. W. N. Glover and J. J. van der Bij, *Higgs boson pair production via gluon fusion*, *Nucl. Phys.* **B309** (1988) 282–294.
- [238] D. de Florian and J. Mazzitelli, *Two-loop virtual corrections to Higgs pair production*, *Phys. Lett.* **B724** (2013) 306–309, [[arXiv:1305.5206](#)].

- [239] D. de Florian and J. Mazzitelli, *Higgs Boson Pair Production at Next-to-Next-to-Leading Order in QCD*, *Phys. Rev. Lett.* **111** (2013) 201801, [[arXiv:1309.6594](#)].
- [240] D. Y. Shao, C. S. Li, H. T. Li, and J. Wang, *Threshold resummation effects in Higgs boson pair production at the LHC*, *JHEP* **07** (2013) 169, [[arXiv:1301.1245](#)].
- [241] D. de Florian and J. Mazzitelli, *Higgs pair production at next-to-next-to-leading logarithmic accuracy at the LHC*, *JHEP* **09** (2015) 053, [[arXiv:1505.0712](#)].
- [242] P. Nogueira, *Automatic Feynman graph generation*, *J.Comput.Phys.* **105** (1993) 279–289.
- [243] R. Bonciani, V. Del Duca, H. Frellesvig, J. M. Henn, F. Moriello, and V. A. Smirnov, *Next-to-leading order QCD corrections to the decay width $H \rightarrow Z\gamma$* , *JHEP* **08** (2015) 108, [[arXiv:1505.0056](#)].
- [244] T. Gehrmann, S. Guns, and D. Kara, *The rare decay $H \rightarrow Z\gamma$ in perturbative QCD*, *JHEP* **09** (2015) 038, [[arXiv:1505.0056](#)].
- [245] G. Puhlfürst, *The evaluation of loop integrals via differential equations*, Master’s thesis, 2012.
- [246] M. Caffo, H. Czyz, S. Laporta, and E. Remiddi, *The Master differential equations for the two loop sunrise selfmass amplitudes*, *Nuovo Cim.* **A111** (1998) 365–389, [[hep-th/9805118](#)].
- [247] S. Laporta and E. Remiddi, *Analytic treatment of the two loop equal mass sunrise graph*, *Nucl. Phys.* **B704** (2005) 349–386, [[hep-ph/0406160](#)].
- [248] S. Bloch and P. Vanhove, *The elliptic dilogarithm for the sunset graph*, *J. Number Theor.* **148** (2015) 328–364, [[arXiv:1309.5865](#)].
- [249] E. Remiddi and L. Tancredi, *Schouten identities for Feynman graph amplitudes; the Master Integrals for the two-loop massive sunrise graph*, [arXiv:1311.3342](#) .
- [250] L. Adams, C. Bogner, and S. Weinzierl, *The two-loop sunrise graph with arbitrary masses*, *J. Math. Phys.* **54** (2013) 052303, [[arXiv:1302.7004](#)].
- [251] L. Adams, C. Bogner, and S. Weinzierl, *The two-loop sunrise graph in two space-time dimensions with arbitrary masses in terms of elliptic dilogarithms*, *J. Math. Phys.* **55** (2014), no. 10 102301, [[arXiv:1405.5640](#)].
- [252] L. Adams, C. Bogner, and S. Weinzierl, *The two-loop sunrise integral around four space-time dimensions and generalisations of the Clausen and Glaisher functions towards the elliptic case*, *J. Math. Phys.* **56** (2015), no. 7 072303, [[arXiv:1504.0325](#)].

- [253] L. Adams, C. Bogner, and S. Weinzierl, *The iterated structure of the all-order result for the two-loop sunrise integral*, *J. Math. Phys.* **57** (2016), no. 3 032304, [[arXiv:1512.0563](#)].
- [254] S. Bloch, M. Kerr, and P. Vanhove, *Local mirror symmetry and the sunset Feynman integral*, [arXiv:1601.0818](#) .
- [255] E. Remiddi and L. Tancredi, *Differential equations and dispersion relations for Feynman amplitudes. The two-loop massive sunrise and the kite integral*, *Nucl. Phys.* **B907** (2016) 400–444, [[arXiv:1602.0148](#)].
- [256] S. C. Borowka, *Evaluation of multi-loop multi-scale integrals and phenomenological two-loop applications*. PhD thesis, Munich, Tech. U., 2014. [arXiv:1410.7939](#) .
- [257] V. Smirnov, *Feynman integral calculus*, .
- [258] G. Cullen et al., *GOSAM-2.0: a tool for automated one-loop calculations within the Standard Model and beyond*, *Eur. Phys. J.* **C74** (2014), no. 8 3001, [[arXiv:1404.7096](#)].
- [259] J. A. M. Vermaseren, *New features of FORM*, [math-ph/0010025](#) .
- [260] J. Kuipers, T. Ueda, J. A. M. Vermaseren, and J. Vollinga, *FORM version 4.0*, *Comput. Phys. Commun.* **184** (2013) 1453–1467, [[arXiv:1203.6543](#)].
- [261] A. von Manteuffel, E. Panzer, and R. M. Schabinger, *A quasi-finite basis for multi-loop Feynman integrals*, *JHEP* **02** (2015) 120, [[arXiv:1411.7392](#)].
- [262] S. Catani and M. Seymour, *A General algorithm for calculating jet cross-sections in NLO QCD*, *Nucl.Phys.* **B485** (1997) 291–419, [[hep-ph/9605323](#)].
- [263] G. P. Lepage, *VEGAS: An adaptive multidimensional integration program*, .
- [264] T. Hahn, *CUBA: A Library for multidimensional numerical integration*, *Comput. Phys. Commun.* **168** (2005) 78–95, [[hep-ph/0404043](#)].
- [265] J. Butterworth et al., *PDF4LHC recommendations for LHC Run II*, *J. Phys.* **G43** (2016) 023001, [[arXiv:1510.0386](#)].
- [266] S. Dulat, T.-J. Hou, J. Gao, M. Guzzi, J. Huston, P. Nadolsky, J. Pumplin, C. Schmidt, D. Stump, and C. P. Yuan, *New parton distribution functions from a global analysis of quantum chromodynamics*, *Phys. Rev.* **D93** (2016), no. 3 033006, [[arXiv:1506.0744](#)].
- [267] L. A. Harland-Lang, A. D. Martin, P. Motylinski, and R. S. Thorne, *Parton distributions in the LHC era: MMHT 2014 PDFs*, *Eur. Phys. J.* **C75** (2015), no. 5 204, [[arXiv:1412.3989](#)].

- [268] **NNPDF** Collaboration, R. D. Ball et al., *Parton distributions for the LHC Run II*, *JHEP* **04** (2015) 040, [[arXiv:1410.8849](#)].